DISSERTATION

GENE THERAPY FOR TREATMENT OF INFECTED NON-UNIONS AND NOVEL METHODS FOR EARLY DIAGNOSIS OF IMPAIRED FRACTURE HEALING

Submitted by

Louise L. Southwood

Department of Clinical Sciences

In partial fulfillment of the requirements

for the Doctor of Philosophy degree

Colorado State University

Fort Collins, Colorado

Summer, 2002

UMI Number: 3064012

ProQuest Information and Learning Company
300 North Zeeb Road
P.O. Box 1346
Ann Arbor, MI 48106-1346

COLORADO STATE UNIVERSITY

JUNE 19, 2002

WE HEREBY RECOMMEND THAT THE DISSERTATION PREPARED UNDER OUR SUPERVISION BY LOUISE L. SOUTHWOOD ENTITLED GENE THERAPY FOR TREATMENT OF INFECTED NON-UNIONS AND NOVEL METHODS FOR EARLY DIAGNOSIS OF IMPAIRED FRACTURE HEALING BE ACCEPTED AS FULFULLING IN PART REQUIREMENTS FOR THE DEGREE OF DOCTOR OF PHILOSOPHY.

Committee on Graduate Work

Co-Advisor

Advisor

Department Head

ABSTRACT OF DISSERTATION

GENE THERAPY FOR TREATMENT OF INFECTED NON-UNIONS AND NOVEL METHODS FOR EARLY DIAGNOSIS OF IMPAIRED FRACTURE HEALING

Non-union and infected non-union are devastating complications of long-bone fracture repair of both human and veterinary patients. Novel methods for treatment of impaired fracture healing, particularly infected non-union, are required. While studies have demonstrated the efficacy of adenoviral transfer of bone morphogenetic protein-2 (Ad-BMP-2) for enhancing healing in non-union models, there have been no studies evaluating the use of Ad-BMP-2 for enhancing healing of infected non-unions.

Early diagnosis of non-union and infected non-union is essential for a favorable outcome. Currently available techniques have limitations for use, particularly when metallic implants are used to stabilize the fracture. Therefore new techniques for early diagnosis of non-union and infected non-union are needed.

The purpose of this study was to evaluate the use of gene therapy for enhancing fracture healing in an infected non-union model and to evaluate the use of nuclear scintigraphy and serum bone marker concentration for early diagnosis of non-union and infected non-union.

The objective of the first part of this study (Chapter 2) was to develop and evaluate an infected non-union model in rabbits. Rabbits were used for economical reasons. A 10-mm middiaphyseal femoral defect, stabilized with bone plates and cortical screws was the basic model. A sclerosing agent was used on the end of the bone

fragments adjacent to the defect to prevent healing and to facilitate the development of osteomyelitis. Rabbits were inoculated with 10^7 colony-forming units of *Staphylococcus aureus* 48 hours after surgery. While there were some complications associated with this model, overall the methods used appeared to result in an infected non-union model that was adequate for evaluating methods to enhance fracture healing.

The objective of the second part of this study (Chapter 3) was to evaluate the use of Ad-BMP-2 for enhancing fracture healing in the infected non-union rabbit model. Radiography, dual energy x-ray absorptiometry, and histomorphometry were used to evaluate healing. Radiographically, rabbits treated with Ad-BMP-2 had earlier initial- and bridging-callus formation, and there were more rabbits with bridging-callus formation compared to control rabbits. Rabbits in the Ad-BMP-2 group also had a higher grade for callus formation. However, there was no difference in bone formation, measured histologically, at 16 weeks between the control and treated rabbits; but treated rabbits that were euthanized prior to 16 weeks did have more endochondral ossification and bone formation compared to control rabbits.

The objective of the final part of this study (Chapters 4 and 5) was to evaluate the use of nuclear scintigraphy and serum bone markers for early diagnosis of non-union and infected non-union. Nuclear scintigraphy using both technetium-labeled diphosphonate and ciprofloxacin was useful for differentiating infected from non-infected fractures in the late phase of healing; however, the accuracy was lower during the early phase. Technetium-labeled diphosphonate may be useful for evaluating callus formation and defect ossification.

Serum markers of bone resorption (deoxypyridinoline crosslinks) peaked at 4 weeks, and markers of bone formation (osteocalcin and bone-specific alkaline phosphatase) peaked at 8 weeks after surgery. Markers of bone formation were lower in infected rabbits at 4 weeks, and osteocalcin was higher in infected rabbits later in healing. The deoxypyridinoline crosslinks were higher in infected rabbits at all time periods. There were only weak associations between serum bone marker concentration and callus formation.

Overall, the results of this study suggest that Ad-BMP-2 may be useful for enhancing healing of infected non-unions; however, in cases with severe cell and tissue damage, *ex vivo* gene transfer may be better. Nuclear scintigraphy has many limitations for diagnosing osteomyelitis associated with long-bone fractures early in the course of fracture healing; however, serum bone markers may be more useful and require further investigation.

Louise L. Southwood
Department of Clinical Sciences
Colorado State University
Fort Collins, CO 80523
Summer, 2002

ACKNOWLEDGEMENTS

There are several people that should be acknowledged for their help and support during the preparation of this thesis.

I would like to acknowledge my graduate committee. Firstly, Dr Wayne McIlwraith for being supportive of a project on fracture healing and osteomyelitis, and providing the initial funding for the pilot studies, which led to us obtaining full funding to complete the main research project. Drs Frisbie and Kawcak for their advice, patience, and support; as well as for their assistance with operating over 70 rabbits. Dr Donna Wheeler assisted with histomorphometric analysis, and Dr Jenny Nyborg with the molecular biological aspects of my PhD studies.

The pilot study evaluating the model was funded by a grant from AO Vet, and the study evaluating novel methods of diagnosis and treatment of impaired fracture healing was funded by Morris Animal Foundation.

Dr Randall Fitch recommended modifications to the surgical technique for the basic non-union model, and Dr Richard Park was integral in developing radiographic grades. Dr Simon Turner performed dual energy x-ray absorptiometry analysis. Dr Philip Steyn assisted in the design of the nuclear scintigraphy part of the study, and John Uhrig performed nuclear scintigraphy scanning. I would also like to thank Dianne Beranek for all her help with preparing the undecalcified histological sections.

This project could not have been completed without the help of Heather Colhoun and Claire Miller, as well as the students that participate in the volunteer

program at the Equine Orthopaedic Research Laboratory. Elisa French at Laboratory Animal Resources provided invaluable assistance with rabbit handling and care. Dr Sophie Morisset and Andi Hume provided continuous assistance with laboratory aspects of the research for my PhD. I would also like to acknowledge Dr Troy Trumble with whom I have shared an office for several years. He has been a great support and his computer knowledge and skill were indispensable during the preparation of this thesis.

I would especially like to thank Eric Parente for all of his love and support during the past 3 years of my PhD program.

PREFACE

Long-bone fractures are not uncommon in horses and complications associated with treatment of long-bone fractures in horses often results in euthanasia. Osteomyelitis is one of the most common complications following fracture repair. Unfortunately euthanasia is often performed after a prolonged period of treatment, at both a financial and emotional cost to the client.

Two cases in particular stimulated this PhD research project. "Cash" was a neonatal Belgian colt that sustained an open metatarsal fracture as a consequence of being stepped on by the mare. The fracture was repaired with bone plates and cortical screws. Unfortunately, wound drainage began a few days after surgery; the foal was treated with antimicrobials and surgical debridement. Numerous radiographs were taken over several months; however, there were no radiographic changes indicative of non-union or osteomyelitis. A diagnosis of infected non-union, with sequestration of the metatarsus, was finally made at surgery, after several months of unsuccessful treatment, and the foal was euthanized. "Bill" was a mature Quarter Horse that sustained an open, non-displaced, distal radial fracture as a result of a kick from another horse. There was a long delay in treatment, and despite the poor prognosis, the owners elected to treat the fracture and osteomyelitis. Unfortunately, the osteomyelitis progressed and the fracture failed to heal. "Bill" was euthanized.

These cases exemplify the problems with fracture healing in horses, particularly in the presence of infection. Therefore, novel methods for treatment of infected non-unions, and improved techniques for early diagnosis of non-union and osteomyelitis are required.

TABLE OF CONTENTS

CHAPTER 1

LITERATURE REVIEW:

IMPAIRED FRACTURE HEALING

CLINICAL PROBLEM OF NON-UNION AND INFECTED NON-UNION OF LONG-BONES

Long-bones have a unique ability to heal without scar tissue, and remodel to their original histological and geometrical structure. While normal healing of long-bone fractures occurs rapidly and without complication, fracture healing is occasionally impaired. Impaired fracture healing (delayed- or non-union) is a devastating clinical complication in both human and veterinary surgery. Osteomyelitis, or infected non-union, is one cause of impaired fracture healing. Non-union or infected non-union can lead to amputation of the affected limb in human or small animal patients, and usually results in euthanasia of equine patients following a prolonged and expensive treatment period. Novel methods for treatment and diagnosis of impaired fracture healing are needed.

Human Patients

In humans, healing of 5 to 10% of the estimated 6 million fractures in the United States each year is delayed or impaired.[1] More specifically, there are 1.5 million long-bone fractures each year in the United States[2] and approximately 100,000 become non-unions.[3] Non-union and infected non-union may ultimately lead to chronic, persistent pain, or amputation of the affected limb.[4] The majority of long-bone non-unions occur in the tibia,[2] and tibial non-unions are particularly problematic to treat.[5] In addition to the physical and psychological impairment to the individual, the estimated direct and indirect cost of fractures approaches 20 billion dollars per year with an associated 101.3 million days of restricted activity each year.[6] These statistics emphasize the importance of

research into methods for enhancing fracture healing as well as techniques for early diagnosis of impaired healing.

Equine Patients

Long-bone fractures in adult horses have a guarded to poor prognosis for survival.[7-10] In retrospective studies, success rates of less than 20% for repair of long-bone fractures in adult horses have been reported.[7-10] Impaired fracture healing and osteomyelitis are among the most common causes of failure of treatment of long-bone fractures in horses, with an occurrence rate of 30-40% following treatment.[7-10] Approximately 70-90% of horses that develop either impaired healing or osteomyelitis are euthanized.[7-10]

Inherent characteristics associated with long-bone fractures in horses include poor vascularity and minimal soft tissue support of the distal limb, high-energy trauma and subsequent massive bone, vascular, and soft tissue damage associated with fracturing an adult long-bone, body weight and temperament of the horse, necessity for early weight bearing on the affected limb, and a contaminated environment in which the horses are housed. These characteristics predispose the horse to complications associated with fracture healing.[11]

Euthanasia of horses with complications following treatment of long-bone fractures usually follows a prolonged course of treatment and hospitalization, at both a high emotional and financial cost to the owner. The clinical situation in horses underscores the importance of the need for improved methods of treatment and early diagnosis of impaired fracture healing.

ANIMAL MODELS OF FRACTURE HEALING, NON-UNION, AND OSTEOMYELITIS

Animal models are an essential part of the development and evaluation of new methods for treatment and diagnosis of impaired fracture healing. While the horse is the target species of our research, horses are more expensive to purchase and maintain compared to other species, and are prone to complications such as support-limb laminitis associated with prolonged lameness and gastrointestinal tract disease associated with general anesthesia, various medications, and surgery. Therefore, pilot studies in small animal models to demonstrate efficacy of the basic principle (proof of principle), are critical prior to clinical application.

Fracture Healing Models

The classical long-bone fracture healing model is a closed tibial or femoral fracture created using a guillotine or three-point bending and stabilized with a cast, intramedullary Kirschner wire, or external skeletal fixator.[12-14] Rats, mice, rabbits, and dogs have been used most commonly.[12-14] Fracture healing with this type of model occurs within weeks of surgery. There are several important aspects of fracture healing models that should be considered when selecting a model for a particular study.

Skeletal Maturity

The use of skeletally mature animals is critical for evaluation of fracture healing.[15] Skeletal maturity is usually defined by growth plate closure, rather than based

on the body weight of the animal, because body weight charts have been shown to give a premature indication of skeletal maturity.[15] This is important because fracture healing in mature animals is a different process compared to immature animals or children. Young animals with open growth plates have been shown to heal more rapidly than mature animals with closed growth plates.[15,16]

The difference in the physiology of fracture healing between old and young animals is illustrated in a study by Meyer and coworkers.[16] Old rats (15 months) had slower healing compared to young rats (1.5 months). Old rats also had lower expression of osteocalcin (OC), type I collagen, and the bone morphogenetic protein (BMP) receptor compared to young rats. Bone morphogenetic protein-4 expression was higher in older rats possibly as a result of tissue resistance and subsequent feedback mechanisms.[16] Older rats also had a longer duration of expression of type II collagen, BMP-2, and the BMP receptor compared to younger rats; however, there was a premature reduction in expression of genes required in fracture healing, which was reflected in slower healing.[16]

In vitro studies have also shown a difference in response to cells from immature compared to mature rats. Cells from older rats (24- and 48-week old) had a reduced response to demineralized bone matrix (DBM) compared to younger rats (4-week old).[17] Older rats had a lower stimulation of alkaline phosphatase synthesis, a marker of osteoblastic phenotype, and a similar, but less pronounced, change in morphology.[17] These studies make a strong case that there are differences in both the rate as well as the physiological process of fracture healing in young and older animals.

Small Animal Models

While biopsies obtained during surgical revision from human malunions, which heal normally but in an incorrect position, are ideal for evaluating normal fracture healing in humans and have recently been used in several studies,[18-20] this type of tissue is in limited supply. Therefore, animal models are needed. Small animal models, which include rat, mice, and rabbit models, have some commonly recognized limitations. Rats and mice have plexiform bone, which heals and remodels differently than Haversian bone, found in higher vertebrates such as humans and horses. This is especially important since fracture healing is slower and associated with more complications in animals with Haversian bone that are higher on the phylogenetic scale compared to animals lower on the phylogenetic scale.[15] An example of this is that cartilage production in human fracture callus was found to be less exuberant and the process of callus mineralization occurred later in humans compared to the rat.[15] While this observation refers to the histomorphometric changes, it most likely reflects differences in the physiology of fracture healing between higher and lower vertebrates. Despite the recognized limitations with the use of small animal models, it is believed that they more accurately represent the processes of fracture healing as compared to *in vitro* cell culture techniques. Because small animals or rodents are more economical and easier to purchase and maintain than large animal models which would include dogs, ruminants, horses, and non-human primates, they are better suited for use in pilot studies and to evaluate proof of principle.

While animal models of fracture healing are useful for evaluating the physiology of normal healing, they do not provide information regarding the pathophysiology of

non-union or infected non-union. Further, because normal fracture healing occurs rapidly it may be difficult to evaluate new methods to enhance healing in normal-healing models because repair is already at an optimum. Large numbers of animals, euthanized at several time periods early in the process of healing, are required to determine the benefits of treatment modalities using these normal-healing models. Therefore, non-union models have been developed to examine the pathophysiology of impaired healing and, in particular, to evaluate methods to enhance fracture healing.

Non-Union Models

Several non-union animal models have been described including unicortical bone defects, mandibulectomy, nasal defects, and craniotomy.[15] Because the focus of our research is on the treatment of long-bone fractures, the following sections will focus on non-union models using long-bones. Long-bone non-union fracture models that have been used to evaluate the use of BMPs for enhancing fracture healing at the time of this manuscript are listed in Tables 2 and 4 in the section on "Treatment of Non-Union and Infected Non-Union."

Long-bone non-union models usually involve the creation of segmental defect in the middiaphyseal region of the femur, tibia, radius, or ulna. The fracture defect has typically been stabilized using either splinting or casting; an intramedullary pin, nail, or Kirschner wire; external fixation; or with a bone plate (stainless steel or synthetic material) and cortical screws or threaded Kirschner wire. Animal species in these studies include mice, rats, rabbits, dogs, sheep, goats, and non-human primates.[15]

A non-union can be produced by preventing bone regeneration through instability, interposition of soft tissue, infection, inadequate blood supply, and systemic disease.[15] Alternatively, a non-union can be produced by creating a critical sized defect (CSD), where bone regeneration is optimal and physiologically normal, but fails to heal the defect because the size of the defect exceeds the ability of the body to regenerate bone.[15] While CSD models may be useful for evaluation of methods to heal bone defects resulting from various surgical procedures, the non-union models may be more representative of non-unions resulting from the majority of traumatic fractures.

Critical Sized Defect Models

A CSD is, by definition, the smallest intraosseus wound that will not heal during the lifetime of the animal.[21] The definition of a CSD has been modified by some authors to a defect that has less than 10 percent bone regeneration during the lifetime of the animal.[15] Using this definition of a CSD, most experimental models used to evaluate treatment of non-unions are too short of a duration (less than 16 weeks) to be classified as CSD models and are therefore non-union models.[15] Schmitz and coworkers[22] postulated that the cause of non-union in CSD is a lack of growth factors, which are produced by the bone ends in the center of the defect.

There have been numerous studies aimed at determining the amount of bone that needs to be removed to create a CSD, which varies depending on both the species and the particular bone.[15] Key reported that "the diameter of the bone roughly determines the (maximum) length of the section which can be removed from the shaft of this bone and not result in union. For example, in adult dogs this length is 1.5 times the diameter."[23]

Similar observations have been made in cats.[24] Several studies have supported Key's[23] findings that the amount of resected bone required to create a non-union is dependent on the diameter of the bone. For example, resection of the ulna equal to twice the diameter of the midshaft created a persistent non-union in dogs.[25] When a 3 mm defect was created in the radius of large breed dogs the defects healed by 3 months; however, when similar defects were created in smaller dogs (at least 2% of the length of the radius) the defects did not heal.[26]

Non-Union Models

A non-union, on the other hand, has the broader definition of failure to restore the continuity and function of the bone and, therefore, can be composed of various amounts of bone and fibrous tissue.[15] Hence, there may be more variability between non-union models than CSD models. This has led some authors to conclude that a CSD model is more useful experimentally because it is more consistent.[15] On the other hand, variability exists between clinical cases of impaired fracture healing, and as mentioned previously, non-union models may be more representative of some clinical cases.

Different methods to inhibit bone regeneration have been tried and most non-union models combine some of the principles of a CSD in addition to creating an environment to inhibit bone regeneration (Table 2 and 4). Removal of periosteum, endosteum, and bone marrow from the bone adjacent to the defect is thought to be important to prevent healing in segmental defect models (Baltzer AWA, Personal Communication). Other methods that have been used to inhibit bone regeneration are the use of silastic material to plug the bone ends or wrapped about the diaphysis.[27-29] The

latter methods inhibit bone marrow and adjacent soft tissues and blood vessels from contributing to fracture healing. The soft tissue, periosteum, endosteum, and bone marrow are essential for fracture healing as described in the section on "Physiology of Fracture Healing".

Recently, Brownlow and coworkers[30] developed a new non-union model in rabbits, where a small (2-mm) defect was created in the middiaphysis of the tibia by slight fragment distraction and stabilized with an external skeletal fixator. A non-union was created by excising the periosteum and removing the bone marrow for a length equal to the diameter of the tibia. The duration of this study was 16 weeks and rabbits with the periosteum and bone marrow removed had a clinically unstable fracture, minimal callus formation, and a fibrous tissue non-union (atrophic non-union). In contrast, rabbits that did not have the periosteum or bone marrow removed developed clinical, radiographical, and histological union.

Fujita and coworks[31] also established a non-union, without making an ostectomy, by creating a tibial fracture in rats using three-point bending, stabilizing the fracture with an intramedullary pin, and interposing muscle between the bone fragments. The periosteum, endosteum, and bone marrow were preserved. The duration of the study was two years, and rats had clinical, radiographical, and histological atrophic non-union at the end of the study period.

Fracture Stabilization

The method of defect stabilization is also important and should simulate that used in the clinical cases. Because of the inherent stability provided by the adjacent bone,

radial and ulna fracture defects are generally not surgically stabilized in most experimental models. The disadvantage of radial and ulna defects are that 1) both the biomechanics and biology of healing are different than that of a fractures stabilized with implants;[15] 2) there is bone, either the radius or ulna, immediately adjacent to the defect which may promote healing, and 3) there is a risk of fracture of the supporting bone particularly if any damage is caused to this bone during surgical creation of the defect.

Fractures stabilized with external skeletal fixators result in minimal disruption to the soft tissue, vasculature, and bone, and some authors report that they are not well tolerated by small animals.[15] Comparatively, the intramedullary fixation devices cause more disruption to the endosteal and marrow tissue and bone plates and screws disrupt the soft tissue and periosteum. These three methods of stabilization also result in biomechanically different environments at the fracture site because the stabilizing structure is placed either externally at a distance from the bone, along the approximate central axis of the bone, or on the surface of the bone. Therefore, the method of stabilization for non-union models for evaluation of methods to enhance healing should be carefully chosen based on the objective of the study.

Morbidity and Mortality

Mortality rates of up to 20% have been reported for non-union models.[34,35] Reported complications include transient or persistent lameness,[25,32] and migration of intramedullary pins.[33] Bone-implant failure,[32,34,35] anesthetic complications,[34] and infection[34] are common causes of euthanasia, as well as loss of rabbits as a result of anorexia and enterocolitis.[36]

Osteomyelitis Models

Animal models of osteomyelitis typically involve surgical creation of a cortical drill hole or fracture in either the femur or tibia, and inoculation of the medullary cavity or fracture site with *Staphylococcus aureus* (Table 1).[37-57] Hematogenous models of osteomyelitis have also been developed;[37,38] however, the pathophysiology associated with acute hematogenous osteomyelitis is most likely different from post traumatic osteomyelitis associated with long-bone fractures. The development of osteomyelitis is defined by clinical signs of lameness, swelling, and drainage, laboratory findings of leukocytosis and increase in erythrocyte sedimentation rate, positive culture results of soft tissues or bone, and radiographic and histological findings of bone lysis and necrosis.[37-51] Inoculation of the medullary cavity through a cortical drill hole in the absence of a foreign body (such as an implant or polymer), sclerosing agent (such as sodium morrhuate or sodium tetradecylsodiumsulfate), fracture, or devitalized bone either does not result in osteomyelitis, [37-57] or is attainable only at doses that cause death of the animal from sepsis or suppurative arthritis requiring euthanasia.[37-40]

Sodium Morrhuate

Sodium morrhuate was first used as a sclerosing agent by Scheman and coworkers[39] and caused aseptic necrosis of bone and subsequent osteomyelitis. Sodium morrhuate, a fish oil product containing fatty acids and arachidonic acid,[38] is a detergent sclerosant that causes cell damage. An aggregation of detergent molecules forms a lipid bilayer in the form of a sheet, a cylinder, or a micelle, that disrupts the cell surface

Table 1. Examples of animal models of *Staphylococcus aureus* osteomyelitis

Author	Species	Bone/Lesion	Dose (cfu)	Infection Rate	Mortality Rate
Norden& Kennedy 1970[40]	Rabbit	Tibia/ 0.1mL 5%NaM	10^6	89%	30%
Adriole et al 1973[47]	Rabbit	Tibia/ Fracture + IM Pin	10^8	88%	0%
Deysine et al 1976[52]	Dog	Tibia/ $BaSO_4$ in Nutrient Artery	10^5	100%	100%[1]
Zak et al 1982[44]	Rat	Tibia/ 0.05mL 5%NaM	10	100%	<5%
Fitzgerald 1983[57]	Dog	Tibia/ PMMA	10^9	100%	0%
Rodeheaver et al 1983[46]	Rabbit	Femur/PMMA	10^5/ 10^6	81%	0%/ 75%
Jacob et al 1984[49]	Rabbit	Tibia/ Fracture + 3% TDSS	10^7	77%	24%
Passl et al 1984[50]	Guinea Pig	Femur/ Fracture + IM Wire	10^4	100%	0%
Rissing et al 1985[45]	Rat	Femur/ 0.05mL 5%NaM	10	81%	0%
Petty et al 1985[60]	Dog	Femur/None, PMMA, SS, CO, PE	10^4-10^8	20-80%	0%
Worlock et al 1988[48]	Rabbit	Tibia/ Fracture +IM Pin/Plate	10^7	80%	<5%
Eerenberg et al 1994[42]	Rabbit	Femur/ IM Pin	10^5	100%	0%
Melcher et al 1994[56]	Rabbit	Tibia/ IM Nail	10^3-10^7	10-100%	5%
Arens et al 1996[55]	Rabbit	Tibia/ Bone Plate & Screws	10^3-10^6	13-100%	0%
Smeltzer et al 1997[43]	Rabbit	Radius/Devascularized bone	10^3-10^6	75-100%	0%
Kaarsemaker et al 1997[41]	Sheep	Tibia/ 1mL 3%TDSS	10^8	100%	21%[2]
Hill et al 1999[54]	Sheep	Tibia/ IM Nail	10^7	100%	0%
Schulz et al 2001[51]	Rabbit	Femur/0.1mL 5%NaM + IM Pin	10^5	100%	25%

NaM=sodium morrhuate, IM=intramedullary, TDSS=tetradecylsodiumsulphate, PMMA=polymethylmethacrylate implant, SS=stainless steel implant, CO=cobalt chromium implant, PE= polyethylene implant. 1. Death of all animals in 4 to 16 weeks, 2. Mortality of 58% was reduced with the use of a single dose of antibiotics 1 hour after inoculation.

membrane, and removes essential proteins from the cell membrane surface.[58] Sodium morrhuate also results in an inflammatory response and fibrosis.[58]

Implants

Several studies have also shown that the use of a foreign body, such as a surgical implant, reduces the bacterial inoculation required to induce infection by 10,000-fold.[59-61] There is a lot of variability in the infection rate with different types of implants. For example, stainless steel implants have a higher infection rate than titanium implants when inoculated with the same dose of *S. aureus*. Therefore, creation of bone damage and the use of surgical implants in experimental osteomyelitis models allow the use of a dose of *S. aureus* that results in a high infection rate without causing severe systemic signs.

Bacterial Inoculation

Staphylococcus aureus is the most commonly used microbial organism in experimental models of osteomyelitis.[37-57] *Staphylococcus aureus* is a common pathogen that can cause osteomyelitis in both human[62] and veterinary patients,[63] and has several characteristics that make it a better microorganism for use in osteomyelitis models compared to other bacteria. These include a very low risk to laboratory personnel and a high rate of establishment of osteomyelitis at a lower dose compared to other bacteria. Specifically, *Staphylococcus intermedius, Proteus mirabilis, and Escherischia coli* were found to have a low rate of infection in animal models,[40,60] and *Pseudomonas aeruginosa* caused a more indolent, less destructive infection, with less extraosseus extension, as well as more proliferation and less lysis radiographically compared to *S. aureus*.[37]

The virulence factors associated with *S. aureus* are most likely the reasons for the high occurrence of *S. aureus* osteomyelitis. Virulence factors associated with *S. aureus* that cause osteomyelitis are the ability to adhere to fibronectin (through cell surface teichoic acids), and collagen, bone sialoprotein (BSP), and laminin through other cell surface receptors. Secretion of a glycocalyx or polysaccharide capsule (biofilm) inhibits chemotaxis and allows the organism to evade the host immune system. The protein A component of the cell surface binds the Fc receptor of immunoglobulins (IgG1, IgG2, and IgG4) preventing antibody-mediated immunity. Extracellular protein A is also capable of binding and inactivating antibodies. Bound coagulase (clumping factor) binds fibrinogen and converts it to insoluble fibrin. There are also several cytolytic toxins (alpha, beta, delta, gamma, and leukocydin) and enzymes (coagulase, catalase, hyaluronidase, fibrinolysin (staphylokinase), lipase, nuclease, and penicillinase) which both enhance survival of the *S. aureus* organism as well as cause damage to the surrounding tissue.[64,65]

Morbidity and Mortality

The morbidity associated with models of osteomyelitis includes weight loss, lameness, and soft tissue infection with drainage and an open wound.[37-57] Rabbits are also usually bacteremic postinoculation.[40] Mortality is highly variable and is mostly attributed to sepsis. A mortality of 25-30% may be expected in studies using animal models of osteomyelitis.[40,41,49,51] Fracture of the inoculated limb[39] and septic arthritis[37,38] are also causes of euthanasia.

Although the mortality rate of animals used in models of osteomyelitis appears disappointingly high, it is important to recognize that acute bacterial osteomyelitis in humans had a 50% mortality, due to overwhelming sepsis and metastatic abscesses, prior to the introduction of antibiotics into clinical practice.[66] This fact emphasizes both the importance of the disease as well as the difficulty in establishing chronic osteomyelitis with acceptable maintenance of the animals systemic condition.

Virulence and Inoculation Dose: It appears that the mortality associated with sepsis may be high in these models as a result of either a large dose or virulence of the particular *S. aureus* strain.[42] There are also variations in the dose and virulence of *S. aureus* required to establish osteomyelitis (Table 1). Low doses and/or low-virulence strains cause a lower infection rate as well as less radiographic and histological signs of osteomyelitis compared to high doses and/or highly virulent strains.[43] However, high doses and virulent strains cause severe sepsis and death.

Andriole and coworkers[47] showed that 10^8 colony forming units (cfu) of a particular strain of *S. aureus* caused almost 100% mortality in rabbits, but the same dose of another strain did not appear to affect the rabbits while causing a high infection rate. Smeltzer and coworkers[43] reported a 75% infection rate with 10^3 cfu of one strain, and very little disease with 10^6 cfu of another strain. The use of a less virulent strain, however, may not cause persistent or chronic osteomyelitis, and increasing the dose of a less virulent strain to cause osteomyelitis may result in a higher mortality. The frustration with achieving a high infection rate but low mortality rate is illustrated in the study by Rodeheaver and coworkers,[46] where a dose of 10^5 cfu resulted in an infection rate of only

81% and no mortality but a dose of 10^6 cfu caused a 75% mortality within 14 days of inoculation.

Route of Inoculation and Study Duration: The method of inoculation may also be important. Deysine and coworkers[52] inoculated dogs with 10^5 cfu of *S. aureus* in the nutrient artery of the tibia and while the infection rate was high, there was 100% mortality over 4 to 16 weeks. Most animals developing severe systemic signs of sepsis either died or required euthanasia within 1 to 2 weeks of inoculation. Therefore, the duration of the study also determines the mortality rate. For example, Whalen and coworkers[53] were able to inoculate rabbits with 10^8 cfu of *S. aureus*; however, rabbits were euthanized within 7 days of inoculation and most rabbits within 48 hours of inoculation.

Low Infection Rate to Prevent Mortality: Some authors have recommended using a lower infection rate (less than 75%), because of the concomitant reduced mortality.[55,56] A lower infection rate may be useful for studies evaluating methods to prevent or treat osteomyelitis because infection rates with the different treatments can be compared. When treatment modalities to enhance fracture healing in infected non-unions are being evaluated, however, a consistent model is required. Further, in many of the previously described models of osteomyelitis, animals are usually euthanized within a few weeks of inoculation; therefore, a lower inoculation dose may be adequate to create osteomyelitis of a short duration. Experimental models used to evaluate methods to enhance fracture healing of infected non-unions not only require a consistently high incidence of infection (90-100%) but the animals need to be infected for the duration of the study which is often

12 to 16 weeks. The challenge is to create a high incidence of osteomyelitis without high morbidity and mortality.

Antimicrobials to Prevent Mortality: Administration of a single dose of an antimicrobial 1 hour postinjection was found to reduce the incidence of mortality due to sepsis, without reducing the incidence of infection.[41] Other studies, however, have found that the use of antimicrobials significantly reduces the incidence of infection (91% versus 30 to 51%).[67] Therefore, while the use of antibiotics in an infected non-union model may reduce the mortality, it may also add undesirable variability to the infection rate, and the effect of antimicrobials on the model should be evaluated prior to use in a large study.

Infected Non-Union

While the classical osteomyelitis models[39-46,48,51-57,59,60] that have intact bone have provided information on methods to establish osteomyelitis as well as provide a model for evaluation of methods to prevent and treat osteomyelitis, they are not suitable for evaluating methods to enhance fracture healing in infected non-unions. There have been a few osteomyelitis models where a fracture was created prior to inoculation and, while these models may actually be useful for evaluating healing, the previous studies have not determined whether or not these models were representative of a non-union.[47-50] Until recently there have been no infected non-union models.

Chen and coworkers[68] recently reported the use of an infected non-union model in rats to evaluate the use of BMP-7 (osteogenic protein-1) to enhance fracture healing. A 6-mm middiaphyseal femoral defect was created and stabilized with a polyacetyl plate, four threaded Kirschner wires and two cerclage wires. Rats were inoculated with 10^5 cfu of *S.*

aureus. Euthanasia was performed at 2, 4, and 9 weeks after surgery and inoculation. Therefore the study was of a short duration compared to other studies evaluating methods to enhance healing of non-unions. None of the rats in the non-infected groups had a positive culture and there were no fixation failures. There was a 100% infection rate in the groups of rats that were inoculated; however, a positive culture only was used to define infection. Other studies have used a quantitative count greater than either 10^4 or 10^5 cfu/gram of tissue to define infection. There were no animals in the infected groups with draining wounds, weight loss, or lameness; however, there was cortical bone fracture, fixation failure, and limb deformity of animals in the infected groups.

While the model of Chen and coworkers[68] appears to be an ideal infected non-union model, the study was of short duration and with cortical fracture and fixation failure the rats may have become lame enough to require euthanasia in a study of longer duration. Further, cortical fracture in some of the animals adds a lot of variability to the model with regard to biomechanics and bone metabolism. Shortcomings of the rat-model are that rats are small, limiting the number of samples that can be taken at necropsy and prohibiting procedures such as repeated blood collection, and rats have plexiform rather than Haversian bone. Rabbits, on the other hand, are larger, but have the advantage over large animal models of being more economical and easier to purchase and maintain. Currently there are no infected non-union models in rabbits. Our first objective, therefore, was do develop an infected non-union model in rabbits as outlined in Chapter 2.

PHYSIOLOGY OF FRACTURE HEALING

An understanding of the physiology of normal fracture healing is important for both discerning the causes of impaired healing as well as developing novel methods to enhance fracture healing.

Histomorphology

General Histological Changes

Fracture healing involves three basic stages that include: inflammation, repair (soft-tissue and hard-tissue callus formation), and remodeling. Each stage has distinct tissue and cellular features.[69,70] These overlapping phases of fracture healing are characterized histologically by the formation of a fracture hematoma and granulation tissue, the formation of fibrous tissue and cartilage, and then bone. Coinciding with the various stages of matrix production there are progressive changes in the cell population. The initial cells at the fracture site are macrophages and undifferentiated mesenchymal cells, followed by fibroblasts, chondroblasts, then osteoblasts, and finally mature osteocytes.

Immediately following fracture, there is damage to the bone, soft tissue, and blood vessels, which results in hemorrhage leading to hematoma formation, migration and accumulation of inflammatory and undifferentiated mesenchymal cells at the fracture site, and release of numerous cytokines, including growth factors. Inflammatory cells, particularly macrophages, lymphocytes, and dendritic cells are responsible for removal of debris, initiating an immune response, as well as the release of growth factors and other cytokines which initiate the healing response.[71,72] Platelets are critical for hemostasis and

the release of growth factors and other cytokines. The damaged bone matrix itself is also a reservoir of growth factors. These growth factors, which are released as a result of fracture, coordinate the process of fracture healing including angiogenesis and neovascularization, as well as migration, proliferation, differentiation, and matrix production by undifferentiated mesenchymal cells.[73]

Osteoprogenitor and Undifferentiated Mesenchymal Cells

The sources of undifferentiated mesenchymal cells include the periosteum, endosteum, bone marrow, ingrowth of blood vessels and perivascular tissue, muscle, and surrounding soft tissues.[73,74] As mentioned previously, these undifferentiated mesenchymal cells proliferate and are capable of differentiating into fibroblasts, chondroblasts or osteoblasts, and synthesizing matrix proteins for fibrous tissue, cartilage, or bone, depending on the stage of healing and the biological and mechanical environment at the fracture site.

Periosteum: The cells in the cambium layer of the periosteum are both undifferentiated mesenchymal and osteoprogenitor cells that proliferate, hypertrophy, and differentiate into osteoblasts or chondrocytes. They produce bone through endochondral ossification or intramembranous bone formation (periosteal callus).[75] These cells proliferate in response to injury and the presence of the fracture hematoma,[76] most likely in response to growth factors released from the damaged bone and in the hematoma.

Bone Marrow and Endosteum: Following fracture, the bone marrow loses its normal architecture. A hematoma forms, which is composed of pyknotic, degenerating stromal cells and erythrocytes. An area of high cellular density with predominantly

undifferentiated mesenchymal cells forms adjacent to the hematoma. There are no blood vessels present in this area, which is thought to be a result of vessel damage and transformation of endothelial and reticular cells into mesenchymal cells.[70] An area of low cellular density with low numbers of undifferentiated mesenchymal cells, but with numerous blood vessels and enlarged capillary and venous endothelial cells, forms adjacent to the avascular region.[70] These areas of altered morphology contribute both osteoprogenitor cells and blood supply to the fracture site.

Small foci of new bone, lined by enlarged osteoblasts, with associated capillaries, form in the areas of undifferentiated mesenchymal cells within 24 hours of fracture (medullary callus).[70] Enlarged endosteal osteoblasts also form bone through intramembranous ossification.[70] The importance of bone marrow in fracture healing was illustrated in a non-union model with the marrow cavities plugged, and fracture healing occurred only when bone marrow was placed into the defect.[77]

Other Sources of Osteoprogenitor Cells: Additional sources of cells are pericytes, which are connective tissue cells associated with capillary walls. Pericytes migrate to the fracture site and are thought to be precursors of either bone or cartilage.[74] Fibroblasts also have the ability to transform into chondrocytes and osteoblasts under appropriate environmental conditions.[75]

Type of Bone Healing

Primary and Secondary Healing: The type of bone healing (primary or secondary) and the process of bone formation in secondary healing (intramembranous or endochondral ossification) are dependent on the environment at the fracture site. Primary

bone healing involves direct osteonal repair, where bone-forming units (cutting cones) unite the fragment ends. This type of healing is dependent on stability and the absence of a fracture gap. True primary bone healing is, therefore, rare.

The two classifications of secondary bone healing are endochondral and intramembranous ossification. These processes of ossification are similar to bone formation during skeletal development; however, are temporally and spatially less organized.[75] Intramembranous ossification involves formation of bone from fibrous tissue whereas endochondral ossification involves the replacement of fibrous tissue by cartilage, followed by bone (Figure 1). The initial formation of cartilage (endochondral ossification) or bone (intramembranous ossification) is dependent on fracture stability and the proximity of the tissue to the fracture site. Cartilage is formed in areas with high motion or strain, low oxygen tension, and in areas adjacent to the fracture site.[78]

Endochondral Ossification: Endochondral ossification involves hypertrophy of terminally differentiated chondrocytes, which have vesicles containing acid phosphatases that degrade the cartilaginous matrix. When the phosphates precipitate with calcium it results in matrix ossification. Vascularization occurs following formation of the calcified cartilage matrix, which is also called primary spongiosa. Osteoblasts follow the capillary ingrowth and produce osteoid on the calcified cartilage matrix. The calcified cartilage matrix is resorbed by osteoclasts, chondroclasts, and macrophages. The remaining cartilage struts are osteoconductive. Controversy exists whether hypertrophic chondrocytes undergo cell death[73] or begin to express an osteoblastic phenotype and produce bone matrix.[79-82] It is thought that woven bone (secondary spongiosa) is deposited on cartilage matrix struts either by transformed chondrocytes (lacuna bone) or

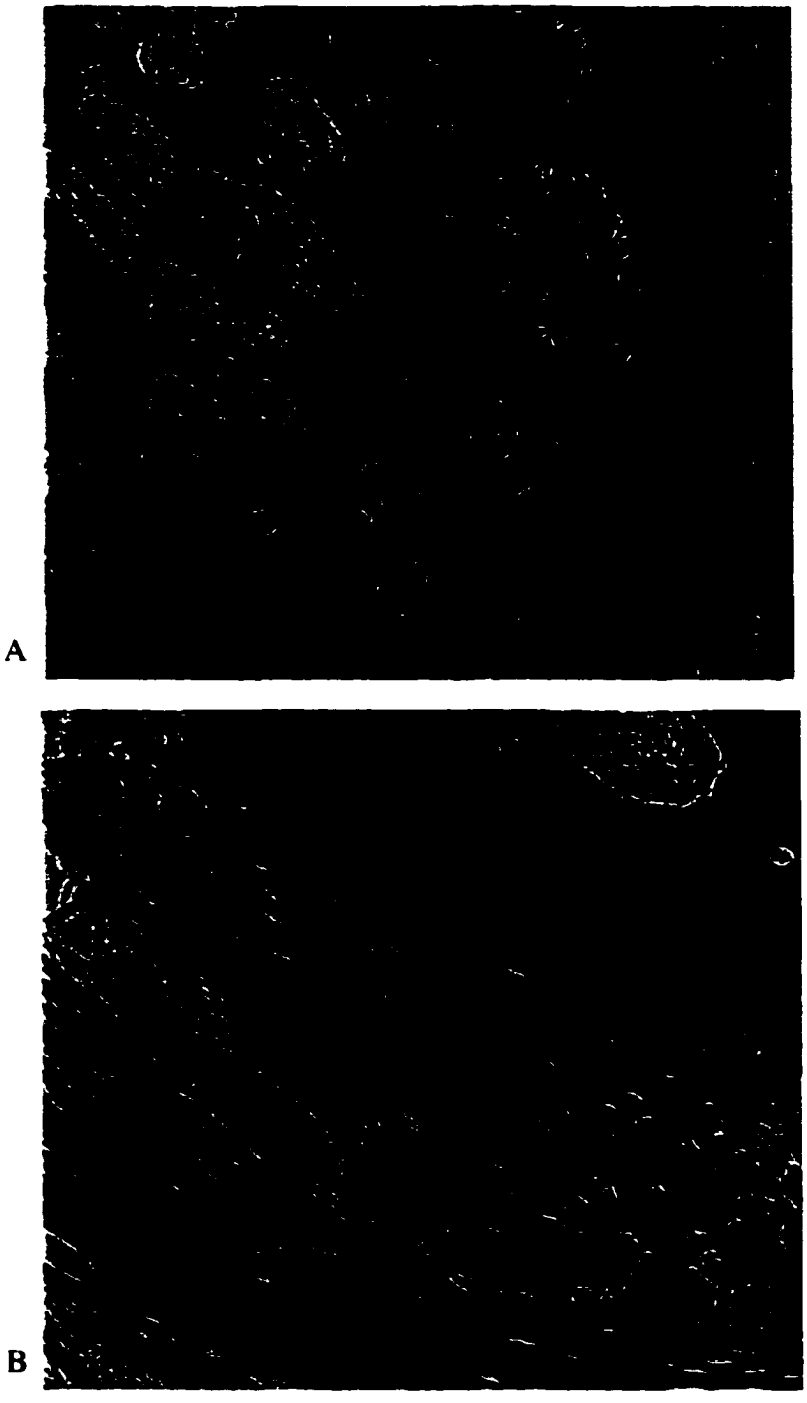

Figure 1. Histological sections illustrating endochondral (A) and intramembranous ossification (B). Endochondral ossification involves cartilage deposition on a fibrous tissue matrix, hypertrophy of chondrocytes, ossification of the cartilage matrix (primary spongiosa), and deposition of woven bone (secondary spongiosa) on the ossified cartilage matrix struts by osteoblasts. Intramembranous bone formation involves direct formation of woven bone without an intermediate cartilaginous stage. Histological sections are taken from rabbit femoral fractures and stained with hematoxylin and eosin. Magnification 200X.

osteoblasts associated with ingrowing vessels (vascular bone).[78] Subsequent to this process the woven bone is remodeled to mature lamellar bone.

The fate of the cells during endochondral ossification has also been a topic of study and may be important in the pathophysiology of impaired healing and represent an area of potential therapeutic intervention. Programmed cell death has been determined to occur in hypertrophic chondrocytes by measuring expression of terminal deoxyuridyl transferase-mediated deoxyuridine triphosphate-biotin nick end label (TUNEL) and using electron microscopy.[73] There is also evidence that hypertrophic chondrocytes begin to express an osteoblastic phenotype.[79] Late hypertrophic chondrocytes at the growth plate begin to express typical bone proteins, such a alkaline phosphatase, osteonectin, osteopontin, BSP, and OC.[80] Bone matrix proteins were also detectable within chondrocytic lacunae of the cartilage remnants soon after vascular invasion, and often before appositional bone had been laid down by the osteoblasts associated with the in growing capillaries. Bone sialoprotein has been identified in the matrix of callus cartilage prior to ossification, suggesting the ability of some chondrocytes to synthesize bone proteins.[81] Other studies[82] have also demonstrated a shared phenotype between chondroblasts and osteoblasts at the junction of cartilaginous and osseous tissue suggesting plasticity in phenotypic differentiation of mesenchymal cells. Specifically, cells with chondrocyte morphology expressed messenger ribonucleic acid (mRNA) for OC and type I collagen, and osteoblastic cells were found to express type II collagen mRNA in addition to expression of their own phenotype. This was a transient finding that diminished with the expression of the expected mRNA.[82]

Asymmetric cell division within chondrocytic lacunae may account for the findings of both chondrocyte death and altered chondrocyte phenotype. The fate of the two daughter cells may be different: one cell dies by apoptosis and another cell replicates and expresses and osteogenic phenotype.[80]

Intramembranous Ossification: Intramembranous ossification involves osteoblastic deposition of woven bone on a fibrous tissue matrix at the same time as vascular ingrowth. As with endochondral ossification, there is an intimate association between blood vessel ingrowth and osteoblastic new bone formation[70] and woven bone is remodeled to form lamellar bone.

Matrix Proteins

The histomorphological changes that occur during both endochondral and intramembranous fracture healing are coupled with a temporal change in the pattern of matrix protein, which is essential for restoring bone function.[75,83-86] The tissue matrix as a whole consists of collagenous and non-collagenous proteins.[84]

Collagenous Proteins

The following section on collagenous proteins will focus on proteins found during fracture healing. Type III collagen is expressed by preosteoblasts and fibroblasts. Granulation and fibrous tissues have predominantly type III and V collagen. Type V collagen, which is associated with type I and III collagen fibrils, is thought to control fibril diameter of these collagens. Type V collagen can also be found in close contact with blood vessels. Cartilage has predominantly type II collagen, but also has type IX, X,

XI collagen. Type IX and XI collagen are found of the surface of collagen fibrils in cartilage and are thought to mediate interactions between collagen molecules and proteoglycans. Type X collagen is associated with hypertrophic chondrocytes. Additionally, type VIII collagen is produced by endothelial cells and is found in periosteum and bone. Osteoid has no type III collagen, and bone is composed predominantly of type I collagen.

Non-collagenous Proteins

Non-collagenous proteins, such as aggrecan, matrix gla protein, biglycan, and decorin are found in cartilage matrix. Osteonectin, OC, osteopontin, thrombospondin, proteoglycan core protein, and osteopontin are found in bone. The following section on non-collagenous proteins will focus on non-collagenous proteins found in bone and those that are important in bone formation.

Osteonectin: Osteonectin is a phosphorylated calcium binding glycoprotein, which binds type I collagen, and has a high affinity for calcium and hydroxyapatite. Osteonectin is thought to be important in bone and cartilage mineralization through binding of mineral to collagen fibers. It is the most abundant non-collagenous organic component of bone and production peaks during the time of matrix ossification.[83] Osteonectin was also detected in proliferating periosteal cells early in fracture healing, suggesting a role in callus formation.[84]

Osteocalcin: Osteocalcin, which is also known as bone gamma-carboxyglutamic acid (gla) protein, is a vitamin-K dependent, gla-containing, bone-specific protein. It is thought to bind calcium and hydroxyapatite, as well as regulate calcium deposition and

hydroxyapatite crystal growth suggesting an important role in matrix mineralization.[83] Osteocalcin is expressed exclusively by osteoblasts and, therefore, is important in bone but not cartilage formation.[85,86]

Osteopontin: Osteopontin, which is also known as BSP, is a sialic acid-rich phosphorylated glycoprotein and is thought to promote attachment of osteoblasts to bone matrix via a class of receptors called integrins. Osteopontin is detected in osteoblasts, osteocytes, and hypertrophic chondrocytes.[85,86]

Other Non-collagenous Proteins: Thrombospondin is another protein found in bone matrix and can bind osteonectin and calcium.[86] Proteoglycan core protein is a structural component of cartilage, and is important in mineralization during endochondral ossification. Fibronectin is found in the immature callus and is important for anchoring matrix proteins and for differentiation of mesenchymal cells to chondral cells. Matrix gla protein is a vitamin-K dependent, gla-containing protein, and is important in cartilage formation and chondrocyte development.

Growth Factors

The changes matrix protein synthesis that are critical to successful fracture healing are controlled by growth factors.[88-90] *In vivo* methodologies that have been used to determine the presence of growth factors at the fracture site include polymerase chain reaction (PCR), *in situ* hybridization, and immunohistochemistry. Each one of these techniques has specific uses. Polymerase chain reaction is important because it can be used to detect very small quantities of mRNA that may not be detected using other techniques, such as *in situ* hybridization. However *in situ* hybridization can be used to

localize the expression of the mRNA to a particular cell type. Messenger RNA expression does not confirm the presence of an active protein; therefore, immunohistochemistry is critical for localizing the presence of a protein to the tissue and cell type. The BMPs are probably one of the most important and most studied growth factors associated with fracture healing.[89,91] Platelet derived growth factor (PDGF), acidic and basic fibroblastic growth factor (a and bFGF), transforming growth factor-beta (TGF-β), insulin-like growth factor (IGF), vascular endothelial growth factor (VEGF) have also been found in association with fractures.[89,91]

Growth factors exert their biological function by binding to the extracellular domain of large cell-surface transmembrane receptors on the target cells. This binding leads to stimulation of the intracellular domain, and secondary signaling then activates specific protein kinases. Protein kinases activate transcription of the growth factor gene into mRNA, which is translated into a growth factor protein.[91]

Growth factors and other cytokines are released from the damaged bone, platelets, inflammatory cells, and undifferentiated mesenchymal cells immediately post fracture. Growth factors that have been found in bone include BMPs, TGF- β, FGF, and IGF.[79,92-94] Platelets produce TGF-β and PDGF; macrophages produce TGF-β, bFGF, PDGF, interleukin-1 (IL-1), tumor necrosis factor (TNF), and prostaglandin E_2 (PGE_2); and T lymphocytes produce IL-1 and –2.[80] These growth factors act in an autocrine, paracrine, and endocrine manner to control cell migration, proliferation, differentiation, and matrix synthesis. The amount and type of growth factor expression varies with the stage of fracture healing.

In vitro fracture healing studies involving growth factors have yielded conflicting results. Growth factor effects are dependent on: concentration, the type and maturity of cells involved, and the presence of other growth factors in the environment. These factors may explain some of the disparate *in vitro* compared to *in vivo* results. There are also most likely numerous growth factors and cytokines not yet identified that are crucial to fracture healing.[95]

Transforming Growth Factor-Beta

The two forms of TGF-β (I and II) are highly conserved and produced by many cells.[98] All cell types also have TGF-β receptors-I, -II, and –III and respond to TGF-β.[98] The effects of TGF-β are dependent on the cell type and stage of differentiation,[97] and its effect on osteoblasts depends on the environment. Transforming growth factor-β is released in latent form and requires activation.[97] Therefore the biological functions of TGF- β are complex.

Transforming growth factor-β is one of the key growth factors associated with fracture healing.[96-101] While TGF-β is expressed by differentiated osteoblasts and chondroblasts, the largest source of TGF-β is in the bone matrix and the highest concentration is in platelets.[98] Transforming growth factor-β is responsible for differentiation, proliferation, and matrix synthesis by osteoblasts and chondrocytes, and it inhibits osteoclasts.[96-100] The expression of TGF-β has been shown to increase during fracture repair.[99] Transforming growth factor-β alters the expression of other growth factors, such as PDGF A and B chains as well as VEGF.[101-103]

Insulin-Like Growth factors

The IGFs, which are also called somatomedins, mediate the growth-promoting actions of growth hormone. The concentration of the IGFs in serum is modulated by growth hormone.[105] The IGFs are also regulated upstream by parathyroid hormone (PTH), glucocorticoids, and prostaglandins. The IGFs act through IGF type I receptors, which are homologous to insulin receptors, and have a wide range of functions on numerous cell types. Expression of IGF-I and –II has been shown to peak 7 days after surgery.[83,89,104,105] Insulin-like growth factor-I and –II are powerful mitogens, promote cell proliferation and matrix synthesis by chondrocytes and osteoblasts, particularly type I collagen, and are also reported to be angiogenic.[83,89,104,105]

Platelet-Derived Growth Factor

Platelet-derived growth factor is either a homo- or heterodimer protein composed of A and B polypeptide chains.[106] There are alpha and beta receptors for PDGF.[106] The alpha receptor is thought to be responsible for cell proliferation and the beta receptor for cell migration. Platelet-derived growth factor is a potent mitogen of cells of mesodermal origin, and is also chemotactic for fibroblasts, monocytes, and osteoblasts. Therefore, PDGF is thought to be important in initiation of healing.[106] Platelet-derived growth factor has been shown to increase expression of *c-myc* and *c-fos* protooncogenes.[108]

Platelet-derived growth factor is important in initiating healing and has been found in all stages of fracture repair.[106-110] It is produced by macrophages, osteoblasts, and platelets (alpha granules), and is stored in bone matrix.[106-110] In normally healing human fractures PDGF was found in the hematoma, presumably released from platelets.

Platelet-derived growth factor-A was found in endothelial and mesenchymal cells in granulation tissue, as well as osteoblasts, chondrocytes (proliferating and hypertrophic), and osteoclasts during later phases of healing. Platelet-derived growth factor-B was found in mesenchymal cells during the inflammatory phase[106] and in osteoblasts at the stage of bone formation.[107]

Fibroblastic Growth Factors

Acidic and basic FGF are also important in fracture healing.[83,89,111,112] They both bind the same receptor and have similar biological activities.[83] Acidic FGF is a potent stimulator of cell division in fibroblasts as well as chondro- and osteoprogenitor cells. Acidic FGF gene expression peaked during chondrogenesis and bFGF was present during all stages of fracture repair.[83,89] Acidic FGF was confined to cells of the cambium layer of the periosteum during the stage of fibrous tissue and cartilage formation,[89] and intracellularly in macrophages, preosteoblasts and immature chondrocytes throughout healing. Basic FGF was found in macrophages in granulation tissue, osteoblasts during intramembranous and endochondral ossification, in the nucleus of immature chondrocytes, the cytoplasm of mature chondrocytes, and in the bone matrix associated with intramembranous ossification.[83,89]

Vascular Endothelial Growth Factor

Vascular endothelial growth factor, a dimeric heparin-binding glycoprotein, is an endothelial cell specific mitogen and chemoattractant, and vascular smooth muscle cell chemoattractant.[102,118] Vascular endothelial growth factor is important for healing various

types of tissues,[119,120] and is associated with capillary development during intramembranous and endochondral ossification in fracture healing[113] and in the growth plate during development.[114-117] Vascular endothelial growth factor has also been shown to increase BMP expression. Expression of VEGF is increased by PGE_1, PGE_2, IGF, PDGF, and vitamin D_3.[102,121-123] It is expressed in normal rat tibia,[121] produced by hypertrophic chondrocytes during endochondral ossification,[116,117] and osteoblasts in response to hypoxia.[124] Serum and local levels of VEGF were found to increase following fracture in humans.[125] In humans with acute fractures a fifteen-fold increase in concentration of VEGF is found in the fracture hematoma compared to circulating serum levels.[125]

Other Factors

Other proteins that are important in fracture healing are the interleukins. For example, Il-1β is thought to play a part in osteoblast differentiation (not proliferation), matrix synthesis, and apoptosis.[126] Matrix metalloproteinase-9 is produced by osteoclasts and important in bone resorption.[127] Matrix metalloproteinase-13 or collagenase-3 was found to be expressed throughout fracture healing and peaked at day 14 coinciding with the peak in callus formation and the transition of collagen gene expression from type II to I. Messenger RNA and protein expression of MMP-13 was found in hypertrophic chondrocytes and immature osteoblasts and was thought to be important in initiation of the cartilage matrix degradation as well as bone remodeling. Because degraded type II collagen during induces vascular endothelial cell migration, the authors concluded that MMP-13 induces vascular invasion into the cartilage matrix during endochondral

ossification.[127] Expression of MMP-13 by immature osteoblasts initiates osteoclastic bone resorption and therefore bone remodeling.[127]

Indian hedgehog (IHH) is a cytokine found in growth plates during embryogenesis and has been identified in prehypertrophic and hypertrophic chondrocytes in the fracture callus, as well as osteoblasts at the endochondral ossification front.[128,129] Indian hedgehog is up regulated by TGF-β and both proteins have similar patterns of expression.[128] Indian hedgehog is a negative regulator of chondrocyte differentiation, and may regulate the number of proliferating chondrocytes and the size of the cartilage callus. Indian hedgehog was also found in bone marrow early in fracture healing, and has been found to promote osteoclastogenesis and bone remodeling, and was therefore thought to be important in the initial stages of fracture repair.[128] Because of the negative control on chondrocyte differentiation as well as its presence early in fracture healing IHH may be implicated in delayed and non-union.[128,129]

Although all cells have complete genomic DNA, only certain genes are expressed in an individual cell. Gene expression is carried out by transcription factors. Transcription factors are the products of other genes such as the proto-oncogenes and their appearance is the common signal of cell activation. Each proto-oncogene contains the instructions for making a protein, such as *c-fos*, *c-jun* and *c-myc*. Proto-oncogenes such as *c-fos*, *c-myc*, and *c-jun* regulate growth and development of cells and organs and act by causing the production of growth factors or by altering the surface receptors of cells.[130-132] Cells in the periosteum, endosteum, surrounding soft tissue, and Haversian canals in bone were positive for *c-jun* and *-myc*.[130] Hypertrophic chondrocytes, which are not capable of proliferation, were not positive. Similarly, *c-fos* was expressed by osteoblasts in the

callus prior to expression of osteoblastic marker genes, suggesting *c-fos* may be associated with osteoblastic differentiation.[131] Mechanical stimulation is thought to be the trigger for production of proto-oncogenes, and was shown *in vivo* to stimulate synthesis of *c-fos*.[132]

Probably the most important growth factors associated with fracture healing are the BMPs. While the other groups of growth factors are obviously important in healing, the BMPs have received the most attention, in part because of their strong osteoinductive capacity.

Physiology of the Bone Morphogenetic Proteins in Fracture Healing

Brief History

The BMPs are the most potent osteoinductive proteins currently recognized. The BMPs were first described by Urist in 1965[133] as the protein in DBM that induces endochondral ossification when deposited in subcutaneous tissue or muscle. When BMP was injected heterotopically the histological changes were identical to the process of endochondral ossification during skeletogenesis and fracture healing.[134] Histological changes included migration of undifferentiated mesenchymal cells to the site of injection, cellular proliferation, production of a cartilage matrix by chondroblasts, hypertrophy of chondrocytes, vascularization of the cartilage matrix by hematopoetic and endothelial cells, and then osteoblasts and osteoclasts caused mineralization and resorption of the cartilage matrix, respectively.[134]

Interestingly, Rosen and coworkers[135] further evaluated the induction of bone formation by the BMPs and found that bone formation did not occur without cartilage

formation (endochondral ossification), a threshold amount of BMP was required to direct cartilage and bone formation, and that the time between new cartilage and new bone formation was dependent on the amount of BMP. The BMPs have become the most studied growth factors with regard to the physiology of fracture healing as well as treatment of impaired healing.[134-158]

Protein Structure

There have been 15 BMPs identified.[134] Bone morphogenetic protein-2 to -9 are members of the TGF-β superfamily based on their amino acid sequence.[136,153] Bone morphogenetic protein-1 is a procollagen-C-proteinase,[136] and BMP 10 to 15 have not been classified.[136,146]

The BMPs are synthesized as large inactive precursor monomers. The molecule is cleaved at a dibasic peptide sequence during secretion, with the approximately 130 amino acid residues at the carboxy terminal being the mature protein.[146] Disulfide-bonded dimerization is also required for the molecule to be activated. There are seven cysteine residues on the carboxy terminal where the disulfide bonds are formed.[136] Dimerization is essential for induction of bone formation.[154]

Mature BMPs are 30 kDa proteins on SDS-PAGE gels and can be reduced to 16 to 20 kDa proteins.[134] The variation in the size of the reduced molecule was attributed to variations in glycosylation. The carboxy terminal is the active portion of the molecule and is highly conserved between the different BMPs. Bone morphogenetic protein-2 and –4 have 92% homology, and BMPs-5, -6, and –7 have 89% homology.[155] While the TGF-βs are secreted in a latent form, the BMPs are not. Hence, mature BMPs are glycosylated

dimers (cysteine disulfide-bridges). Variation in dimerization and glycosylation are thought to affect the activity of the BMPs; however, the importance of this with regard to fracture healing is unknown.

Intracellular Mechanism of Action

The BMPs are responsible for osteoprogenitor cell differentiation into osteoblasts[132] and initiation of intracellular responses that result in mineralization of the matrix.[146] This process is regulated upstream by five proteins: noggin, chordin, gremlin, dan, and cerberus.[153]

The mechanisms of intracellular signaling has been described by Schmitt and coworkers[153] as well as Sakou and coworkers.[146] Briefly, the BMPs act through cell surface heterotetrameric serine/threonine kinase receptors (types IA, IB, and II) and intracellular signaling proteins, namely SMADs (Figure 2).[153] The heterotetrameric receptor complex is required for high-affinity binding of BMPs. While the type II receptors are autophosphorylating (continuously active), it is the type I receptors that are actually required to initiate an intracellular signal. Therefore, when BMP-2, -4, and –7 are bound, the type-II receptor kinase phosphorylates the type I receptor, which initiates intracellular signaling events via the SMADs. SMAD-1 is phosphorylated by the type I receptor and then SMAD-1 and -4 form a heterooligomer which accumulate in the nucleus. SMAD-5 is also activated by BMP-2 and also associates with SMAD-4. SMAD-6 inhibits SMAD-1 by binding to the type I receptor and then competing with SMAD-4 to produce an inactive complex. Additional secondary signally pathways are also thought to modulate the cellular activity.

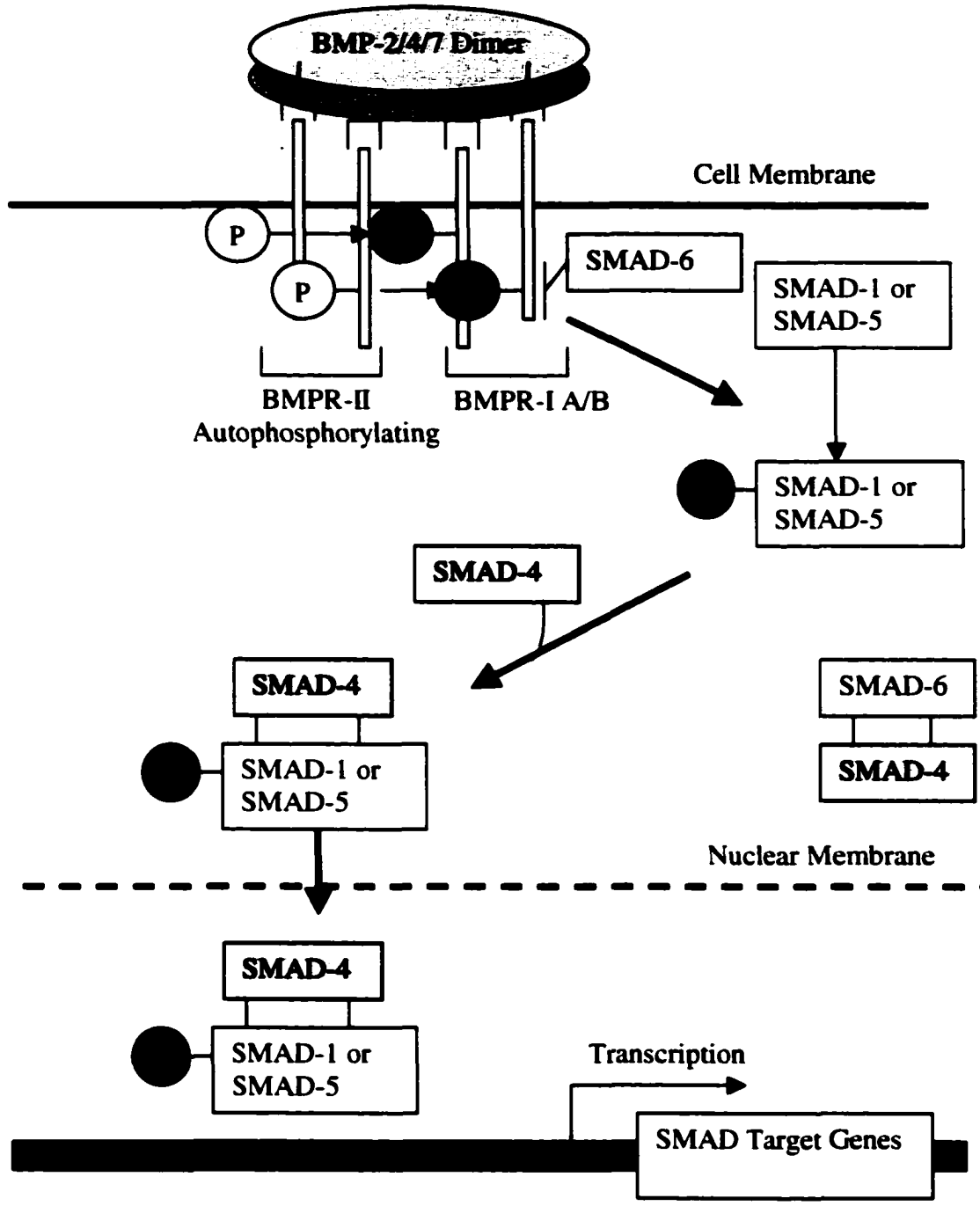

Figure 2. A schematic representation of the basic intracellular signaling mechanism of the BMPs. The active bone morphogenetic protein (BMP) dimer binds with high affinity to the BMP receptor (BMPR)-I and –II heterotetrameric complex. The BMPR are serine/threonine kinase receptors. The BMPR-II is continuously active (autophosphorylating). Following binding of the BMP to the receptors, the BMPR-II phosphorylates (P) BMPR-I, which then phosphorylates either SMAD-1 or SMAD-5 that bind to SMAD-4 and enter the nucleus. SMAD-1 or –5 may bind nuclear elements or proteins and activate gene transcription; alternatively, SMADs may act as transcription factors. Modified from Schmitt and coworkers.[153]

Methods of Measuring the Effects of BMPs

The heterotopic rat model used in the early studies[135] described above has subsequently been used to assess the ability of the purified and recombinant BMPs, other growth factors, as well as transfer of the genes for the BMPs to produce *de novo* bone *in vivo*. However, most of the studies evaluating the function of the BMPs have been performed *in vitro*. The BMPs basically cause undifferentiated mesenchymal cells, including immortalized cell lines and bone marrow cells, to differentiate along the osteoblastic cell lineage.[136] The osteogenic cell phenotype is defined by the production of alkaline phosphatase, the chondrogenic cell phenotype by positive alcian blue staining, and adipocytic phenotype by positive oil red O staining. The morphology of the cells (spindle-shaped fibroblastic versus round chondroblastic), the presence of clumping, and the expression of different collagen types are also used. While *in vitro* studies have been used to evaluate various functions of the different BMPs, the results are often conflicting. The conflicting results may reflect poor simulation of the *in vivo* environment with *in vitro* models.

Biological Function of BMPs

The BMPs are the only proteins capable of *de novo* bone formation,[137] and do not appear to have the pleotrophic effects of other growth factors, specifically TGF-β1 and –β2. These properties are some of the indications that the BMPs are ideal proteins for enhancing fracture healing.[136] While all the details of the mechanism of *de novo* bone formation by the BMPs has not been elucidated, various studies have found different BMPs to induce cell migration, proliferation, and differentiation. A concentration effect

as well as a different effect with different BMPs has been observed.[135] For example, milligram quantities of purified BMP and microgram quantities of recombinant human BMPs (rhBMP) are required to stimulate bone formation *in vivo* as described in Table 2 in the section on "Enhancement of Fracture Healing with Bone Morphogenetic Proteins".

Osteoinduction: The BMPs are principally osteoinductive proteins, that is, they are capable of inducing immature and multipotent stem cells to differentiate along the osteoblastic lineage.[136] Mature cells are not responsive to osteoinduction by the BMPs.[136,138] There are variations in the osteoinductive potency of different BMPs.[136] Heterodimers of the BMPs have been shown to be more osteoinductive than homodimers.[136] The ability of cells to differentiate into chondro- and osteo-progenitor cells is species dependent, with marrow stromal cells, muscle-derived pericytes, and embryonic myoblasts being capable of differentiation in rodents, whereas marrow stromal cells are more inducible in dogs and non-human primates.[138] This is important when considering the use of BMPs to enhance fracture healing in different animal models if it is not the target species.

Osteogenesis: *In vitro* studies comparing the osteogenic or mitogenic ability of the different BMPs, that is, the ability to stimulate cell proliferation, have had variable results, with different BMPs having different osteogenic capabilities.[136] The BMPs are reportedly required in nanogram quantities to be osteogenic *in vitro*.[140] In one study, DNA synthesis, a measure of cell proliferation, increased more after treatment with BMP-2 and –4 than the other BMPs.[140]

Chemotaxis: The BMPs were found to be chemotactic *in vitro* at femptomolar concentrations. Bone morphogenetic proteins-3, -4, and –7 were chemotactic for

monocytes,[141,142] BMP-7 for neutrophils and fibroblasts, and BMP-2 for mature osteoblasts.[143]

Angiogenesis: Whereas most authors have indicated that the target cells of the BMPs are undifferentiated mesenchymal cells, some authors have also proposed that the target cells may be pericytes and that BMP may be angiogenic.[139] The concept that the BMPs are angiogenic was supported by the finding that BMP-7 increased the expression of VEGF *in vitro*.[144] Inhibition of VEGF also reduced the effects of BMP-7 (alkaline phosphatase activity and mineralized nodule formation).[144] The relationship between BMP and VEGF is reflected in the close association of osteoblasts and blood vessels in both endochondral and intramembranous ossification.

Cell Adhesion: In one study, BMP-2 was found to regulate cell adhesion, predominantly by down regulating the $\alpha 3\beta 1$ integrin cell surface receptor at the transcriptional level and inhibiting the adhesion of cells to laminin 5, a protein found on basement membranes, and the ligand for $\alpha 3\beta 1$.[145] Although the exact importance of the latter function is unknown, the authors proposed that it may be important for apoptosis during development and fracture healing in allowing the process of endochondral ossification to progress.

Organogenesis: Although the BMPs are mostly recognized for their importance in skeletogenesis and fracture healing, they are also found in numerous other tissues suggesting a broader organogenic function.[146] The BMPs are homologous to proteins critical to development in arthropods (*Drosophilia* decapentaplegic (Dpp) and 60A) and chordates (Vgl). Interestingly, when Dpp and 60A are injected heterotopically in mammals bone is also formed[147] and BMP can substitute for the developmental proteins

found in *Drosophilia* spp. Therefore, in addition to its effects in multiple tissues in higher vertebrates, it has been highly conserved from animals lower on the phylogenetic scale. Several of the cellular mechanisms of BMP function have been determined as a result of the similarity to proteins in *Drosophilia* spp.

The Localization of BMPs in Normal Bone and During Fracture Healing

Normal Bone Matrix: Bone morphogenetic proteins are stored in the normal bone matrix, which is an important source of BMP in fracture healing. Bone morphogenetic protein is distributed along the collagen fibers in normal bone matrix, and in the cells in the periosteum and along the margin of the marrow cavity.

Fracture Healing: There have been several studies evaluating the expression of the BMPs during fracture healing. In one study evaluating healing in the rabbit mandible BMP-2 was expressed by undifferentiated mesenchymal cells in the fracture hematoma and granulation tissue, and by differentiating osteoblasts and chondroblasts at the stage of intramembranous bone formation and chondrogenesis.[96]

Bone morphogenetic protein-2/4 has been shown to be expressed following fracture.[87] Because of the high homology in the carboxy terminal domain between BMP-2 and -4, these proteins cannot be distinguished using immunohistochemical techniques.[87] Bone morphogenetic protein-2/4 was located in the cambium cell layer of periosteum (intracellular and pericellular) proximal and distal to the fracture site. While there was minimal BMP-2/4 in fracture hematoma, undifferentiated mesenchymal cells produced BMP-2/4. The authors[87] proposed that growth factors at the fracture site in the fracture hematoma (TGF-β or PDGF) might initiate the secretion of the BMPs by the

undifferentiated mesenchymal cells. There was a decrease in BMP-2/4 with increase in maturity of cells and bone. Prechondroblasts showed maximum expression just before becoming chondroblasts, and mature and hypertrophic chondrocytes had less expression. Similarly, osteoblasts lining the calcified cartilage matrix and woven bone also stained intensely for BMP-2/4, however, staining disappeared as lamella bone replaced the woven bone.

Other studies[150-152] have also found BMP-2/4 and -7, as well as, BMP receptor (BMPR)-II in the thickened periosteum at the fracture ends in early bone healing, and later in proliferating chondrocytes and fibroblast-like spindle cells. While BMP-7 disappeared in proliferating and mature chondrocytes later in fracture healing, BMP-2/4 persisted throughout healing. Therefore BMP-7 was thought to act predominantly in the initial phase of endochondral ossification, and BMP-2/4 throughout the fracture healing process. The BMPR-II was also present during intramembranous and endochondral ossification. The BMP-2/4 and –7 were present in the newly formed bone. Interestingly, BMP-2/4 and –7 and BMPR-II were also present in osteoclasts, suggesting that the BMPs are also important for osteoclastic function and bone resorption.

During the remodeling phase of fracture healing, the staining of BMP in the fracture site was found to be similar to that in normal bone.[148,149] This suggests that the BMPs may be less important during this stage of fracture healing.

The results of these studies indicate that BMP-2 is expressed most intensely early in fracture healing and in the undifferentiated mesenchymal cells and less intensely later in healing and in the mature osteoblasts and chondroblasts. This supports the primary role of the BMPs in cell differentiation or osteoinduction.

Transcription is stimulated by carboxy-terminal binding of SMADs to DNA. SMADs either act as transcriptional factors or bind nuclear elements and/or other proteins to stimulate transcription. The carboxy-terminal domain of SMAD-1 is required to activate gene transcription. Schmitt and coworkers[153] hypothesized that the phosphorylated SMADS activate the osteoblast-specific factor-2 (core-binding factor-1) gene. The osteoblast-specific factor-2 protein is related to transcriptional activators and binds to and activates the OC transcriptional promoter region via binding to the osteoblast-specific element-2 sequence. Osteoblast-specific element-2 sequence is also found in promoters of α1(I) collagen, BSP, and osteopontin.[153]

The importance of these regulators in enhancing fracture healing are illustrated by the fact that over expression of SMADS 1 and 5 converts myoblasts to osteoblasts independent of BMP activation.[156] Osteoblast-specific factor-2 can promote differentiation of non-osteoblastic cells into osteoblasts, and expression of BSP, OC, and α1(I) collagen.[157] Therefore, while BMPs are currently being used to successfully enhance fracture healing, regulation of fracture healing may be improved by manipulating proteins at the transcription level.

Protein Purification and Recombinant Protein Production

The BMPs (1 to 3) were initially purified by Wang and coworders.[132] Purification was difficult, however, and only produced microgram quantities. The protein had to be purified 300,000 fold.[134] Purification involves removal of the mineralized part with either an acid (HCl) or chelating agent (EDTA). The BMPs are tightly associated with the remaining matrix and require removal with strong dissociating agents (4M guanidine HCl

or 6M urea).[158] Because of the technical difficulties associated with protein purification as well as the small quantities of protein obtained, Wozney and coworkers[154] produced BMPs as recombinant proteins. Recombinant protein production involved identification and cloning of the bovine genes. the clones were used as probes to identify the human gene sequence. and the complementary DNAs for human BMP were cloned and sequenced from human osteosarcoma cells. The genes were expressed in Chinese hamster ovarian cells and *E. coli* to produce large quantities of the specific BMP.

Comparison of BMP Function

The most important finding from heterotopic injection of BMPs in rats was that while BMP-2, -4, -5, and –7 were all capable of *de novo* bone formation, BMP-2 was the most osteoinductive. When 0.5 μg of rhBMP-2 was injected heterotopically, bone was formed in 14 days and there was more rapid bone formation at higher doses. Recombinant human BMP-4 required a dose twice as high as that of rhBMP-2 to produce the same amount of bone, and rhBMP-5 and –7 were also found to be less osteoinductive.[137] Therefore, BMP-2 is most likely to be the best choice of BMP for enhancing healing in complicated fractures.

PATHOPHYSIOLOGY OF DELAYED- OR NON-UNION

Clinical Causes of Delayed- or Non-Union

By definition, delayed-union occurs when a fracture requires a healing time longer than the average period of time and non-unions do not heal without treatment.[159] Radiographically, non-unions are defined by a lack of bridging callus or defect

ossification and histologically consist of the persistence of either fibrous or cartilaginous tissue in the fracture defect, with variable amounts of new bone formation.[30] Sclerosis of the fragment ends and a mature periosteal callus are reported to be the best indicators of non-unions. Histologically, these fractures have less cellularity and vascularity.[161] Early in fracture healing, non-unions have also been shown to have a persistence of hematoma, where normal healing fractures had hematoma, granulation tissue, fibrous tissue, endochondral ossification, and bone.[30]

While the pathophysiology of non-unions is classified as primary or secondary, they do not appear to be mutually exclusive and in many clinical cases both may apply. Primary or biological non-unions occur when the local conditions for fracture healing are created but the biological mechanisms fail. Secondary or technical non-unions occur because the conditions for fracture healing are not created.[159] While secondary non-union is commonly a result of surgical technique, in some cases of equine as well as human traumatic long-bone fractures it is not possible to create favorable conditions for fracture healing as a result of the initial injury. Subsequently the biological mechanisms fail (primary non-union).

Causes of primary non-union are systemic disease such as old age, chronic disease, and starvation, inadequate regional acceleratory phenomenon, failure to make callus, maldifferentiation of tissue where the defect fills with fibrous tissue and fat, and failure or delay in modeling and remodeling.[159] Primary non-unions also occur in the distal limb where there is less soft tissue and vasculature. It has been proposed that non-union in this region may be attributed to a lack of revascularization of the fracture site.[159] Primary non-unions can also occur following damage to the medullary arterial supply.

Secondary non-unions are associated with the following: infection subsequent to contamination at the initial injury or surgery, poor fracture reduction where the bone ends are not well aligned, bone defects, distraction where the bone ends are too far apart, inadequate immobilization and too much motion, loss of blood supply, and bone necrosis.[159,160]

Non-unions are also classified as hypertrophic or atrophic. Hypertrophic non-unions have an excessive amount of callus which does not bridge the defect, and are usually associated with inadequate stabilization.[30] Atrophic non-unions have almost no callus formation, are considered non-reactive, and have been associated with a lack of blood supply and/or infection.[30]

Excessive Inflammation and Granulation Tissue

While inflammatory cells are critical for debridement of non-viable tissue and debris and initiating the healing response, excessive or prolonged inflammatory response, as a result of too much contamination or infection, is detrimental to healing.[78] Inflammatory cells stimulate fibroblast synthesis of type III collagen and inhibit synthesis of type I collagen. This results in the formation of granulation tissue. Excessive granulation tissue inhibits osteogenesis and impairs fracture healing.[83]

Inflammatory cells are not normally present in association with cartilage and bone formation. The presence of CD4 T-lymphocytes has been associated with the formation of a non-union.[71,72] Other studies have shown that local activation of macrophages at the fracture site induced an immature hypertrophic callus with reduced biomechanical characteristics. Local activation of macrophages during the initial phase of bone repair

impairs healing.[162] This may be a result of increased cytokine production by the T-lymphocytes (IL-1 and –2) and activated macrophages (TGF-β, IL-1, TNF, and PGE_2) with excessive removal of the fibrin meshwork, damage to the endothelium, fibroblasts, and parenchymal cells, and release of growth factors that support fibrous tissue formation. Cytokines released by T-lymphocytes and activated macrophages may also activate osteoclastic resorption of bone. Although PGE_2 has been found to increase cartilage matrix production in callus healing, it may delay callus maturation and reduce the biomechanical strength of bone.[162] Therefore any complication that prolongs the inflammatory response may lead to impaired fracture healing.

Cell Differentiation and Matrix Protein Synthesis

Cell differentiation is crucial in the progressive change in matrix synthesis and consequent mechanical properties of the fracture callus. *In vitro* studies evaluating cells from experimental non-unions in dogs have found that cells from acute (7 days) and chronic (84 days) non-unions were undifferentiated mesenchymal cells and not chondroblasts or osteoblasts.[163] The authors concluded that failure of cells at the fracture site to differentiate was a major part of the pathophysiology of non-unions.[163] Encouragingly, when cells taken from both human clinical and canine experimental non-union were exposed to BMP they had an increase in messenger ribonucleic acid (mRNA) levels for alkaline phosphatase (ALP) and collagen genes, as well as an increase in hyaluronic acid synthesis.[164] This study showed that while cells from non-union are undifferentiated they are still capable of responding to the BMPs.[164] The authors

suggested that BMP may be deficient in non-unions and that BMP may be useful for prevention and treatment of non-unions.[163]

The progressive improvement in the mechanical properties of the fracture callus is associated with an increase in expression of type I collagen genes and decrease in expression of type II and III collagen genes. Non-union fracture callus fibroblasts, and most importantly osteoblasts, on the surfaces of woven bone exhibited expression of type III collagen.[165] Immature osteoblasts secrete type III collagen, but mature osteoblasts should secrete osteoid with no type III collagen. Further, in non-unions, osteoblasts were found to express matrix gla protein. In normal unions, matrix gla protein was absent in osteoblasts on woven bone, but these osteoblasts were positive for osteonectin, osteopontin, and OC.[166] Matrix gla protein has been used as a marker of the chondrogenic lineage, with osteoblasts appearing uniformly negative.[65] Matrix gla protein appears to inhibit mineralization based on experimental studies in mice.[167] Undifferentiated mesenchymal cells and immature osteoblasts that do not proceed through the normal differentiation process are fundamental components of non-unions. The lack of differentiation and maturation cause the formation of a callus that is incapable of restoring bone function. Mechanisms to enhance differentiation of mesenchymal cells, such as use of BMPs, may be important to prevent development of non-unions.

In experimental non-unions, histologically, healing progressed normally until about 3 weeks with an organizing hematoma and periosteal proliferation.[169] However, while cartilage formed on the fracture ends it did not bridge the fracture gap. The cartilage in the fracture gap did not become mineralized and was replaced by fibrous tissue. Type I collagen was found in the periosteal callus; however, there was no type I

collagen found in the center of the defect. Type II collagen was found with cartilage and type III collagen was found in the central area of the defect. These authors[169] concluded that if fracture healing does not heal normally in a defined time period, then fibroblasts, type III collagen, and fibronectin are formed in the gap. Subsequently a fibrous non-union ensues and bone formation is inhibited. Supporting these findings, other studies have found an increase in type III collagen in delayed unions,[170] and Joerring and coworkers[171] as well as Kurdy and coworkers[172] found that human patients with non unions have abnormally high markers of type III collagen in serum.

Cellular activity has also been evaluated in normal and non-unions using proliferating cell nuclear antigen (PCNA) and adenosine triphosphate (ATP) concentrations.[30,31] In normal healing fractures, PCNA was found in immature and mature chondrocytes early in the course of healing,[85,31] and decreased after 3 weeks in normal union with the onset of endochondral ossification.[31] In non-unions, however, PCNA was initially found in immature chondrocytes and disappeared prior to the onset of endochondral ossification. Proliferating cell nuclear antigen was detected in fibroblasts in the fracture defect. Therefore, there was an early decline in the activity of chondrocytes in the defect, but the fibroblasts in non-unions remained active. This was also supported by another study[30] that demonstrated a decrease in ATP in normal healing fractures; however, the non-unions with fibrous tissue in the defect had a persistent elevation in ATP. These studies suggest that a non-union may not be associated with a lack of cellular activity, but activity of inappropriate cells. This supports the theory of poor cellular differentiation or differentiation of cells along an inappropriate cell lineage.

Growth Factors

Because of the integral role that growth factors have in normal fracture healing, the lack of cellular differentiation and failure to synthesize a mature callus in non-unions could be attributed to a lack of growth factors. Brownlow and coworkers,[173] evaluated the presence or absence of TGF-β, PDGF, bFGF, and BMP-2/4 in experimental unions versus non-unions. Unions were fractures that were allowed to heal normally, and healing in non-unions was inhibited by removal of the periosteum and bone marrow adjacent to the defect. At 1 week there was no difference between normal and non-unions in growth factor expression in the fracture hematoma. Non-unions, however, had no granulation tissue in the defect, as well as a lack of periosteum or bone marrow, all of which were important sources of both growth factors and undifferentiated mesenchymal cells. At 8 weeks unions were filled with bone, which expressed growth factors associated with endochondral ossification and remodeling; whereas non-unions had fibrous tissue in the defect and there was no expression of growth factors by fibroblasts. While these authors suggested that the non-union was not associated with a lack of growth factors, this can only be concluded for the fracture hematoma, because the lack of granulation tissue, periosteum, endosteum, and bone marrow caused a lack of both growth factors and cells, which most likely contributed to formation of a non-union.

Blood Supply

Inadequate blood supply is thought to be an important contributing factor in atrophic, but not hypertrophic, non-unions. Hausman and coworkers[174] showed complete inhibition of fracture healing, with formation of an atrophic non-union, when an

angiogenesis inhibitor (TNP-470) was placed in the fracture site of closed femoral fractures in rats. In another study,[175] the tissue in the fracture gap of non-unions was found to be void of vessels early in healing (1 week) which was in contrast to the richly vascularized tissue of normal unions; however, later in healing (8 weeks) the defect of non-unions was well vascularized but the vessels were small and immature. Although hypertrophic non-unions are thought to be associated with excessive motion at the fracture site, and not inadequate blood supply, there was no difference in the vascularity between hypertrophic and atrophic non-unions late in fracture healing and there were trends for atrophic non-unions to have an increase in vascularity compared to hypertrophic non-unions.[161,175,176] Therefore, poor vascularity early in healing may be important in the development of non-unions. Avascularity early in healing may be because of a lack of growth factors to stimulate angiogenesis, or may actually be the cause of the non-union because of a lack of growth factors and cells delivered to the fracture site.

Fracture Stability

The physiology of fracture healing in stabilized and non-stabilized fractures has been evaluated. The mechanical environment alters expression of growth factors as well as differentiation of cells and matrix production. The tissue matrix, and subsequently the cells in the matrix, particularly osteocytes, which have been shown to function as mechanosensors, receives mechanical stress associated with fracture instability. The cells transmit mechanical signals to the cytoskeleton via mechanoreceptors and convert mechanical stress to biochemical reactions.[177] Mechanical stress has been shown to alter

expression of numerous factors including nitric oxide, prostaglandin synthetase, cyclic adenosine monophosphate, *c-fos*, IGF, and BMP-2 and –4.[175] Alterations in pH associated with micromotion[178] as well as the effect of stability facilitating or preventing vascular ingrowth[180] will alter the expression of growth factors, migration and differentiation of cells, and subsequently the type of matrix.

The type of matrix deposited at the fracture site is dependent on the fracture stability. Granulation tissue and fibrous tissue will form with strain up to 100%, cartilage with strain less than approximately 10%, and bone with a strain of less than approximately 2%. Cartilage is not seen after the initial phase of healing if the fracture is stable because rapid mineralization occurs in the hypertrophic cartilage zone when adequate stability is attained and fracture healing proceeds by endochondral ossification.[180] Tissue morphology is in part a reflection of matrix protein and growth factor expression. Type II collagen synthesis depends on the mechanical environment and is only abundant if the healing fracture is unstable. Pre-hypertrophic and hypertrophic chondrocytes expressed IHH during fracture healing and embryogenesis. Indian hedgehog regulates chondrocyte maturation through a feedback loop involving BMP6 and gli3.[180] Expression of type II collagen, IHH, and collagen X were found in unstable but not stable fractures.[180] There was also a lack of BMP-6 and gli3 expression in stable fractures. Interestingly, the callus in stable fractures did not appear to mature or form lamella bone more rapidly than callus in unstable fractures.[180] The authors suggested that, under normal conditions, stable and unstable fractures heal at the same rate but with or without a cartilaginous intermediate.[180] Hypertrophic non-unions are associated with unstable fractures and the molecular changes during the formation of a non-union are

most likely involve alterations in the described process, ultimately resulting in failure to provide enough stability to healing the fracture.

Other Causes of Non-Union

Another important cause of non-union is the encroachment of soft tissue in the defect: this is reportedly one of the most important causes of non-union in humans.[31] One study reported that 30% of human patients having open reduction and internal fixation of fractures had muscle, often necrotic, interposed in the fracture site.[31] In addition to interposition of adjacent soft tissue, maldifferentiation[159] of undifferentiated mesenchymal cells migrating to the fracture site may occur. These maldifferentiated cells proliferate and synthesize matrix more rapidly than bone, filling the defect with fibrous tissue or fat.[159] Another cause of non-union is the formation of sclerotic bone ends resulting from previous osteomyelitis.[159]

PATHOPHYSIOLOGY OF OSTEOMYELITIS

Clinical Causes and Signs of Osteomyelitis

Traumatic musculoskeletal injuries often result in fractures associated with severe trauma to the soft tissues, vasculature, and fracture fragments, as well as heavy bacterial contamination at the time of injury. Furthermore, motion at the fracture site, surgical trauma, use of internal fixation techniques, and a compromised patient predispose the site to infection and osteomyelitis. Although internal reduction and fixation of fractures are commonly used in human and veterinary surgery, and provides the best stability of fracture fragments, it can exacerbate infection.[159] This is in part because of additional

tissue trauma, foreign body implantation, and the formation of a biofilm (bacterial glycocalyx),[159] which can provide a reservoir for bacteria.

Patients with osteomyelitis have clinical signs of redness, swelling, and pain or lameness. Drainage from a traumatic or surgical wound is also common. Radiographically signs of osteomyelitis are bone lysis, proliferation, sclerosis, sequestration, and periosteal thickening and elevation, as well as soft tissue swelling. Histologically there is fibrosis, bone resorption and formation, necrosis, and the presence of inflammatory cells.[182]

Acute Versus Chronic Osteomyelitis

Acute osteomyelitis is a suppurative infection of bone accompanied by edema, vascular congestion, and small-vessel thrombosis. The vascular supply is compromised because of extension of infection into the soft tissues, as well as swelling in a non-distensible structure. Sequestra occur when the medullary and periosteal blood supplies are compromised. Chronic osteomyelitis is the simultaneous presence of organisms, necrotic bone, and compromised soft tissue.[181] Osteomyelitis is considered chronic when signs have lasted for 4-6 weeks, previous treatment has been instituted, or when it follows open fractures or surgery.

The presence of bacteria alone is not adequate to establish osteomyelitis. Establishment of osteomyelitis is dependent on both the number and virulence of inoculating bacteria as well as local and systemic host factors. There have been several reviews of the pathophysiology of osteomyelitis.[62,159,181-188]

Local Trauma and Implants

Trauma has been shown to delay the inflammatory response and depress cell mediated immunity[62,184] by impairing the function of neutrophils, including chemotaxis and superoxide production, and increasing the numbers of T-lymphocyte suppressor cells leading to progression of the infection. Chronic osteomyelitis, once established, also decreases chemotaxis, immunoglobulin concentration, and the number of T-lymphocytes. The metals used in implants have been found to inhibit lymphocyte proliferation and cytokine production.[61,183] Therefore the combination of trauma associated with the injury and surgery, as well as the presence of implants, impair the local immune response. This facilitates the formation and persistence of osteomyelitis and infected non-union.

Fracture Stability

Fracture instability has also been shown to increase infection rate with one study[189] reporting a 35% infection rate in stable and 71% infection rate in unstable fractures. The increase in infection rate in unstable fractures is most likely a result of an increase in damage to the fractured bone, dead space, hematoma formation, and tissue necrosis, as well as a decrease in revascularization, which lead to impairment of local humoral and cellular immunity.[189]

Bacterial Adherence

Implants

Following inoculation of the fracture site, the bacteria adhere to either damaged bone and/or implants. Foreign body surfaces acquire a glycoproteinaceous film composed

mainly of fibronectin when implanted. The glycoproteinaceous film is anionic and initially repels the anionic bacteria. However, van der Waals forces and the presence of hydrophobic molecules on both the film and bacteria allow bacteria to maintain close proximity to the implants and form irreversible attachments to the fibronectin.[184] The surface area as well as the biocompatibility of the implants are critical in bacterial adherence.[60] The modification of implant surfaces is a separate area of research[184] and will not be covered in this review.

Bone

Bacteria are also capable of attachment to bone. Normal bone is relatively resistant to infection as discussed in the section on "Osteomyelitis Models". Necrotic bone, however, was found to be more important in the development of osteomyelitis than the presence of an inoculated hematoma with associated dead space.[185] Interestingly, some strains of bacteria more readily adhere to bone than to metallic implants. In this situation the inoculation dose required to establish osteomyelitis is lower in the absence of an implant because of the increased amount of exposed bone.[186] Removal of the periosteum and bone necrosis provide an acellular surface with exposed collagenous and non-collagenous proteins for bacteria to bind.[184] For example, many bacteria have receptors to type I and II collagen as well as other proteins such as elastin and laminin that are exposed as a result of injury or surgical trauma to bone and other tissues.[62,183,187] *Staphylococcus aureus*, in particular, has numerous cell surface receptors that bind BSP. Many bacteria, including *S. aureus*, are capable of binding to fibronectin which covers damaged bone soon after injury. Bone also lacks the surface defenses that are present on

tissues covered by cutaneous and mucosal surfaces, making damaged bone and implants essentially inanimate objects that resemble surfaces to which bacteria naturally adhere.[184]

Following adhesion of bacteria to either the implant or bone, some bacteria secrete a biofilm. The biofilm forms strong bonds with glycoproteins of tissue,[62] and facilitates evasion of the host immunity and antimicrobial therapy. The bacteria proliferate and an infection becomes established. Both the host immune response and bacterial toxins and enzymes are responsible for the development of osteomyelitis.

Inflammatory and Immune Response

Following bacterial inoculation inflammatory and immune responses are elicited by the host. The presence of bacteria initiates both the complement cascade as well as a specific humoral and cell-mediated immune response.[182] Complement activation ultimately leads to bacterial lysis, which causes further release of bacterial toxins and enzymes. Bacteria release toxins and enzymes to cause host cellular and tissue destruction. Host cell death, in particular neutrophils and macrophages, result in release of proteins, enzymes, and peptides such as histamine, seratonin, and bradykinin, which cause vasodilation, increased vascular permeability, and pain. The combination of proteins released as a consequence of host cell death and complement activation causes chemotaxis and diapedesis of neutrophils and monocytes. Monocytes become tissue macrophages. Neutrophils and macrophages phagocytose bacteria, particularly bacteria that have been opsonized by compliment. Macrophages present antigens from ingested bacteria to T- and B-lymphocytes, which then elicit a more specific cellular and humoral immune response, respectively. In addition cytokines, including interleukins, interferon,

and tumor necrosis factor are released by macrophages which stimulate T- and B-lymphocytes.[62] The accumulation of proteinaceous material, bacterial and cellular debris, as well as neutrophils and macrophages result in formation of a purulent exudate.

The exudate produced from the inflammatory response initially accumulates and in the bone marrow, and then extends into the Haversian and Volkmann canals. Accumulation of exudate in the bone marrow causes infarction of marrow fat and hematopoetic cells.[62] The extension of exudate into the Haversian canals causes avascular necrosis of osteocytes adjacent to the canal and in the Volkmann canals may cause sequestration of the periosteal and endosteal surfaces.[188]

The exudate may reach the subperiosteal space via the Haversian and Volkmann canals and either elevate the periosteum causing avascular necrosis of the underlying bone (young animals and humans) or enter the adjacent soft tissue and create a soft tissue abscess and drainage (cloaca; older animals and humans). A proliferative response occurs in the periosteum and viable bone adjacent to necrotic bone (involucrum). Soft tissue infection and abscessation further compromise the blood supply to the bone. The ultimate result is accumulation of necrotic bone, inflammatory cells, fibrosis, as well as a host bone response, which may be periosteal proliferation or the formation of an involucrum.

Bone Necrosis and Resorption

While vascular occlusion from accumulation of exudate is a one cause of bone necrosis, there are also numerous other key factors which lead to bone necrosis and resorption. Bacterial toxins and enzymes (phosphatases, proteases, and hyaluronidases) may both inhibit bone formation and cause tissue necrosis as outline in the section on

"Osteomyelitis Models". The exact role of all factors involved has not been elucidated.[190] Lipopolysaccharide of gram negative bacteria and surface associated protein of *S. aureus* have been associated with bone resorption.[62,190]

An oxidative burst accompanies neutrophil activation, with consequent degranulation of neutrophils. While these enzymes are supposed to be directed against bacteria, they also degrade bone. Enzymes released from inflammatory cells include collagenase and gelatinase which degrade type I collagen, fibronectin, laminin, and denatured proteoglycans; and elastase which degrades terminal non-helical cross linking peptides of type I collagen.[190] In addition, lysosomal enzymes released from neutrophils and macrophages also cause bone necrosis.[159] Macrophages are also capable of mobilizing calcium and hydroxyproline and causing bone resorption directly.[190]

Most authors agree that bacterially induced cytokine release is an important cause of bone resorption.[62,183,190] Cytokines associated with bone resorption are IL-1β, IL-6, and TNF-α. Lymphotoxin, IL-1, and TNFα are considered osteoclast-activating factors.[183] Metabolites of arachidonic acid, such as prostaglandin E_2, are also thought to increase osteoclastic activity.[183]

Osteoclasts are multinucleated giant cells derived from hematopoetic tissue, and are the only cells capable of bone resorption.[191] With the appropriate stimulus osteoclasts attach to bone, form a sealing zone which encompasses the Howship's lacuna, and forms a secretory ruffled border.[191] Hydroxyapatite dissolution is brought about by the release of acid into the Howship's lacunae. Acid is produced by an ATPase proton pump, with generation of protons by carbonic anhydrase II.[191] Matrix proteins are degraded through

the action of cysteine proteinases, matrix metalloproteinases, serine proteinases, and phosphatases, such as tartrate-resistant acid phosphatase.[191]

Osteoblasts are also thought to be critical in regulating osteoclastic bone resorption.[191] Osteoblasts are thought to release an "osteoclast-activating factor" in response to activators of bone resorption.[191] Osteoblasts have receptors for prostaglandin E_2 and IL-1, and produce collagenase.[190] Tumor necrosis factor, for example, is thought to exert its effect by stimulating osteoblasts to activate osteoclasts via IL-6.[183] Osteoblasts are also reported to secrete proteolytic enzymes that degrade osteoid.[191]

Infected Non-Union

Chronic osteomyelitis associated with fractures develops as result of the presence of necrotic bone, implants, as well as characteristics of some bacteria, such as *S. aureus*, that can survive intracellularly and acquire a slow metabolic rate (small colony variants) avoiding the host immune response, being resistant to antimicrobials, and often avoiding detection on tissue culture. The presence of cytokines causing bone resorption, the continued presence of necrotic bone, as well as sclerotic bone ends inhibits fracture healing. Recently, extracts of *S. aureus* and *S. epidermis* caused decrease in bone matrix formation *in vitro*.[192]

The result of the combination of factors mentioned under the section of "Pathophysiology of Delayed- and Non-Union" as well as chronic osteomyelitis is an infected non-union. Infected non-unions in human and veterinary patients are expensive, challenging, and ultimately frustrating to treat, and cases often result in amputation of the

affected limb or euthanasia of the animal at a physical, mental, and emotional cost to the affected individual.

TREATMENT OF NON-UNION AND INFECTED NON-UNION

Basic Principles and Conventional Treatment

Non-Union

Currently, the basic principles of treatment of non-union are fracture stabilization (intramedullary nail or bone plate with cortical screws), debridement of sclerotic or fibrotic tissue, and the use of a bone graft. Most recently, Devnani[193] reported the successful treatment of 25 patients with non-unions of long-bones by debriding the bone ends, opening the medullary canal, stabilizing the fracture with bone plate and cortical screws, and using autogenous cancellous bone graft (ACG) at the fracture site. All of these patients healed the non-union in 18 weeks.[193]

Infected Non-Union

While the treatment of bone infection has come a long way since "the application of burning wood (1500 to 800 BC), iodine pellet fillings, and a mixture of antibiotic and whipped blood"[194] management of infected non-union is still one of the greatest challenges to both human and veterinary orthopedic surgeons. The basic principles of treating an infected non-union are debridement of necrotic soft tissue and bone, removal of implants, fracture stabilization usually with an external skeletal fixator, obliteration of dead space, wound irrigation and drainage, bone grafting, soft tissue coverage, and the use of both local and systemic antibiotics based on results of culture and

sensitivity.[188,194,195] The success of treating osteomyelitis in human patients is between approximately 60 and 90%,[194] which is markedly higher than the success in equine patients, most likely as a result of the economic constraints and complications associated with treatment in horses.

Antimicrobial Delivery

Systemic delivery of antimicrobials alone is often ineffective in treating osteomyelitis because the antimicrobial is unable to reach the site of infection. The topic of local antimicrobial delivery to the site of osteomyelitis is a large and rapidly expanding area of research and has been reviewed by Rudd[188] and Dernell.[195] In summary, recent developments in prevention and treatment of bone infection include local and sustained delivery of antimicrobials in synthetic polymers and antimicrobial-coated implants. Materials used for local delivery have included polymethylmethacrylate (PMMA), polylactic acid (PLA), copolymers of polylactic acid and polyglycolide (PGLA), polyanhydrides, plaster of paris (calcium sulfate), hydroxyapatite, and collagen.[195] The use of antibiotic-impregnated PMMA was used successfully in open fractures in horses.[196] Regional limb perfusion, either via intravenous or intramedullary route, is another method of antimicrobial delivery used to obtain high concentrations of antibiotics at the site of infection.[188,195] Regional limb perfusion has also been used successfully to treat clinical cases of osteomyelitis in horses.[197] In addition to resolving the infection, novel methods to enhance fracture healing in the presence of infection or osteomyelitis are required.

Bone Graft

Bone grafting is the mainstay of treatment for non-union and infected non-union. The benefits of bone graft were initially realized in the late 19th century by Senn[198] who found an acceleration of bone healing in patients with osteomyelitis treated with bone graft.

Bone grafts may be autogenic, allogenic, or xenogenic. Allogenic and xenogenic bone grafts are not biologically active, have minimal osteoinductive capacity, a high rate of resorption, inferior revascularization, are at risk of becoming infected, and may induce an immune response that can delay fracture healing.[199] There is also the risk of disease transmission with allogenic and xenogenic grafts.[200] Autogenic bone graft (cancellous and corticocancellous), on the other hand, is the most effective substance for stimulating fracture healing, and is currently the gold standard to which all other methods of osteoinduction, osteogenesis, and osteoconduction are compared. Cancellous bone grafts are biocompatible and provide both pluripotent osteogenic cells as well as numerous growth factors. Autogenic bone graft was superior to both allogenic bone and DBM for enhancing fracture healing,[201] as a result of immunity and infection, which delayed healing in the allogenic bone grafts and DBM.

Autogenous cancellous bone graft is the ideal treatment for enhancing fracture healing, because of a potential for an 80 to 90% success rate.[202-204] There are several limitations, however, associated with the donor site. Problems with donor site morbidity including pain, local infection, hypersensitivity, paresthesias, or anesthesia of the buttocks occur in 6 to 20% of patients, and 3 to 9% of patients have major complications,[205,206] for an average of 5 years after surgery.[207] Excessive blood loss from

the donor site at the time of surgery is not uncommon. Further, there is limited supply of ACG in both small animals and children as well as in adults requiring repeat grafting. Autogenous cancellous graft was also found to increase infection at the fracture site in one experimental study.[186] The proposed cause of the increase in infection rate in this study was an increase in adherence of bacteria to the bone in the graft.[186] Although some authors have reported a good success rate with ACG,[202-204] other authors have reported failure rates of up to 30% in cases of segmental bone defects.[208-211]

Conversely, autogenous bone marrow is also osteoinductive, but less invasive to harvest, and has been used successfully to enhance fracture healing.[212] The problems with the use of autogenous bone marrow include rapid diffusion from the fracture site and low numbers of chondrogenic or osteogenic cells within the marrow.[212] While bone marrow enriched in undifferentiated mesenchymal cells, also called bone marrow stromal cells, has shown some clinical applicability,[212] this methodology is technically difficult and time consuming.

While bone graft substitutes including DBM, hydroxyapatite, tricalcium phosphate, and other ceramic materials have been developed, these materials are only osteoconductive and do not have the osteoinductive and osteogenic properties of ACG, they induce a foreign body response, lower the inoculation dose required to establish infection, and in some cases may actually inhibit bone healing.

Other Methods to Enhance Fracture Healing

Methods to enhance fracture healing have been recently reviewed by Einhorn.[213] Ultrasound, electromagnetic, and mechanical stimulation have been used to enhance

fracture healing. Although these methods of mechanical stimulation may have shown improvements in healing, these treatment modality have not had widespread acceptance because none of these methods have provided rapid and reliable treatment to manage pain, loss of function, or morbidity associated with impaired fracture healing.[5] Further, there is evidence that the most likely mechanism of action is through stimulation of various growth factors.[214-217] including BMP-2 and -4,[217] and angiogenic growth factors such as VEGF.[216] Therefore, direct use of these growth factors at the fracture site should be a better way to enhance fracture healing.

Growth Factors

Growth factors that are important in fracture healing are TGF-β, FGF, PDGF, IGF, and the BMPs.

Transforming Growth Factor-Beta

Exogenous administration of TGF-β increased the strength of long-bone fractures in the rat[218,219] and accelerated healing of CSDs in long-bones.[219-221] Subperiosteal injections of TGF-β into the non-fractured rat femur resulted in mesenchymal cell proliferation and initiation of chondrogenesis and intramembranous bone formation.[100] The cartilage mass increased until TGF-β injections were discontinued and the bone remodeled resulting in thickened cortical bone. While these studies would suggest that TGF-β would be a useful growth factor for enhancing healing of non-unions and infected non-unions, this thought is not uniformly accepted.[224-228]

In general, the effects of TGF-β on bone healing are not as favorable as other growth factors, such as the BMPs.[224] Firstly, the biological effects of TGF-β on cell proliferation and matrix synthesis depends on the cell type, cell density, and culture conditions.[225] Secondly, TGF-β isoforms are ineffective in initiating bone formation in the extra skeletal sites, that is, they are incapable of *de novo* bone formation,[226] and TGF-β has been shown to actually inhibit mineralization of extracellular matrix.[98] Finally, there have been other studies to show that TGF-β did not significantly enhance healing of chronic non-unions, and did not result in a synergistic response when used in combination with BMP-2.[227,228] Therefore, the conclusions were that TGF-β was inferior to BMP-2 for enhancing fracture healing.[228]

Fibroblastic Growth Factor

While the FGFs are important in the physiological process of fracture healing, when aFGF was injected into the soft callus during early chondrogenesis it resulted in increased cartilage in the callus and delayed endochondral ossification; that is, it stimulated chondrocyte proliferation but delayed maturation.[112] Further, although the FGFs stimulate DNA synthesis and cell replication in a number of mesodermal tissues, they may actually inhibit fibrous tissue formation, and synthesis of collagens and proteoglycans,[104] as well as endochondral ossification.[111,112] Therefore, the use of FGFs may actually be contraindicated in fracture healing.

Platelet-Derived Growth Factor

When placed in tibial osteotomies in rabbits PDGF enhanced intramembranous bone formation.[109] In another study, injection of suramin, which inhibits PDGF, reduced intramembranous bone formation.[229,230] Subperiosteal injection of PDGF stimulated mesenchymal proliferation in the cambial layer of the periosteum, intramembranous ossification, and the formation of bone.[88] The bone was remodeled and the final result was a thickened cortex.[88] Although PDGF enhanced mitosis of osteoblasts[110] and intramembranous bone formation,[109] it may also increase fibroblast proliferation and fibrous tissue formation, increase collagen degradation,[110] and inhibited chondrogenesis.[110] Therefore, although PDGF is important in fracture healing, the inhibition of chondrogenesis and the fact that it is unable to facilitate all phases of fracture healing and create bone *de novo* signify that PDGF is unlikely to be useful for therapeutic enhancement of fracture healing.

Insulin-Like Growth Factor

Some authors have suggested that IGF-I and –II may be useful to enhance fracture healing because of their presence at the fracture site[231] and their ability to increase bone turnover in patients with low bone mineral density. However, local application of IGF-I to the fracture did not enhance healing.[232]

In summary, based on these studies as well as the effects of these growth factors in the physiology of fracture healing, the use of TGF-β, FGF, PDGF, and IGF to enhance fracture healing are either contraindicated or would not result in as favorable results as use of the BMPs.

ENHANCEMENT OF FRACTURE HEALING WITH BONE MORPHOGENETIC PROTEINS

Recombinant Proteins

Recombinant BMPs have been evaluated for enhancing healing in long-bone fractures,[25,26,33,34,36,233-252] spinal fusion, bone formation in periodontal disease, reattachment of soft tissues to bone, prostheses, bone defects from neoplasia or craniotomy, and craniomaxillofacial reconstruction.[253-255] Additionally, BMP-2 has been shown to enhance healing of allografts[235] as well as induce bone formation in irradiated tissue.[256] The volume of research in these areas is extensive; therefore, the focus of information on bone healing with recombinant BMPs in this thesis will be mainly on long-bone fractures.

In Vitro *Studies*

Purified and recombinant BMPs, including BMP-2, -3, -4, and -7 have been shown to increase cell proliferation, collagen and proteoglycan synthesis, alkaline phosphatase (ALP) activity, and OC production in a variety of bone-derived cells *in vitro*. Both ALP and OC are important because they are indicators of the osteoblastic phenotype suggesting a potential role for BMPs in cell differentiation.[225]

Experimental Studies

There have been numerous studies demonstrating successful use of different BMPs for enhancing fracture healing (Table 2). Both non-union and fracture healing (union) models have been used. These studies have all demonstrated an increase in the

rate or amount of radiographic and histological healing, and biomechanical strength of the healed tissue. Healing in large animal non-union models generally occurs within 12 weeks with rBMPs.[25,242] with signs of new bone formation occurring as early as 4 weeks.[239] In fracture healing models, the benefit of the BMPs appears to occur early in fracture healing. For example, BMP-7 was shown to increase stiffness and strength and the amount of lamellar bone at 2 weeks whereas there was no difference between treated and control animals at 4 weeks.[237] This is probably a result of a combination of fracture healing being at a biological optimum in these models, the main effect of BMP being on differentiation of undifferentiated mesenchymal cells, and early release of BMP from the carrier matrix.

Because ACG is the gold standard for enhancing fracture healing, treatment with rBMP in a carrier matrix is often compared to treatment with bone graft. Gerhart and coworkers[242] found that defects treated with either rhBMP-2 or ACG healed in the 12-week period and there was no difference in mechanical testing between the two groups. While both autogenous corticocancellous bone graft and recombinant bovine BMP (rbBMP: 100mg) had similar amounts of bone formation and bone union was achieved in both groups at 12 weeks, the rhBMP-treated dogs developed fibrocartilage during the process of healing and had lamella bone whereas the grafted dogs had woven bone.[25] Biomechanical analysis was not performed in the latter study, and the authors rationalized that rbBMP treated animals would have had an increase in strength because of the increase in lamellar bone.

Table 2. Studies evaluating BMPs for enhancing healing of long-bone fractures.

Author	Model[1]	Dose (μg)	BMP[2]	Carrier	Response
Nilsson et al 1986[25]	Dog/ ulna/25	$100x10^3$	bBMP	Protein	Union
Heckman et al 1991[26]	Dog/ radius/3	$15x10^3$	cBMP c/bBMP	PLA BDBM/PLA	Union NS
Yasko et al 1992[34]	Rat/ femur/5	1.4/11	rhBMP-2	DBM	Dose Effect
Stevenson et al 1994[234]	Rat/ femur/8	100	BMP-3	HA/TCA	Union
Gerhart et al 1993[242]	Sheep/ femur/25	1.5×10^3	rhBMP-2	SDBM	Union
Cook et al 1994[240]	Rabbit/ ulna/15	3-400	rhBMP-7	RDBM	Union
Cook et al 1994[241]	Dog/ ulna/25	0.625/1.2/ $2x10^3$	rhBMP-7	BDBM	Union Dose Effect
Lee et al 1994[246]	Rat/ femur/5	0.93/3.1/ 9.3	rhBMP-2	PLGA (small/large)	Dose Effect
Cook et al 1995[33]	Primate/ Ulna/Tibia/20	0.25- $2x10^3$	rhBMP-7	BCOL	Union
Kirker-Head et al 1995[243]	Sheep/ femur/25	$1.5x10^3$	rhBMP-2	SDBM	Union
Bostrom et al 1996[36]	Rabbit/ ulna/20	20-300	rhBMP-2	PLGA	Dose Effect
Zegzula et al 1997[236]	Rabbit/ radius/20	17/35/70	rhBMP-2	PLA	Dose Effect
Welch et al 1998[238]	Goat/tibia/ fracture	860	rhBMP-2	COL Sponge; Wrap/ Onlay	↑ Bone
Heckman et al 1999[227]	Dog/ radius/3	$1.5x10^3$ $15x10^3$	cBMP	PLGA	↑ Bone
Ohura et al 1999[239]	Rat/ Femur/5	1.26/6.28	rhBMP-2	TCP-MCPM	Dose Effect
Bax et al 1999[245]	Rabbit/tibia/ 0.5 Unstable	120	rhBMP-2	Injected	Increased healing
	Stable/Unstable	54/360	rhBMP-2	PLGA/ COL gel	Delayed/NS
Blokhuis et al 2001[237]	Goat/tibia/ Fracture	1000	rhBMP-7	Injected/COL	Union
Bouxsein et al 2001[244]	Rabbit/ulna/ 0.5-1.0	40	rhBMP-2	COL	Union

rh=recombinant human, c=canine, b=bovine, PLA=polylactic acid, PLGA=copolymer polylactic/polyglycolic acid, DBM= demineralized bone matrix (inactive), COL=collagen. NS=no significant effect, Dose Effect= there was an increase in fracture healing with an increase in BMP. 1. Species, bone, defect size (mm), 2. BMP is purified protein and the type of BMP was not specified by the authors.

In a study using an ulnar and tibial non-union model in non-human primates, although both tibia treated with BMP-7 and ACG healed, the BMP-7 treated animals healed sooner, were stronger, and had more mature bone (lamella bone with marrow) by 20 weeks compared to the ACG treated tibia.[33] The BMP-7 treated animals had biomechanical strength that was not significantly different from the contralateral limb and both BMP-7 treated tibia and the contralateral limb failed by comminution.[33] In the latter study, however, the ulna did not heal with ACG and a fibrous non-union developed, whereas the ulnas treated with BMP-7 healed. Therefore, fractures treated with rhBMP heal at a similar rate to fractures treated with bone graft, the advantage of the recombinant protein being a lack of donor site morbidity. As pointed out by one author,[243] while the dose of rhBMP-2 used was 25,000-times the dose in bone graft (1.5 mg versus 0.06 μg) bone graft has numerous growth factors as well as osteoprogenitor cells which would further enhance fracture healing.[242,243]

Clinical Studies

The first human clinical studies evaluating the use of purified human BMP protein were performed by Johnson and coworkers.[247-249] The BMP was delivered with other noncollagenous proteins in various carrier matrices (Table 3). Patients in these studies had femoral and tibial non-unions, and had had several previous surgeries with internal fixation and bone grafting indicating that there was an established non-union. While most patients healed, there was one patient with an infection at the fracture site that did not heal. Although these studies demonstrate the potential use of BMPs for enhancing healing in clinical cases, the studies were not controlled prospective blinded clinical

Table 3. Studies on the evaluation of BMP in clinical cases of non-union

Author	Species	No[1]	Site	Dose (mg)	BMP	Carrier	Time to union[2] (Mo; No)
Friedlander et al 2001[5]	Human	63	Tibia	3.5/ 7.0	rhBMP-7	COL (1or2g)	9; c.80%
Bulstra et al 1999[250]	Human	24	Fibula	2.5	rhBMP-7	COL (1g)	12; 96%
Johnson et al 1998[249]	Human	15	Femur	100	hBMP/ NCP	AAA (8g)	5.6; 100%
Johnson et al 1992[248]	Human	25	Femur, tibia, humerus	100	hBMP/ NCP	AAA (6.6g)	6; 96%
Johnson et al 1990[247]	Human	4	Tibia	50-100	hBMP/ NCP	PLGA, GEL, AAA	4.4; 100%
Itoh et al 1998[251]	Dog	1	Femur	0.26	rhBMP-2	PLGA/ GS	9; NA
Meng-Hai et al 1996[252]	Dog	17	Femur	50	bBMP	Plaster of Paris (1g)	5.7; 94%

AAA=allogeneic antigen extracted autolyzed human bone, COL=type I collagen, PLGA=copolymer of polylactic and polyglycolic acid, GS=gelatin sponge, GEL=absorbable gelatin, NCP=noncollagenous protein, NA=not applicable because there is only one animal, c=circa or approximately. 1. Number of patients, 2. Average months to union or time to which union was achieved; the percentage of patients with bone union.

trials. Therefore, the real benefit of rhBMP compared to conventional treatment is unknown.

Recently, a prospective human clinical trial was performed in 122 patients with tibial non-unions using rhBMP-7 in a type-1 collagen carrier matrix (Novos, Stryker Biotech, Natick MA).[5] Patients were treated with either ACG or rhBMP-7. There was a trend for patients treated with ACG to have an increase in duration of hospitalization, surgery time, and blood loss from the donor site during surgery. Additionally, all of the patients had donor site pain, which was most often described as moderate to severe, and 13% of patients had donor site pain that persisted to 12 months after surgery. The incidence of infection at the fracture site was significantly lower in patients receiving rhBMP-7 compared to bone graft (21 versus 3%). There were 81% of patients in the rhBMP-7 and 85% of patients in the ACG groups that developed union at 9 months; the difference was not statistically significant. There were 5% of patients that had antibodies to the carrier and 10% to the rhBMP-7; however, this was not reported to affect healing.

Bulstra and coworkers[250] also reported successful healing of fibular ostectomies, which were created following tibial osteotomy for osteoarthritis of the femorotibial joint. Patients treated with rhBMP-7 in a collagen matrix (Novos, Stryker Biotech) had an increase in healing that was not significantly different from patients treated with DBM, but was superior to controls treated with the collagen matrix alone. Patients had new bone formation at 6 weeks and bridging callus at 1 year. Interestingly, patients treated with DBM had centrally healing defects, whereas patients treated with BMP-7 had bone formation that started medially or laterally at the external borders of the defect. While the patients in the BMP-7 treated groups appeared subjectively to have earlier callus

formation. those treated with DBM had denser bone. Similar to the study by Friedlaender and coworkers[5] there were a few patients with an anticollagen reaction that did not appear to delay healing. Interestingly, patients in the BMP-7 treated group had an increase in pain at the ostectomy site compared to patients treated with DBM or the collagen carrier only.[250]

The BMPs have also been used clinically in veterinary patients. Bone morphogenetic protein-2 in a poly D, L lactic-co-glycolic acid (PGLA) and gelatin sponge complex was used successfully to treat a persistent femoral non-union in a dog.[251] Callus formation was observed at 2 weeks and radiographic union at 8 weeks. Additionally bovine BMP in plaster of paris was used successfully to treat 17 persistent non-unions in dogs (total dose of BMP 80-200mg).[252]

Protein Purity and Species Specificity

The greater the protein purity the lower the dose of BMP that is required.[240] For example, defect healing with 6.25μg of rhBMP-7 was equivalent to 250μg of purified bovine BMP-7 in a rabbit ulnar non-union model.[240] Although species specificity in lower vertebrates appears not to be problematic, in a canine non-union model bovine BMP-2 failed to heal the defect, whereas canine BMP-2 resulted in bone formation.[26] Therefore, the use of a recombinant protein from the target species would seem to provide optimal healing.

Dose of BMP

There are wide ranges of doses of BMP that have been used. The dose for rodents is much lower than that for higher vertebrates (Table 2). A dose effect with BMP-2 has been observed in several studies.[34,36,236,239-241,246] In one study a higher dose of rhBMP-7 resulted in more bone and faster healing, but the end result appears to be the same for doses over 6.25μg in rabbits.[240] Zegzula and coworkers[236] found there was an increase in bone formation earlier in the course of fracture healing with high doses of rhBMP-2 (35 and 70μg), although after 4 weeks there was no difference in callus formation between the high and low (17μg) doses. In rats, 6.28 μg of rhBMP-2 resulted in a large callus and union at 3 weeks but 1.26 μg rhBMP-2 resulted in only 41% of the rats healing at 9 weeks.[234] Similarly, Yasko and coworkers[34] reported bone formation by 7 days and complete healing by 3 weeks in 80% of animals treated the high dose (11.5μg) of rhBMP-2, but no radiographic signs of healing until 3-4 weeks and inadequate healing in animals treated with a low dose (1.4μg). Another study also found a dose-dependent effect up to a certain threshold in non-human primates.[33] These studies suggest that animals treated with a higher dose of BMP had more healing bone formation and more rapid healing but a larger callus; however, there appears to be a plateau effect.

Heckman and coworkers[227] found that in a chronic canine non-union model a lower dose (1.5mg) of recombinant canine BMP (rcBMP) induced more endosteal bone formation than the higher dose (15 mg). Animals treated with the lower dose of rcBMP also had a higher new bone and lamella bone volume than animals treated with the higher dose. Both doses, however, created significantly more new bone compared to untreated defects and defects treated with TGF-β. This study suggested that BMP at higher doses

may actually inhibit bone formation.[227] Other authors have also reported that a higher dose of BMP-2 (360μg) may induce more bone and less callus formation than a lower dose (54μg).[245] Therefore one challenge with using recombinant proteins is determining the optimal dose, which will vary depending on the species, site, and potentially the individual patient. The optimal dose is important to determine because if excessive BMP is used this may result in adverse effects and higher cost.

Exuberant Callus Formation

One disadvantage with the use of rBMP compared to ACG was that animals were found to have an exuberant callus response, whereas the animals treated with ACG did not.[25] Other studies have not reported this problem.[242] The area of callus was also found to increase with higher doses of rhBMP-2 (35 and 70 μg).[236] And some studies have observed focal areas of reactive bone eccentrically formed and on the opposite side of the bone to the bone plate;[34] that is, the plate was placed laterally and bone formed on the medial aspect of the bone. Others have found bone formation only in the defect and no excessive callus or radioopaque bone densities away from the defect.[237]

Histological Changes

In general, defects treated with BMP had more new bone formation, osteoblastic activity,[227] cartilage and endochondral ossification,[34,237,242] as well as more lamella bone with formation of the marrow cavity. Although carrier matrix and multinucleated giant cells were present, some studies showed less foreign body reaction, less inflammation, and more rapid dissolution of the carrier matrix in BMP-treated defects.[227] Although most

studies have found cartilage formation to be a part of ossification associated with BMP treatment,[237] other studies have found no cartilage in the defects of BMP treated animals at 4 and 8 weeks.[236] This is most likely a reflection of the dose of BMP, the type of BMP, and the time of evaluation. Control defects generally produce a fibrous tissue non union, or pseudoarthrosis, and may have a few millimeters of callus but in general do not bridge the defect.[240]

In a long-term study of 12-months duration using sheep, it was difficult to differentiate new bone from old bone on gross examination and on histological examination there was a distinct medullary cavity and remodeling cortical bone. While there were focal adhesions between the soft tissues and diaphysis, there was no lameness and no adverse effects. [243] This study demonstrated that there were no long-term adverse effects associated with the use of rhBMP-2.

The results of these studies appear favorable based on histological evaluation. The carrier matrix, however, clearly incites a foreign body reaction based on the presence of multinucleated giant cells, and this may be detrimental to fracture healing.

Carrier Matrix

The rBMPs are usually delivered using a carrier matrix. One challenge with the use of recombinant proteins is the design of a carrier matrix.[259,260] The carrier matrix is critical to the outcome of the study, with sustained release of appropriate concentrations as well as adequate degradation of the matrix required for optimal fracture healing.[258,259] The ideal carrier should be non-immunogenic, non toxic, bioabsorbable, and easily manufactured. Carrier matrices that have been used are shown in Table 2. There are

variations in protein release characteristics with different matrices. For example, type I collagen sponge reportedly causes a sustained release, deorganified bovine bone a burst-release, and PLGA a dose-dependent sustained release.[258,259] One study suggested that the advantage of the carrier was that there was less exuberant callus or ectopic bone formation because the carrier kept the protein in the local proximity of the defect and provided a scaffold for cell adherence and proliferation as well as bone formation, which was not provided in the adjacent soft tissues.[34]

The synthetic polymers, such as PLA or glycolic acid (PGA), are biodegradable, biocompatible, have initial physical characteristics similar to the surrounding tissue, provide a scaffold for ingrowth of bone, [259] and elicit minimal foreign body and allergic reaction.[227,259] They are also readily availability and can be synthesized with diverse characteristics.[259] The addition of PGA and/or higher porosity of the implant may result in more rapid resorption of the carrier which may be advantageous to fracture healing. In one study using rats,[246] fracture defects treated with rhBMP-2 delivered in PLGA with small particles had greater torsional stiffness and strength compared to PLGA with large particles. These findings probably reflect both protein release as well as matrix resorption and bone ingrowth. Although studies have shown that the protein is released from these scaffolds with an initial high dose in the first 48 hours and then by a continuous release over a 12 week period associated with polymer degradation,[258] other studies have found no burst release.[259] These studies suggest that there may be variability in protein release properties with different types of carrier matrices.

There are several limitations with the use of synthetic polymers. Synthetic polymers still result in a significant foreign body reaction, with multinucleated giant cells

and lymphocytes found at the fracture site.[236,245] Another complication includes the release of acids associated with degradation, which cause inflammation and toxicity,[258] as well as bone demineralization.[212] The use of a more porous implant allowing buffering of the acid was thought to reduce this complication.[227] In one study, however, the use of PLA was found to result in a massive inflammatory response and actual bone degradation.[260] Polymer degradation is obviously variable and may not coincide with the requirements for fracture healing. The presence of the protein affects the porosity and crystallization which in turn affects the degradation rate.[258,258] The local environment, particularly the amount of water, may also affect the degradation rate.[258,259] In addition to the protein release kinetics, there is also biomechanical variability associated with degradation which may be important in fracture healing.[259] In addition to the problems associated with the synthetic polymers, the disadvantage of the calcium phosphate-based delivery systems is that they are not biodegradable.[236]

Demineralized bone matrix is predominantly composed of collagen and may have a lot of variation in its osteoinductive properties depending on the extraction process and the amount of growth factors remaining in the matrix. Inactivated DBM does not enhance bone healing, but allows for controlled release of BMP, it keeps the BMP local, is osteoconductive, and may contain some growth factors that either interact with the BMP or the cells in the fracture site.[34] Some studies have found an increase in new bone formation with DBM,[212,250] yet most other studies have not. The DBM was resorbed in a 12 week period in one study;[242] however, other authors have found that it is slow (longer than 12 weeks) to resorb because degradation involves an immune-mediated process.[26] Demineralized bone matrix also has variable properties depending on the donor, and

there are complications associated with the use of allogenic and xenogenic tissue such as infection, immunological response, and disease transmission. Demineralized bone matrix has also been associated with an inflammatory response, most likely a result of alteration in the matrix structure or contaminants from the demineralization and extraction process.[26] While pure collagen molecules are not strongly immunogenic, cellular debris, ground substance, and other impurities are strongly antigenic and can impair fracture healing.[246]

Variation in fracture healing with BMPs has been found with different carriers. When bovine DBM was used as a carrier in a canine model, there was no increase in healing with BMPs and the carrier actually acted as a physical barrier to healing.[26] The authors proposed that this was a result of isolation of the BMP from the surrounding tissue, which minimized the effect it may have had on osteoinduction. Polylactic acid, on the other hand, appeared to be osteoconductive and there was induction of bone formation with BMP.[26] Bax and coworkers[245] also found that the use of BMP-2 in a matrix actually delayed healing compared to untreated controls, whereas delivery of the BMP-2 without a carrier matrix increased the rate callus formation in unstable fractures only. Most studies have been performed using a fracture defect, whereas this study used no defect. The rate or amount of fracture healing was not enhanced in stable fractures, suggesting that BMP-2 cannot accelerate normal fracture healing.[245] In unstable fractures, the rate of callus formation was increased and defect ossification did not occur until fracture stability was achieved.[245] The actual amount of cartilage and bone formed was not greater in BMP-2 treated fractures, therefore these authors[245] concluded that the matrix could act as a physical barrier to healing. Matrix to bone contact was thought to be

critical for fracture healing. The authors concluded from these results that biomechanical factors were important in fracture healing following treatment with BMP-2.

The configuration of the carrier is also important. Recombinant hBMP-2 in a collagen sponge placed in a wrap rather than an onlay configuration was superior and may have provided an increased osteoconductive or chemotactic environment.[238] The authors[238] proposed that the increased callus was a result of an increase in the number of osteoprogenitor cells because the mineral apposition rate and bone formation rate were not different suggesting that they were already optimal in normal fracture healing. Similarly, Bouxsein and coworkers[244] found that fractures in rabbits treated with rhBMP-2 in a collagen sponge wrapped around the osteotomy resulted in 33% faster healing compared to untreated controls. These studies did not place an implant in the defect, which in other studies was shown to inhibit healing. The latter study actually demonstrated that healing of normal fractures could also be enhanced with rhBMP-2.

Osteopromotive Membranes and BMPs

Osteopromotive membranes consist of a fenestrated material, such as polytetrafluoroethylene (PTFE), placed around the bone at the fracture site. The use of osteopromotive membranes was initially used to overcome the problem of non-union associated with soft tissue interposition. Osteopromotive membranes are thought to inhibit migration of fibroblasts and soft tissue into the defect but maintain growth factors and osteoinductive cells from the bone marrow in the defect providing uninhibited bone formation.[261]

New bone formation was enhanced with the use of an osteopromotive membrane in combination with BMPs. Expanded PTFE in combination with BMP-2 in a PGLA matrix carrier induced new bone formation more than either treatment alone.[257,261] Defects treated with rhBMP-2 alone had exuberant bone formation.[261] Therefore, the resulting contour with a PTFE osteopromotive membrane is better than that seen with BMP treatment alone.[261]

The rate of bone formation is dependent on the porosity of the membrane.[260] One study failed to show improvement in healing with osteopromotive membranes when BMP-2 in a collagen carrier was used, this was thought to be associated with a lack of access of inflammatory cells and macrophages with the use of small or no pores in an osteopromotive membrane.[257] Further, in another study the use of an unperforated PLA membrane caused bone graft necrosis because of inadequate vascularization.[263]

Polytetrafluoroethylene is not biodegradable and therefore would require a second surgery for removal. Additionally, PTFE cannot be easily shaped to contour to the bone.[261] The use of a bioabsorbable membrane may make this technology useful in the future.

Infected Non-Union Model

Until recently, there were no reports of successful use of recombinant protein in a carrier matrix in infected non-union. Chen and coworkers[68] however reported enhancement of fracture healing with BMP-7 in an infected non-union rat model. This study was the first to show that recombinant proteins in a carrier matrix are capable of enhancing fracture healing in a contaminated or infected environment.

Problems with Recombinant Proteins

Reported complications associated with the use of rhBMPs to stimulate fracture healing include a poor osteogenic response of the tissue surrounding the defect, loss of function caused by extraskeletal bone formation, and problems with restoration of the original dimensions of the bone.[264] Although infection has not been reported in these models, these defects are created using aseptic conditions and atraumatically. The use of recombinant BMPs in a carrier matrix in open or more complicated fractures may delay healing or increase the risk of osteomyelitis because of the presence of foreign carrier matrix.

Recombinant proteins are expensive to produce, have a short shelf life, require high doses (milligrams), and molding of the carrier matrix to the defect is difficult. Overall, the use of recombinant proteins has shown that the BMPs can be used to enhance fracture healing. However, the limitations make alternate methods for delivery of these growth factors more desirable. Additionally, because of the high cost, proteins cannot be used routinely in treating fractures, particularly in large animals.

Gene Therapy

Gene therapy may overcome the limitations associated with the use of recombinant proteins. Firstly, DNA has a longer shelf life compared to proteins, and is less expensive because it involves *in vivo* protein production at the fracture site rather than by cells in culture with subsequent protein purification. When the protein is synthesized *in vivo* it may have more recognizable ligands because of posttranslational

modification making it more biologically responsive.[265] Gene therapy has been used for spinal fusion, maxillofacial surgery, and fracture healing.[266] The major limitations of gene therapy for treatment of genetic, congenital, or chronic diseases is the short duration of gene expression and the associated immunological response; the short duration of expression is desirable for treatment of long-bone fractures and local application reduces the potentially fatal complication of an acute type-4 hypersensitivity reaction.

Basic Principles of Gene Therapy

Gene therapy involves delivering and transfer of the gene sequence for the desired protein to cells, which then produce a biologically active protein *in situ*. Gene therapy can provide high, sustained concentrations of growth factors locally. The gene is delivered to the cells either as naked DNA or by a vector. There are both viral and non-viral vectors.

Non-Viral Vectors: Non-viral vectors include plasmids, cationic and anionic liposomes, polypeptides, and condensed DNA with polycations.[265] Non-viral vectors often have the advantages of being economical to produce in large quantities, are reported to have a relatively low immunogenicity allowing repeated dosing and possibly prolonged transgene expression, no risk of recombination and reversion to an infectious virus, and potentially have more diversity with respect to characterization and manufacture.[268] However, although their immunogenicity is low compared to viral vectors, they may cause a non-specific inflammatory response, are currently a poorly defined system, unstable, susceptible to DNA aggregation, and most importantly have low, variable, and transient transduction rates.[267,268] Although research is being

performed to overcome some of these limitations,[268] viral vectors are currently preferred methods of gene delivery for enhancing fracture healing.

Viral Vectors: Viral vectors include retroviruses (for example, murine leukemia virus (MLV) and lentiviruses), adenoviruses, herpesvirus, and adenoassociated virus. Although retroviruses are thought to have prolonged transgene expression because they permanently modify the host genome, this may cause malignancy and other diseases. They can only transduce dividing cells (MLV) and recombination with the wild-type virus may risk development of systemic viral disease (Lentivirus). Prolonged transgene expression may be unnecessary and disadvantageous in fracture healing with excessive bone production potentially altering the function of adjacent soft tissues.

Herpesviral vectors has the advantage of the possibility for a large insert and the potential for multiple transgene insertion, and transient gene expression, however this virus is associated with disease, and the large, complex genome makes recombination challenging.[267]

Adenoassociated viruses are non-pathogenic, transduce both dividing and non-dividing cells, and are easily manipulated. However adenovirus contamination may occur in some preparations because helper-virus may be required for replication in some systems. Results of studies evaluating the use of adenoassociated viruses for joint disease have produced mixed results.[267]

Adenoviruses have several advantages over other viral as well as non-viral vectors, and are currently the most frequently used and best vector for delivery of genes to the fracture site. The characteristic features of adenoviral vectors have been extensively reviewed by Oligino and coworkers[267] as well as Horwitz and coworkers[269]

and will not be repeated here. Briefly, adenoviruses are associated with many diseases,[269] including upper respiratory tract infections ("common cold").[267] Serological types 2 and 5 are most commonly used as vectors. Following infection the virus is located episomally in the nucleus, where transcription, replication, and viral packaging occur. There are early (E1 to E4), middle, and late viral genes (open reading frames; ORF). The early genes encode proteins required for the lifecycle of the virus; E1 is essential for transcription of the other early genes, including DNA polymerase and DNA-binding protein in the E2 region.[269] The late genes encode packaging proteins.[269] Modifications to the wild-type virus are used for gene transfer.

Deletion of the E1 region, and partial deletion of the E3 region, results in a replication-incompetent virus and reduces the risk of oncogenic transformation of the host cell[269] (first generation adenoviral vector). Complete deletion of the E3 region increases the immune response the virus and decreases the duration of expression. The E3 region is involved with avoidance of the host immune response by interactions with the class I major histocompatibility complex (MHC-I), which decreases recognition of the infected cell by CD8+ T-lymphocytes and inhibition of the cytolytic effects of TNF-α.[269] Partial E3 deletions, however, allow transgene insertion without creating too large a genomic structure.

The virus is propagated on 293 cells that supply the E1 and E3 function. The 293 cells also express Cre recombinase, which facilitates the isolation of recombinant vectors because of negative selection against non-recombinant viruses by the effect of Cre recombinase on *lox*P sites, incorporated in the parent adenoviral vector (Ψ5).[270] Basically, there are two *lox*P sites flanking the viral packaging gene sequence; in the

presence of high concentrations of Cre recombinase, the packaging genes are deleted and the adenoviral vector is unable to replicated. Cre recombinase also catalyzes recombination of Ψ5 and the shuttle plasmid containing the gene to be delivered by the vector, a single *lox*P site, and a normal packaging sequence. Therefore, when the gene to be expressed by the vector is inserted there is only one *lox*P site, the packaging genes are not deleted, and the virus can replicate on 293 cells.[270]

The duration of expression of adenoviral vectors is short. This is in part because the virus resides episomally in the nucleus and is not replicated with the cell. However, the main limitation with the use of first generation adenoviral vectors is the immune response and inflammation, which limits transgene expression to weeks.[267] At doses greater than 10^8 particles/mL expression may be less than 1 week.[267] Hence, the development of second generation and gutless viruses was pursued.

Second generation adenoviral vectors involved deletion of parts of the E2 or E4 regions.[267] The virus is propagated on 293 cells modified to express the deleted genes.[267] Although second generation adenoviral vectors have reduced immunogenicity, deletion of the E4 region actually decreases transgene expression.[267] Gutted or gutless adenoviral vectors have all the viral genes removed with the exception (usually) of the packaging signal and consequently are helper dependent for propagation.[267] Gutless viruses therefore have a larger region for transgene insertion, lack viral protein expression, and are less immunogenic; however, purification is more difficult because of the helper viruses required for propagation.[267]

Therefore, in summary, adenoviruses have the advantage of being easily purified using cesium chloride density gradients because they are non-enveloped and produced in

high titers (up to 10^{14} particles/mL).[267] Adenoviruses have a high and transient period of gene expression,[266] a high transduction rate, and they are able to transduce both dividing and non-dividing cells.[271] Because the transduced genes reside extrachromosomally, the mutation rate is low.[272] The extrachromosal location of the vector is also in part responsible for the transient expression because the virus is not usually replicated with the cell. The main problem with currently used adenoviral vectors is the host immune response.

In Vivo Versus *Ex Vivo* Gene Transfer: Gene transfer may be *in vivo* or *ex vivo*. *In vivo* gene transfer has the main advantage of being minimally invasive and simple, requiring an injection containing the vector with the gene of interest into the fracture site. *In vivo* gene transfer however requires introduction of a live virus into the patient and is dependent on viable cells at the fracture site. *Ex vivo* gene transfer, while technically more complicated, places transduced cells in the fracture site. *Ex vivo* gene transfer is more cumbersome. Both forms of gene therapy have been used successfully to enhance fracture healing in experimental models. Because of the simplicity associated with *in vivo* gene therapy, it is most likely to gain clinical acceptance particularly for initial or prophylactic use, however in resistant or complicated cases *ex vivo* gene transfer may be required.

Host Immune Response

While there have been no studies evaluating the host immune response following the use of gene transfer for enhancing fracture healing, there have been several studies assessing the immune response following the use of gene therapy for other diseases. The host immune response is one reason for the short duration of transgene expression.

The immune response is the most problematic limitation with the use of adenoviral vectors. Both innate and acquired immunity are induced by gene therapy.[273-284] The host immune response is to both the viral structural proteins (hexon, penton, fiber)[282] as well as the foreign transgene proteins.[273-284] Expression of viral genes leads to destruction of the transduced cells, inflammation, and repopulation with non-transduced cells.[277,280] Recombinant adenoviral vectors in which the transgene to be expressed is derived from the host should induce a minimal immune response, whereas a transgene from a different species induces a greater immune response, with reduced duration of expression.

Innate immunity, in addition to anatomic and physiologic barriers, consists of endocytic and phagocytic barriers, and the inflammatory response resulting in endocytosis of foreign molecules, phagocytosis of foreign particles, and a local and systemic inflammatory response consisting of vasodilation, increased capillary permeability, and the influx of phagocytic cells.[285] Innate immunity is an important part of the initial host response to the virus and expressed protein,[273] and is thought to be a critical factor limiting the duration of expression of the proteins.

Acquired immunity involves both cellular and humoral immune responses.[285] The cellular immune response involves both cytotoxic (CTL) and helper (TH-1 and TH-2) T-lymphocytes. The CTL have a CD8+ receptors and the TH cells have CD4+ receptors; TH-1 cells produce IL-1 and TH-2 cells produce IL-4 and INFγ. The cellular immune response is directed against both the viral structural proteins and the transgene product.[274,276,277] The major histocompatibility complex class 1-restricted CD8+ CTLs are thought to be the primary immune effectors limiting gene expression,[275,278,280] and the TH

cellular response is thought to be insufficient to mediate cell destruction despite activation of the TH-1 cells.[275,280]

The humoral immunity (antibody, secondary, memory response) associated with the β-lymphocyte response, which involves production of antibodies to both the adenoviral structural proteins and the transgene product is thought to be an important part of the limited protein expression following reinoculation with the recombinant adenovirus.[276,282] In addition to reinoculation, human patients are likely to have had previous exposure to and therefore antibodies directed against the human adenoviruses that are used as vectors for gene therapy.[279,282,283] To overcome this limitation in humans, canine, bovine, and ovine adenoviruses have been evaluated as an alternative to the human adenovirus for gene transfer to minimize the immune response for gene therapy, because human patients are unlikely to have been exposed to adenoviruses from other species.[279,283] Although repeated inoculation is likely to be required for treatment of congenital and neoplastic diseases, reinoculation for fracture healing should not be necessary with this type of treatment, based on research in experimental models. Further, horses should not have previous exposure to human adenovirus, and should not have preexisting antibody titers; therefore, although the immune response is an important issue in adenoviral gene transfer and should be addressed, this aspect of the immune response should not interfere with treatment.

The genomic structure of the viral vector has been found to be important in the immune repsonse.[274,276,280] Manipulation of the adenoviral vector has been found to reduce the immune response. Deletions of E4 have been shown to reduce the humoral immune response which would be important for diseases in which redosing was

important;[276] and deletions in E2a were shown to reduce the CD8+ T cell response in the airway epithelium, however did not prolong transgene expression or reduce the immune response in the alveolar epithelium.[280] Chimeric adenoviral vectors have been shown to overcome the secondary immune response which complicates redosing.[281] Manipulation of host immunity by using immunosuppressive drugs may also prolong transgene expression; this is associated with inherent complications, and would not be suitable for incorporation in a regimen directed at accelerating fracture healing. The E3 region of the adenoviral vector is retained because, as mentioned previously, the E3 proteins inhibit the host immune response.[286] Partial deletions of E3 has been shown to increase the MHC on the cell surface, increase the immune response, and therefore decrease transgene expression. Despite the problems with host immunity, adenoviral vectors are still the most commonly used vectors for delivering BMP genes to the fracture site.

Expression of Marker Genes at the Fracture Site following In Vivo *Gene Transfer*

Initially studies evaluating gene transfer were performed with marker genes, ß-galactosidase (LacZ) and the firefly luciferase gene (LUC). These studies demonstrated transduction of the cells either in muscle (heterotopic site) or in the fracture defect (orthotopic site) and gene expression of a biologically active protein.[272,287,288-290]

Following heterotopic injection, muscle cells, mononuclear cells (fibroblasts, pericytes, myogenic stem cells, bone marrow-derived cells) along the injection site and in perimysium between muscle fascicles were transduced with LacZ by *in vivo* adenoviral gene transfer.[290] Mature muscle cells were not transduced by the adenovirus because fascial barriers and basement membrane are thought to inhibit adenoviral entry;

adenoviruses infect only immature myotubes and myoblasts which are not present in uninjured mature muscle; and the internalization receptor for adenovirus contains av-integrin which is low in mature muscle. Implantation of a gene activated matrix containing the LacZ gene resulted in transduction of and protein expression of cells migrating into the matrix.[289]

Cells that were transduced in the fracture site included osteoblasts, osteocytes, periosteal cells, inflammatory cells, and mesenchymal cells in the bone, bone marrow, muscle and soft tissue surrounding the defect.[272,287,291] Protein expression following adenoviral gene transfer has been found to be between 3 and 6 weeks.[287,289] High expression of marker genes in the surrounding muscle and soft tissue is reported to be up to 3 weeks, whereas that in the cut ends of the bone in the fracture defect up to 6 weeks.[287] Similarly in another study, protein expression was found to be more prolonged in cells in the fracture defect compared to cells adjacent to the defect.[272]

There were no signs of cytotoxicity or inflammation associated with adenoviral delivery of gene products, and fracture healing was found to progress normally.[272] There does no appear to be systemic distribution of marker genes to the liver, lung, spleen, or contralateral limb.[272,287] Therefore, these studies have shown that adenoviral gene transfer is simple, and that there is repeatable, transient expression of marker genes.

Expression of the BMP-2 Gene at Heterotopic Sites: Ex Vivo *and* In Vivo *Transduction*

Ex Vivo: Gene transfer of BMP-2 to heterotopic sites, particularly muscle, results in new bone production (Table 4). *Ex vivo* transduction of W-20 marrow stromal cells ($5x10^6$ cells) was performed using adenoviral transfer of the BMP-2 gene (Ad-BMP-2),

and the transduced cells were capable of bone formation in muscle in severe combined immunodeficient mice (SCID) whereas the LUC and DBM controls did not produce bone;[271] similarly C3H/10T ½ cells (10^7 cells) were transduced using Ad-BMP-2 and produced bone in nude mice.[292] Mesenchymal stem cells (C3H/10T ½ cells) were found to proliferate and differentiate along the osteoblastic lineage *in vitro* following adenoviral transduction with the BMP-gene, and were capable of bone formation *in vivo*.[293] More recently, Laurencin and coworkers[294] used *ex vivo* retroviral transfer of the BMP-2 gene to W-20 cells, in a PGLA-HA carrier, as a vehicle for delivery of BMP-2.

In Vivo: *In vivo* transduction has also been used successfully, with bone formation at heterotopic sites. Injection of athymic nude mice with Ad-BMP-2 ($7.5x10^8$ particles/7.5μL) resulted in heterotopic bone formation; however, immunocompetent mice did not form bone but had an inflammatory response at the site of injection.[295] An E1a-, E1b- and partial E3-gene deleted adenoviral vector was used in that study.[295] The use of an E1- and E3-gene deleted adenoviral vector ($1.5x10^9$ particles/20μL) resulted in bone formation in both SCID and immunocompetent mice.[290] Bone production in the immunocompetent mice, however, was slower, there was less bone, there was more inflammatory response, and fewer cells were transduced as indicated by expression of the marker gene (LacZ). Therefore, although the immune response appears to reduce transgene expression in immunocompetent animals, bone is produced which supports the use of *in vivo* gene transfer for enhancement of fracture healing.

Table 4. Studies evaluating gene transfer of the bone morphogenetic proteins at heterotopic and orthotopic sites.

Author	Species	Delivery	Vector	Model[1]	Carrier
Fang et al 1996[288]	Rats	*In vivo*	Plasmid	5mm; femur	GAM
Lieberman et al 1997[298]	SCID mice	*Ex vivo* W-20 cells[2]	Retroviral	Heterotopic	DBM
Lieberman et al 1998[271]	SCID mice/ Nude Rats	*Ex vivo* W-20 cells[2]	Adenoviral	Heterotopic/ 8mm; femur	DBM
Lieberman et al 1999[296]	Nude Rats	*Ex vivo* Bone marrow cells	Adenoviral	8mm; femur	DBM
Musgrave et al 1999[290]	SCID mice/ Mice	*In vivo*	Adenoviral	Heterotopic	NA
Alden et al 1999[295]	Rats/ Nude rats	*In vivo*	Adenoviral	Heterotopic	NA
Gazit et al 1999[293]	Mice	*Ex vivo* C3H/10T ½ cells[2]	Adenoviral	2.5mm; radius	COL
Lou et al 1999[292]	Nude mice	*Ex vivo* C3H/10T ½ cells[2]	Adenoviral	Heterotopic	-
Baltzer et al 2000[300]	Rabbits	*In vivo*	Adenoviral	13mm; femur	NA
Spector et al 2000[272]	Rat	*In vivo*	Adenoviral	0.5mm; mandible	NA
Laurencin et al 2001[294]	SCID mice	*Ex vivo* W-20 cells[2]	Retroviral	Heterotopic	PLGA/ HA

GAM=gene activated matrix (collagen), DBM=demineralized bone matrix, COL=collagen, PLGA=polylactic acid-polyglycolic acid copolymer, HA=hydroxyapatite, NA=not applicable. 1. Model was heterotopic or orthotopic using various sites. The defect size and the bone used for orthotopic models are recorded. 2. Pluripotent mesenchymal cells

Enhancement of Fracture Healing

Ex Vivo: Both *ex vivo*[271,293,296-298] and *in vivo*[272,288,299,300] gene transfer have been shown to enhance fracture healing in laboratory animal models (Table 4). Lieberman and coworkers[271,296-298] have demonstrated enhanced fracture healing with *ex vivo* transduction of both an immortalized cell line as well as autologous bone marrow stromal cells using both adenovirus and retrovirus vectors in rats. Interestingly, in one study,[296] there were 2 rats that did not heal the defect. These rats were shown to have reduced BMP-2 on Western blot analysis compared to the other rats, suggesting some variability in protein production, which may have been a result of reduced transduction efficiency. Defect healing is usually achieved in 8 weeks in these studies.[271,293] Although one author observed ectopic bone formation adjacent to the implant, it was later resorbed and therefore unlikely cause a long-term problem in clinical cases.

One advantage of *ex vivo* transduction is that depending on the cell type used the transduced cells may differentiate into osteoblasts *in vivo* and produce bone, therefore both autocrine and paracrine mechanisms can be used to enhance healing.[292] *Ex vivo* transduction with osteoprogenitor cells (C3H10T ½) enhances callus formation compared to gene transfer with non-progenitor cells (CHO) in immunosuppressed mice,[292] even though *in vitro* the non-progenitor cells produced more BMP-2. Transduced progenitor cells were found lining the trabecules of new bone whereas wild-type cells were in the connective tissue.

Although gene expression by cells in culture is limited with adenoviral gene transfer because the gene is extrachromosal and is not replicated with the cell, and therefore becomes diluted by untransduced cells,[271] transduced cells have been shown to

survive for up to 8 weeks.[293] Immunosuppression is required however, when autologous cells are not used. *Ex vivo* transduction of cultured periosteal cells with BMP-7 using a retrovirus vector induced new bone formation and healed defects.[267] Autologous bone marrow stromal cells have also been used successfully and are also osteoinductive as well as easy to harvest.[271]

While bone marrow stromal cells appear to be a logical cell choice for *ex vivo* transduction, there are several limitations. The isolation process is difficult, cell proliferation is slow *in vitro* requiring several weeks for cell culture, a low percentage of the cells in bone marrow are stromal cells, and the biopsy procedure is invasive. Muscle cells, on the other hand, can be easily isolated and cultured, they grow more rapidly in culture compared to bone marrow stromal cells, and the cell population is greater in muscle than bone marrow. Muscle cells are an efficient gene delivery vehicle, and are capable of being transformed into osteoblasts when stimulated with BMP-2. Because cell turnover *in vivo* is slower there may be a more prolonged transgene expression. Muscle cells have been found to successfully express marker gene in a fracture defect.[301] Other studies have also strongly supported the use of muscle cells for *ex vivo* gene transfer.[302-304] These studies showed no toxicity associated with gene transfer, osteogenic differentiation of muscle cells, and bone formation *in vivo* equivalent to that with marrow stromal cells.[302] Other cells that have been used are articular chondrocytes, fibroblasts, and an *osteogenesis imperfecta* stromal cell line.[303]

While, in addition to the advantages mentioned in the previous paragraph, *ex vivo* transduction has the advantage of not introducing foreign genetic material, or a virus that may regain its pathogenicity by recombination with wild-type viruses, into the host, it is

technically more demanding and requires harvesting of the patient's cells for transduction. The latter two requirements may prohibit the routine use of *ex vivo* transduction, particularly in equine surgery, and limits its use to resistant non-unions. The use of a carrier matrix, such as a collagen sponge[293] or PGLA,[294] which is often used to deliver the transduced cells to the fracture site following *ex vivo* transduction, introduces some of the disadvantages that were discussed in association with the use of recombinant proteins. Therefore, *in vivo* gene transfer has several advantages over *ex vivo* gene transfer.

In Vivo: *In vivo* direct gene transfer of BMP-2 has been shown to enhance fracture healing in several laboratory animal models.[272,288,299,300] The first studies evaluating gene therapy for enhancing fracture healing were performed using plasmids, with the BMP-4 and parathyroid hormone genes, in a collagen sponge (gene-activated matrix), in non-union models in rats and 8-mm bored defects in the distal femur of dogs. Bridging callus was attained by 9 weeks with BMP-4 alone and by 4 weeks with BMP-4/PTH combination.[288,299] The authors proposed that the matrix was beneficial to healing because it provided a scaffold for new bone formation as well as cell migration allowing cell-plasmid contact, it also protected the plasmids and provided sustained release. The response was found to be dose-dependent.[289]

The limitation with the use of plasmids are that transduction and subsequent protein production is dependent on cells migrating to the fracture site, which may result in reduced transduction efficiency particularly in non-unions that may be relatively acellular and avascular. *In vivo* gene delivery with plasmids often requires a scaffold, and

the collagen scaffold has been found to actually impede *in vivo* cell transduction by adenoviral vectors.[300]

Direct *in vivo* gene transfer using an adenoviral vector is probably the simplest and most efficacious method of gene therapy for routine used in fracture healing. Previous work by our collaborators[300] has demonstrated enhancement of fracture healing in rabbits using *in vivo* adenoviral transfer of the BMP-2 gene. In this study, fractures treated with Ad-BMP-2 had radiographic evidence of fracture healing at 7 weeks, and complete ossification seen histologically across the defect at 8 weeks. This was unlike control rabbits, which developed a radiographic and histologic non-union at 12 weeks (Figure 3). Fractures treated with Ad-BMP-2 were stronger and stiffer in bending compared to control rabbits.

Despite the previous findings of expression in muscle and surrounding soft tissue, bone formation adjacent to the defect was not found.[300] This was attributed to cell death as a result of high concentrations of BMP.[300,303] High concentrations of BMP have been found to cause cell death *in vitro*, while high concentrations of the viral vector did not cause cell death.[305] Formation of hydroxyapatite was thought to be responsible for the cell death.[305] Another study showed while there was a dose dependent increase in proliferation with increase in Ad-BMP-2 dose, higher doses of Ad-BMP-2 reduced cell proliferation which was thought to be a result of toxicity or occupation of the cell machinery with the BMP-2 gene.[292] It is interesting, however, that the high BMP dose damages cells adjacent to the defect and not cells in the defect. Another explanation for the lack of bone formation adjacent to the defect may be that biomechanical factors are also be important in the pattern of callus formation following treatment with BMPs.[245]

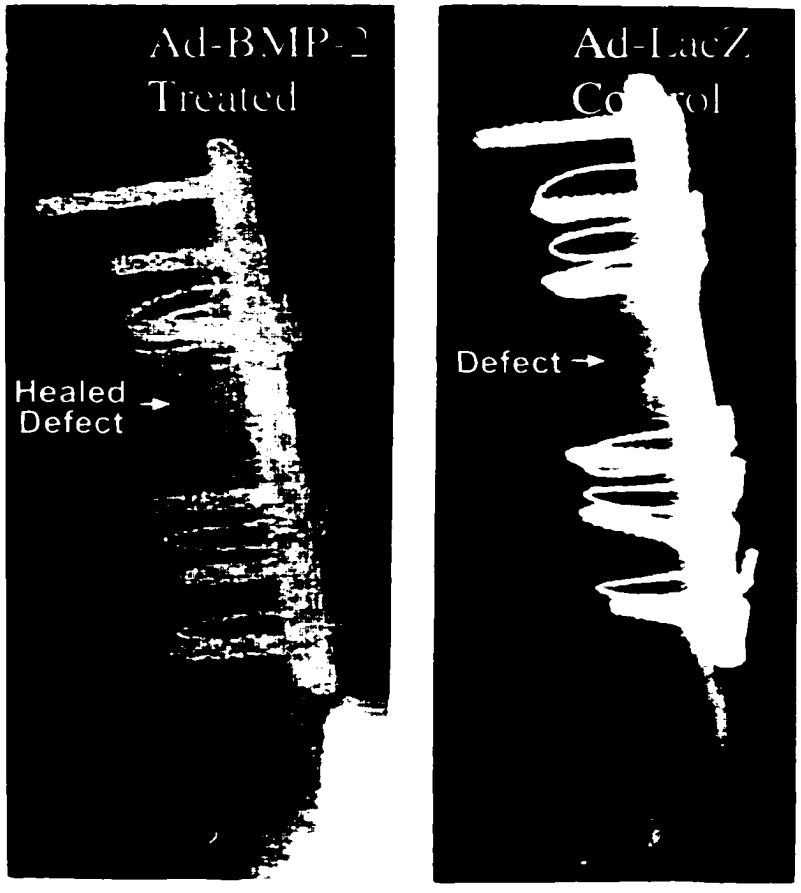

Figure 3. A craniocaudal radiographic view of two rabbit femurs at 12 weeks. The femurs were treated with either Ad-BMP-2 (treated) or Ad-LacZ (control). There was more healing or radiographic ossification of the defect in the rabbits treated with Ad-BMP-2 compared to rabbits in the Ad-LacZ control group. The figure was copied and modified from Baltzer and coworkers.[228]

Gene Transfer Versus Recombinant Protein

Overall, studies evaluating gene transfer of the BMP-2 gene have demonstrated improved healing, and with smaller quantities of protein, compared to the use of recombinant proteins.[288] This is thought to be a result of the production of a more biologically active protein, more favorable protein-release kinetics, and the presence of the osteoprogenitor cells with *ex vivo* gene transfer.

Ex vivo gene transfer with BMP-2 resulted in a greater total volume of bone, based on histomorphometric analysis, compared to defects treated with rhBMP-2.[296] The bone in the animals treated with gene transfer had more course trabecular compared to the thin, lace-like bone in animals treated with the recombinant protein.[296]

Similarly, in another study the use of rhBMP-2 resulted in less efficient and less organized bone formation compared to *ex vivo* transfer of the BMP-2 gene.[293] While microgram quantities of rhBMP are required to produce bone *in vivo*, fibroblasts, muscle-derived cells, and bone marrow stromal cells all produce nanogram quantities of BMP-2 when transduced with Ad-BMP-2 and new bone formation occurs at these quantities.[287] Therefore bone induction and fracture healing with gene therapy requires a smaller dose of BMP.

A more recently recognized advantage of gene therapy is the ability to exogenously regulate transgene expression.[306] Expression of the BMP-2 gene by genetically engineered mesenchymal stem cells was regulated by exogenous administration of doxycycline (a tetracycline analogue) via a tetracycline-regulated expression vector. Doxycycline was shown to control both bone formation and angiogenesis.[306] This type of technology, combined with improvements in our knowledge

on the physiology of fracture healing, may be ideal for use of multiple growth factors for enhancing healing of complicated fractures.

Enhancement of Fracture Healing in an Infected Non-Union using Ad-BMP-2

Based on previous research of both the physiology of fracture healing as well as the use of growth factors for enhancing fracture healing, it may be concluded that BMP-2 is the best method for enhancing healing of infected non-unions. In addition, it is currently available in an adenoviral vector. While there are limitations with *in vivo* gene transfer using an adenoviral vector, it is simple and effective, and importantly does not require a carrier matrix, which may exacerbate infection in more complicated or open fractures. There have been no studies evaluating the use of gene transfer of BMP for enhancing healing in an infected non-union model. Therefore, the purpose of this study was to evaluate the use of adenoviral transfer of the BMP-2 gene for enhancing healing in infected non-union as described in Chapter 3.

EARLY DIAGNOSIS OF NON-UNION AND INFECTED NON-UNION

Although advances have been made in the treatment of non-union and infected non-union, early diagnosis is thought to be essential for a favorable clinical outcome. The diagnosis of impaired fracture healing and osteomyelitis can be challenging. While history and physical examination are still the most fundamental diagnostic tools, findings often lack specificity and sensitivity for non-union and infected non-union. History and physical examination findings of pain, fever, heat, swelling, redness, and drainage are often associated with the initial traumatic incident causing the fracture, the surgical

procedure to repair the fracture, or infection involving the soft tissue only. Laboratory findings of leukocytosis, increase in erythrocyte sedimentation rate, and increase in acute phase protein, such as fibrinogen and c-reactive protein, may occur after trauma or surgery, and are not specific or sensitive for osteomyelitis.[307,308] Therefore, in post traumatic or postoperative cases, clinicians rely on imaging modalities to evaluate fracture healing and osteomyelitis. Imaging techniques are complementary[308] and when combined the diagnostic accuracy may be at least 90%.[309]

Radiography

Radiography is the most commonly used technique for evaluating fracture healing and osteomyelitis, particularly in the initial evaluation. Radiography is easy, quick, economical, and readily available.

Early radiographic signs of osteomyelitis are soft tissue swelling and loss of fascial planes, which is followed sequentially by periosteal thickening and elevation, osteopenia, cortical destruction, sequestration, formation of an involucrum and cloaca.[308] Chronic osteomyelitis is associated with a periosteal reaction, lysis, and sclerosis.[308]

The main limitation with the use of radiography for evaluating fracture healing and diagnosing osteomyelitis is the lack of sensitivity. A spherical lesion in trabecular bone needs to be greater than 15 mm in diameter, and 30 to 50% of the calcium lost before it can be discerned radiographically.[310] Radiographic signs may not be visible for up to 14 days after onset of the disease process.[311] Changes consistent with osteomyelitis are visible in less than 5% of patients initially, less than 30% at 1 week, and then approximately 90% are positive at 3 to 4 weeks.[309] One study showed radiography alone

to have a sensitivity of 62.5% and specificity of 57.1% for diagnosing the presence of osteomyelitis in a canine model 8 weeks after inoculation.[312] In another study assessing the reliability of radiography for evaluating fracture healing in goats treated with BMP-7, although visibility of the fracture line correlated with mechanical strength there was a poor correlation between radiographic scores and results of mechanical testing.[313] Therefore, other imaging modalities should be used in combination with radiography.

Ultrasound

Ultrasound has been used both to evaluate fracture healing[314] and diagnose osteomyelitis.[308,315-319] Ultrasound is simple, rapid, non-invasive, and inexpensive. In one study evaluating fracture healing, the fracture was detected as a discontinuity, step, or irregular depression with ultrasound.[314] During healing the callus was initially hypoechoic, followed by isoechoic, then hyperechoic compared to the cranial tibial muscle. In this study, the presence of a hyperechoic callus correlated 100% with histological findings of a hard callus, and there was a good correlation between ultrasound and histological findings for the percentage of bone in the callus.[314] An ultrasonic diagnosis of union was made on average 5.6 weeks after surgery, whereas a radiographic diagnosis was made at 7.3 weeks.[314] Ultrasound was also used successfully for evaluating healing of tibial fractures stabilized with an intramedullary nail in human patients.[314] These reports suggest that ultrasound may be useful for assessing fracture healing; however, the presence of a large soft tissue mass and metallic implants may alter the accuracy in some patients.

Osteomyelitis is diagnosed with ultrasound based on finding fluid directly adjacent to the bone.[315-319] If there is soft tissue interposed between the fluid and the bone then a diagnosis of osteomyelitis cannot be made, and the patient is more likely to have an abscess or cellulitis.[317] Other signs include soft tissue swelling, gas associated with an anaerobic infection, fluid-filled tracts, irregular bone surface, as well as fragments and sequestra.[316] Ultrasonographic signs of osteomyelitis are usually detected prior to radiographic signs.[316,317] Changes in acute osteomyelitis may be detected 1 to 2 days after the onset of clinical signs.[308] While in a human study ultrasound had a sensitivity of 83% for diagnosing osteomyelitis,[318] soft tissue infection was associated with false positive results in another study.[315]

Ultrasound would also have limited use posttrauma and postoperatively because of an open would and hematoma formation adjacent to the bone which has a similar appearance to the exudate associated with osteomyelitis.[300] Therefore, ultrasound may not be the best imaging modality for early diagnosis of osteomyelitis following fracture repair.

Computerized Tomography

Computerized tomography (CT) is highly specific and sensitive for evaluating fracture healing and osteomyelitis.[308,320] Computerized tomography integrates the attenuation values of ionizing radiation to create cross-sectional images.[221] Compared to magnetic resonance imaging (MRI), CT provides a superior image of the cortical bone, is more sensitive, and provides better spatial resolution compared to radiography. Changes consistent with acute hematogenous osteomyelitis are intramedullary gas or increased

marrow density. Sclerosis, demineralization, periosteal reaction, and sequestra are detected with chronic osteomyelitis.[308] The use of quantitative CT (QCT) has also been evaluated for assessing fracture healing.[322] The authors concluded that QCT may predict density alteration in the fracture callus more accurately than radiography.[322] However, as pointed out by the authors in the latter study, while QCT accurately measures the mineral content of the fracture callus, other factors, such as the collagen orientation, are important for mechanical strength of the healed fracture. Markel and coworkers[323,324] have also evaluated the use of QCT for evaluating fracture healing. They found that QCT correlated with the mechanical properties of bone (r^2=>0.6) and had better correlation than MRI, dual energy x-ray absorptiometry (DEXA), and single photon absorptiometry (SPA).

Despite its high sensitivity and accuracy for detection of cortical changes, there are limitations with the use of CT for evaluating fracture healing and diagnosis of osteomyelitis. In general, CT delivers a high radiation dose to the patient, which is undesirable in young human patients and human patients requiring reevaluation, and metallic implants cause an artifact that may preclude visibility of the fracture site. Further, for horses, CT is expensive, requires general anesthesia, which may be contraindicated in horses with long-bone fractures, and is not readily available. Therefore, alternate methods for evaluating fracture healing and diagnosing osteomyelitis associated with long-bone fractures are required.

Magnetic Resonance Imaging

Magnetic resonance imaging is a multiplanar imaging modality that provides excellent soft tissue and bone marrow resolution.[308] Magnetic resonance imaging creates

images from resonance of hydrogen nuclei within the body. Osteomyelitis can be detected in the acute phase of the disease process with MRI by detection of bone marrow abnormalities as a result of the marrow fat being replaced by water associated with edema, exudate, hyperemia and ischemia.[308] Similarly, with chronic osteomyelitis changes are consistent with an increase in the water content of the bone marrow associated with granulation tissue formation. The specificity and sensitivity was reported to be greater than 90% for detection of primary osteomyelitis in human patients.[308,321]

While MRI is sensitive for detection of bone marrow changes associated with primary osteomyelitis, these changes are not specific for osteomyelitis associated with long-bone fractures because false-positive results as a consequence of hematoma formation occur with fractures. Additionally, MRI provides poor cortical detail[311] and the image may be obscured with metallic implants.[308, 321] In patients with metallic implants with magnetic attraction, such as stainless steel, MRI cannot be used because of the strong magnetic field. In a study evaluating fracture healing, MRI had the poorest association with mechanical properties of bone.[324] As with CT, MRI is expensive, required general anesthesia for veterinary patients, and is not commonly available, particularly for horses.

Dual Energy X-Ray Absorptiometry

Dual energy x-ray absorptiometry is most commonly used for evaluating patients with metabolic bone disease; however, studies have evaluated the use of DEXA for evaluating fracture healing.[325,326] In a canine non-union model, the sensitivity for detecting non-union with DEXA was 100% at 8 weeks and the specificity 78% at 16

weeks. A fracture was classified as a non-union by DEXA on average at 2.6 weeks and by radiography at 4.6 weeks.[326] Both DEXA and SPA were superior to MRI for evaluation of mineral content and indentation stiffness,[324] with correlation coefficients with material properties of approximately 0.8 and 0.73 for SPA and DEXA, respectively.[325] Therefore, DEXA may be useful for evaluating fracture healing, however is not readily available, particularly for large animals. There have been no studies using DEXA to diagnose osteomyelitis.

Nuclear Scintigraphy

While the previously mentioned imaging techniques provide high quality anatomical information, trauma, surgery, and metallic implants alter the normal anatomy, making these imaging modalities difficult to interpret. Nuclear scintigraphy, on the other hand, which evaluates physiological rather than anatomical changes[327] may be superior to these techniques for evaluation of fracture healing and osteomyelitis. In general, radionuclide uptake reflects both vascularity and metabolic activity of bone.[328]

Fracture Healing

Historical Radionuclides: Nuclear scintigraphy using various radionuclides has been used to evaluate fracture healing. Radionuclides that have been used include strontium (Sr)-85, Sr-87m, fluorine (F)-18, and various phosphates (PO) which bind calcium, hydroxyl, and phosphate ions in hydroxyapatite, respectively.[329] There are 2 physiological pools of hydroxyapatite in bone: the large, slowly changing pool, and the small, rapidly exchangeable pool which allows exchange of ions, such as Sr, F, and

PO.[329] Although Sr-85 was the original nuclide for evaluating bone physiology and osteomyelitis,[330] it was not useful for early diagnosis of impaired fracture healing, had a low count rate requiring a long scanning time, a long half-life, delivers a high radiation dose, dosing cannot be repeated, and therefore was not useful clinically.[331-333]

Strontium-87m and F-18 have been shown to be useful for evaluating fracture healing and prostheses, as well as diagnosing osteomyelitis. They have a shorter half-life, and deliver a lower radiation dose.[334-338] Patients with normal union were found to have a focal uptake of Sr-87m, patients with delayed union a diffuse uptake, and patients with non-union or infection had a persistent uptake.[338] Similarly in another study, patients with normal healing had a focal increase in uptake of Sr-87m, whereas patients with non-union had two peaks, one proximal and one distal.[335] Non-stable fractures had a more intense uptake for a prolonged period compared to stabilized fracutres.[335] Human patients with a hypertrophic non-union had an increase, and patients with an atrophic non-union a decrease in uptake compared to normal.[335] Other studies have failed to demonstrate a difference in radionuclide uptake between patients with normal and abnormal healing.[336] Chronologically, there are two peaks with Sr-87m in humans; the first peak within weeks of fracture and the second peak associated with the onset of weightbearing.[336]

Because of the short half-life of these radionuclides, scanning must be performed an hour after delivery, at which time the pool-phase has not cleared. Further, Sr-87m has a low count rate and F-18 requires a cyclotron for production, which limits their routine clinical use.[328,334-338]

Technetium-Labeled Phosphates: The use of technetium-99m labeled phosphates (Tc-PO) has overcome many of the limitations associated with the use of other

radionuclides. Technetium-PO has a high sensitivity for bone disease, good image quality, is cheap, simple to prepare, and widely available.[311] The short half life (6 hours) and absence of beta radiation, result in a low level of radiation delivered to the patient, allowing a higher dose of Tc to be administered. Technetium decays by releasing monochromatic 140 kV gamma rays, which are detected by a gamma camera. The higher allowed dose and the decay characteristics produce a high quality image and a short scanning time. Technetium-99m is not protein bound resulting in faster blood clearance and patients can be scanned at 2 to 3 hours postinjection.[328,339,340]

Phosphate compounds that are used include tripolyphosphate, pyrophosphate, and diphosphonate.[328] The best results have been obtained with Tc-methylene diphosphonate (HDP or HMDP; Tc-PO).[328] Technetium-PO accumulates in areas of rapid bone turnover; the mechanism of accumulation is hyperemia, mineral (hydroxyapatite crystals) deposition, as well as immature collagen deposition.[341] Microautoradiography has shown that the radioactivity concentrates in the cement lines at the junction of osteoid and mineralized bone; 50-60% is deposited in the bone and the remainder deposited in urine.[342] Technetium-PO has been shown to be useful for evaluating fracture healing in limited studies.[343,344] One study showed that in normal healing the uptake peaked 4 to 8 weeks after fracture and then decreased, whereas the uptake remained elevated in patients with delayed healing.[343] In three horses with metacarpal or metatarsal fractures, Tc-PO was used to evaluate vascularity and fracture healing;[344] horses with an increase in radionuclide uptake ratio healed the fracture, whereas one horse that did not have an increase in uptake developed an atrophic non-union, with sequestration of the metacarpus

requiring euthanasia. Further studies evaluating the use of Tc-PO for evaluating fracture healing are required.

Osteomyelitis

Technetium-Labeled Phosphates: Nuclear scintigraphy can be used to detect osteomyelitis several months before radiography.[345] Technetium-PO bone scanning is commonly used to diagnose osteomyelitis[346] and is useful for differentiating infected bone from soft tissue.[329,347-352] Osteomyelitis could be distinguished from cellulitis (soft tissue infection) with a specificity of 92% and sensitivity of 84% in children with acute hematogenous osteomyelitis.[350] However, Tc-PO actually has a low specificity for osteomyelitis because there will be an increase in uptake ratio with any cause of increase in bone metabolism. For example, there was an increase Tc-PO with inactive osteomyelitis,[347] and an infected hypertrophic non-union could not be distinguished from a non-infected hypertrophic non-union.[343] In the latter study, infected fractures had an increase in uptake ratio with the pool phase scan, whereas non-infected fractures only had an increase in delayed-phase scans.[343] Therefore, while Tc-PO may be useful for detecting the development of a primary osteomyelitis in patients known to have an infection, it may not be useful for early diagnosis of osteomyelitis following fracture repair.

A lot of research has been performed evaluating the use of Tc-PO for evaluating infection associated with hip prostheses. In general, Tc-PO could not be used to distinguish infection from surgical trauma, thermal necrosis, and fracture, in the early

postoperative period; however, an increase in uptake after 8 months was associated with infection.[345,368-370]

Therefore, Tc-PO bone scans are usually performed in combination with other radionuclides, such as gallium-67 citrate and indium-111 labeled leukocytes, which are thought to be more specific for infection and inflammation.[353-375]

Gallium-67 Citrate: Gallium-67 citrate is a bone seeking radionuclide that localizes with bacterial debris, increased vascular permeability, leukocyte infiltration, and sites of high mitotic activity.[346] Gallium is a transition metal similar to the ferric ion in atomic charge, radius, and inorganic complexes accumulation. It binds to transferrin, lactoferrin, ferritin, and siderophores, which facilitate ion uptake by microorganisms. Gallium-ferritin acts as a macromolecule, hence an increase in vascular permeability and exudation of serum proteins causes an increase in gallium-67 citrate uptake. Gallium-67 citrate also accumulates in leukocytes and bone marrow, is bone seeking, and has been found to accumulate at the site of postoperative wounds and normal fractures.[311] Therefore it is not specific for septic osteomyelitis.[346] Gallium-67 citrate has poor image quality, delivers a high radiation dose to the patient,[353] requires up to 72-hour delay in imaging, and although some studies reported a high specificity and sensitivity for diagnosing postoperative osteomyelitis,[354-356] others have not.[311,343,357-359]

Labeled Leukocytes: Leukocytes have been labeled with indium(In)-III-oxine, In-III-tropolonate, and Tc-99m. Neutrophils only are labeled because they are the most abundant leukocyte and lymphocytes are radiosensitive and therefore do not circulate when labeled. Although indium-111-leukocytes have a high specificity and sensitivity for detecting acute osteomyelitis,[360] the accuracy for chronic infection and infection

associated with other orthopedic disease, such as fracture, is low.[361] The sensitivity for detection of osteomyelitis with In-III-labeled leukocytes was 84% and the specificity 90%.[360]

However, In-111 has poor image quality compared to Tc-99m,[311] leukocytes accumulate in the bone marrow, and there are technical difficulties and health risks to both laboratory personnel and patients associated with labeling leukocytes.[311,357,362] Indium-111 also has a long half-life, high cost, and requires a longer time between injection and scanning (24 to 48 hours) compared to Tc-99m.[363] Although labeling leukocytes with Tc[364,365] and labeling antibodies against leukocytes (antigranulocyte antibodies)[366,367] has overcome some of these problems, these methods are not useful for differentiating inflammation from infection. For example, the overall accuracy of labeled antigranulocyte antibodies was 72% with a sensitivity of 95% but a specificity of only 57% for diagnosis of osteomyelitis.[363]

Other Radiolabeled Products: Other inflammatory mediators have also been labeled and include Tc-99m-nanocolloid which accumulates in the reticuloendothelial system by being phagocytosed by macrophages, endothelial cells, and neutrophils;[363] In-III-labeled non-specific IgG;[367] Tc-99m- or In-III-labeled monoclonal antibodies to adhesion molecules such as E-selectin associated with inflammatory cell migration; and Tc-99m-labeled tetraphenylporphyrin sulfonate, which localize to histamine receptors on inflammatory cells at the site of infection.[362] While these products may overcome some of the previously mentioned problems with gallium-67 citrate and labeled leukocytes, their specificity and sensitivity for diagnosing osteomyelitis associated with a long-bone fracture is unknown.

Technetium-Labeled Ciprofloxacin: Technetium-labeled ciprofloxacin (Infecton; Tc-CIPRO) is one method that has been shown in several studies to distinguish infection from inflammation.[376-380] Ciprofloxacin binds to bacterial DNA gyrase of both sensitive and resistant bacteria, as well as both resting and actively multiplying bacteria, and does not bind to dead bacteria. Ciprofloxacin reportedly penetrates abscesses and may accumulate in inflammatory cells. Technetium-CIPRO does not localize in the bone marrow like labeled leukocytes and local accumulation is independent of the patient's leukocyte count. Technetium-CIPRO is stable *in vivo*. Advantages of Tc-CIPRO over other methods of nuclear scintigraphy for detecting infection include the reported high specificity, handling of blood is not required, there are low levels of radioactivity, and there is minimal time, technical skills, and laboratory equipment required for preparation because there is a commercially available kit. The sensitivity of Tc-CIPRO for diagnosing infection and osteomyelitis was reported to be between 70 and 84%, and the specificity 91 to 96%.[376,377,379] The reported causes of false positive results were fractures and accumulation of Tc-CIPRO in neutrophils and activated macrophages at a site of sterile inflammation.[377] Treatment with antibiotics, and subsequent bacterial death, may cause a false negative result.[377,379] Because of its high specificity for infection, Tc-CIPRO may be a useful method for early diagnosis of infected fracture site. There have been no controlled studies evaluating the use of Tc-CIPRO for differentiation of infected and non-infected fractures.

The purpose of part of this study (Chapter 4) was to evaluate the use of Tc-PO for assessing fracture healing and to compare the use of Tc-PO and –CIPRO for diagnosing

osteomyelitis associated with fractures in a non-union and infected non-union rabbit model.

Serum Bone Markers

Serum bone markers have been used traditionally to evaluated systemic bone diseases, particularly osteoporosis and Paget's disease.[381-385] More recently they have been used to assess fracture healing.[163,170,386-414] The advantage of measuring serological markers of bone resorption and formation for detection of non-union and infected non-union are that it is easier, less invasive, more economical and does not require general anesthesia or prolonged restraint compared to imaging techniques, and may be useful to detect abnormalities earlier.[170]

Osteonecrosis associated with the initial injury and surgical treatment, infection, bone resorption, lameness, reduced activity, immobilization, physical unloading of the limb, remodeling, as well as soft tissue injury, hemorrhage, infection, and systemic diseases may all affect serum bone marker concentration.[391,409] However, despite the potential for multiple causes of alteration in serum bone marker concentration, studies have indicated that they may be useful for evaluating fracture healing. Further studies are required, however, to determine the effects of these factors on the usefulness of serum bone marker concentration for evaluating fracture healing.

Bone Formation

Markers of bone formation include OC, bone-specific alkaline phosphatase (BS-ALP), and procollagen type I carboxy (C) or amino (N) -terminal peptide.

Osteocalcin: Osteocalcin is the most abundant non-collagenous protein in bone and is a specific product of osteoblasts.[386] Although OC is thought to be important in matrix mineralization, the precise function of OC is unknown.[387,388] A fraction of the OC molecule is released into the blood during incorporation of OC into bone during bone formation.[389] and serum levels of OC are thought to reflect osteoblastic activity accurately.[390]

It is important to recognize that there is variability in OC, as well as BS-ALP, because of circadian, seasonal, age- related, and hormonal factors. Additional variability between OC assays is associated with the heterogeneity of circulating OC. There are circulating intact OC molecules (36%) as well as fragments from proteolytic hydrolysis of peptide bonds involving arginine residues, including the large N-terminal mid fragment (30%), and smaller N-terminal, mid, and C-terminal fragments (34%; Figure 4a).[415] Proposed sources of fragmented molecules include bone resorption, and proteolysis in blood or other tissues. Therefore, OC can be measured as an intact molecule or the N-terminal mid fragment. While measurement of the N-terminal mid fragment has the advantage of being more stable during storage resulting in less variability associated with degradation,[391] the actual concentration with this method may be misleading because there may be multiple fragments measured for each OC molecule. The OC concentration will also be lower if there is hemolysis and lipemia.[415]

Studies have shown an increase in OC following fracture.[391-393] A significant increase in OC has been reported following fracture with peaks at 2-4,[396] 6,[389] 8,[391,392] 16,[393-395] and 24[391] weeks. In the latter study, OC increased from week 8 to 24, which was the completion of the study.[391] There appears to be a lot of variability in the pattern of

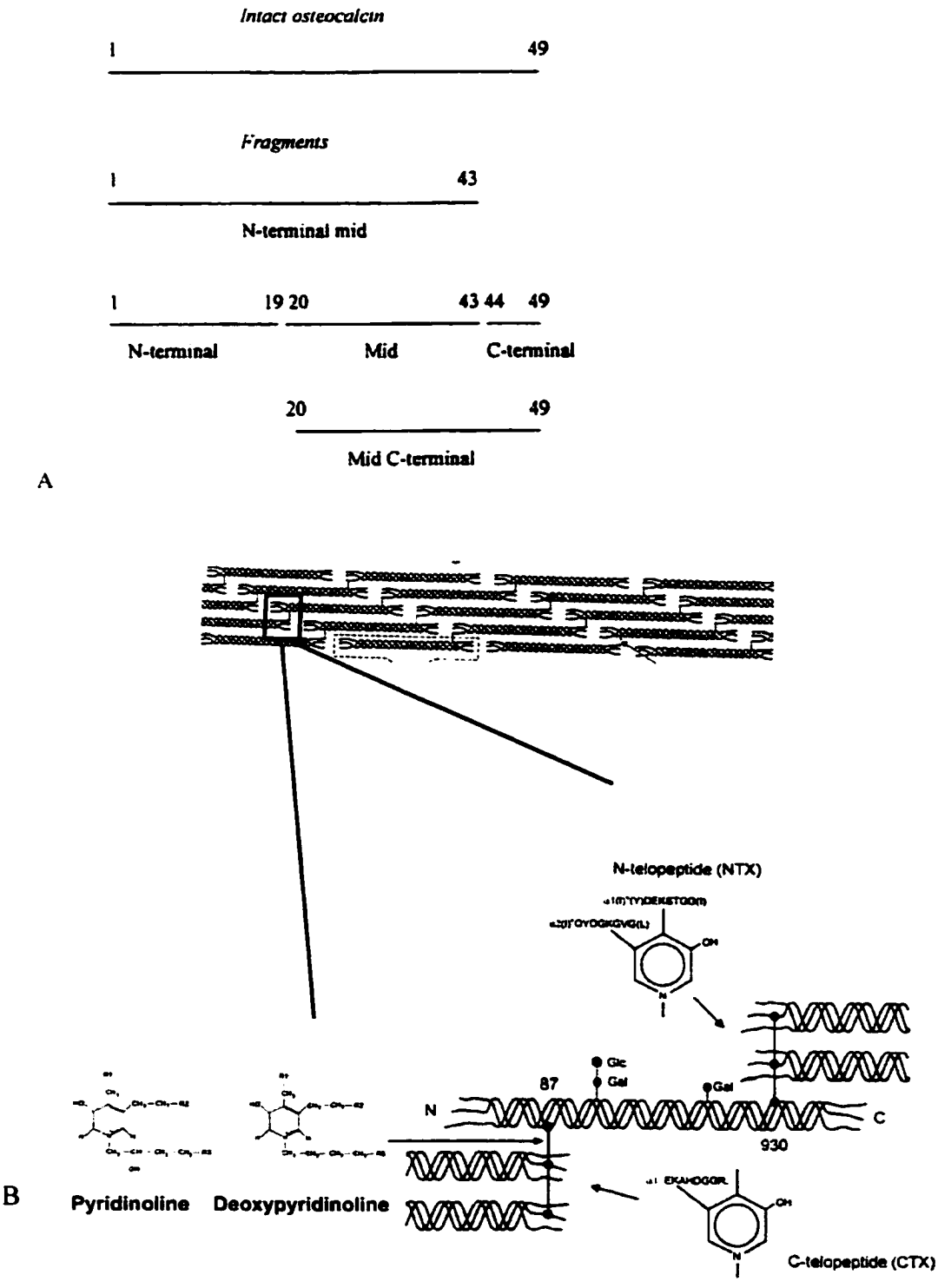

Figure 4A. A schematic illustration of the both the intact osteocalcin molecule and the fragments. B. A schematic illustustration of N- and C-terminal telopeptides, and pyridinoline and deoxypyridinoline crosslinks. Adapted from Naylor and Eastell[415] and Kraenzlin and Seibel[417].

change in OC concentration between different types of fractures. For example, OC increased from week 8 in patients with osteosynthesis for femoral neck fractures and not in patients with hemiarthroplasty or vertebral compression fractures.[391] Similarly, in another study patients with hip fracture repair had a postoperative increase in OC, whereas patients with hip prosthesis did not, possibly because the fracture site was removed.[410]

Recently, researchers have begun to evaluate OC for differentiating non-union from normal fracture healing. Patients with high-energy fracture and delayed healing were found to have lower OC at various times during fracture healing compared to patients with normal healing.[389,397] In the same study, patients with delayed healing had prolonged elevations, whereas in patients with normal unions the levels decreased after 6 weeks.[389]While these studies suggest that OC concentration may be useful for differentiating normal union from non-union, other studies have shown no difference between patients with normal and impaired healing.[398] Therefore, further studies are required to more definitively define the changes in OC concentration during fracture healing.

There have been very few studies evaluating the use of OC for diagnosis of osteomyelitis. One author concluded that OC is not a useful marker of chronic osteomyelitis;[399] however, other studies have found an increase in OC in infected femoral fractures repaired with intramedullary nail. In the latter study the OC peaked at week 2 in infected fractures; however, there were no non-infected controls and the duration of the study was only 4 weeks.[400] Therefore, conclusions on the use of serum markers to differentiate infected from non-infected fractures could not be made from this study.

Bone-Specific Alkaline Phosphatase: BS-ALP is secreted by osteoblasts and is involved in calcification of bone matrix. Alkaline and acid phosphatase are found in osteoblasts at the fracture site immediately post fracture, and it is thought to play a role in the formation and mineralization of the protein matrix of bone.[401,402]

Although an increase in total ALP following fracture has been reported,[395,397,403,404] it is not a useful marker of bone formation because of a lack of specificity for bone as a result of production by most body tissues including the liver and kidney. While a single gene encodes liver-specific ALP and BS-ALP, posttranslational modifications have enabled specific detection of BS-ALP. Bone-specific ALP, however, has been shown to increase at various times between 8 and 12 weeks after fracture.[389,406] In one study, an increase in ALP occurred earlier than OC,[395] most likely because BS-ALP is involved in the initiation of mineralization whereas OC is actually released during the mineralization process.

The concentration of BS-ALP has also been used to evaluate non-unions. Bone-specific-ALP was lower in patients with delayed healing between 4 and 7 weeks,[398] yet another study showed no difference in BS-ALP between normal and delayed healing, but there was a difference in both BS-ALP and markers of type I collagen late in healing at 20 weeks.[412]

As with OC there have been limited studies evaluating the association between osteomyelitis and BS-ALP. Total ALP was shown to be significantly increased in patients with chronic osteomyelitis,[407] and was increased in dogs with infected fracture, peaking at 2 weeks and then returning to normal values.[400] As mentioned previously, there were no non-infected controls in the latter study.

Procollagen Type I (PICP) and III (PIIINP) Terminal Peptide: Types I and III collagen are synthesized from larger types I and III procollagens. The carboxy terminal extension peptide of type I procollagen is released during synthesis of type I collagen. The amino-terminal extension peptide of type III procollagen is partly cleaved during formation type III collagen, and also released during degradation, therefore represents collagen III turnover.[408]

Several studies have evaluated turnover of collagen I and III in fracture healing.[170,408,412] Turnover of collagen increases after fracture, reaching peak values at 2 weeks and then decreasing.[408] In normal healing, there is an early increase in PIIINP and later a more gradual increase in PICP.[412] This represents the type III collagen in granulation tissue and type I collagen in bone.[412]

Humans with delayed healing of tibial fractures had a trend toward higher PICP and PIIINP at 2 weeks, compared to humans with normal healing.[408] Therefore, delayed healing may be associated with an increase in turnover of types I and III collagen. There was a higher relative increase in PIIINP compared with PICP, suggesting greater synthesis of type III compared to type I collagen early in fracture healing.[408] Delayed healing could, therefore, be a result of an increase in collagen turnover, or the severity of the injury may require an increase in turnover and subsequently delayed healing. In one study, there was an increase in PIIINP at 10 weeks in patients with delayed union; however, the evidence for decreased osteoblastic activity, that is decreased PICP and BS-ALP, did not appear to occur until week 20.[170] This study[170] suggests that normal healing was impaired and healing with type III collagen was occurring; that is, while there was adequate production of both type I and III collagen, there was excessive type III collagen

production. The inadequate osteoblastic response late in healing could have been a result rather than a cause of delayed union. Other studies have also shown excessive type III collagen produced by osteoblasts in non-union.[163] Because soft tissue damage from trauma or surgery may cause alterations in collagen markers, the role of soft tissue injury on collagen markers needs to be determined before collagen markers can be used to evaluate fracture healing and osteomyelitis.[408,412]

Markers of Bone Resorption

Markers of bone resorption include hydroxyproline, hydroxylysine, urinary calcium, pyridinoline and deoxypyridinoline crosslinks (PYR and DPYR), C- and N-terminal telopeptides of type I collagen (IC(N)TP), and tartrate-resistant acid phosphatase (TRAP)[395,414,416,417] which is a measure of osteoclastic activity. Most of the studies evaluating fracture healing and osteomyelitis have measured PYR, DPYR and IC(N)TP. Type I collagen makes up greater than 90% of the bone matrix, during bone resorption, collagen is degraded, and PYR, DPYR, and IC(N)TP are released into the blood (Figure 4b).

Pyridinoline and Deoxypyridinoline Crosslinks: Both PYR and DPYR are non-reducible crosslinks that stabilize collagen molecules within extracellular matrix, and are formed as a posttranslational modification of collagen molecules following secretion of the molecule into the extracellular matrix.[416] They covalently link collagen molecules between two telopeptides and a triple-helical sequence at two intermolecular sites.[417] Deoxypyridinoline reflects specific bone and dentine, whereas PYR is abundant in all connective tissues and therefore less specific for bone.[391]

An increase in serum and urinary PYR and DPYR was found at 2 and 6 weeks after fracture.[391,396] Urinary PYR and DPYR started to increase at week 1, peaked between week 4 and 8, and returned to normal by week 24 in patients with hemiarthroplasty and osteosynthesis for hip fractures. However, there was no change in urinary PYR or DPYR in patients with vertebral compression fractures.[391] Other studies have shown no changes in markers of bone resorption with fracture healing.[395]

C- and N-Terminal Telopeptides of Type I Collagen: ICTP have been shown to increase at 2 and 6 weeks after fracture.[391,396] While patients with delayed healing were shown to have a trend toward an increase in telopeptide at 2 weeks in one study,[408] other studies have shown no difference in concentration in patients with normal and delayed healing fractures.[385,398] The initial increase in ICTP may be associated with bone necrosis from the injury and surgery, and later increases may reflect the remodeling phase of healing.[408] Collagen cross-linked N-telopeptides have been used successfully as a marker for evaluating particulate osteolysis,[413] and ICTP increased over a 4 week period in dogs with infected femoral fractures.[400]

There have been no controlled studies evaluating the use of serum markers of bone formation and resorption for assessing fracture healing and early diagnosis of osteomyelitis. The purpose of the final part of this study, as outlined in Chapter 5, was to evaluate OC, BS-ALP, and DPYR for early diagnosis of non-union and infected non-union in a rabbit model.

References

1. Praemer A, Furner S, Rice DP. Musculoskeletal conditions in the United States. Park Ridge, IL, Am Acad Orthop Surg; 1992.
2. Praemer A, Furner S, Rice DP. Musculoskeletal conditions in the United states. Rosemont, IL, Am Acad Orthop Surg; 1999.
3. Calandruccio R (Ed) Musculoskeletal System Research: Current and Future Research Needs. Chicago: American Academy of Orthopedic Surgeons, 1981.
4. Johnson EE, Urist MR, Finerman AM. Resistant nonunion and partial or complete segmental defects of long bones. Clin Orthop Rel Res 1992; 277:229-237.
5. Friedlaender GE, Perry CR, Dean CJ, Cook SD, Cierny G, Muschler GF, Zych GA, Calhoun JH, LaForte AJ, Yin S. Osteogenic protein-1 (bone morphogenetic protein-7) in the treatment of tibial nonunions: A prospective, randomized clinical trial comparing rhOP-1 with fresh bone graft. J Bone Joint Surg 2001; 83A:S151-S158.
6. Yelin E, Callahan LF. The economic cost and social and psychological impact of musculoskeletal conditions. Arthritis Rheum 1995; 38:1351-1362.
7. Auer JA, Watkins JP. Treatment of radial fractures in adult horses: An analysis of 15 clinical cases. Equine Vet J 1987; 19: 103-110.
8. Sanders-Shamis M, Bramlage LR, Gable AA. Radius fractures in the horse: A retrospective study of 47 cases. Equine Vet J 1986; 18:432-437.
9. Crawford WH, Fretz PB. Long bone fractures in large animals. A retrospective study. Vet Surg 1985; 14:295-302.

10. Hance SR, Bramlage LR, Schneider RK, Embertson RM. Retrospective study of 38 cases of femur fractures in horses less than one year of age. Equine Vet J 1992; 24:357-363.

11. Ducharme NG, Nixon AJ. Delayed Union, Non-Union, and Malunion. In Nixon AJ: Equine Fracture Repair. Philadelphia, WB Saunders Co., 1996, p 354-358.

12. Bonnarens F, Einhorn TA. Production of a standard closed fracture in laboratory animal bone. J Orthop Res 1984; 2:97-101.

13. Oni OO. Protein immunohistochemistry as a means of unraveling the mysteries of fracture repair. Injury 1995; 26:523-525.

14. Bourque WT, Gross M, Hall BK. A reproducible method for production and quantifying the stages of fracture repair. Lab Anim Sci 1992; 42:369-374.

15. Hollinger JO, Kleinschmidt JC. The critical size defect as an experimental model to test bone repair materials. J Craniofacial Surg 1990; 1:60-68.

16. Meyer RA, Meyer MH, Phieffer LS, Banks DM. Bone morphogenetic proteins and osteocalcin mRNA expression during fracture healing in young and older rats. Proc 45th Ann Mtg Orthop Res Soc 1999; 475.

17. Becerra J, Andrades JA, Ertl DC, Sorgente N, Nimni ME. Demineralized bone matrix mediates differentiation of bone marrow stromal cells in vitro: Effect of age of cell donor. J Bone Min Res 1996; 11:1703-1714.

18. Andrew JG, Hoyland J, Andrew SM, Freemont AJ, Marsh D. Demonstration of TGF-β1 mRNA by *in situ* hybridization in normal human fracture healing. Calcif Tissue Int 1993; 52:74-78.

19. Andrew JG, Hoyland J, Freemont AJ, Marsh D. Insulin-like growth factor gene expression in human fracture callus. Calcif Tissue Int 1993; 53:97-102.

20. Andrew JG, Hoyland J, Freemont AJ, Marsh D. Platelet-derived growth factor expression in normally healing human fractures. Bone 1995; 16:455-460.

21. Schmitz JP, Hollinger JO. The critical size defect as an experimental model for craniomandibulofacial nonunions. Clin Orthop Rel Res 1986; 205:299-308.

22. Schmitz JP, Schwartz Z, Hollinger JO, Boyan BS. Characterization of rat calvarial nonunion defects. Acta Anat 1990; 138:185-192.

23. Key JA. The effect of a local calcium depot on osteogenesis and healing of fractures. J Bone Joint Surg 1934; 16A:176-184.

24. Toombe JP, Wallace LJ, Bjorling DE, Rowland GN. Evaluation of Key's hypothesis in the feline tibia: an experimental model for augmented bone healing studies. Am J Vet Res 1985; 46:513-518.

25. Nilsson OS, Urist MR, Dawson EG, Schmalzried TP, Finerman GAM. Bone repair induced by bone morphogenetic protein in ulna defects in dogs. J Bone Joint Surg 1986; 68B:635-642.

26. Heckman JD, Boyan DB, Aufdemorte TB, Abbott JT. The use of bone morphogenetic protein in the treatment of nonunion in a canine model. J Bone Joint Surg 1991; 73A: 750-764.

27. Rigby H. The pathophysiology of fracture healing and non-union. Mechanical influences. DM Thesis. University of Nottingham, Nottingham, 1986.

28. Watkins P. A study of mechanical influences on fracture healing. PhD Thesis. University of Bristol, Bristol, 1986.

29. Oni OO. A non-union model of the rabbit tibial diaphysis. Injury 1995; 26:619-622.

30. Brownlow HC, Simpson AHRW. Metabolic activity of a new atrophic nonunion model in rabbits. J Orthop Res 2000; 18:438-442.

31. Fujita M, Matsui N, Tsunoda M, Saura R. Establishment of a non-union model using muscle interposition without osteotomy in rats. Kobe J Med Sci 1998; 44:217-233.

32. Kirker-Head CA. Recombinant bone morphogenetic proteins: Novel substances for enhancing bone healing. Vet Surg 1995; 24:408-419.

33. Cook SD, Wolfe MW, Salkeld SL, Rueger DC. Effect of recombinant human osteogenic protein-1 on healing of segmental defects in non-human primates. J Bone Joint Surg 1995; 77A:734-750.

34. Yasko AW, Lane JM, Fellinger EJ, Rosen V, Wozney JM, Wang EA. The healing of segmental bone defects, induced by recombinant human bone morphogenetic protein (rhBMP-2). J Bone Joint Surg 1992; 74A:659-670.

35. Claes L, Augat P, Suger G, Wilke HJ. Influence of size and stability of the osteotomy gap on the success of fracture healing. J Orthop Res 1997; 15:577-584.

36. Bostrom M, Lane JM, Tomin E, Browne M, Berberian W, Turek T, Smith J, Wozney J, Schildhauer T. Use of bone morphogenetic protein-2 in the rabbit ulnar nonunion model. Clin Orthop Rel Res 1996; 327:272-282.

37. Mader JT. Animal Models of Osteomyelitis. Am J Med 1985; 78:213-217.

38. Rissing JP. Animal Models of Osteomyelitis. Infect Dis Clin N Am 1990; 4:377-390.

39. Scheman L, Janota M, Lewin P. The production of experimental osteomyelitis. J Am Med Assoc 1941; 117:1525-1529.

40. Norden, CW and Kennedy E. Experimental osteomyelitis. I. A description of the model. J Infect Dis 1970; 122:410-418.

41. Kaarsemaker S, Walenkamp GHIM, vd Bogaard AEJ. New model for chronic osteomyelitis with *Staphylococcus aureus* in sheep. Clin Orthop Rel Res 1997; 339:246-252.

42. Eerenberg JP, Patka P, Haarman HJTHM. A new model for posttraumatic osteomyelitis in rabbits. J Invest Surg 1994; 7:453-465.

43. Smeltzer MS, Thomas JR, Hickmon SG, Skinner RA, Nelson CL, Griffith D, Parr TR, Evans RP. Characterization of a rabbit model of Staphylococcal osteomyelitis. J Orthop Res 1997; 15:414-421.

44. Zak O, Zak F, Rich R, Tosch W, Dradolfer F, Scheld WM. Experimental staphylococcal osteomyelitis in rats: Therapy with rifampin and cloxacillin alone or in combination. In Perti P, Grassi G (Eds): Current Chemotherapy and Immunotherapy. Washington, American Society for Microbiology, 1982, p 973-974.

45. Rissing JP, Buxton TB, Weinstein RS, Shockley RK. Model of experimental chornic osteomyelitis in rats. Infect Immun 1985; 47:581-586.

46. Rodeheaver GT, Rukstalis D, Bono M, Bellamy WA. A new model of bone infection used to evaluate the efficacy of antibiotic-impregnated polymethylmethacrylate cement. Clin Orthop Rel Res 1983; 178:303-311.

47. Andriole VT, Nagel DA, Southwick WO. Chronic Staphylococcal osteomyelitis: An experimental model. Yale J Biol Med 1974; 1:33-39.

48. Worlock P, Slack R, Harvey L, Mawhinney R. An experimental model of post-traumatic osteomyelitis in rabbits. Br J Exp Pathol 1988; 69:235-244.

49. Jacob E, Arendt DM, Brook I, Durham LC, Falk MC, Schaberg SJ. Enzyme-linked immunosorbent assay for detection of antibodies to *Staphylococcus aureus* cell walls in experimental osteomyelitis. J Clin Microbiol 1985; 22:547-552.

50. Passl R, Müller C, Zielinski CC, Eibl MM. A model of experimental post-traumatic osteomyelitis in guinea pigs. J Trauma 1984; 24:323-326.

51. Schulz S, Steinhart H, Mutters R. Chronic osteomyelitis in a new rabbit model. J Invest Surg 2001; 14:121-131.

52. Deysine M, Rosario E, Isenberg HD. Acute hematogenous osteomyelitis: an experimental model. Surgery 1976; 79:97-99.

53. Walen JL, Fitzgerald RH, Morrissy RT. A histological study of acute hematogenous osteomyelitis following physeal injuries in rabbits. J Bone Joint Surg 1988; 70A:1383-1392

54. Hill PF, Watkins PE, Clasper JC, Parker SJ. Intramedullary nailing of a contaminated fracture in an experimental model. Proc 45th Ann Mtg Orthop Res Soc 1999; p 497

55. Arens S, Schlegel U, Printzen G, Ziegler WJ, Perren SM, Hansis M. Influence of materials for fixation implants on local infection. J Bone Joint Surg 1996; 78B:647-651.

56. Melcher GA, Claudi B, Schlegel U, Perren SM, Printzen G, Munzinger J. Influence of type of medullary nail on the development of local infection. J Bone Joint Surg 1994; 76B:955-959.

57. Fitzgerald RH. Experimental osteomyelitis: description of a canine model and the role of depot administration of antibiotics in the prevention and treatment of sepsis. J Bone Joint Surg 1983; 65A:371-380.

58. Feied CF. Mechanism of action of sclerosing agents and rationale for selection of a sclerosing solution. American Vein Institute (www.veins.com) 2001; p 1-8.

59. Christensen GD, Simpson WA, Bisno AL, Beachey EH. Experimental foreign body infections in mice challenged with slime-producing Staphylococcus epidermis. Infect Immun 1983; 40:407-410.

60. Petty W, Spanier S, Shuster JJ, Silverthorne C. The influence of skeletal implants on incidence of infection. J Bone Joint Surg 1985; 67A:1236-1244.

61. Grewe SR, Stephens BO, Perlino C, Riggins RS. Influence of internal fixation on wound infections. J Traum Injury Infect Crit Care 1987; 27:1051-1054.

62. Tsukayama DT. Pathophysiology of posttraumatic osteomyelitis. Clin Orthop Rel Res 1999; 360:22-29.

63. Moore RM, Schneider RK, Kowalski J, Bramlage LR, Mecklenberg LM, Kohn CW. Antimicrobial susceptibility of bacterial isolates from 233 horses with musculoskeletal infection during 1979-1989. Equine Vet J 1992; 24:450-456.

64. Murray PR, Rosenthal KS, Kobayashi GS. Chapter 22: Staphylococcus and Related Organisms. In Murray PR, Rosenthal KS, Kobayashi GS (Ed): Medical Microbiology, 3rd Ed, Mosby, St Louis MO, 1998; p 175-188.

65. Tally FP, Barg NL. Chapter 11: Staphylococci: Abscesses and Other Diseases. In Schaechter M, Engleberg NC, Eisenstein B, Medoff G (Eds): Mechanics of Microbial Disease, 3rd Ed, Lipincott, Philadelphia, PA, 1999; p 135-142.

66. Joyner AL, Smith DT. Acute staphylococcus osteomyelitis. Surg Gynecol Obstet 1936; 63:1-6.

67. Worlock P, Slack R, Harvey L, Mawhinney R. The prevention of infection in open fractures. J Bone Joint Surg 1988; 70A:1341-1347.

68. Chen X, Kidder LS, Lew WD. Osteogenic protein-1 induced bone formation in an infected segmental defect in the rat femur. J Orthop Res 2002; 20:142-150.

69. McKibbin B. The biology of fracture healing in long bones. J Bone Joint Surg 1978; 60B:150-162.

70. Brighton CT, Hunt RM. Early histological and ultrastructural changes in medullary fracture callus. J Bone Joint Surg 1991; 73A:832-847.

71. Andrew JG, Andrew SM, Freemont AJ, Marsh DR. Inflammatory cells in normal human fracture healing. Acta Orthop Scand 1994; 65:462-466.

72. Hendricson A, Hulth A, Johnell O. The occurrence of accessory immunological cells in bone induction. Clin Orthop Rel Res 1991; 264:270-277.

73. Lee FYI, Choi YW, Behrens FF, DeFouw DO, Einhorn TA. Programmed removal of chondrocytes during endochondral fracture healing. J Orthop Res 1998; 16:144-150.

74. Diefenderfer DL, Brighton CT. Microvascular pericytes express aggrecan message with is regulated by BMP-2. Biochem and Biophys Res Comm 2000; 269:172-178.

75. Sandberg M, Aro H, Multimaki P, Aho H, Vuorio E. In situ localization of collagen production by chondrocytes and osteoblasts in fracture callus. J Bone Joint Surg 1989; 71A:69-77.

76. Eyre-Brook AL The periosteum: its function reassessed Clin Orthop 1983; 189:300-307.

77. Takagi K, Urist MR. The role of bone marrow in bone morphogenetic protein-induced repair of femoral massive diaphyseal defects. Clin Orthop Rel Res 1982; 171:224-31.

78. Markel MD, Wikenheiser MA, Chao EYS. Formation of bone in tibial defects in a canine model. J Bone Joint Surg 1991: 915-923.

79. Stafford HJ, Roberts MT, Oni OOA, Hay J, Gregg P. Localization of bone-forming cells during fracture healing by osteocalcin immunocytochemistry: An experimental study of the rabbit tibia. J Orthop Res 1994; 12:29-39.

80. Scammell BE, Roach HI. A new role for the chondrocyte in fracture repair: endochondral ossification includes direct bone formation by former chondrocytes. J Bone Min Res 1996; 11: 737-745.

81. Oni OOA. Protein immunohistochemistry as a means of unraveling the mysteries of fracture repair. Injury 1995; 26:523-525.

82. Hughes SS, Hicks DG, O'Keefe RJ, Hurwitz SR, Crabb ID, Krasinskas AM, Loveys L, Puzas JE, Rosier RN. Shared phenotypic expression of osteoblasts and chondrocytes in fracture callus. J Bone Min Res 1995; 10:533-544.

83. Sandberg MM, Aro HT, Vuorio EI. Gene expression during bone repair. Clin Orthop Rel Res 1993; 289:292-312.

84. Yamazaki M, Jajeska RJ, Moriya H, Einhorn TA. Role of osteonectin during fracture healing. Proc 43rd Ann Mtg Orthop Res Soc 1997; p 254.

85. Jingushi S, Joyce ME, Bolander ME. Genetic expression of extracellular matrix proteins correlates with histologic changes during fracture repair. J Bone Min Res 1992; 7:1045-1055.

86. Hirakawa K, Hirota S, Ideda T, Amaguchi A, Takemura T, Nagoshi J, Yoshiki S, Suda T, Kitamura Y, Nomura S. Localization of the mRNA for bone matrix proteins during fracture healing as determined by *in situ* hybridization. J Bone Min Res 1994; 9:1551-1557.

87. Bostrom MPG, Lane JM, Berberian WS, Missri AA, Tomin E, Weiland A, Doty SB, Glaser D, Rosen VM. Immunolocalization and expression of bone morphogenetic proteins 2 and 4 in fracture healing. J Orthop Res 1995; 13:357-367.

88. Bolander ME. Regulation of fracture repair by growth factors. Proc Soc Exp Biol Med 1992; 200:165-170.

89. Bourque WT, Gross M, Hall BK. Expression of four growth factors during fracture repair. Int J Dev Biol 1993; 37:573-579, 1993.

90. Kovacs EJ. Fibrogenic cytokines: the role of immune mediators in the development of scar tissue. Immunol Today 1991; 12: 17-23.

91. Khan SN, Bostrom MGP, Lane JM. Bone growth factors. Orthop Clin N Am 2000; 31:375-387.

92. Hauschka PV, Mavrakos AE, Iafrati MD, Doleman SE, Klagsbrun M. Growth factors in bone matrix: Isolation of multiple types by affinity chromatography on heparin-sepharose. J Biol Chem 1986; 261:12665-12674.

93. Seyedin SM, Thomas TC, Thompson AY, Rosen DM, Piez KA. Purification and characterization of two cartilage-inducing factors from bovine demineralized bone. Proc Natl Acad Sci USA 1985; 82:2267-2271.

94. Frolik CA, Ellis LF, Williams DC. Isolation and characterization of insulin-like growth factor-II from human bone. Biochem Biophys Res Commun 1988; 151:1011-1018.

95. Hadjiargyrou M, Ahrens W, Rubin CT. Temporal expression of the chondrogenic and angiogenic growth factor CR61 during fracture repair. J Bone Min Res 2000; 15:1014-1023.

96. Si XH, Jin Y, Yang LJ, Tipoe GL, White FH. Expression of BMP-2 and TGF-β1 mRNA during healing of the rabbit mandible. Eur J Oral Sci 1997; 105:325-330.

97. Kasperk CH, Wergedal JE, Mohan S, Long DL, Lau KH, Baylink DJ. Interaction of growth factors present in bone matrix and bone cells: effects on DNA synthesis and alkaline phosphatase. Growth Factors 1990; 3:147-55.

98. Bonewald LF, Mundy GR. Role of Transforming growth factor-beta in bone remodeling. Clin Orthop Rel Res 1990; 250:261-276.

99. Joyce ME, Jingushi S, Bolander ME. Transforming growth factor-beta in the regulation of fracture repair. Orthop Clin North Am 1990; 21:199-209.

100. Joyce ME, Roberts AB, Sporn MB, Bolander ME. Transforming growth factor-beta and the initiation of chondrogenesis and osteogenesis in the rat femur. J Cell Biol 1990; 110:2195-2207.

101. Battegay EJ, Ranes EW, Seifert RA, Bowen-Pope DF, Ross R. TGF-beta induces bimodal proliferation of connective tissue cells via complex control of an autocrine PDGF loop. Cell 1990; 63:515-524.

102. Saadeh PB, Mehrara BJ, Steinbrech DS, Dudziak ME, Greenwald JA, Luchs JS, Spector JA, Ueno H, Gittes GK, Longaker MT. Transforming growth factor-β1 modulates the expression of vascular endothelial growth factor by osteoblasts. Am J Physiol 1999; 277:C628-C637.

103. Massague J. The transforming growth factor-B family. Annu Rev Cell Biol 1990; 6:597.

104. Canalis E, McCarthy T, Centrella M. Growth factors and the regulation of bone remodeling. J Clin Invest 1988; 81:277.

105. McCarthy TL, Centrella M, Canalis E. Regulatory effects of insulin-like growth factors I and II on bone collagen synthesis in rat calvarial cultures. Endocrinology 1989; 124:301.

106. Fujii H, Kitazawa R, Maeda S, Mizuno K, Kitazawa S. Expression of platelet-derived growth factor proteins and their receptor alpha and beta mRNAs during fracture healing in the normal mouse. Histochem Cell Biol 1999; 112:131-138.

107. Andrew JG, Hoyland JA, Freemont AJ, Marsh DR. Platelet-derived growth factor expression in normally healing human fractures. Bone 1995; 16:455-460.

108. Muller R, Bravo R, Burckhardt J, Currant T. Induction of *c-fos* gene and protein by growth factors precedes activation of *c-myc*. Nature 1984; 312:716.

109. Nash T, Howlett CR, Martin C, Steele J, Johnson KA, Hicklin DJ. The effect of PDGF on tibial osteotomies in rabbits. Calcif Tisssue Int 1992; 50:A11.

110. Canalis E, McCarthy TL, Centrella M. Effects of platelet-derived growth factor on bone formation *in vitro*. J Cell Physiol 1989; 140:530-537.

111. Canalis E., Centrella M, McCarthy T. Effects of basic fibroblast growth factor on bone formation *in vitro*. J Clin Invest. 1998; 81:1572-1577.

112. Jingushi S, Hydemann A, Kana SK, Macey LR, Bolander ME. Acidic fibroblast growth factor (aFGF) injection stimulates cartilage enlargement and inhibits cartilage gene expression in rat fracture healing. J Orthop Res 1990; 8:364-371.

113. Collin-Osdoby P. Role of vascular endothelial cells in bone biology. J Cell Biochem 1994; 55:304-309.

114. Garcia-Ramirez M, Toran N, Anduluz P, Carrascosa A, Audi L. Vascular endothelial growth factor is expressed in human fetal growth cartilage. J Bone Min Res 2000; 15:534-540.

115. Horner A, bishop NJ, Bord S, Beeton C, Kelsall AW, Coleman N, Compston JE. Immunolocalisation of vascular endothelial growth factor (VEGF) in human neonatal growth plate cartilage. J Anat 1999; 194:519-24.

116. Ferrara N. Molecular and biological properties of vascular endothelial growth factor. J Mol Med 19991 77:527-43.

117. Gerber HP, Vu TH, Ryan AM, Kowalski J, Werb Z, Ferrara N. VEGF couples hypertrophic cartilage remodeling, ossification, and angiogenesis during endochondral bone formation. Nature Medicine 5:623-8, 1999.

118. Grosskreutz CL, Anand-Apte, Dpulaa C, Quinn TP, Terman BI, Zetter B, D'Amore PA. Vascular endothelial growth factor-induced migration of vascular smooth muscle cells in vitro. Microvascular Res 1999; 58:128-136.

119. Corral CJ, Siddiqui A, Wu L, Farrell CL, Lyons D, Mustoe TA. Vascular endothelial growth factor is more important than basic fibroblastic growth factor during ischemic wound healing. Arch Surg 1999; 134:200-5.

120. Boyer MI, Towler DA, Gelberman RH. Expression of messenger RNA for vascular endothelial growth factor during the early phase of flexor tendon healing. Proc 45th Ann Mtg Orthop Res Soc, 1999, p1082.

121. Harada S, Nagy JA, Sullivan KA, Thomas KA, Endo N, Rodan GA, Rodan SB. Induction of vascular endothelial growth factor expression by prostaglandin E2 and E1 in osteoblasts. J Clin Invest 1994; 93:2490-2496.

122. Goad DL, Rubin J, Wang H, Tashjian AH, Patterson C. Enhanced expression of vascular endothelial growth factor in human SaOS-2 osteoblast-like cells and murine osteoblasts induced by insulin-like growth factor I. Endocrinology 1996; 137:2262-2268.

123. Wang DS, Yamazaki K, Nohtomi K, Hizume K, Ohsumi K, Shibuya M, Demura H, Sato K. Increase of vascular endothelial growth factor mRNA expression by 1.25-dihydroxyvitamin D3 in human osteoblast-like cells. J Bone Min Res 1996; 11:472-479.

124. Steinbrech DS, Mehrara BJ, Saadeh PB, Chin G, Dudziak ME, Gerrets RP, Gittes GK, Longaker MT. Hypoxia regulates VEGF expression and cellular proliferation by osteoblasts in vitro. Plastic Reconst Surg 1999; 104:738-747.

125. Street J, Winter D, Wang JH, Wakai A, McGuinness A, Redmond HP. Is human fracture hematoma inherently angiogenic? Clin Orthop Rel Res 2000; 378:224-237.

126. Olmedo ML, Landry PS, Sadasivan KK, Albright JA, Meek WD, Routh R, Marino AA. Regulation of osteoblast levels during bone healing. J Orthop Trauma 1999; 13:356-362.

127. Yamagiwa H, Tokunaga K, Hayami T, Hatano H, Uchida M, Endo N, Takahashi HE. Expression of metalloproteinase-13 (collagenase-3) is induced during fracture healing. Bone 1999; 25:197-203.

128. Murakami S, Noda M. Expression of Indian hedgehog during fracture healing in adult rat femora. Calcif Tissue Int 2000; 66:272-276.

129. Ito H, Akiyama H, Shigeno C, Iyama K, Matsouka H, Nakamura T. Hedgehog signaling molecules in bone marrow cells at the initial stage of fracture repair. Biochem Biophys Res Comm 1999; 262:443-451.

130. Oni OOA. Proto-oncogene expression during fracture repair. Injury Int J Care Injured 2000; 31:363-366.

131. Ohta S, Yamamuro T, Lee K, Okumura H, Kasai R, Hiraki Y, Ikeda T, Iwasaki R, Kikuchi H, Konishi J, Shigeno C. Fracture healing induces expression of the proto-oncogene *c-fos in vivo*. Fed Eur Biochem Soc 1991; 284:42-45.

132. Closs EI, Murray AB, Schmidt J, Schon A, Erfle V, Strauss PG. *c-fos* expression precedes osteogenic differentiation of cartilage cells in vitro. J Cell Biol 1990; 111:1313-23.

133. Urist MR. Bone: Formation by autoinduction. Science 1965; 150:893-899.

134. Wang EA, Rosen V, Cordes P. Purification and characterization of other distinct bone-inducing factors. Proc Natl Acad Sci USA 1988; 85; 9484-9488.

135. Rosen V, Wozney JM, Wang EA, Cordes P, Celeste A, McQuaid D, Kurtzberg L. Purification and molecular cloning of a novel group of BMPs and localization of BMP mRNA in developing bone. Connective Tissue Res 1989; 20:313-319.

136. Groeneveld EHJ, Burger EH. Bone morphogenetic proteins in human bone regeneration. Eur J Endocrin 2000; 142:9-21.

137. Wozney JM. Bone morphogenetic proteins. Prog Growth Factor Res 1989; 1:267-280.

138. Komaki M, Katagiri T, Suda T. Bone morphogenetic protein-2 does not alter the differentiation pathway of committed progenitors of osteoblasts and chondroblasts. Cell Tissue Res 1996; 284:9-17.

139. Lindholm TS, Urist MR. A quantitative analysis of new bone formation by induction in compositive grafts of bone marrow and bone matrix. Clin Orthop Rel Res 1980; 150:288-300.

140. Mayer H, Scutt AM, Ankenbauer T. Subtle differences in the mitogenic effects of recombinant human bone morphogenetic proteins-2 and –7 on DNA

synthesis in primary bone forming cells and identification of BMP-2/4 receptor. Calcified Tissue Int 1996; 58:249-255.

141. Cunningham NS, Paralkar V, Reddi AH. Osteogenin and recombinant bone morphogenetic protein 2B are chemotactic for human monocytes and stimulate transforming growth factor beta 1 expression. Proc Natl Acad Sci USA 1992; 89:11740-11744.

142. Postlethwaite AE, Raghow R, Stricklin G, Ballou L, Sampath TK. Osteogenic protein-1, a bone morphogenic protein member of the TGF-β superfamily, shares chemotactic but not fibrogenic properties with TGF-β. J Cell Physiol 1994; 161:562-570.

143. Lind M, Eriksen EF, Bunger C. Bone morphogenetic protein-2 but not bone morphogenetic protein-4 and –6 stimulates chemotactic migration of human osteoblasts, human marrow osteoblasts, and U2-OOS cells. Bone 1996; 18:53-57.

144. Yeh LC, Lee JC. Osteogenic protein-1 increases gene expression of vascular endothelial growth factor in primary cell cultures of fetal rat calvaria cells. Molecular Cellular Endocrinol 1999; 153:113-124.

145. Nissinen L, Pirila L, Heino J. Bone morphogenetic protein-2 is a regulator of cell adhesion. Exp Cell Res 1997; 230:377-385.

146. Sakou T. Bone morphogenetic proteins: From basic studies to clinical approaches. Bone 1998; 22:591-603.

147. Sampath TK, Rashka KE, Doctor JS, Tucker RF, Hoffmann FM. Drosophila TGF-B superfamily proteins induce endochondral bone formation in mammals. Proc Natl Acad Sci USA 1993; 90:6004-6008.

148. Yan J, Lianjia Y, White FH. An immunocytochemical study of bone morphogenetic protein in experimental fracture healing of the rabbit mandible. Chin Med Sci J 1994; 9 (2): 91-95

149. Lianjia Y, Yan J. Immunohistochemical observations on bone morphogenetic protein in normal and abnormal conditions. Clin Orthop Rel Res 257:249-256, 1990).

150. Ishidou Y, Kitajima I, Obama H, Maruyama I, Murata F, Imamura T, Yamada N, ten Dijke P, Miyazono K, Sakou T. Enhanced expression of type I receptors for bone morphogenetic proteins during bone formation. J Bone Min Res 10:1651-1659, 1995.

151. Nakase T, Nomura S, Yoshikawa H, et la. Transient and localized expression of bone morphogenetic protein 4 messenger RNA during fracture healing. J Bone Miner Res 9:651-9, 1994

152. Onishi T, Ishidou Y, Nagamine T, Yone K, Imamura T, Kato M, Sampath TK, ten Dijke P, Sakou T. Distinct and overlapping patterns of localization of bone morphogenetic protein (BMP) family members and a BMP type II receptor during fracture healing in rats. Bone 1998; 22:605-612.

153. Schmitt JM, Hwang K, Winn S, Hollinger JO. Bone morphogenetic proteins: An update on basic biology and clinical relevance. J Orthop Res 1999; 17:269-278.

154. Wozney JM, Rosen V, Celeste AJ, Mitsock LM, Whitters MJ, Kriz RW, Hewick RM, Wang EA. Novel regulators of bone formation: Molecular clones and activities. Science 1988; 242:1528-1534.

155. Wozney JM. Bone morphogenetic proteins and their gene expression. In Noda M (Ed): Cellular and Molecular Biology of Bone. San Diego: Academic 1993; p 131-167.

156. Yamamoto N, Akiyama S, Katagiri T, Namiki M, Kurokawa T, Suda T. Smad1 and Smad5 act downstream of intracellular signalings of BMP-2 that inhibits myogenic differentiation and induces osteoblast differentiaion in C2C12 myoblasts. Biochem Biophys Res Commun 1997; 238:574-580.

157. Ducy P, Zhang R, Geoffroy V, Ridall AL, Karsenty G. Osf2/Cbfa1: a transcriptional activator of osteoblast differentiation. Cell 1997; 89:747-754.

158. Kirker-Head CA. Recombinant bone morphogenetic proteins: Novel substances for enhancing bone healing. Vet Surg 24:408-419, 1995

159. Woodward JC, Riser WH. Morphology of fracture nonunion and osteomyelitis. Vet Clin N Am Sm Anim Pract 1991; 21:813-844.

160. Frost HM. The biology of fracture healing. An overview for clinicians. Part II. Clin Orthop Rel Res 1989; 248:293-309.

161. Andrew JG, Marsh DR, Andrew SM, Sugden P, Freemont AJ. An investigation of the relationship between histological and radiological features of human non unions. J Bone Joint Surg 1995; 77B:S92.

162. Grundnes O, Reikeraas O. Effects of macrophage activation on bone healing. J Orthop Sci 2000; 5:243-247.

163. Boyan BD, Caplan AI, Heckman JD, Lennon DP, Ehler W, Schwartz Z. Osteochondral progenitor cells in acute and chronic canine nonunions. J Orthop Res 1999; 17:246-255.

164. Boyan BD, Schwartz Z, Swain LD, Khare AG, Heckman JD, Ramirez V, Peters P, Carnes DL. Initial effects of partially purified bone morphogenetic protein on the expression of glycosaminoglycan, collagen, and alkaline phosphatase in nonunion cell cultures. Clin Orthop Rel Res 1992; 278:286-304.

165. Lawton DM, Andrew JG, Marsh DR, Hoyland JA, Freemont AJ. Mature osteoblasts in human non-union fractures express collagen type III. J Clin Pathol: Mol Pathol 1997; 50:194-197.

166. Lawton DM, Andrew JG, Marsh DR, Hoyland JA, Freemont AJ. Expression of the gene encoding the matrix gla protein by mature osteoblasts in human fracture non-unions. J Clin Pathol Mol Pathol 1999; 52:92-96.

167. Lou G, D'Souza R, Hogue D, Karsenty G. The matrix gla protein gene is a marker of the chondrogenesis cell lineage during mouse development. J Bone Mineral Res 1995; 10:325-334

168. Luo G, Ducy P, McKee MD, Pinero GJ, Loyer E, Behringer RR, Karsenty G. Spontaneous calcification of arteries and cartilage in mice lacking matrix GLA protein. Nature 1997; 358:78-81.

169. Hietaniemi K, Lehto MUK, Paavolainen P. Major fibrillar collagens and fibronectin in an experimental nonunion. Acta Orthop Scand 1998; 69:545-549.

170. Anderson AM, Hastings GW, Fisher TR, Ross ERS, Shuttleworth A. Collagen types at human fracture sites – A preliminary report. Injury 1986; 17:78-80.

171. Joerring S, Krogsgaard M, Wilbek H, Jensen LT. Collagen turnover after tibial fractures. Arch Orthop Trauma Surg 1994; 113:334-336.

172. Kurdy NMG. Serology of abnormal fracture healing: The role of PIIINP, PICP, and BsALP. J Orthop Trauma 2000; 14:48-53.

173. Brownlow HC, Reed A, Simpson AH. Growth factor expression during the development of atrophic non-union. Injury 2001; 32:519-524.

174. Hausman MR, Schaffler MB, Majeska RJ. Prevention of fracture healing in rats by an inhibitor of angiogenesis. Bone 2001; 29:560-564.

175. Brownlow H, Simpson AHRW, Kenwright J. The vascularity of atrophic non-union gaps. J Bone Joint Surg 1999; 81B:S331.

176. Reed A, Joyner C, Brownlow H, Simpson H. A comparison of vessel density in human hypertrophic and atrophic non-union fractures. J Bone Joint Surg 2000; 82B:S132.

177. Wang N, Butler JP, Ingber DE. Mechanotransduction across the cell surface and through the cytoskeleton. Science 1993; 260:1124-1127.

178. Nomura S, Takano-Yamamoto T. Molecular events caused by mechanical stress in bone. Matrix Biol 2000; 19:91-96.

179. Brighton CT, Hunt RM. Early histological and ultrastructural changes in microvessels periosteal callus. J Orthop Trauma 1997; 11:244-253.

180. Le AX, Hu MD, Helms JA. Molecular aspects of healing in stabilized and non-stabilized fractures. J Orthop Res 2001; 19:78-84.

181. Mader JT, Norden C, Nelson JD, Calandra GB. Evaluation of new anti-infective drugs for the treatment of osteomyelitis in adults. Clin Invest Dis 1992; 15:S155-161.

182. McGuire MH. The pathogenesis of adult osteomyelitis. Orthop Rev 1989; 18:564-570.

183. Ciampolini J, Harding KG. Pathophysiology of chronic bacterial osteomyelitis. Why do antibiotics fail so often? Postgrad Med J 2000; 76:479-483.

184. Gristina AG, Naylor PT, Myrvik QN. Mechanisms of musculoskeletal sepsis. Orthop Clin N Am 1991; 22:363-371.

185. Evans RP, Nelson CL, Harrison BH. The effect of wound environment on the incidence of acute osteomyelitis. Clin Orthop Rel Res 1993; 286:289-297.

186. Cordero J, Munuera L, Folgueira MD. Influence of bacterial strains on bone infection. J Orthop Res 1996; 14:663-667.

187. Wadström T. Molecular aspects of bacterial adhesion, colonization, and development of infections associated with biomaterials. J Investig Surg 1989; 2:353-360.

188. Rudd RG. A rational approach to the diagnosis and treatment of osteomyelitis. Compend Contin Educ 1986; 8:225-234.

189. Worlock P, Slack R, Harvey L, Mawhinney R. The prevention of infection in open fractures: an experimental study of the effect of fracture stability. Injury 1994; 25:31-38.

190. Gillespie WJ, Allardyce RA. Mechanisms of bone degradation in infection: A review of current hypotheses. Orthop 1990; 13:407-410.

191. Lerner UH. Osteoclast formation and resorption. Matrix Biol 2000; 19:107-120.

192. Lerner UH, Sundqvist G, Ohlin A, Rosenquist JB. Bacteria inhibit biosynthesis of bone matrix proteins in human osteoblasts. Clin Orthop Rel Res 1998; 346:244-254.

193. Devnani AS. Simple approach to the management of aseptic non-union of the shaft of long-bones. Singapore Med J 2001; 42:20-25.

194. Meadows SE, Zuckerman JD, Koval KJ. Posttraumatic tibial osteomyelitis: diagnosis, classification, and treatment. Bull Hosp Joint Dis 1993; 52:11-16.

195. Dernell WS. Treatment of severe orthopedic infections. Vet Clin N Am Sm Anim Pract 1999; 29:1261-1274.

196. Holcombe SJ, Schneider RK, Bramlage LR, Embertson RM. Use of antibiotic-impregnated polymethyl methacrylate in horses with open or infected fractures or joints: 19 cases (1987-1995). J Am Vet Med Assoc 1997; 211:889-893.

197. Whitehair KJ, Adams SB, Parker JE, Blevins WE, Fessler JF. Regional limb perfusion with antibiotics in three horses. Vet Surg 1992; 21:286-292.

198. Senn N. On the healing of aseptic bone cavities by implantation of antiseptic decalcified bone. Am J Med Sci 1889; 98:219.

199. Goldberg VM, Stevenson S, Shaffer JW. Biology of autografts and allografts. In Bone and Cartilage Allografts: Biology and Clinical Applications. GE Friedlaender, VM Goldberg (ED) Park Ridge, IL, The American Academy of Orthopaedic Surgeons, 1991, p 3-12.

200. Leads from the MMWR. Transmission of HIV through bone transplantation: case report and public health recommendations. J Am Med Assoc 1988; 260:2487-2488.

201. Heiple KG, Chase SW, and Herndon CH. A comparative study of the healing process following different types of bone transplantation. J Bone Joint Surg 1963; 45A:1593-1616.

202. Heppenstall RB. The present role of bone graft surgery in treating nonunion. Orthop Clin North America 1984; 15:113-123.

203. Reckling FW, Waters CH III. Treatment of non-unions of fractures of the tibial diaphysis by posterolateral cortical cancellous bone-grafting. J Bone Joint Surg 1980; 62A:936-941.

204. Enneking WF, Eady JJL, Burchardt H. Autogenous cortical bone grafts in the reconstruction of segmental skeletal defects. J Bone Joint Surg 1980; 62A:1039-1058.

205. Cockin J. Autologous bone grafting. Complications at the donor site. J Bone Joint Surg 1971; 53B:153.

206. Younger EM, Chappman MW. Morbidity at bone graft donor sites. J Orthop Trauma 1989; 3:192-195.

207. Summers BN, Eisenstein SM. Donor site pain from the ilium. A complication of lumbar spine fusion. J Bone Joint Surg 1989; 71B:677-680.

208. Albertson KS, Medoff RJ, Mitsumaga MM. The use of periosteally vascularized autografts to augment the fixation of large segmental allografts. Clin Orthop Rel Res 1991; 269:113-119.

209. Zaslav KR, Meinhard BP. Management of resistant pseudoarthrosis of long bones. Clin Orthop Rel Res 1988; 233:234-242.

210. Moroni A, Rollo G, Guzzardella M, Zinghi G. Surgical treatment of isolated forearm non-union with segmental bone loss. Injury 1997; 28:497-504.

211. Südkamp NP. Incidence of non-unions in open fractures: analysis of 948 open fractures. Akt Traumatol 1993; 23:59-67.

212. Niyibizi C, Kim M. Novel approaches to fracture healing. Exp Opin Invest Drugs 2000; 9:1573-1580.

213. Einhorn TA. Enhancement of fracture healing. J Bone Joint Surg 1995; 77A:940-956.

214. Zhuang H, Wang W, Seldes RM, Tahernia AD, Fan H, Brighton CT. Electrical stimulation induces the level of TGF-β1 mRNA in osteoblastic cells by a mechanism involving calcium/calmodulin pathway. Biochem Biophys Res Commun 1997; 237:225-229.

215. Zhuang H, Wang W, Tahernia AD, Levitz CL, Luchetti WT, Brighton CT. Mechanical strain-induced proliferation of osteoblastic cells parallels increased TGB-beta 1nRNA. Biochem Biophys Res Commun 1996; 229:449-453.

216. Reher P, Doan N, Bradnock B, Meghji S, Harris M. Effect of ultrasound on the production of IL-8, basic FGF, and VEGF. Cytokine 1999; 11:416-423.

217. Sato M, Ochi T, Nakase T, Hirota S, Kitamura Y, Nomura S, Yasui N. Mechanical tension-stress induces expression of bone morphogenetic protein (BMP)-2 and BMP-4, but not BMP-6, BMP-7, and GDF-5 mRNA, during distraction osteogenesis. J Bone Min Res 1999; 14:1084-1095.

218. Nielsen HM, Andreassen TT, Ledet T, Oxlund H. Local injection of TGF-beta increases the strength of tibial fractures in the rat. Acta Orthop Scand 1994; 65:37-41.

219. Lind M, Schumacker B, Soballe K, Keller J, Melsen F, Bunger C. Transforming growth factor-beta enhances fracture healing in rabbit tibiae. Acta Orthop Scand 1993; 64:553-556.

220. Beck LS, Duguzman L, Lee WP. Transforming growth factor beta 1 bound to tricalcium phosphate persists at segmental radial defects and induces bone formation. Trans Orthop Res Soc 1995; 20:593.

221. Beck LS, Duguzman L, Lee WP. Bone marrow augments the activity of transforming growth factor beta 1 in critical sized bone defects. Trans Orthop Res Soc 1996; 21:626.

222. Heckman JD, Aufdemorte TB, Athanasiou KA. Treatment of acute ostectomy defects in the dog radius with rhTGF-β1. Trans Orthop Res Soc 1995; 20:590.

223. Peterson DR, Glancy TP, Bacon-Clarke R. A study of delivery timing and duration of the transforming growth factor beta 1 induced healing of critical-size long bone defects. J Bone Min Res 1997; 12:S304.

224. Rosier RN, O'Keefe RJ, Hicks DG. The potential role of transforming growth factor beta in fracture healing. Clin Orthop Rel Res 1998; 355S:S294-S300.

225. Baylink DJ, Finkelman RD, Mohan S. Growth factors to stimulate bone formation. J Bone Min Res 1993; 8:S565-S572.

226. Reddi AH. Regulation of cartilage and bone differentiation by bone morphogenetic proteins. Curr Opinion Cell Biol 1992; 4:850-855.

227. Heckman JD, Ehler W, Brooks BP, Aufdemorte TB, Lohmann CH, Morgan T, Boyan BD. Bone morphogenetic protein but not transforming growth factor-beta enhances bone formation in canine diaphyseal nonunions implanted with a biodegradable composite polymer. 1999; 81A:1717-1729.

228. Baltzer AWA, Latterman C, Whalen JD, Ghivizzani S, Wooley P, Krauspe R, Robbins PD, Evans CH. Potential role of direct adenoviral gene transfer in enhancing fracture repair. Clin Orthop Rel Res 2000; 379:S120-S125.

229. Joyce ME. Jingushi S. Scully SP. Bolander ME. Role of growth factors in fracture healing. Prog Clin Biol Res 1991; 365:391-416.

230. Joyce ME, Heydemann A, Bolander ME. Platelet-derived growth factor regulates the initiation of fracture repair. Orthop Trans 1990; 14:363.

231. Steinbrech DS, Mehrar BJ, Rowe NM, Dudziak ME, Saadeh PB, Gittes GK, Longaker MT. Gene expression of insulin-like growth factors I and II in rat membranous osteotomy healing. Ann Plast Surg 1999; 42:481-487.

232. Aspenberg P, Albrektsson T, Thorngren KG. Local application of growth-factor IGF-I to healing bone. Experiments with a titanium chamber in rabbits. Acta Orthop Scand 1989; 60:607.

233. Urist MR, Dawson EG, Schmalzried TP, Finerman GAM. Bone repair induced by bone morphogenetic protein in ulna defects in dogs. J Bone Joint Surg 1986; 68B:635-642.

234. Stevenson S. Cunningham N. Toth J, Davy D, Reddi AH. The effect of osteogenin (a bone morphogenetic protein) on the formation of bone in orthotopic segmental defects in rats. J Bone Joint Surg 1994; 76A:1676-1687.

235. Lee FY. Hazan EJ. Trahan C. Snyder B, Gebhardt MC, Mankin HJ. Bone morphogenetic protein (BMP-2) can initiate and conduct repair process at the allograft osteotomy site in an animal experimental model. Proc 45th Ann Mtg Orthop Res Soc 1999; p 620.

236. Zegzula HD. Buck DC. Brekke J. Wozney JM, Holllinger JO. Bone formation with use of rhBMP-2 (recombinant human bone morphogenetic protein-2) J Bone Joint Surg 1997; 79A:1778-1790.

237. Blokhuis TJ. den Boer FC. Bramer JAM. Jenner JMG. Bakker FC. Patka P. Haarman HJThM. Biomechanical and histological aspects of fracture healing stimulated with osteogenic protein –1. Biomaterials 2001; 22:725-730.

238. Welch RD. Jones AL. Bucholz RW. Reinert CM. Tjia JS. Pierce WA. Wozney JM. Li XJ. Effect of recombinant human bone morphogenetic protein-2 on fracture healing in a goat tibial fracture model. J Bone Min Res 1998; 13:1483-1490.

239. Ohura K. Hamanishi C. Tanaka S. Matsuda N. Healing of segmental bone defects in rats induced by a β–TCP-MCPM cement combined with rhBMP-2. J Biomed Mater Res 1999; 44:168-175.

240. Cook SD. Baffes GC. Wolfe MW. Sampath TK. Reuger DC. Whitecloud TS. The effect of recombinant human osteogenic protein-1 on healing of large segmental bone defects. J Bone Joint Surg 1994; 76A:827-838.

241. Cook SD, Baffes GC, Wolfe MW, Sampath TK, Rueger DC. Recombinant human bone morphogenetic protein-7 induces healing in a canine long-bone segmental defect model. Clin Orthop Rel Res 1994; 301:302-312.

242. Gerhart TN, Kirker-Head CA, Kriz MJ, Holtrop ME, Hennig GE, Hipp J, Schelling SH, Wang E. Healing segmental femoral defects in sheep using recombinant human bone morphogenetic protein. Clin Orthop Rel Res 1993; 293:317-326.

243. Kirker-Head CA, Gerhart TN, Schelling SH, Hennig GE, Wang E, Holtrop ME. Long-term healing of bone using recombinant human bone morphogenetic protein 2. Clin Orthop Rel Res 1995; 318:222-230.

244. Bouxsein ML, Turek TJ, Blake CA, D'Augusta D, Li X, Stevens M, Seeherman HJ, Wozney JM. Recombinant human bone morphogenetic protein-2 accelerates healing in a rabbit ulnar osteotomy model. J Bone Joint Surg 2001; 83A:1219-1230.

245. Bax BE, Wozney JM, Ashhurst DE. Bone morphogenetic protein-2 increases the rate of callus formation after fracture of the rabbit tibia. Calcif Tissue Int 1999; 65:83-89.

246. Lee SC, Shea M, Battle MA, Kozitza K, Ron E, Turek T, Schaub RG, Hayes WC. Healing of large segmental defects in rat femurs is aided by RhBMP-2 in PLGA matrix. J Biomed Mater Res 1994; 28:1149-1156.

247. Johnson EE, Urist MR, Finerman GAM. Resistant nonunions and partial or complete segmental defects of long bones. Clin Orthop Rel Res 1992; 277:229-237

248. Johnson EE, Urist MR, Finerman GAM. Distal metaphyseal tibial nonunion. Clin Orthop Rel Res 1990; 250:234-240.

249. Johnson EE, Urist MR. One-stage lengthening of femoral nonunion augmented with human bone morphogenetic protein. Clin Orthop Rel Res 1998; 347:105-115.

250. Bulstra SK, Geesink RGT, Hoefnagels NHM. Osteogenic activity of OP-1, bone morphogenetic protein-7 (BMP-7), in a human fibular defect model. Proc 45th Ann Mtg Orthop Res Soc 1999; p62.

251. Itoh T, Mochizuki M, Fuda K, Nishimura R, Matsunaga S, Kadosawa T, Sasaki N. Femoral nonunion fracture treated with recombinant human bone morphogenetic protein-2 in a dog. J Vet Med Sci 1998; 60:535-538.

252. Meng-Hai B, Xing-Yan L, Bao-Feng G, Chao Y, Dong-An C. An implant of a composite of bovine bone morphogenetic protein and plaster of paris for treatment of femoral shaft nonunions. Int Surg 1996; 81:390-392.

253. Xiang W, Baolin L, Yan J, Yang X. The effect of bone morphogenic protein on the osseointegration of titanium implants. J Oral Maxillofac Surg 1993; 51:647-651.

254. Sigurdsson TJ, Lee MB, Kubota K, Turek TJ, Wozney JM, Wikesjo UME. Peridontal repair in dogs: Recombinant human bone morphogenic protein-2 significantly enhances peridontal regeneration. J Periodontol 1995; 66:131-138.

255. Sandu HS, Kanim LEA, Kabo BF, Zeegen EN, Liu D, Seeger LL, Brekke JH, Smith JL, McKay BF, Dawson EG. Evaluation of rhBMP-2 with OPLA

carrier in a canine posterolateral (transverse process) spinal fusion model. Trans Orthop Res Soc 1995; 41:43.

256. Howard BK, Brown KR, Leach JL, Chang CH, Rosenthal DI. Osteoinduction using bone morphogenic protein in irradiated tissue. Arch Otolaryngol Head Neck Surg 1998; 124: 985-988.

257. Linde A, Hedner E. Recombinant bone morphogenetic protein-2 enhances bone healing, guided by osteopromotive e-PTFE membranes: An experimental study in rats. Calcif Tissue Int 1995; 56:549-553.

258. Agrawal CM, Best J, Heckman JD, Boyan BD. Protein release kinetics of a biodegradable implant for fracture non-unions. Biomaterials 1995; 16:1255-1260.

259. Athanasiou KA, Niederauer GG, Agrawal CM. Sterilization, toxicity, biocompatibility and clinical applications of polylactic acid/polyglycolic acid copolymers. Biomaterials 1996; 17:93-102.

260. Suganuma J, Alexander H. Biological response of intramedullary bone to poly-L-lactic acid. J Applied Biomater 1993; 4:13-27.

261. Zellin G, Linde A. Treatment of segmental defects in long bones using osteopromotive membranes and recombinant human bone morphogenetic protein-2. Scand J Plast Reconstr Hand Surg 1997; 31:97-104.

262. Zellin G, Linde A. Effects of different osteopromotive membrane porosities on experimental bone neogenesis in rats. Biomaterials 1996; 17:695-702.

263. Gerber A, Gogolewski S. Treatment of large diaphyseal bone defects using polylactide membrane in combination with autogenic cancellous bone graft. Proc 5th World Biomaterials Congress 1996; p32.

264. Khouri RK, Koudsi B, Reddi H. Tissue transformation into bone *in vivo*. J Am Med Assoc 1991; 266:1953-1955.

265. Niyibizi C, Baltzer A, Latterman C, Oyama M, Whalen JD, Robbins PD, Evans CH. Potential role for gene therapy in the enhancement of fracture healing. Clin Orthop Rel Res 1998; 355S:S148-S153.

266. Chen Y. Orthopedic applications of gene therapy. J Orthop Sci 2001; 6:199-207.

267. Oligino TJ, Yao Q, Ghivizzani SC, Robbins P. Vector systems for gene transfer to joints. Clin Orthop Rel Res 2000; 379S:S17-S30.

268. Zhang YP, Sekirov L, Saravolac EG, Wheeler JJ, Tardi P, Clow K, Leng E, Sun R, Cullis PR, Scherrer P. Stabilized plasmid-lipid particles for regional gene therapy: formulation and transfection properties. Gene Therapy 1999; 6:1438-1447.

269. Horwitz MS, Tufariello J, Grunhaus A, Fejer G. Model systems for styding the effects of adenovirus E3 genes on virulence in vivo. In Doerfler W and Böhm (Eds): The Molecular Repertoire of Adenoviruses III. Springer, NY, p195-211.

270. Hardy S, Kitamura M, Harris-Stansil T, Dai Y, Phipps ML. Construction of Adenovirus vectors through Cre-*lox* recombination. J Virol 1997; 71:1842-1849.

271. Leiberman JR, Le LQ, Wu L, Finerman GAM, Berk A, Witte ON, Stevenson S. Regional gene therapy with a BMP-2 producing murine stromal cell line induces heterotopic and orthotopic bone formation in rodents. J Orthop Res 1998; 16:330-339.

272. Spector JA, Mehrar BJ, Luchs JS, Greenwald JA, Fagenholz PJ, Saadeh PB, Steinbrech DS, Longaker MT. Expression of adenovirally delivered gene products in healing osseous tissues. Ann Plast Surg 2000; 44:522-528.

273. Worgall S, Wolff G, Falck-Pedersen E, Crystal RG. Innate immune mechanisms dominate elimination of adenoviral vectors following in vivo administration. Hum Gene Ther 1997; 8:37-44.

274. Kaplan JM, Armentano D, Sparer TE, Wynn SG, Peterson PA, Wadsworth SC, Couture KK, Pennington SE, St George JA, Gooding LR, Smith AE. Characterization of factors involved in modulating persistence of transgene expression from recombinant adenovirus in the mouse lung. Hum Gene Ther 1997; 8:45-56.

275. Yang Y, Ertl HCJ, Wilson JM. MHC Class 1-Restricted cytotoxic T lymphocytes to viral antigens destroy hepatocytes in mice infected with E1-deleted recombinant adenoviruses. Immunity 1994; 1:433-443.

276. Chirmule N, Hughes JV, Gao GP, Raper SE, Wilson JM. Role of E4 in eliciting CD4 T-cell and B-cell responses to adenovirus vectors delivered to murine and nonhuman primate lungs. J Virol 1998; 72:6138-6145.

277. Yang Y, Nunes FA, Berencsi K, Furth EE, Gönczöl E, Wilson JM. Cellular immunity to viral antigens limits E1-deleted adenoviruses for gene therapy. Proc Natl Acad Sci 1994; 91:4407-4411.

278. DeMatteo RP, Yeh H, Friscia M, Caparrelli D, Burke C, Desai N, Chu G, Markmann JF, Raper SE, Barker CF. Cellular immunity delimits adenoviral gene therapy strategies for the treatment of neoplastic diseases. Ann Surg Oncol 1999; 6:88-94.

279. Rasmussen UB, Benchaibi M, Meyer V, Schlesinger Y, Schughart K. Novel human gene transfer vectors: Evaluation of wild-type and recombinant animal adenoviruses in human-derived cells. Hum Gene Ther 1999; 10:2587-2599.

280. Engelhardt JF, Litzky L, Wilson JM. Prolonged transgene expression in cotton rat lung with recombinant adenoviruses defective in E2a. Hum Gene Ther 1994; 5:1217-1229.

281. Roy S, Shirley PS, McClelland A, Kaleko M. Circumvention of immunity to the adenoviral major coat protein hexon. J Virol 1998; 72:6875-6879.

282. Gahery-Segard H, Farace F, Godfrin D, Gaston J, Lengagne R, Tursz T, Boulanger P, Guillet JG. Immune response to recombinant capsid proteins to adenovirus in humans: Antifiber and anti-penton base antibodies have a synergistic effect on neutralizing activity. J Virol 1998; 72:2388-2397.

283. Hofmann C, Löser P, Chichon G, Arnold W, Both GW, Strauss M. Ovine adenovirus vectors overcome preexisting humoral immunity against human adenoviruses in vivo. J Virol 1999; 73:6930-6936.

284. Juillard V, Villefroy P, Godfrin D, Pavirani A, Venet A, Guillet JG. Long-term and cellular immunity induced by a single immunization with replication-defective adenovirus recombinant vector. Eur J Immunol 1995; 25:3467-3473.

285. Kuby J. Overview of the Immune System. In Kuby J: Immunology, Ed 2, WH Freeman & Co., New York, 1994, p 2-20.

286. Ahrens M, Ankenbauer T, Schroder D, Hollnagel A, Mayer H, Gross G. Expression of human bone morphogenetic proteins 2 or 4 in murine mesenchymal progenitor C3H10T1/2 cells induces differentiation into distinct mesenchymal cell lineage. DNA Cell Biol 1993; 12:871-880.

287. Baltzer AWA, Lattermann C, Whalen JD, Braunstein S, Robbins PD, Evans CH. A gene therapy approach to accelerating bone healing. Evaluation of gene expression in a New Zealand white rabbit model. Knee Surg, Sports Traumatol, Arthrosc 1999; 7:197-202.

288. Fang J, Zhu YY, Smiley E, Bonadio J, Rouleau JP, Goldstein SA, McCauley LK, Davidson BL, Roessler BJ. Stimulation of new bone formation by direct transfer of osteogenic plasmid genes. Natl Acad Sci USA 1996; 93:5753-5758.

289. Goldstein SA, Bonadio J. Potential role for direct gene transfer in the enhancement of fracture healing. Clin Orthop Rel Res 1998; 355S:S154-S162.

290. Musgrave DS, Bosch P, Ghivizzani S, Robbins PD, Evans CH, Huard J. Adenovirus-mediated direct gene therapy with bone morphogenetic protein-2 produces bone. Bone 1999; 24:541-547.

291. Mehrara BJ, Saadeh PB, Steinbrech DS, Dudziak M, Spector JA, Greenwald JA, Gittes GK, Longaker MT. Adenovirus-mediated gene therapy of osteoblasts in vitro and in vivo. J Bone Min Res 1999; 14:1290-1301.

292. Lou J, Xu F, Merkel K, Manske P. Gene therapy: adenovirus-mediated human bone morphogenetic protein-2 gene transfer induces mesenchymal progenitor cell proliferation and differentiation in vitro and bone formation in vivo. J Orthop Res 1999; 17:43-50.

293. Gazit D, Turgeman G, Kelley P, Wang E, Jalenak M, Zilberman Y, Moutsatsos I. Engineered pluripotent mesenchymal cells integrate and differentiate in regenerating bone: A novel cell-mediated gene therapy. J Gene Med 1999; 1:121-133.

294. Laurencin CT, Attawia MA, Lu LQ, Borden MD, Lu HH, Gorum WJ, Lieberman JR. Poly(lactide-co-glycolide)/hydroxapatite delivery of BMP-2-producing cells: a regional gene therapy approach to bone regeneration. Biomaterials 2001; 22:1271-1277.

295. Alden TD, Pittman DD, Hankins GR, Beres EJ, Engh JA, Das S, Hudson SB, Kerns KM, Kallmes DF, Helm GA. *In vivo* endochondral bone formation using a bone morphogenetic protein 2 adenoviral vector. Hum Gene Ther 1999; 10:2245-2253.

296. Leiberman JR, Daluiski A, Stevenson S, Wu L, McAllister P, Lee YP, Kabo JM, Finerman GA, Berk AJ, Witte ON. The effect of regional gene therapy with bone morphogenetic protein-2 producing bone-marrow cells on the repair of segmental femoral defects in rats. J Bone Joint Surg 1999; 81A: 905-917.

297. Lieberman JR, Le LQ, Tomin E, Stevenson S, Rosen V, Finerman GAM, Witte ON. Genetic transfer of recombinant BMP-2 into a stromal cell line induces bone formation in vivo. Trans Orthop Res Soc 1996; 42:198.

298. Lieberman JR, Le LQ, Stevenson S, finerman GAM, Witte ON. *In vivo* bone induction via retroviral gene transfer of BMP-2 into a stromal cell line. Trans Orthop Res Soc 1997; 43:223.

299. Bonadio J, Smiley E, Patil P, Goldstein S. Localized, direct plasmid-gene delivery in vivo: prolonged therapy results in reproducible tissue regeneration. Nat Med 1999; 5:753-759.

300. Baltzer AWA, Lattermann C, Whalen JD, Wooley P, Weiss K, Grimm M, Ghivizzani SC, Robbins PD, Evans CH. Genetic enhancement of fracture repair: healing of an experimental segmental defect by adenoviral transfer of the BMP-2 gene. Gene Ther 2000; 7:734-739.

301. Day CS, Bosch P, Kasemkijwattana C, Menetrey J, Moreland MS, Fu FH, Ziran B, Huard J. Use of muscle cells to mediate gene transfer to the bone defect. Tissue Engineering 1999; 5:119-125.

302. Musgrave DS, Pruchnic R, Wright V, Bosch P, Ghivizzani SC, Robbins PD, Huard J. The effect of bone morphogenetic protein-2 expression on the early fate of skeletal muscle-derived cells. Bone 2001; 28:499-506.

303. Musgrave DS, Bosch P, Lee JY, Pelinkovic D, Ghivizzani SC, Whalen J, Niyibizi C, Huard J. *Ex vivo* gene therapy to produce bone using different cell types. Clin Orthop Rel Res 2000; 378:290-305.

304. Bosch P, Musgrave DS, Lee JY, Cummins J, Shuler T, Ghivizzani TC, Evans T, Robbins TD, Huard J. Osteoprogenitor cells within skeletal muscle. J Orthop Res 2000; 18:933-944.

305. Mason JM, Grande DA, Barcia M, Grant R, Pergolizzi RG, Breitbart AS. Expression of human bone morphogenetic protein 7 in primary rabbit periosteal cells: potential utility in gene therapy for osteochondral repair. Gene Ther 1998; 5:275-282.

306. Moursatsos IK, Turgeman G, Zhou S, Kurkalli BG, Pelled G, Tzur L, Kelly P, Stumm N, Mi S, Muller R, Zilberman Y, Gazit D. Exogenously regulated stem cell-mediated gene therapy for bone regeneration. Molecular Ther 2001; 3:449-461.

307. Spangehl MJ, Younger ASE, Masri BA, Duncan CP. Diagnosis of infection following total hip arthroplasty. J Bone Joint Surg 1997; 79A:1578-1588.

308. Sammak B, Abd El Bagi A, Al Shahed M, Hamilton D, Al Nabulsi J, Youssef B, Al Thagafi M. Osteomyelitis: a review of currently used imaging techniques. Eur Radiol 1999; 9:894-900.

309. Wegener WA, Alavi A. Diagnostic imaging of musculoskeletal infection. Orthop Clin N Am 1991; 22:401-418.

310. Letts RM, Afifi A, Sutherland JB. Technetium bone scanning as an aid in the diagnosis of atypical acute osteomyelitis in children. Surg Gynecol Obstet 1975; 140:899-902.

311. Munoz P, Bouza E. Acute and chronic adult osteomyelitis and prosthesis-related infections. Bailliere's Clinical Rheumatology 1999; 13:129-147.

312. Braden TD, Tvedten HW, Mostosky UV, Thomas M, Stickle RL, Kaneene JB. The sensitivity and specificity of radiology and histopathology in the diagnosis of posttraumatic osteomyelitis. Vet Comp Orthop Traum 1989; 3:98-103.

313. Blokhuis TJ, de Bruine JHD, Bramer JAM, den Boer FC, Bakker FC, Patka P, Haarman HJThM, Manoliu RA. The reliability of plain radiography in experimental fracture healing. Skeletal Radiol 2001; 30:151-156.

314. Craig JG, Jacobson JA, Moed BR. Ultrasound of fracture and bone healing. Radiol Clin N Am 1999; 37:737-751.

315. Abiri MM, DeAngelis GA, Kirpekar M, Abou AA, Ablow RC. Ultrasound detection of osteomyelitis. Invest Radiol 1992; 27:111-113.

316. Reef VB, Reimer JM, Reid CF. Ultrasonographic findings in horses with osteomyelitis. Proc Am Assoc Eq Pract 1991; 37:381-391.

317. Nath AK, Sethu AU. Use of ultrasound in osteomyelitis. Br J Radiol 1992; 65:649-652.

318. Abiri M, Kirpekar M, Ablow RC. Osteomyelitis: Detection with US. Radiol 1989; 172:509-511.

319. Kaplan PA, Matamoros Jr A, Anderson JC. Sonography of the musculoskeletal system. Am J Roent 1990; 155:237-245.

320. Magid D. Computed tomographic imaging of the musculoskeletal system. Radiol Clin N Am 1994; 32:255-274.

321. Schawecker DS, Braunstein EM, Wheat LJ. Diagnostic imaging of osteomyelitis. Infect Dis Clin N Am 1990; 4:441-463.

322. Korkusuz F, Akin S, Akkus O, Korkusuz P. Assessment of mineral density and atomic content of fracture callus by quantitative computerized tomography. J Orthop Sci 2000; 5:248-255.

323. Markel MD, Morin RL, Wikenheiser MA, Lewallen DG, Chao EY. Quantitative CT for the evaluation of bone healing. Calcif Tissue Int 1991; 49:427-432.

324. Markel MD, Wikenheiser MA, Morin RL, Lewallen DG, Chao EY. Quantification of bone healing. Comparison of QCT, SPA, MRI, and DEXA in dog osteotomies. Acta Orthop Scand 1990; 61:487-498.

325. Markel MD, Wikenheiser MA, Morin RL, Lewallen DG, Chao EY. The determination of bone fracture properties by dual energy x-ray absorptiometry and single-photon absorptiometry: a comparative study. Calcif Tissue Int 1991; 48:392-399.

326. Markel MD, Bogdanske JJ, Xiang Z, Klohnen A. Atrophic nonunion can be predicted with dual energy x-ray absorptiometry in a canine ostectomy model. J Orthop Res 1995; 13:869-875.

327. Buscombe J. The challenge of nuclear medicine. Br J Hosp Med 1995; 54: 68-9.

328. Hughes S. Radionuclides in orthopaedic surgery. J Bone Joint Surg 1980; 62B:141-150.

329. Letts RM, Afifi A, Sutherland JB. Technetium bone scanning as an aid in the diagnosis of atypical acute osteomyelitis in children. Surg Gynecol Obstet 1975; 140:899-902.

330. Bauer GCH, Lindberg L, Naversten Y, Sjöstrand L-O. ^{85}Sr radionuclide scintimetry in infected total hip arthroplasty. Acta Orthop Scand 1973; 44:417-425.

331. Segmuller G, Cech O, Bekier AM. Diagnostic use of Sr-85 in the preoperative evaluation of non-union. Acta Orthop Scand 1970; 41:150.

332. Wendeberg B Mineral metabolism of fractures of the tibia in man studied with external counting of Sr85. Acta Orthop Scand 1961; S52:135.

333. Asnis SE, Shoji H, Bohne WHO. Scintimetric evaluation of complications after femoral neck fractures. Clin Orthop Rel Res 1976; 121:149-156.

334. Feith R, Slooff TJJH, Kazem I, van Rens TJG. Strontium 87m bone scanning for the evaluation of total hip replacement. J Bone Joint Surg 1976; 58B:79-83.

335. Muheim G. Assessment of fracture healing in man by serial 87mstrontium-scintimetry. Acta Orthop Scand 1973; 44, 621-627.

336. Johannsen A. Fracture healing controlled by 87m-Sr uptake. Acta Orthop Scand 1973; 44:628-639.

337. McGrail JW, Vulpetti AT, Shifrin LZ. 18F scintigraphy of non-neoplastic skeletal lesions. Clin Orthop Rel Res 1974; 101:292-298.

338. Fueger GF, Tscherne H, Schwarz G, Szyszkowitz R. Szintigraphische untersuchungen mit 87m-strontium-zitrat zur Beurteilung der Frakturheilung. In

Glauner R (Ed): Angiologie und Szintigraphie bei Knochen- und Gelenkerkrankungen. Stuttgart, Georg Thieme Verlag, 1971; p 133-143.

339. Subramanian G, McAfee JG, Blair RJ, Kallfelz FA, Thomas FD. Technetium-99m-methylene diphosphonate-a superior agent for skeletal imaging: comparison with other technetium complexes. J Nucl Med 1975; 16:744-755.

340. Hendler A, Hershkop M. When to use bone scintigraphy. It can reveal things other studies cannot. Bone Scint 1998; 104:54-61.

341. Rosenthall L, Lisbona R, Hernandez M, Hadkipavlou A. 99mTc-PO4 and Ga-67 imaging following the insertion of orthopaedic devices. Radiol 1979; 133:717-721.

342. Tilden RL, Jackson J, Enneking WF, DeLand FH, McVey JT. 99mTc-polyphosphonate: Histological localization in human femurs by autoradiography. J Nucl Med 1973; 14:576-578.

343. Hadjipavlou A, Lisbona R, Rosenthall L. Difficulty of diagnosing infected hypertrophic pseudoarthrosis by radionuclide imaging. Clin Nucl Med 1983; 3:45-49.

344. Markel MD, Snyder JR, Hornof WJ, Meagher DM. Nuclear scintigraphic evaluation of third metacarpal and metatarsal bone fractures in three horses. J Am Vet Med Assoc 1987; 191:75-77.

345. Creutzig H. Bone imaging after total replacement arthroplasty of the hip joint. Eur J Nucl Med 1976; 1:177-180.

346. Peters AM. The use of nuclear medicine in infections. British J Radiol 1998; 71: 252-261.

347. Lisbona R, Rosenthal L. Observations on the sequential use of 99m-Tc-phosphate complex and 67Ga imaging in osteomyelitis, cellulites, and septic arthritis. Radiol 1977; 123:123-129.

348. Gilday DL, Paul DJ, Paterson J. Diagnosis of osteomyelitis in children by combined blood pool and bone imaging. Radiol 1975; 117:331-335.

349. Treves S, Khettry J, Broker FH, Wilkinson RH, Watts H. Osteomyelitis: Early scintigraphic detection in children. Pediatrics 1976; 57: 173-86.

350. Gelfand MJ, Silberstein EB. Radionuclide Imaging. Use in diagnosis of osteomyelitis in children. J Am Med Assoc 1977; 237: 245-247.

351. Atcheson SG, Coleman RE, Ward JR. Septic arthritis mimicking cellulitis: Distinction using radionuclide bone imaging. Clin Nuclear Med 1979; 4:79-81.

352. Lutzker LG, Koenigsberg M, Freeman LM. Focal bone pain. Infection or infarction? J Am Med Assoc 1976; 235:425-426.

353. Palestro CJ. The current role of gallium imaging in infection Semin Nucl Med 1994; 24:128-41.

354. Deysine M, Rafkin H, Russell R, Teicher I, Aufses AH. The detection of acute experimental osteomyelitis with 67Ga citrate scannings. Surg Gynecol Obstet 1975; 141:40-42.

355. Deysine M, Robinson R, Rafkin H, Teicher I, Silver L, Aufses AH. Clinical infections detected by 67Ga scanning. Ann Surg 1974; 180:897-901.

356. Deysine M, Rafkin H, Teicher I, Silver L, Robinson R, Manly J, Aufses AH. Diagnosis of chronic and postoperative osteomyelitis with gallium 67 citrate scans. Am J Surg 1975; 129:632-635.

357. Oyen WJG, Corstens FHM. Scintigraphic techniques for delineation of infection and inflammation. Br J Hosp Med 1995; 54:75-80.

358. Merkel KD, Brown ML, Dewanjee MK, Fitzgerald RH. Comparison of indium-labelled-leukocyte imaging with sequential technetium-gallium scanning in the diagnosis of low grade musculoskeletal sepsis. A prospective study. J Bone Joint Surg 1985; 67:465-76.

359. Seabold JE, Napola JV, Conrad GR Marsh JL, Montgomery WJ, Bricker JA, Kirchner PT. Detection of osteomyelitis at fracture non union sites: comparison of two scintigraphy methods. Am J Roentogenol 1989; 152:1021-1027.

360. Schauwecker DS. Osteomyelitis: Diagnosis with In-111-labeled leukocytes. Radiol 1989; 171:141-146.

361. Datz FL. Indium-111 labelled leukocytes for the detection of infection: Current status. Semin Nucl Med 1994; 24:92-109.

362. Ali SA, Cesani F, Nusynowitz ML, Briscoe EG, Shirtliff ME, Mader JT. Skeletal scintigraphy with technetium-99m-tetraphenyl porphyrin sulfonate for the detection and determination of osteomyelitis in an animal model. J Nucl Med 1997; 38:1999-2002.

363. Rüther W, Hotze A, Möller F, Bockisch A, Heitzmann P, Diersack HJ. Diagnosis of bone and joint infection by leucocyte scintigraphy. Arch Orthop Trauma Surg 1990; 110:26-32.

364. Aktolun C, Ussov WY, Arka A, Glass D, Gunasekera RD, Peters AM. Technetium-99m and indium-111 double labeling of granulocytes for kinetic and clinical studies. Eur J Nucl Med 1995; 22:330-334.

365. Long CD, Galuppo LD, Waters NK, Hornof WJ. Scintigraphic detection of eqine orthopedic infection using Tc-HMPAO labeled leukocytes in 14 horses. Vet Radiol Ultrasound 2000; 41:354-359.

366. Morrel EM, Tompkins RG, Fischman AJ, Wilkinson RA, Yarmush ML. Imaging infections with antibodies. J Immunol Methods 1990; 130:39-48.

367. Oyen WJG, Claessens AMJ, Van der Meer JWM, Rubin RH, Strauss HW, Corstens FHM. Indium-111 labelled human non-specific immunoglobulin G: a new radiopharmaceutical for imaging infectious and inflammatory foci. Clin Infect Dis 1992; 14:1110-1119.

368. Spinelli R. The role of scintigraphy in the diagnosis of late complications of total prosthesis of the hip. Italian J Orthop Traum 1975; 2:79-87, 1975.

369. Williamson BRJ, McLaughlin RE, Wang GJ, Miller CW, Teates CD, Bray ST. Radionuclide bone imaging as a means of differentiating loosening and infection in patients with a painful total hip prosthesis. Radiol 1979; 133:723-725.

370. Williams ED, Tregonning RJ, Hurley PJ. 99Tcm-diphosphonate scanning as an aid to diagnosis of infection in total hip joint replacements. Br J Rad 1977; 50:562-566.

371. Thrall JH, Geslien GE, Corcoron RJ, Johnson MC. Abnormal radionuclide deposition patterns adjacent to focal skeletal lesions. Radiol 1975; 115:659-663.

372. Genant HK, Bautovich GJ, Singh M, Lathrop KA, Harper PV. Bone-seeking radionuclides: an *in vivo* study of factors affecting skeletal uptake. Radiol 1974; 113:373-382.

373. Oyen WJG, Claessens RAMJ, Van der Meer JWM, Corstens FHM. Biodistribution and kinetics of radiolabeled proteins in rats with focal infection. J Nucl Med 1992; 33:388-94.

374. Hagan PL, Taylor A, Chauncey DM, Schelbert H. Comparison of 131I-tetracycline and 67Ga-citrate as abscess localizing agents. Nucl Medizin 1977; 16:76-78.

375. Oyen WJG, Corstens FHM. Scintigraphic techniques for delineation of infection and inflammation. Br J Hospital Med 1995; 54:75-80.

376. Britton KE, Vinjamuri S, Hall AV, Solanki K, Siraj QH, Bomanji J, Das S. Clinical evaluation of technetium-99m infecton for the localisation of bacterial infection. Eur J Nucl Med 1997; 24:553-556.

377. Hall AV, Solanki KK, Vinjamuri S, Britton KE, Das SS. Evaluation of the efficacy of 99mTc-Infecton, a novel agent for detecting sites of infection. J Clin Pathol 1998; 51:215-219.

378. Jayaraman S, Al-Nahhas AM, Vivian G, Gilbert TJ, Hughes PM. Demonstration of spinal osteomyelitis with Ga-67 citrate, Tc-99m MDP, and Tc-99m ciprofloxacin with provisionally negative results of MRI. Clin Nucl Med 2000; 25:224-226.

379. Vinjamuri S, Hall AV, Solanki KK, Bomanji J, Siraj Q, O'Shaughnessy EO, Das SS, Britton KE. Comparison of 99mTc-infecton with radiolabeled white cell imaging the evaluation of bacterial infection. Lancet 1996; 347:233-235.

380. Amaral H, Morales B, Pruzzo R, Britton KE. Cold-hot mismatch between Tc-99m HMPAO-labeled leukocytes and Tc-99m ciprofloxacin in axial skeleton infections: a report of three cases. Clin Nucl Med 1999; 24:855-888.

381. Russell RGG. The assessment of bone metabolism *in vivo* using biochemical approaches. Horm Metab Res 1997; 29: 138-144.

382. Bettica P, Moro L, Robins SP, Taylor AK, Talbot AK, Singer FR, Baylink DJ. Bone-resorption markers galactosyl hydroxlysine, pyridinium crosslinks, and hydroxyproline compared. Clin Chem 1992; 38:2313-2318.

383. Garnero P, Shih WJ, Gineyts E, Karpf DB, Delmas PD. Comparison of new biochemical markers of bone turnover in late postmenopausal osteoporotic women in response to alendronate treatment. J Clin Endocrin Metab 1994; 79:1693-1700.

384. Bollen AM, Kiyak HA, Eyre DR. Longitudinal evaluation of a bone resorption marker in elderly subjects. Osteoporosis Int 1997; 7:544-549.

385. Turner AS, Alvis M, Myers W, Stevens ML, Lundy MW. Changes in bone mineral density and bone-specific alkaline phosphatase in ovariectomized ewes. Bone 1995; 17:395S-402S.

386. Hauschka PV, Lian JB, Gallop PM. Direct identification of the calcium-binding amino acid, gamma-carboxyglutamate in mineralized tissue. Proc Natl Acad Sci USA 1975; 72:3925-3929.

387. Lian JB, Gundberg CM. Osteocalcin: Biochemical considerations and clinical applications. Clin Orthop Rel Res 1988; 226:267-271.

388. Price PA, Poser JW, Raman N. Primary structure of the gamma carboxy glutamic acid containing protein from bovine bone. Proc Natl Acad Sci USA 1976; 73:3374-3375.

389. Nyman MT, Paavolainen P, Forsius S, Lamberg-Allardt C. Clinical Evaluation of fracture healing by serum osteocalcin and alkaline phosphatase. Annales Chirurgiae et Gynaecologiae 1991; 80:289-293.

390. Price PA, Williamson MK, Lothringer JW. Origin of the vitamin K-dependent bone protein found in plasma and its clearance by kidney and bone. J Biol Chem 1981; 256:12760.

391. Ohishi T, Takahashi M, Kushida K, Hoshino H, Tsuchikawa T, Naitoh K, Inoue T. Changes in biochemical markers during fracture healing. Arch Orthop Trauma Surg 1998; 118:126-130.

392. Obrant KJ, Merle B, Bejui J, Delmas PD. Serum bone-gla protein after fracture. Clin Orthop Rel Res 1990; 258:300-303.

393. Akesson K, Vergnaud Ph, Delmas PD, Obrant KJ. Serum osteocalcin increases during fracture healing in elderly women with hip fracture. Bone 1995; 16:427-430.

394. Bowels SA, Kurdy N, Davis AM, France MW, Marsh DR. Serum osteocalcin, total and bone-specific alkaline phosphatase following isolated tibial shaft fracture. Ann Clin Biochem 1996; 33:196-200.

395. Mallmin H, Ljunghall S, Larsson K. Biochemical markers of bone metabolism in patients with fracture of the distal forearm. Clin Orthop Rel Res 1993; 295:259-263.

396. Ingle BM, Hay SM, Bottjer HM, Eastell R. Changes in bone mass and bone turnover following distal forearm fracture. Osteoporos Int 1999; 10:399-407.

397. Oni OOA, Mahabir JP, Iqbal SJ, Gregg PJ. Serum osteocalcin and total alkaline phosphatase levels as prognostic indicators in tibial shaft fractures. Injury 1989; 20: 37-38.

398. Emami A, Larsson A, Petrén-Mallmin M, Larsson S. Serum bone markers after intramedullary fixed tibial fractures. Clin Orthop Rel Res 1999; 368:220-229.

399. Peters KM, Rosendahl T, Heller KD, Weigmann R, Zilkens KW. Osteocalcin levels in chronic osteomyelitis. Arch Orthop Trauma Surg 1994; 114:53-55.

400. Philipov JP, Pascalev MD, Aminkov BY, Grosev CD. Changes in serum carboxyterminal telopeptide of type I collagen in an experimental model of canine osteomyelitis. Calcif Tissue Int 1995; 57:152-154.

401. Raekallio J, Mäkinen PL. Alkaline and acid phosphatase activity in the initial phase of fracture healing. Acta Path Microbiol Scandinav 1969; 75:415-422.

402. Volpin G, Rees JA, Ali SY, Bently G. Distribution of alkaline phosphatase activity in experimentally produced callus in rats. J Bone Joint Surg 1986; 68B:629-634.

403. Urist MR, Mazet R, McLean FC. Pathogenesis and treatment of delayed union and non-union. J Bone Joint Surg 1954; 36A:931.

404. Lal SK, Jacob KC, Nagi ON, Annamalai AL, Nair CR. Variations of some plasma components after closed fractures. J Trauma: Injury Infect Crit Care 1976; 16: 206-211.

405. Bowles SA, Kurdy N, Davis AM, France MW. Changes in serum bone-specific alkaline phosphatase following tibial fracture. Ann Clin Biochem 1997; 34:690-691.

406. Leung KS, Fung KP, Sher AHL, Li CK, Lee KM. Plasma bone-specific alkaline phosphatase as an indicator of osteoblastic activity. J Bone Joint Surg 1993; 75B:288-292.

407. Brozmanová E, Škrovina B. Serum enzyme activity in bone tumors and osteomyelitis (LDH, GOT, GPT, CPK, CHE, ALP, AP, PP, ALD). Neoplasia 1977; 24:109-117.

408. Joerring S, Krogsgaard M, Wilbek H, Jensen LT. Collagen turnover after tibial fractures. Arch Orthop Trauma Surg 1994; 113:334-336.

409. Wichmann MW, Arnoczky SP, DeMaso CM, Ayala A, Chaudry IH. Depressed osteoblast activity and increased osteocyte necrosis after closed bone fracture and hemorrhagic shock. J Trauma: Injury, Infection, and Critical Care 1996; 41:628-633.

410. Slovik DM, Gundberg CM, Neer RM, Lian JB. Clinical evaluation of bone turnover by serum osteocalcin measurements in a hospital setting. J Clin Endocrin Metab 1984; 59:228-230.

411. Kjaersgaard-Anderson P, Pedersen P, Kristensen SS, Schmidt SA, Pedersen NW. Serum alkaline phosphatase as an indicator of heterotopic bone formation following total hip arthroplasty. Clin Orthop Rel Res 1988; 234:102-109.

412. Kurdy NMG, Bowles S, March DR, Davies A, France M. Serology of collagen types I and III in normal healing of tibial shaft fractures. J Orthop Trauma 1988; 12:122-126.

413. Antoniou J, Huk O, Zukor D, Eyre D, Alini M. Collagen cross-linked N-telopeptide as a marker for evaluating particulate osteolysis. Proc 43rd Ann Mtg Orthop Res Soc 1997.

414. Rico H, Villa LF. Serum tartrate-resistant acid phosphatase (TRAP) as a biochemical marker of bone remodeling. Calcif Tissue Int 1993; 52:149-150.

415. Naylor KE, Eastell R. Ch 27: Measurement of biochemical markers of bone formation. In Seibel MJ, Robins SP, and Bilezikian JP (Eds): Dynamics of Bone and Cartilage Metabolism. San Diego, CA, Academic Press 1999; p 401-410.

416. Delmas PD. Biochemical markers of bone turnover. J Bone Min Res 1993; 8:S549-S555.

417. Kraenzlin ME, Seibel MJ. Ch 28: Measurement of biochemical markers of bone resorption. In Seibel MJ, Robins SP, and Bilezikian JP (Eds): Dynamics of Bone and Cartilage Metabolism. San Diego, CA, Academic Press 1999; p 411-426.

CHAPTER 2

DEVELOPMENT AND EVALUATION OF AN INFECTED NON-UNION MODEL IN RABBITS

Abstract

Objective: The overall objective of this study was to develop an infected non-union model that could be used to evaluate the efficacy of gene transfer of growth factors for enhancing fracture healing in the presence of infection.

Materials and Methods: The basic model was a rabbit mid-diaphyseal femoral defect stabilized with bone plates and cortical screws. *Staphylococcus aureus* was used to establish osteomyelitis. There were five components to this study: (1) the first pilot study was performed to develop the model and determine the dose of *S. aureus* required to establish an infected non-union, (2) the second pilot study was performed to evaluate modifications to the model, (3) the model was then used in a larger study evaluating the use of adenoviral transfer of bone morphogenetic protein-2 (Ad-BMP-2, Chapter 3) for enhancing healing of infected non-unions, (4) post-hoc, the effect of the sclerosing agent on the adenoviral vector was evaluated *in vivo* by evaluating its effect on ectopic bone formation in nude rats following injection of Ad-BMP-2, and (5) by evaluating the effect of the sclerosing agent *in vitro* on the transduction efficiency of Ad-LacZ using production of β-galactosidase by synoviocytes in culture.

Results: Based on the first pilot study, a dose of 10^7 colony-forming units (cfu) of *S. aureus* was chosen. Bone-implant failure, fracture healing, and resolution of infection were the major limitations identified in the first pilot study. Therefore, older rabbits were used, a sclerosing agent was placed on the bone ends adjacent to the defect, and modifications were made to the surgical procedure. Surviving rabbits in the second pilot study developed an infected non-union, but bone-implant failure was a problem. This was resolved with the use of cerclage wires around the proximal and distal fragments. When

the infected non-union model was used in the larger study, the main problems included loss of rabbits from sepsis and lameness. The sclerosing agent attenuated bone production by Ad-BMP-2 *in vivo*, which may have been a result of either cell death resulting in too few cells for the adenovirus to transduce or direct damage to the adenoviral vector. When the transduction efficiency of Ad-LacZ was evaluated *in vitro*, it was not affected by low concentrations of the sclerosing agent.

Conclusion: The model developed appears to be an adequate infected non-union model; however, there are several limitations that may be addressed in future studies. The sclerosing agent did not appear to affect adenovirus transduction efficiency at low concentrations.

Introduction

Non-unions of open long-bone fractures due to osteomyelitis are a relatively common and devastating complication of fracture repair in both human[1] and veterinary surgery.[2] Severe trauma to the soft tissue, vasculature, and fracture fragments, heavy contamination at the time of injury, motion at the fracture site, the use of internal fixation techniques, and a compromised patient predispose the site to impaired healing (delayed- or non-union) and osteomyelitis (infected non-union). Although internal reduction and fixation provides the best stability of fracture fragments and is commonly used to stabilize fractures in human and veterinary surgery, it exacerbates infection because of additional tissue trauma, foreign body implantation, and the formation of a biofilm (bacterial glycocalyx), which provides a reservoir for bacteria. Following the establishment of osteomyelitis, it is difficult to eliminate infection and gain bone union, especially in the presence of implants or an unstable fracture. We hypothesize that enhancement of fracture healing with subsequent early removal of surgical implants would accelerate the resolution of infected non-union in clinical cases.

Growth factors have been shown to enhance fracture healing in several experimental and clinical studies.[3-31] Growth factors are most commonly delivered to the fracture site as a recombinant protein in a carrier matrix. There are several limitations associated with the delivery of growth factors as recombinant proteins.[32] Gene transfer of growth factors has overcome many of these limitations,[32] and has been shown to improve healing in non-union models.[33-43] There have been no studies evaluating the use of gene transfer of growth factors to enhance healing in an infected non-union model.

Historically, models of osteomyelitis have involved surgical creation of a cortical drill hole or fracture in either the femur or tibia, and inoculation of the medullary cavity or fracture site with *Staphylococcus aureus*.[44-52] Inoculation in the absence of a foreign body (such as a medullary pin or polymer) or sclerosing agent (such as sodium morrhuate) has not resulted in osteomyelitis. These traditional models are thought to be of limited value for evaluating treatment of infected non-unions because they do not simulate the biomechanical, physiological, and pathophysiological environment of an infected non-union, including the presence of fracture gaps, excessive motion at the fracture site, damage to the soft tissue, periosteum, endosteum, and marrow, as well as, the presence of implants.

Although some osteomyelitis models have involved creation of a closed mid-diaphyseal fracture that was stabilized with an intramedullary pin,[50,53-56] it is unknown if a persistent infected non-union will result or if the fracture will heal. The use of an infected non-union model was thought to be important in the initial investigation of gene transfer of growth factors for enhancing fracture healing. It is probably difficult to determine the early benefits of treatment if the fracture is allowed to heal normally, and more frequent evaluation intervals as well as more animals are required to determine the effects of treatment in these models.[11]

Recently, an infected non-union model in rats was used to evaluate enhancement of healing with recombinant human BMP-7.[57] Rats are small and difficult to surgically create a fracture defect and stabilize the fracture defect with stainless steel bone plate and cortical screws. The fracture defect in the latter study was stabilized with a polyacetyl plate, threaded Kirschner wires, and cerclage wires.[54] Rabbits, on the other hand, are

larger allowing creation of a fracture defect and stabilization with bone plates and cortical screws, as would be used in human and large animal veterinary surgery. Also, an adequate volume of blood can be collected at regular intervals for measurement of multiple serum bone markers (Chapter 5); and the bone is large enough that it could be easily sectioned longitudinally, with the stainless steel bone plate and cortical screws in place, using a diamond blade saw, for histological analysis of both decalcified and undecalcified tissue. Rabbits have Haversian bone similar to humans, as well as small and large animals. Rats, on the other hand, have plexiform bone. Rabbits are also a commonly used and reliable model for evaluating fracture healing and osteomyelitis.[44] Rabbits have the advantage over large animal models in that they are economical to purchase and house. Non-union models in rabbits have also been used successfully to evaluate adenoviral transfer of growth factors;[33,41] however, there have been no reports of an infected non-union model in rabbits.

The purpose of this study was to develop an infected non-union model in rabbits that could be used to evaluate the use of gene transfer of growth factors for enhancing fracture healing. The model used in the study was a modification of the non-union model used by Baltzer and coworkers[33,41] to evaluate adenoviral transfer of growth factors for enhancing fracture healing.

Materials and Methods

Overview

Development of the infected non-union model initially involved two pilot studies. Pilot study 1 was performed to determine the dose of *S. aureus* required to establish infection, and pilot study 2 to evaluate a modified infected non-union model. Following development and evaluation of the model, it was used in a larger study evaluating adenoviral transfer of the bone morphogenetic-2 gene (Ad-BMP-2) for enhancing fracture healing. There were several limitations identified with the infected non-union model used in the larger study. A major difference between our model and other non-union and infected non-union models was the use of the sclerosing agent. Therefore, post-hoc, the effect of the sclerosing agent on the adenoviral vector was evaluated *in vivo* and *in vitro*.

Determination of the Dose of Staphylococcus aureus *and Development of an Infected Non-Union Model (Pilot Study 1)*

The objective of this study was to determine the dose of *S. aureus* required to create osteomyelitis in a surgically induced and repaired femoral fracture while avoiding severe systemic signs, lameness, and death in rabbits. This lead to the hypothesis that osteomyelitis can be caused in surgically created femoral fractures in rabbits with 10^7 colony forming units (cfu)/mL of *S. aureus* while avoiding severe systemic signs, lameness, and death of rabbits. All procedures were approved by the Colorado State University Animal Care and Use Committee.

Six mature (3-3.3 kg) New Zealand White rabbits were used. Rabbits were assigned to one of three treatment groups receiving either 10^5, 10^6, or 10^7 cfu/mL of *S. aureus* (n=2 rabbits per group). These doses were chosen based on previous studies in rabbits where a dose of 10^4 cfu/mL will not result in osteomyelitis and a dose greater than 10^8 cfu/mL will result in severe sepsis and death of the animal.[44-51] *S. aureus* was chosen as the microbial agent because it is one of the most common causes of osteomyelitis in humans and animals,[58,59] it is routinely used in experimental models of osteomyelitis,[44-51] and it is readily available. Further, other bacteria such as *Staphylococcus intermedius*, *Proteus mirabilis*, and *Escherischia coli* were found to have a low rate of infection in animal models;[51] and *Pseudomonas aeruginosa* results in less bone lysis and more bone proliferation compared to *S. aureus*. Therefore, because of the lower infection rate and excessive proliferation, it may be more difficult to evaluate methods that would enhance fracture healing in an infected non-union.[44]

Rabbits were premedicated with morphine (0.5 mg/kg) and glycopyrrolate (0.03 mg/kg), and anesthesia was induced using isoflurane in oxygen in an induction chamber. The rabbits were intubated (3.0 mm endotracheal tube) for intermittent positive pressure ventilation during surgery (12 cm H_2O; 10-12 breaths per minute), as well as, monitoring of end tidal carbon dioxide and percentage oxygen saturation. A catheter was placed in the auricular artery for direct measurement of blood pressure, as well as, arterial blood collection for blood gas analysis. The auricular vein was catheterized for intravenous administration of polyionic, isotonic fluids (5-6 mL/kg/hr), analgesia, and medication during surgery. Atropine (0.02 mg/kg) was administered for bradycardia and dobutamine (2 mg/kg/min) for hypotension. Rabbits were given intravenous dextrans (4-5 mL/kg)

when there appeared to be excessive hemorrhage. Atracurium (0.1 mg/kg) was administered in some rabbits to reduce the amount of isoflurane required to maintain a surgical-plane of anesthesia.

Perioperative analgesia consisted of preoperative morphine epidurally (0.1 mL/kg) and subcutaneously (SQ; 0.5 mg/kg), fentanyl administered as a bolus (0.02 mg/kg) followed by a constant rate infusion during surgery (20 μg/kg/hr), and flunixin meglumine (0.5 mg/kg SQ) every 12 hours for 72 hours after surgery. Butorphanol (0.4 mg/kg SQ) was administered as needed postoperatively. Enrofloxacin (10mg/kg intramuscularly, IM) was administered preoperatively only.

The left hindlimb was routinely clipped, aseptically prepared, and draped. A routine lateral approach to the femur, between the *vastus lateralis* and *biceps femoris* was made. The soft tissue and periosteum were removed from the femur to prevent fracture healing.[33,41] A 7-hole dynamic compression plate (DCP) with 6, 2.7-mm cortical bone screws was routinely applied to the lateral aspect of the femur. The plate and screws were removed and an 11-mm mid-diaphyseal segmental defect (ostectomy) was created using an oscillating bone saw. The endosteum and marrow were removed using curettage and lavage. The bone plate and cortical screws were then reapplied to the femur. Cerclage wire (20-gauge) was placed around the proximal and distal fragment (one proximal and one distal). The wound was thoroughly lavaged to remove any bone debris. The muscle, subcutaneous tissue and skin were routinely apposed, and a stent bandage was placed over the wound.

Rabbits were inoculated in the fracture defect with 1 mL of 10^5, 10^6, or 10^7 cfu/mL *S. aureus* (S. Schaefler 1428, ATCC # 25923) 48 hours after surgery. The *S.*

aureus used was a clinical isolate and was sensitive to gentamicin and ampicillin. Rabbits were inoculated 48 hours after surgery to allow hematoma formation so that the infection was more likely to persist.

Three colonies of *S. aureus* were placed in 50 mL of brain-heart infusion (BHI) broth and incubated for approximately 22 hours at 37°C under stationary atmospheric conditions. The broth was centrifuged at 12,000 rpm for 10 minutes, and the supernatant fluid removed. The *S. aureus* pellet was resuspended in 50 mL of Dulbecco's phosphate buffered saline (PBS; no Ca^{2+}, no Mg^{2+} Gibco, Grand Island, NY) and 50 mL of sterile 80% glycerol (prepared in sterile distilled water and mixed well). The bacterial suspension was aliquoted (1 mL) into sterile cryovials (Corning Inc., Corning, NY) and immediately frozen at –70°C. The dilution required to obtain a concentration of 10^5, 10^6, and10^7 cfu/mL was determined by serial dilutions. After the vials had been in the freezer overnight, two vials were thawed rapidly at 37°C in a water bath. The cell suspension (1 mL) was transferred to a microcentrifuge tube. The cryovials were rinsed with 300 µL of PBS and the rinse added to the microfuge tube. The 1.3 mL suspension was centrifuged at 12,000 x g at room temperature for 2 minutes, to remove the supernatant containing the glycerol. The pellet was resuspended in 1 mL of PBS. Following resuspension, 100 µL of the bacterial suspension was added to 10 mL of PBS in a 15 mL conical tube (1:100-dilution).

The bacteria were titered by preparing 10^{-1}, 10^{-2}, 10^{-3}, 10^{-4}, 10^{-5}, 10^{-6}, 10^{-7} and 10^{-8} dilutions of the stock 1:100 dilution in BHI broth and plating 100 µL of each dilution onto BHI agar plates. Plates were incubated overnight at 37°C. The number of colonies on each plate containing between 30-300 colonies were counted to determine the

concentration of bacteria in cfu/mL in the stock solution. The dilution required to obtain a concentration of 10^5, 10^6, and 10^7 cfu/mL was calculated. Prior to inoculation, the 1 mL *S. aureus* preparation was thawed rapidly at 37°C, aliquoted to a microfuge tube, and centrifuged for 2 minutes at 12,000 x g. The supernatant was removed and the pellet resuspended in 1 mL of PBS. The *S. aureus* was diluted in PBS to a final concentration of 10^5, 10^6, or 10^7 cfu/mL. Although the concentration of *S. aureus* was determined from the initial titration, the concentration of *S. aureus* for each inoculation was determined by titrating and plating (BHI agar plates) the suspension and calculating the cfu/mL, as described previously: 0.5 mL of the final *S. aureus* preparation was drawn into a tuberculin syringe with a 22-gauge needle prior to inoculation of the fracture defect.

For inoculation the rabbits were anesthetized using isofluorane in 100% oxygen. The medial aspect of the limb was aseptically prepared and the proximal and distal aspect of the defect, which can be palpated percutaneously, inoculated with 1 mL of the *S. aureus* preparation. Approximately 0.5 mL of *S. aureus* was injected into the distal aspect of the proximal fragment and 0.5 mL in the proximal aspect of the distal fragment.

Rabbits were evaluated postoperatively twice a day for signs of systemic illness (fever, inappetence, and recumbency), infection (heat, pain, swelling, and redness), and lameness. Rabbits were given a score from 0 to 4 (0=none, 1=slight, 2=mild, 3=moderate, 4=severe) for attitude, appetite, lameness, and pain associated with the surgical site. The sum of scores from each category was calculated. Appropriate treatment was performed if the scores exceeded a predetermined number. If systemic signs of infection or lameness were severe the rabbit was euthanized.

Radiographic evaluation was performed on day 0, and weeks 4, 8, and 12 postoperatively. The number of weeks to initial- and bridging-callus formation was recorded. The percentage ossification in the defect was subjectively measured, and periosteal proliferation and bone lysis were subjectively graded from 0 to 4 (0=none, 1=slight, 2=mild, 3=moderate, and 4=severe) based on radiographic images.

Rabbits were euthanized 12 weeks after surgery. Following euthanasia the skin was clipped and prepared with alcohol. Gross examination was performed to evaluate the amount of soft tissue and bone damage and accumulation of purulent material. Quantitative aerobic culture was performed on the soft tissue, bone, and screws to confirm to the presence of infection. Infection was defined as $>10^4$ cfu/gram of tissue (g). The left femur was excised, and the soft tissue as well as the bone plate and screws were removed. The bone was sectioned sagittally, and placed in 10% neutral buffered formalin. The section was decalcified in EDTA (Decalcifying Solution, Stephens Scientific Division of Cornwall Corporation, Riverdale, NJ), embedded in paraffin, sectioned (5 μm), and routinely stained with hematoxylin and eosin (H&E). Quantitative histomorphometry was performed on sections that included the fracture defect. Because the original fracture defect was not always readily defined, the defect region of interest (ROI) was defined as being between the two screw holes immediately proximal and distal to the fracture defect. The percentages of total bone tissue (mineralized bone and marrow), live bone, dead bone, fibrocartilage, and fibrous tissue in the defect were measured. Histologically, the tissue in the defect was graded subjectively for inflammation (neutrophils, monocytes, vascularity) from 0 to 4 (0=none, 1=slight,

2=mild, 3=moderate, and 4=severe). Data were analyzed qualitatively because there were small numbers of animals in each group at the completion of the study.

Evaluation of the Modified Infected Non-Union Model (Pilot Study 2)

Six skeletally mature (4.1-4.3 kg; 9 to 10 month old) New Zealand White Rabbits were used to evaluate modifications to the previously developed infected non-union model. General anesthesia, analgesia, and surgical procedures were performed as in Pilot Study 1. Modifications that were made to the surgical procedure described in Pilot Study 1 included: (1) the use of two stacked 1.5-mm cuttable plates with 2.0 mm cortical bone screws, (2) creation of the defect with a side-cutting carbide burr (MicroAire Surgical Instruments, Charlottesville, VA), (3) cerclage wire was not used, and (4) a sclerosing agent (5% Sodium Morrhuate, American Regent Laboratories Inc, Shirley NJ; 0.4 mL) was placed on the bone ends adjacent to the defect. Rabbits were inoculated in the fracture defect percutaneously with 0.5 mL of 10^7 cfu/0.5mL *S. aureus* (S. Schaefler 1428, ATCC # 25923) 48 hours after surgery. Radiographic and histomorphometric evaluation and quantitative aerobic culture were performed as in Pilot Study 1. Data were analyzed qualitatively because there were small numbers of animals in each group at the completion of the study.

Infected Non-Union Model used to Evaluate Adenoviral Transfer of Growth Factors

Sixty-four skeletally mature (4.0-4.4 kg; 9 month old) New Zealand white rabbits were used to evaluate Ad-BMP-2 for enhancing fracture healing, using the infected non-union model developed and evaluated in Pilot Studies 1 and 2. The details of this part of

the study are described in Chapter 3. There was several modifications made to the model developed in Pilot Study 2 including: (1) the use of a longer plate, (2) two cerclage wires (20-gauge) proximally and distally, and (3) the defect was created after bending the plate but prior to placement of the plate and screws. Radiography, gross examination, quantitative aerobic culture, and histomorphometry were performed as previously described in Pilot Studies 1 and 2.

In Vivo *Evaluation of the Effect of Sodium Morrhuate on Adenoviral Transfer of the BMP-2 Gene*

Six skeletally mature nude rats (150-200 g) were used to evaluate the effect of sodium morrhuate on ectopic bone formation following intramuscular injection with Ad-BMP-2. Rats were assigned to one of two experimental groups: (1) Ad-LUC and (2) Ad-BMP-2. The rats were anesthetized with isofluorane in oxygen and the left hindlimb prepared with alcohol. The left quadriceps muscle was injected with 50 μL of sodium morrhuate using a 25-gauge needle and 1-mL syringe. The right quadriceps muscle was not injected. A volume of 50 μL was chosen because it was thought, subjectively, to be a large enough volume that the adenoviral vector could be easily injected at the same site 48 hours later, but that the size of the volume would not cause lameness or excessive tissue damage, and it was thought to be approximately the same ratio of tissue to sodium morrhuate volume that was used in the larger study evaluating the effect of Ad-BMP-2 on healing of infected non-unions. After 48 hours the rats were injected in the left and right quadriceps muscle with either Ad-LUC or Ad-BMP-2 (10^9 plaque-forming units (pfu) in

50 μL Gey's Balanced Salt Solution, Sigma Chemical Co, St. Louis, MO). Analgesia consisted of flunixin meglumine (0.4 mg/kg). The rats were not infected with *S. aureus*.

Rats were euthanized 12 weeks after injection. Radiographs were performed to determine the presence or absence of bone and the areas of bone formation were measured using Image-Pro Plus (Version 4.1) software program (Media Cybernetics, Silver Spring, MD).

At necropsy gross examination of the injection site was performed. The quadriceps muscle was removed, sectioned sagittally and placed in 10% neutral buffered formalin. Following decalcification in EDTA the tissue was stained using H&E for histological evaluation.

Data from the quantitative radiographic evaluation of the area of bone formation was analyzed using a mixed model ANOVA (PROC MIXED, SAS Institute, Cary, NC). The dependent variable was the area of bone formation, the fixed effect variables were the sodium morrhuate group (present or absent), the experimental groups (Ad-LUC or Ad-BMP-2), and the interaction, and the rat was used as the random variable.

In Vitro *Evaluation of the Effect of Sodium Morrhuate on Adenoviral Transfer of the LacZ Gene*

Synovium was collected from the metacarpo-/tarsophalangeal and carpal joint of horses. The synovium was cut into small pieces, placed in 0.2% collagenase in supplemented Ham's F12 media (SHF12; 25 mL 1M Hepes, 300 mg L-glutamine, 30 mg a-ketogutamic acid, 200 mL fetal bovine serum (FBS), 50 mg ascorbic acid, 20,000 U penicillin/streptomycin per 1 L), and incubated at 37°C and 5% CO_2 and gently stirred for

4 hours. The digested synovium was filtered and the filtrate centrifuged at 80 x g for 5 min at 21°C. The cells were washed and then resuspended in SHF12 media. The cells were counted using a hemocytometer and diluted in SFH12 media to a final concentration of approximately 10^6 cells/mL. The cells were seeded into wells (2 mL; 2 x 10^6/ 9.6 cm^2 well). The media was changed every 3 to 4 days until the cells were 80 to 100% confluent. The number of cells per well at approximately 100% confluence was 1.2 x 10^6.

The concentration of sodium morrhuate that caused cell detachment and loss of viability was determined for serum-supplemented and serum-free media. The dilutions of sodium morrhuate were 1:1, 1:2, 1:10, 1:10^2, 1:10^3, and 1:10^4. Ten μL of each dilution of sodium morrhuate was put into each well with 2 mL of media. The analyses were performed in duplicate. The cells were incubated with the dilutions of sodium morrhuate for 4 hours. The cells were rinsed with PBS, and a viability stain (Live/Dead Viability/Cytotoxicity Kit (L3224), Molecular Probes, Inc. Eugene, OR) was used to determine the numbers of live and dead cells.

The effect of sodium morrhuate on the adenoviral vector was then evaluated. There were four major groups: (1) Control (no Ad-LacZ and no sodium morrhuate), (2) Positive control (Ad-LacZ only; 10^{10} particles/ 10 μL; multiplicity of infection (MOI) of 100). (3) Negative control (sodium morrhuate only; 10 μL of 1:10, 1:10^4, or 0 dilution of sodium morrhuate), and (4) Ad-LacZ (1 x 10^{10}particles/ 10 μL) incubated with sodium morrhuate (10 μL of 1:10, 1:10^4, or 0 dilution) for 2 hours prior to cell transduction. The analyses were performed in duplicate. Prior to incubation with Ad-LacZ, the wells were washed twice with sterile PBS. The Ad-LacZ (10 μL) and/or sodium morrhuate (10 μL of 1:10, 1:10^4, or 0 dilution) was added to the cells in 2 mLs of serum-free Ham's F12

media and incubated for 4 hours at 37°C and 5% CO_2. The cells were washed with SHF 12 media, and then incubated in SHF 12 media for 24 hours to allow synthesis of β-galactosidase. The media was removed and the cells fixed in 4% paraformaldehyde (1 mL) for 10 min. The cells were washed with PBS three times and then placed in 1 mL Xgal solution [0.5 mL 20X KC Stock Solution; 0.5 mL 20X Xgal Stock Solution; 9 mL PBS; 10 μL 1M $MgCl_2$; 20X KC Stock Solution (1.05 g $K_4Fe(CN)_6$, 0.82 g $K_3Fe(CN)_6$, PBS 25 mL; stored at –20°C in the dark); 20X Xgal Stock Solution (20 mg Xgal, 1 mL dimethylformamide; stored at –20°C in the dark)] for 4 hours at 37°C and 5% CO_2. Transduction efficiency was evaluated by transduced cells (blue)/total cells.

Data from the calculation of transduction efficiency were analyzed using a mixed model ANOVA (PROC MIXED, SAS Institute, Cary, NC). The transduction efficiency and the percentage of dark blue cells were used as the dependent variables, the experimental group the fixed effect variable, and the well was used as the random variable.

Results

Determination of the Dose of Staphylococcus aureus *(Pilot Study 1)*

The results of the first pilot study are summarized in Table 1. Two rabbits, one in the 10^7 and one in the 10^6 cfu/mL experimental groups, showed mild signs of systemic illness and fever, which responded to treatment with enrofloxacin (10 mg/kg IM) every 12 hours for 4 days, and flunixin meglumine (1.1 mg/kg SQ) every 12 hours for 4 days. One rabbit (Rabbit 3) in the 10^6 cfu/mL group died from hemorrhagic enteritis at 11 weeks. Three rabbits showed signs of mild lameness within 2 weeks of surgery and

Table 1. Summary of the results of a pilot study evaluating a model of osteomyelitis using a femoral fracture with plate and screw fixation in rabbits.

No	Experimental Group	Outcome	Fever[1]	Lame[2]	Infect[3]	Bridg. callus[4]	Defect Ossific[5]
1	10^5 cfu/mL	Radiographic Union	No	No	No	Yes	Yes
2*	10^5 cfu/mL	Surgical Failure	No	Yes	Yes	-	-
3**	10^6 cfu/mL	Infected Non-Union	Yes	Yes	Yes	No	No
4	10^6 cfu/mL	Radiographic Union	No	No	No	Yes	Yes
5*	10^7 cfu/mL	Surgical Failure	Yes	Yes	Yes	-	-
6	10^7 cfu/mL	Infected Non-Union	No	No	Yes	No	No

*Euthanized at the time of implant/bone failure, 7 and 14 days after surgery. **Euthanized at 11 weeks because of severe hemorrhagic enteritis. 1. Fever within 2 weeks of inoculation. 2. Lame within 2 weeks of inoculation, 3. Infected at 12 weeks. 4. Bridging-callus at 12 weeks. 5. Defect ossification at 12 weeks.

inoculation; two of these rabbits fractured the operated limb through the screw holes at 7 and 14 days after surgery and were euthanized (Figure 1; Rabbits 2 and 5 in experimental groups 10^5 and 10^7 cfu/mL). Overall there appeared to be no severe systemic signs or lameness associated with the higher inoculation dose (10^7 cfu/mL) compared to the lower doses (10^5 and 10^6 cfu/mL).

All four rabbits surviving past 14 days (experimental groups 10^5, 10^6, 10^7 cfu/mL) had initial-callus formation at 4 weeks. Two rabbits (experimental groups 10^5, 10^6 cfu/mL) had bridging-callus formation and 80-90% ossification in the defect (radiographic union) at 12 weeks (Figure 2). Results from the radiographic evaluation of periosteal proliferation and bone lysis for all rabbits are shown in Figures 3 and 4. Based on radiographic evaluation of bridging-callus, defect ossification, periosteal proliferation, and bone lysis, rabbits receiving the lower inoculation doses (10^5 and 10^6 cfu/mL *S. aureus*) appeared to be more likely to have a radiographically detectable union and to have minimal radiographic signs of osteomyelitis compared to rabbits receiving the higher inoculation dose (10^7 cfu/mL *S. aureus*)

At 11 and 12 weeks after inoculation two rabbits (experimental groups 10^6 and 10^7 cfu/mL) had gross signs of infection, and had a quantitative aerobic culture of approximately 10^7 cfu/g, which was consistent with infection as defined by our protocol ($>10^4$ cfu/g). The two rabbits (experimental groups 10^5 and 10^7 cfu/mL) that were euthanized 7 and 14 days after inoculation also had gross signs of infection and a quantitative aerobic culture of approximately 10^7 cfu/g. In the rabbits with gross signs of infection there was a large volume of purulent material around the implant and bone. Accumulation of purulent material in the soft tissue resulted in unavoidable superficial

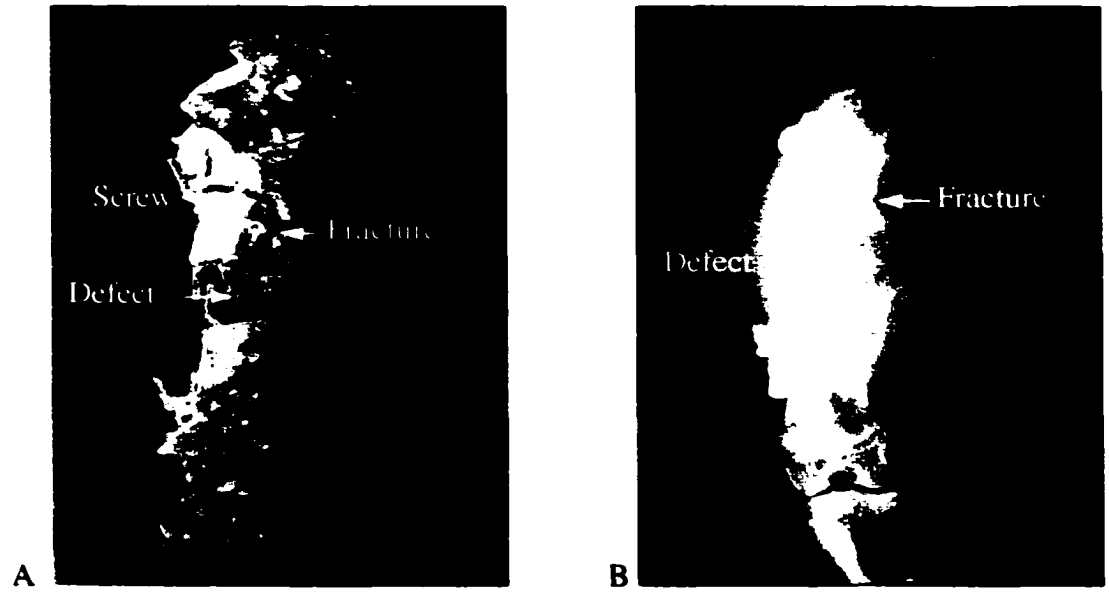

Figure 1. (a) Gross necropsy specimen and (b) craniocaudal radiographic view of Rabbit 2 in Pilot Study 1 following fracture of the operated limb through the screw holes in the proximal fragment.

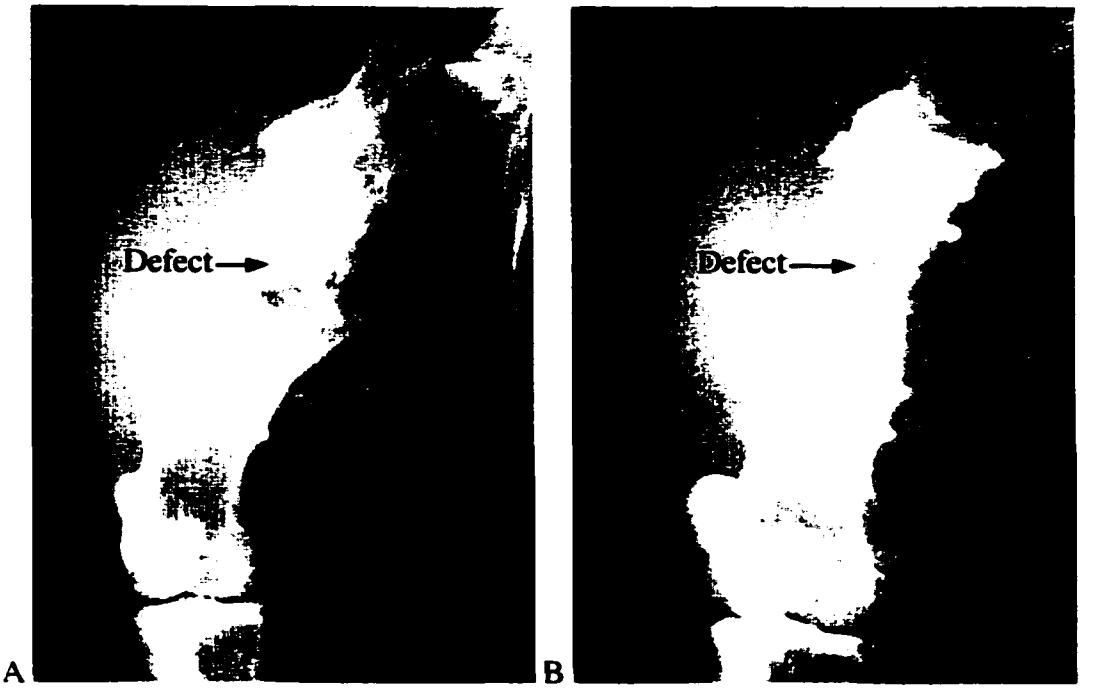

Figure 2. Craniocaudal radiographic views of the rabbits in Pilot Study 1 with healed defects at 12 weeks. (A) Rabbit 1 that was inoculated with 10^5 cfu/mL *S. aureus*. (B) Rabbit 4 that was inoculated with 10^6 cfu/mL *S. aureus*.

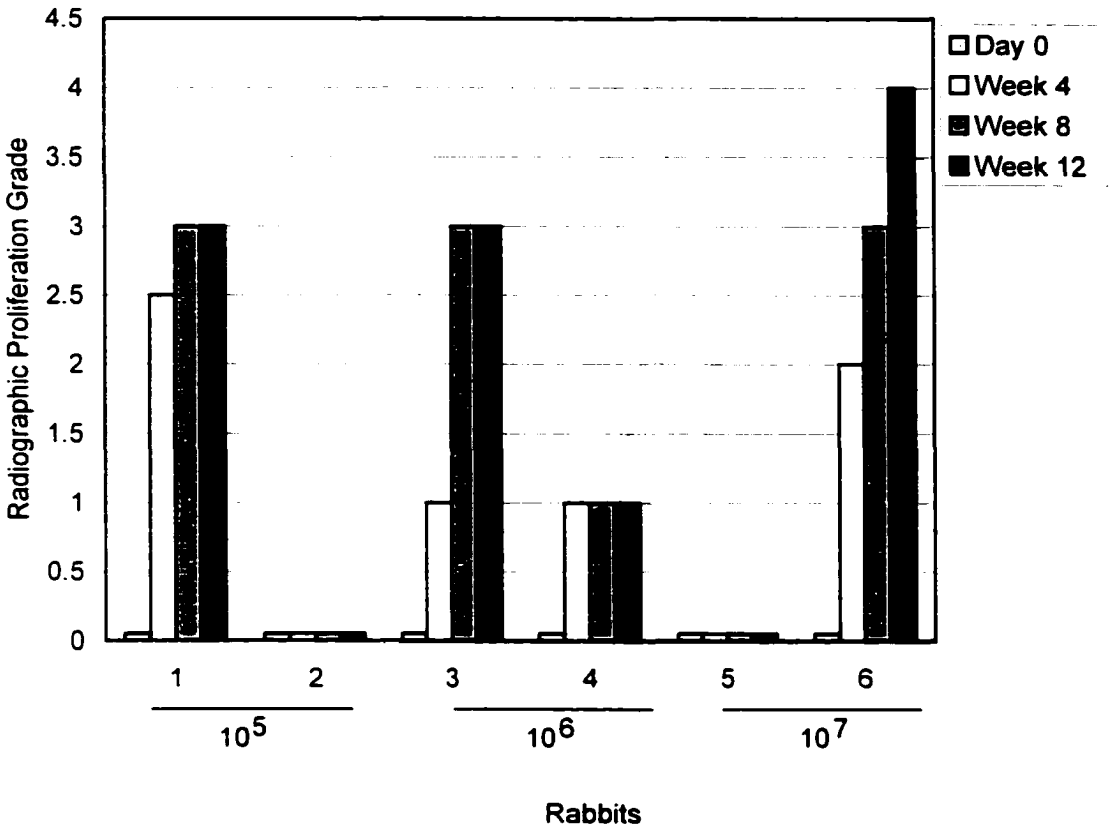

Figure 3. A plot of periosteal proliferation based on radiographic images over the 12-week experimental period (Pilot Study 1). Rabbit Numbers (1 to 6) and Experimental Groups (105, 106, 107 cfu/mL *S. aureus*) are plotted by time period on the x-axis, and the subjective grade for periosteal proliferation is plotted on the y-axis. Proliferation was graded subjectively from 0 to 4 (0=no proliferation, 1=slight proliferation, 2=mild proliferation, 3=moderate proliferation, and 4=severe proliferation). Rabbits 1 and 4 had a readiographically detectable union at 12 weeks; Rabbits 2 and 5 fractured the operated limb within 2 weeks of surgery. There was an increase in proliferation over time in Rabbits 1, 3, and 6. Rabbit 4 developed a radiographic union by defect ossification (Figure 2), and had minimal periosteal proliferation. Rabbit 6, which was inoculated with the highest dose of *S. aureus* (107 cfu/mL), had the highest grade for periosteal proliferation.

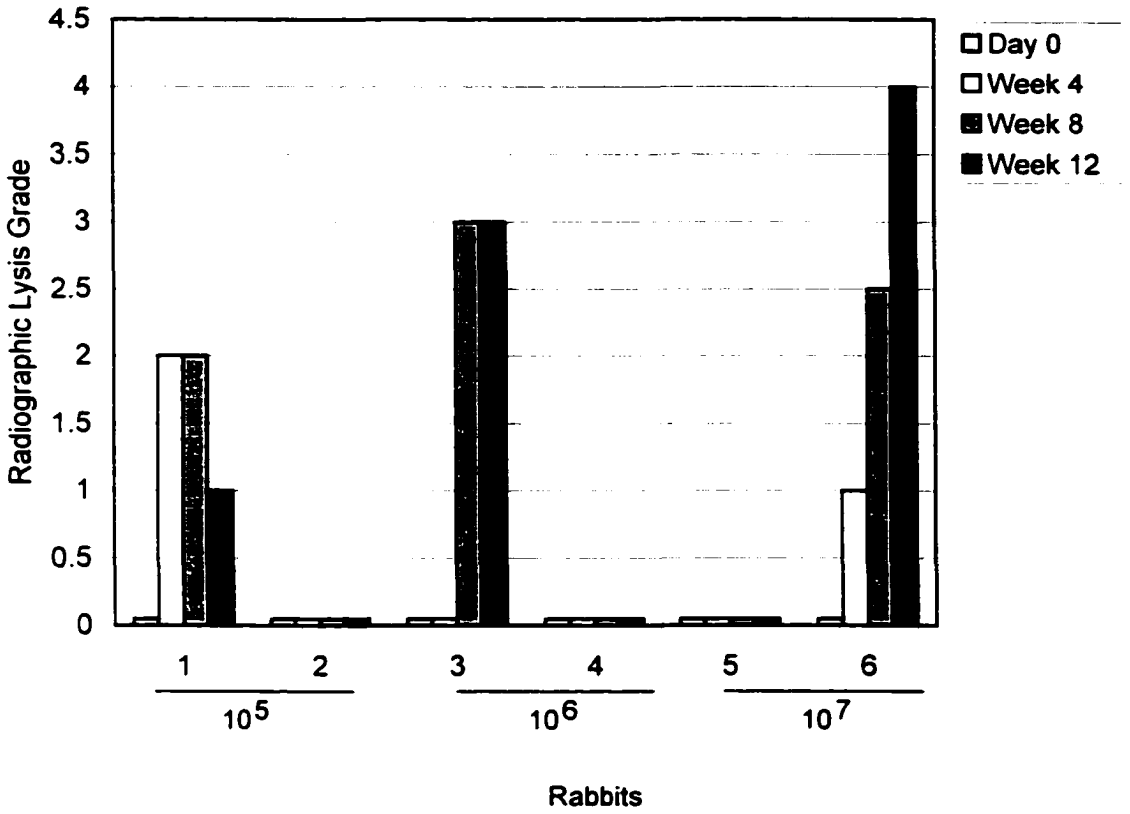

Figure 4. A plot of bone lysis based on radiographic images over the 12-week experimental period (Pilot Study 1). Rabbit Numbers (1 to 6) and Experimental Groups (105, 106, 107 cfu/mL *S. aureus*) are plotted by time period on the x-axis, and the subjective grade for Bone Lysis is plotted on the y-axis. Lysis was graded subjectively from 0 to 4 (0=no lysis, 1=slight lysis, 2=mild lysis, 3=moderate lysis, and 4=severe lysis). Rabbits 1 and 4 had a radiographically detectable union at 12 weeks; Rabbits 2 and 5 fractured the operated limb within 2 weeks of surgery. There was an increase in the grade for bone lysis over time in the two rabbits that developed a radiographic non-union (Rabbits 3 and 6). One rabbit (Rabbit 4) that developed a radiographic union did not show signs of lysis, and the other rabbit (Rabbit 1) that developed a radiographic union initially showed signs of lysis, however the lysis resolved over time.

contamination of the bone, which made it difficult to determine if the infection was actually in the bone or only in the soft tissue based on culture results. There were two rabbits (experimental groups 10^5 and 10^6 cfu/mL) that had no signs of infection grossly and no bacterial growth on aerobic culture of the bone, screws, or soft tissues at 12 weeks. Based on these observations, although there did not appear to be a direct relationship between the inoculation dose and the quantitative aerobic culture results, rabbits receiving the lower inoculation dose (10^5 and 10^6 cfu/mL *S. aureus*) appeared to be less likely to develop a persistent infection.

The composition of the fracture defect (percentage of fibrous tissue, fibrocartilage, and bone) is shown in Figures 5 and 6. The percentage of the total bone tissue that mineralized was 32%, 56%, and 49% for experimental groups inoculated with 10^5, 10^6, and 10^7 cfu/mL *S. aureus*, respectively. The percentage of mineralized bone that was alive was 76%, 76%, and 98% for experimental groups inoculated with 10^5, 10^6, and 10^7 cfu/mL of *S. aureus*, respectively. There was no inflammation associated with samples from either rabbit in experimental group 10^5 and 10^6 cfu/mL, however the rabbit inoculated with 10^7 cfu/mL of *S. aureus* had moderate inflammation (grade 3 out of 4).

Based on the results of this pilot study a dose of 10^7 cfu/mL of *S. aureus* was selected and modifications to the model were made. A second pilot study was performed to evaluate the modified infected non-union model.

Evaluation of the Modified Infected Non-Union Model (Pilot Study 2)

In this study rabbits developed an infected non-union at 12 weeks. There were no rabbits that developed any signs consistent with systemic illness. Radiographically the

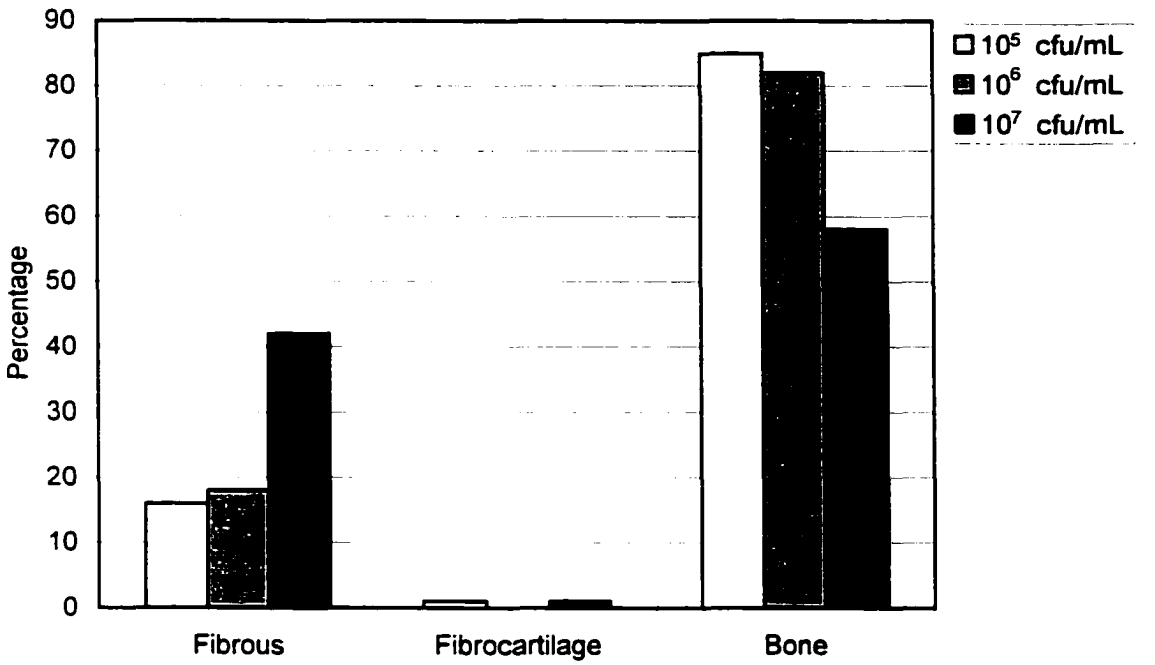

Figure 5. A plot of the type of tissue composing the entire defect area based on quantitative histomorphometry at 12 weeks (Pilot Study 1). Experimental groups (105, 106, 107 cfu/mL *S. aureus*) are plotted by tissue type (fibrous tissue, fibrocartilage, bone) on the x-axis, and the percentage of the type of tissue composing the entire defect area is plotted on the y-axis. There was mroe fibrous tissue and less bone formation associated with the higher inoculation dose. NOTE: bone is defined by total bone tissue, and therefore includes mineralized bone and bone marrow, as well as live and dead bone. There was mineral fibrocartilage in the fracture defect region.

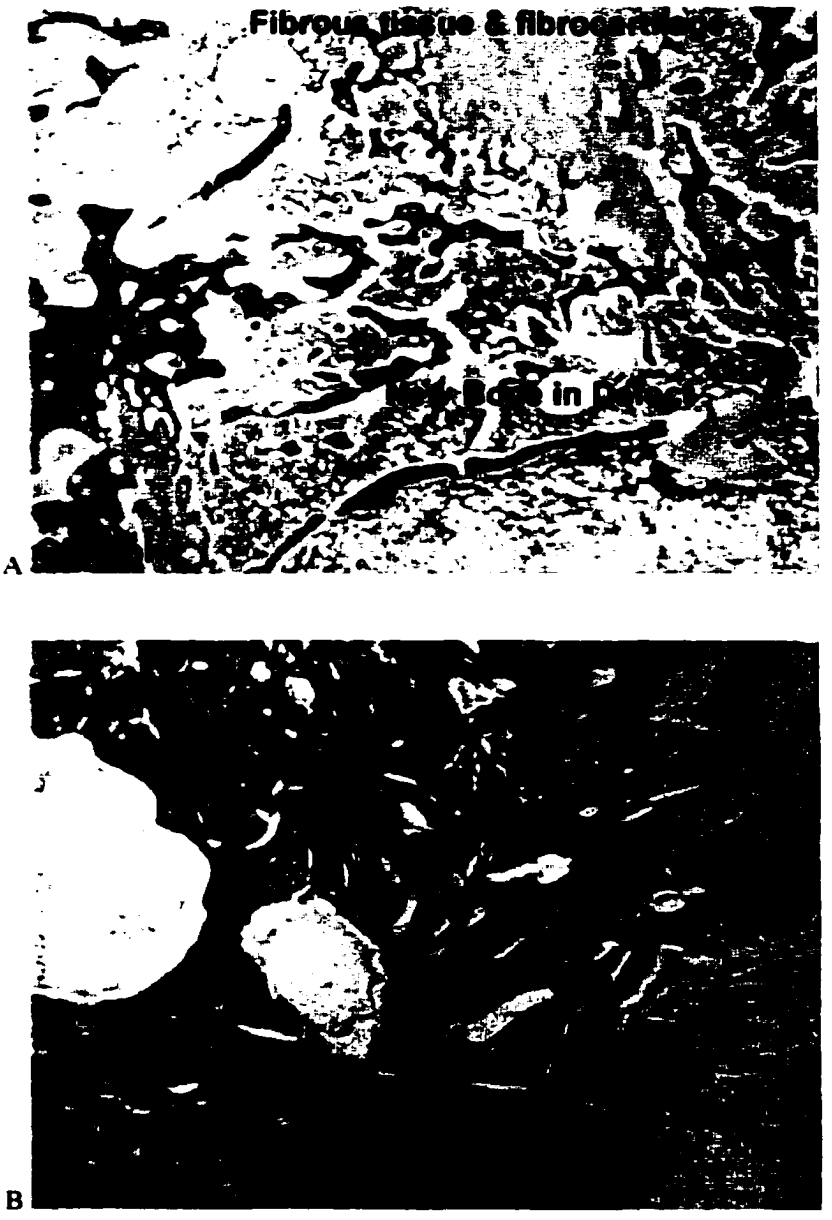

Figure 6. Histological sections of two rabbits from Pilot Study 1, illustrating a large proliferative response and defect ossification at 12 weeks after surgery. There was only a very small amount of fibrous tissue and cartilage in the defect in one rabbit (A).

fractures appeared representative of non-unions, with no ossification in the defect and minimal periosteal bone proliferation (Figure 7). Quantitative aerobic culture at 12 weeks was consistent with infection as defined by our protocol ($>10^4$ cfu/g). Histologically, there was a similar percentage of tissue composing the repair tissue in the fracture defect as compared to the 10^7 cfu/mL *S. aureus* experimental group in the first pilot study. The percentage of mineralized bone that was alive was lower and the inflammation grade was higher (grade 4/4; severe) in the second pilot study where a sclerosing agent was used (Figure 8). The major complication was bone-implant failure, which occurred in four rabbits.

Infected Non-Union Model used to Evaluate Adenoviral Transfer of Growth Factors

The infected non-union model developed in Pilot Studies 1 and 2 was used to evaluate the use of Ad-BMP-2 for enhancing healing of an infected non-union model (Chapter 3). There was minimal morbidity or mortality associated with the rabbits in the non-infected groups. In general, rabbits tolerated general anesthesia and the surgical procedure. The surgical time was approximately 1 to 1.5 hours and the total general anesthesia time was 2.5 to 3 hours. The rabbits did not appear to be lame as a result of the actual fracture defect.

There was a high morbidity and mortality, however, associated with the rabbits in the infected groups. There was one rabbit that had failure of the bone-implant construct early in the study and this rabbit was replaced. The overall mortality was 31% (20/65). The mortality for rabbits in the non-infected group was 16% (5/31) and in the infected group was 44% (15/34). General causes of mortality in both groups were bone-implant

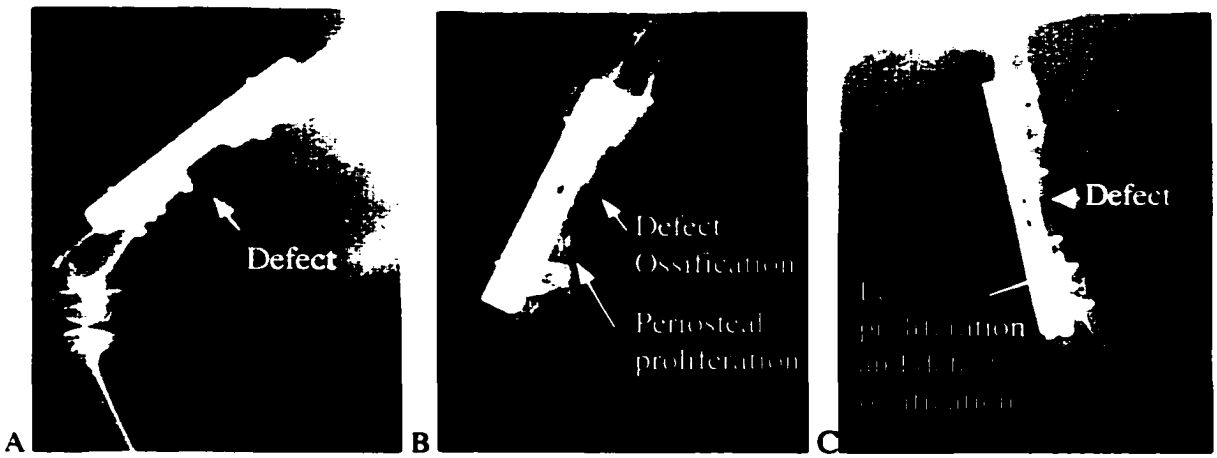

Figure 7. Lateral radiographic views of a surgically created infected non-union fracture. (A) The femoral fracture defect on day 0 following repair with plates and screws. (B) Severe periosteal proliferation around the defect and ossification within the defect at 12 weeks in Rabbit 6 in Pilot Study 1. (C) Less periosteal proliferation and less ossification in the defect at 12 weeks following modification of the model (Pilot Study 2).

Figure 8. Histological section of an operated rabbit femur, at 4 weeks after surgery, illustrating old bone with empty lacunae. It appears that the sclerosing agent has damaged the bone adjacent to the fracture defect. There was no periosteum attached to the old bone and no new bone formation. Muscle from the adjacent soft tissue is encroaching on the fracture defect region. The section was stained with hematoxylin and eosin. Magnification 20X

failure (6/65, 9%), vertebral fracture (4/65, 6%), and anesthetic complications (3/65, 5%). There was one rabbit that fractured its metacarpus and then had failure of the bone-implant construct and there was one rabbit that had lateral femorotibial joint instability and required euthanasia.

The major cause of mortality of rabbits in the infected groups was systemic illness (8/34, 24%). Rabbits became dull and inappetent. Supportive therapy, including subcutaneous fluids and flunixin meglumine, was provided. One rabbit was treated with enrofloxacin. Despite the supportive therapy the rabbits either died or required euthanasia. Hematology and serum biochemistry was performed on one rabbit and revealed severe neutropenia (8,000 cells/μL), anemia (15%), azotemia (blood urea nitrogen 106 mg/dL and creatinine 8.3 mg/dL), hypoglycemia (75 mg/dL), and acidosis (bicarbonate 10.5 mEq/L). Necropsy examination revealed hepatic lipidosis, pleuritis/pneumonia, and/or enterocolitis. Histological evaluation was performed on the liver, spleen, kidney, and lung of one rabbit. The liver had changes consistent with hepatic lipidosis, the spleen was within normal limits except for extramedullary hematopoeisis, the kidney had tubular casts, and the lung had thickening of the alveoli and bronchioles, abscessation, necrosis, inflammation, and fibrin accumulation consistent with fibrinonecrotic pneumonia. All of these findings were consistent with sepsis. *P. aeruginosa* was cultured from the liver and spleen of one rabbit and was considered to be either a contaminant or infection as a result of the rabbit being immunocompromised.

The mortality of infected rabbits increased when, in addition to the surgery, 10 mL of blood was collected for measurement of serum bone markers. The inoculation dose was reduced to 0.5×10^7 cfu/0.5 mL of *S. aureus* and rabbits in both groups were treated

with dextrans, iron, vitamin B, as well as, subcutaneous polyionic isotonic fluids. The mortality associated with systemic illness was zero following reducing the dose of *S. aureus* and increasing the amount of supportive therapy.

Other complications that did not require euthanasia but did cause morbidity were lameness, weight-loss, and abscessation or fistulation. Lameness grades were recorded for 51 rabbits prior to euthanasia, and 19% (5/27) of rabbits in the non-infected groups and 42% (14/24) of rabbits in the infected groups were lame. The lameness was moderate to severe in 11% (3/27) of rabbits in the non-infected groups and 38% (9/24) of rabbits in the infected groups. Lameness was associated with the development of a septic femorotibial joint associated with the distal aspect of the bone plate in infected rabbits (n=10). When the plate was placed more proximally and less dissection was performed adjacent to the femorotibial joint, the incidence of femorotibial joint infection was reduced. These changes were only slight modifications and did not alter the actual model. Rabbits in both non-infected and infected groups developed lameness associated with medial luxation of the patella (n=7). These rabbits were operated later in the study and patella luxation may have been subsequent to less dissection and more retraction on the tissues adjacent to the femorotibial joint. Rabbits in both the non-infected and infected groups also had weight-loss during the duration of the study. There were 65% (17/26) rabbits in the non-infected groups and 94% (17/18) rabbits in the infected groups that lost weight. The average weight-loss was 3.5% of initial body weight for non-infected and 13.8% for infected rabbits. External signs of infection (abscessation and fistulation) were recorded for 47% (9/19) of infected rabbits surviving to 16 weeks.

There was a greater than 90% infection rate in the infected rabbits and there was no infection in the rabbits in the non-infected groups. Infection was classified as whether there was accumulation of purulent material on gross examination, a positive culture, and radiographic lysis at 16 weeks (non-infected = lysis grade of 0.5 of less and infected = lysis grade of 1 or greater). There were only three rabbits that did not meet all three requirements for being infected or non-infected. There was one rabbit in the infected group that had no signs of infection grossly, a negative culture, and no radiographic lysis at 16 weeks, and on further examination of this rabbit's record the culture of the inoculation was negative; therefore, this rabbit was considered to be in the non-infected group. There was one rabbit in the infected group that did not have signs of infection at the fracture site; however, this rabbit had severe infection of the femorotibial joint, and was therefore considered in the infected group. There was one rabbit in the non-infected group that had a small amount of inspissated purulent material at the fracture site; however, this was sterile on culture of the tissue and screw, therefore the rabbit was considered in the non-infected group.

There were 43% (6/14) of rabbits in the non-infected and 67% (6/9) of rabbits in the infected control groups that had some defect ossification. However only one rabbit in the non-infected and one rabbit in the infected control group had >30% defect ossification (95 and 100%). There were two rabbits in the non-infected and one rabbit in the infected control groups that developed bridging-callus formation.

Histological examination of the rabbits euthanized prior to 16 weeks showed that the rabbits appeared to have developed an acellular and avascular defect region (Figure 9). Nuclear scintigraphy (pool phase) also confirmed a photopenic region in the area of

Figure 9. Histological section of an operated femur from a rabbit that was euthanized 24 hours after surgery. There were numerous empty lacunae, the surface of the bone had no periosteum, and there was hemorrhage, fibrin, and necrosis in the marrow cavity. The section was stained with hematoxylin and eosin. Magnification 20X.

the defect suggesting reduced blood flow to the defect region at 4 weeks most likely as a result of the use of a sclerosing agent (Chapter 4). Rabbits euthanized prior to 16 weeks also had muscle and fat in the defect (Figure 8) and rabbits euthanized at 16 weeks also had a large amount of fat in the fracture defect (Chapter 3).

In Vivo *Evaluation of the Effect of Sodium Morrhuate on Adenoviral Transfer of the BMP-2 Gene*

There was no morbidity or mortality associated with injection of the nude rats with sodium morrhuate, Ad-LUC, or Ad-BMP-2. Rats in the Ad-BMP group had bone formation and rats in the Ad-LUC group had no bone formation at 12 weeks. The limb injected with sodium morrhuate formed bone in 1 of 3 rats injected with Ad-BMP-2 (Figure 10). The area of bone formation was significantly higher in the Ad-BMP-2 groups and higher in the Ad-BMP-2 groups without sodium morrhuate (Figure 11). Gross examination at necropsy confirmed the radiographic findings in that there was soft tissue only in the Ad-LUC rats and bone in the Ad-BMP-2 rats; and only 1 of 3 rats injected with sodium morrhuate had bone formation in the muscle tissue. Histomorphometry confirmed bone formation in the rats treated with Ad-BMP and only in 1 of 3 rats treated with Ad-BMP and sodium morrhuate (Figure 12). There was no inflammation associated with injection of sodium morrhuate or Ad-BMP-2 in any of the groups.

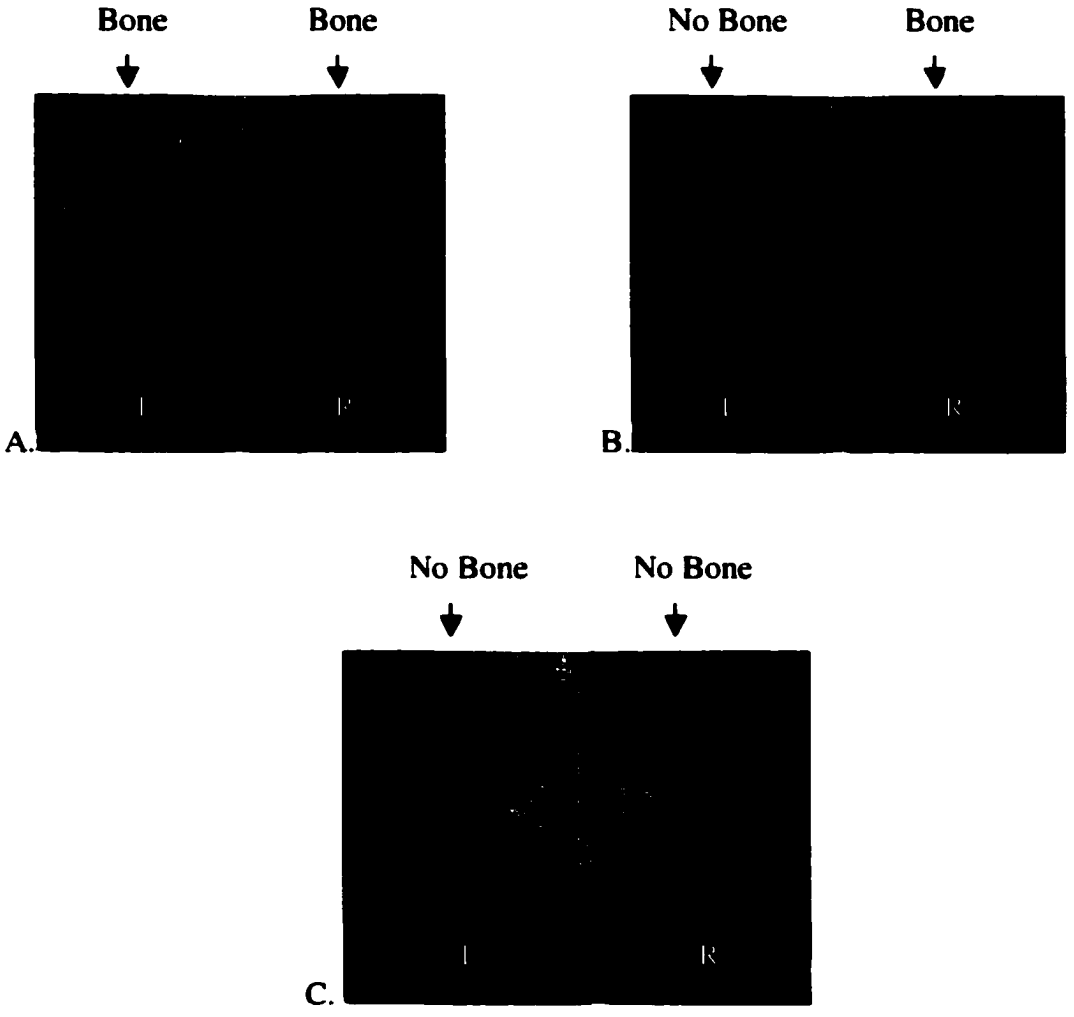

Figure 10. Lateral radiographic views of rats at 12 weeks from the *in vivo* study evaluating the effect of sodium morrhuate on bone formation following injection with Ad-BMP-2. The radiographs illustrate bone formation in the quadriceps muscle. The left quadriceps muscle was injected with sodium morrhuate 48 hours prior to injection with either Ad-LUC (control) or Ad-BMP-2. (A) A rat injected with Ad-BMP-2 with bone formation in both the left (L) and right (R) limbs, and (B) a rat injected with Ad-BMP-2 with bone formation in the right quadriceps only. Therefore, the sodium morrhuate attenuated *de novo* bone formation with Ad-BMP-2. (C) A rat injected with Ad-LUC showing no bone formation in the left or right quadriceps.

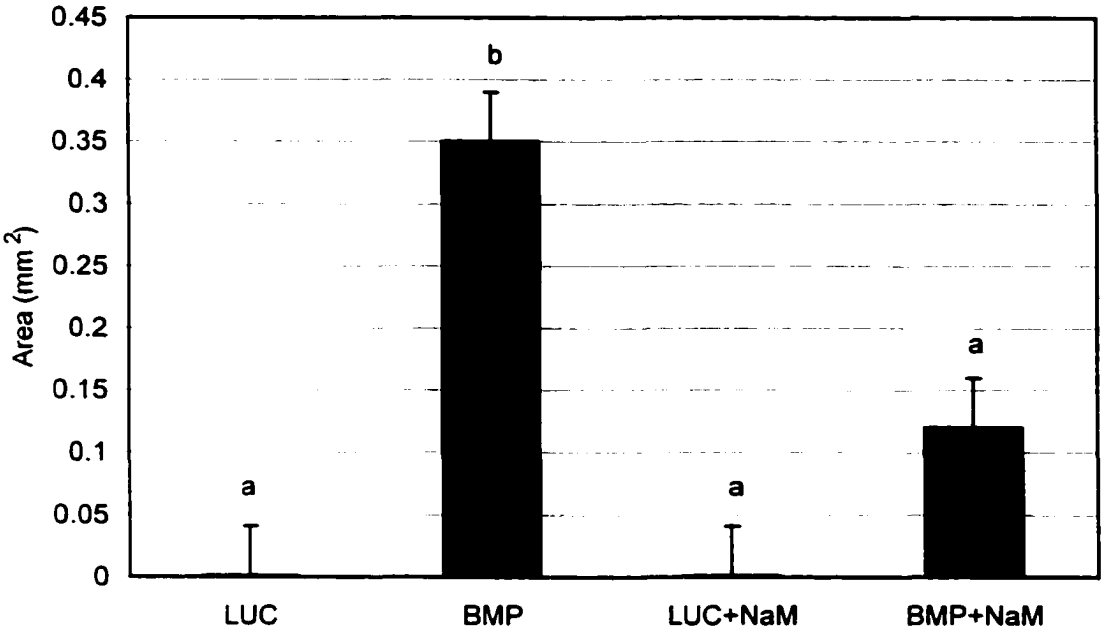

Figure 11. A plot from the *in vivo* study evaluating the effect of sodium morrhuate on bone formation following intramuscular injection with Ad-BMP-2, showing the association between radiographic bone formation and treatment group. Rats in the Ad-BMP-2 groups (BMP) had bone formation whereas those in the Ad-LUC control groups (LUC) did not. There was an attenuation of bone formation when rats were injected with sodium morrhuate (NaM) 48 hours prior to injection with Ad-BMP (BMP+NaM). Different letters represent statistically significant differences. The level of significance was $p<0.05$.

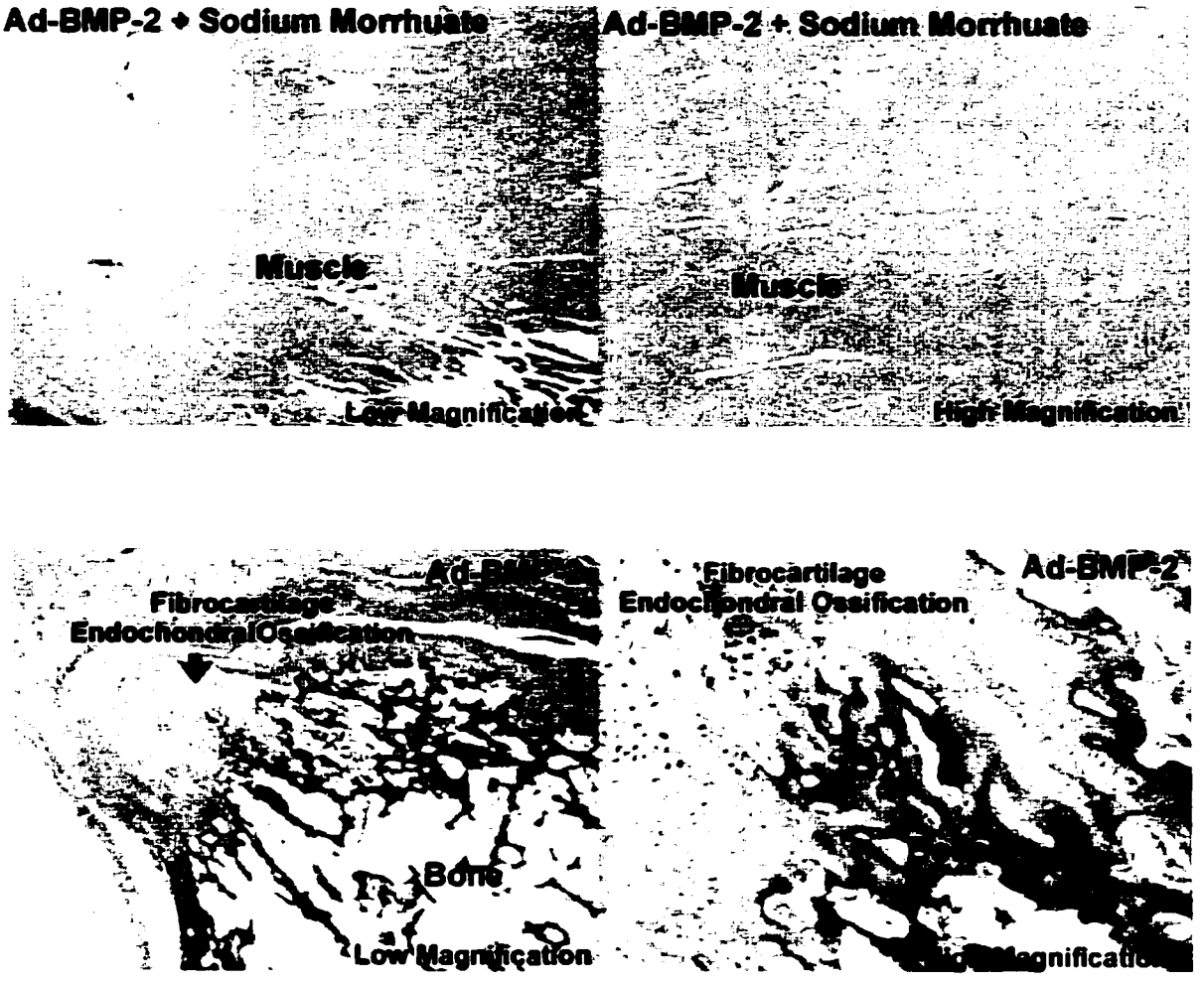

Figure 12. Histological sections of the quadriceps muscle from rats in the *in vivo* study evaluating the effect of sodium morrhuate on bone formation following intramuscular injection with Ad-BMP-2. (A) Left quadriceps that was injected with sodium morrhuate 48 hours prior to injection with Ad-BMP-2 and (B) the right quadriceps that was not injected with sodium morrhuate prior to injection with Ad-BMP-2. There is endochondral ossification and bone formation in the right quadriceps muscle that was not injected with sodium morrhuate prior to Ad-BMP-2, but not in the left quadriceps muscle that was injected with sodium morrhuate. The sections were stained with hematoxylin and eosin.

In Vitro *Evaluation of the Effect of Sodium Morrhuate on Adenoviral Transfer of the LacZ Gene*

Evaluation of the effect of sodium morrhuate on the cells in culture in serum-free media showed that 10 μL of a 1:1 or 1:2 dilution of sodium morrhuate caused the cells to become detached and non-viable (Table 2; Figure 13). Therefore dilutions of 1:10 (high concentration), $1:10^{4}$ (low concentration), and 0 (control) were chosen to evaluate the effect of sodium morrhuate on the transduction efficiency of the adenoviral vector. There was a significant difference in transduction efficiency between the control as well as the sodium morrhuate only (negative control) groups, and Ad-LacZ groups (Figure 14). There was no difference in transduction efficiency between the Ad-LacZ only (positive control) and the Ad-LacZ incubated with the $1:10^{4}$ dilution of sodium morrhuate groups. Because there was variability in the intensity of blue staining between cells, in addition to being transduced (blue) and not transduced (unstained), cells were classified as light and dark blue. There were a greater number of light blue cells in the group treated with Ad-LacZ incubated with $1:10^{4}$ dilution of sodium morrhuate (Figure 15a and b) compared to the Ad-LacZ only (positive control) group. The cells incubated with Ad-LacZ and the 1:10 dilution of sodium morrhuate became detached and did not appear to be transduced based on a lack of blue staining. These cells did not appear to be viable. However, because they were fixed in paraformaldehyde, the viability assay was not performed. Therefore, the effect of a high concentration of sodium morrhuate (1:10 dilution) could not be determined using these techniques because we were unable to differentiate damage to the virus versus damage to the cells.

Table 2. The detachment and percentage viability of cells in culture incubated with different concentrations of sodium morrhuate (NaM) for 4 hours

Media	**Group**	**Detached**	**% Viability**	**Comment**
Serum-Supplemented	NaM1:1	Yes	40 to 60%	Both detached and attached cells viable and non-viable
	NaM1:2	No	>90%	Occasional non-viable cell
	NaM1:10	No	>95%	Almost no non-viable cells
	NaM1:10^{2}	No	>95%	Almost no non-viable cells
	NaM1:10^{3}	No	>95%	Almost no non-viable cells
	NaM1:10^{4}	No	>95%	Almost no non-viable cells
	NaM 0	No	>95%	Almost no non-viable cells
Serum-Free	NaM1:1	Yes	<5%	Almost no viable cells
	NaM1:2	Yes	<5%	Almost no viable cells
	NaM1:10	Yes/No	50 to 80%	Both detached and attached cells viable and non-viable
	NaM1:10^{2}	No	>95%	Almost no non-viable cells
	NaM1:10^{3}	No	>95%	Almost no non-viable cells
	NaM1:10^{4}	No	>95%	Almost no non-viable cells
	NaM 0	No	>95%	Almost no non-viable cells

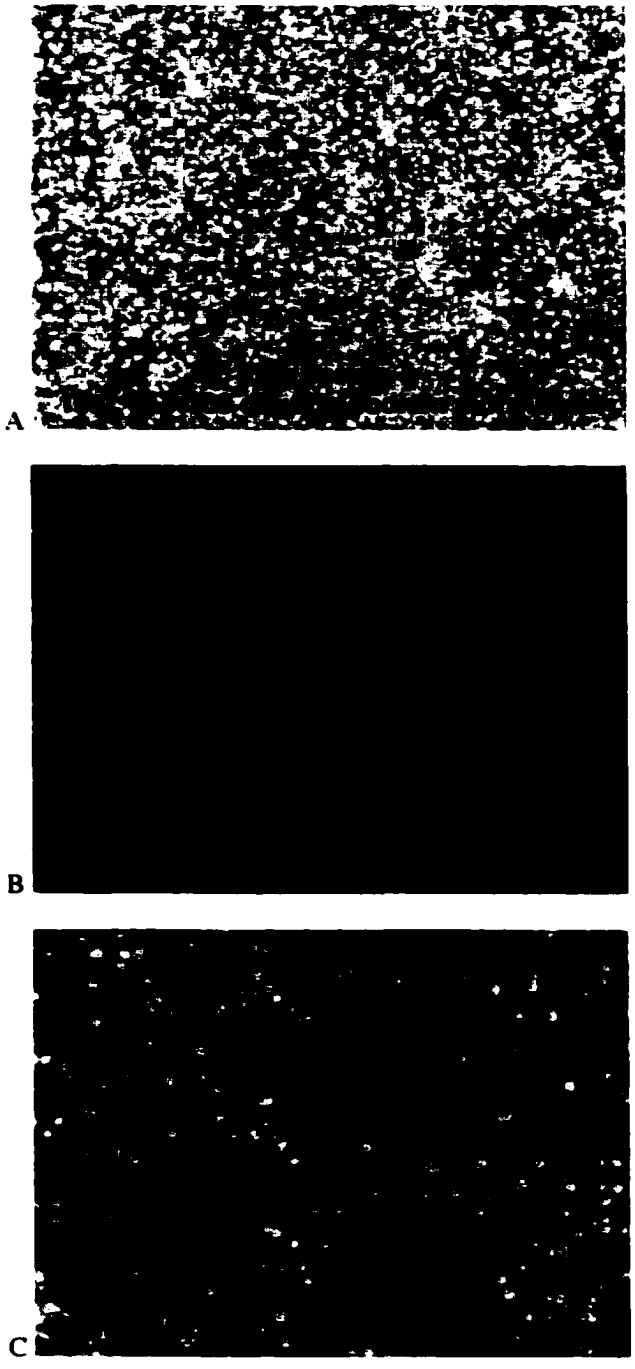

Figure 13. Cytotoxic assay demonstrating the viability of cells incubated for 4 hours with different concentrations of sodium morrhuate in serum-free media. Green cells are viable and red cells are non-viable. Cells incubated with 10 μL of a 1:100 or greater dilution of sodium morrhuate were viable (A), whereas cells incubated with 10 μL of a 1:1 or 1:2 dilution of sodium morrhuate were not viable (B), and there was a lot of variation in the cell viability when cells were incubated with 10 μL of a 1:10 dilution of sodium morrhuate (C).

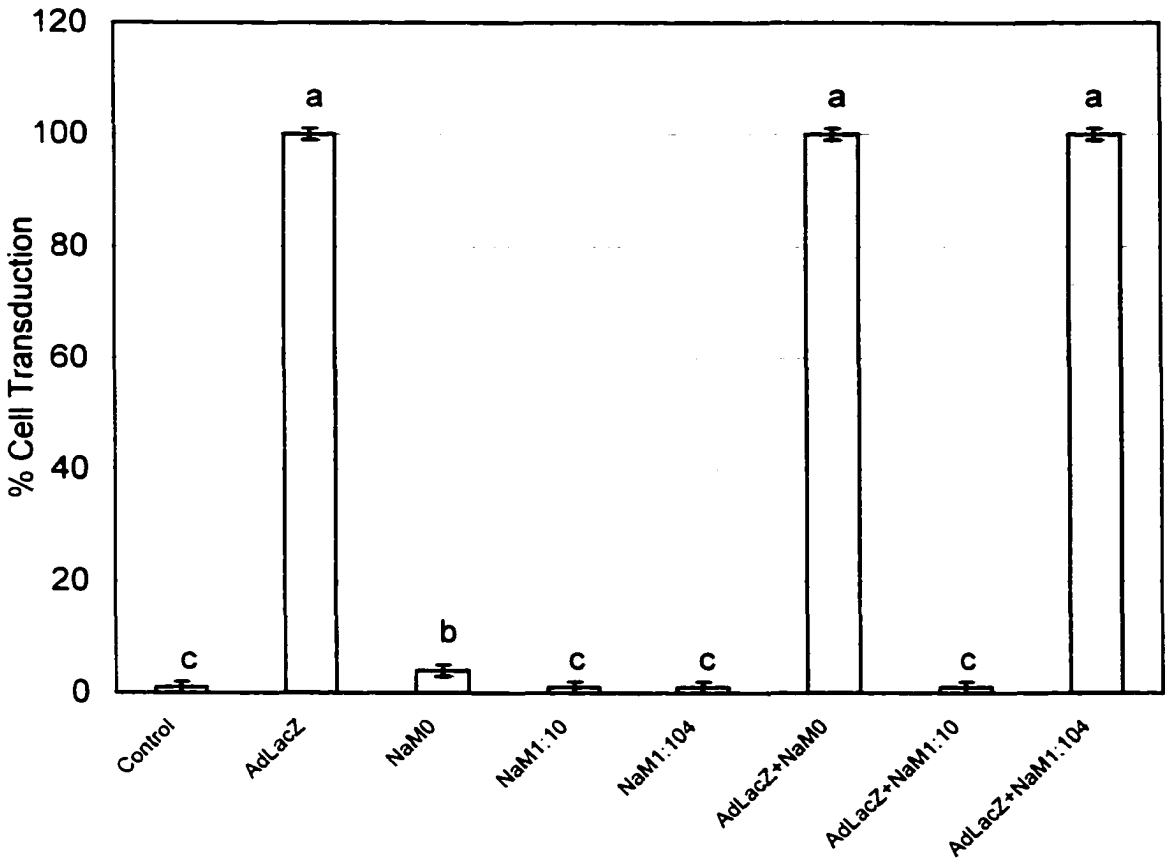

Figure 14. A plot from the *in vitro* study evaluating the effect of sodium morrhuate on transduction efficiency of Ad-LacZ, showing the association between experimental group and the percentage of cells that were transduced. There was no transduction of cells when the adenovirus was incubated with sodium morrhuate (NaM) at a 1:10 dilution (AdLacZ+NaM1:10). However there was no effect on transduction efficiency when Ad-LacZ was incubated with a more dilute solution of NaM (AdLacZ+NaM1:104). Different letters represent values that were statistically significantly different. The level of significance was $p<0.05$.

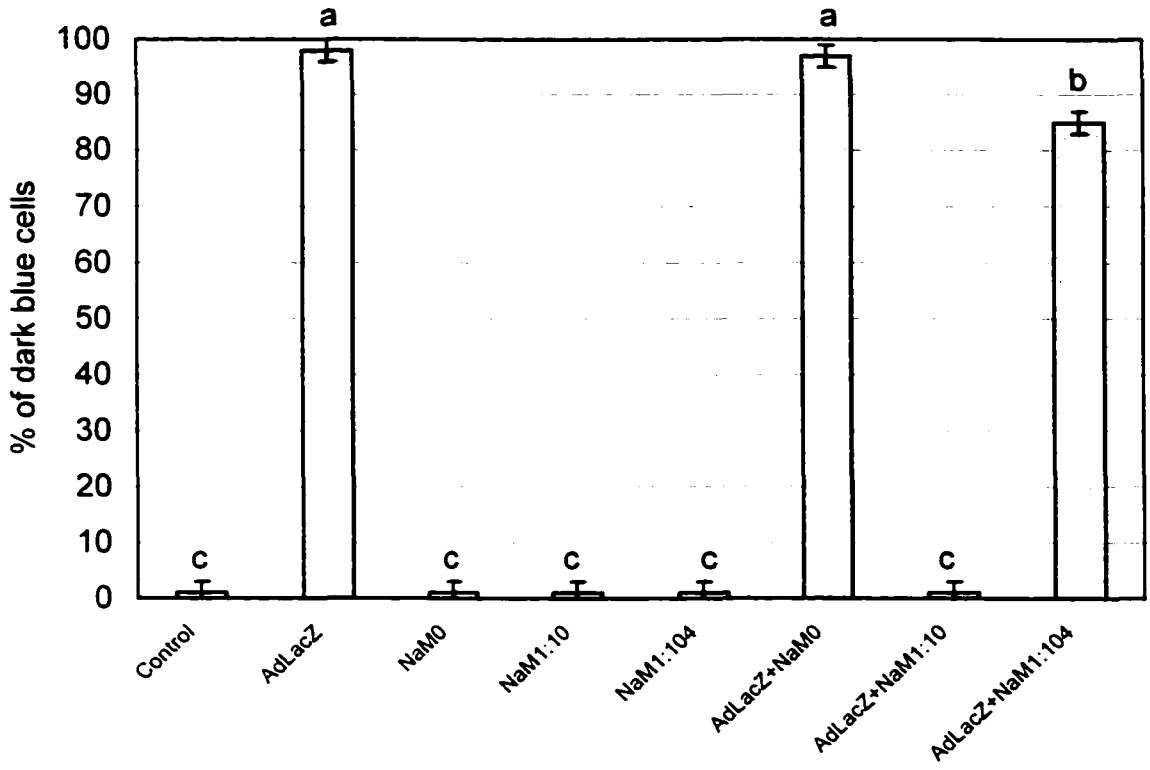

Figure 15a. A plot from the *in vitro* study evaluating the effect of sodium morrhuate on transduction efficiency of Ad-LacZ, showing the association between experimental group and the percentage of dark blue cells. There were fewer dark blue cells when the Ad-LacZ was incubated with NaM at a 1:10 dilution (AdLacZ+NaM1:104) compared to Ad-Lac Z controls. Although the importance of this is unknown, it may be a result of a decrease in β-galactosidase production by cells incubated with sodium morrhuate compared to cells that were not incubated with sodium morrhuate. The decrease in β-galactosidase production may have been a result of cell damage. Different letters represent values that were statistically significantly different. The level of significance was $p<0.05$.

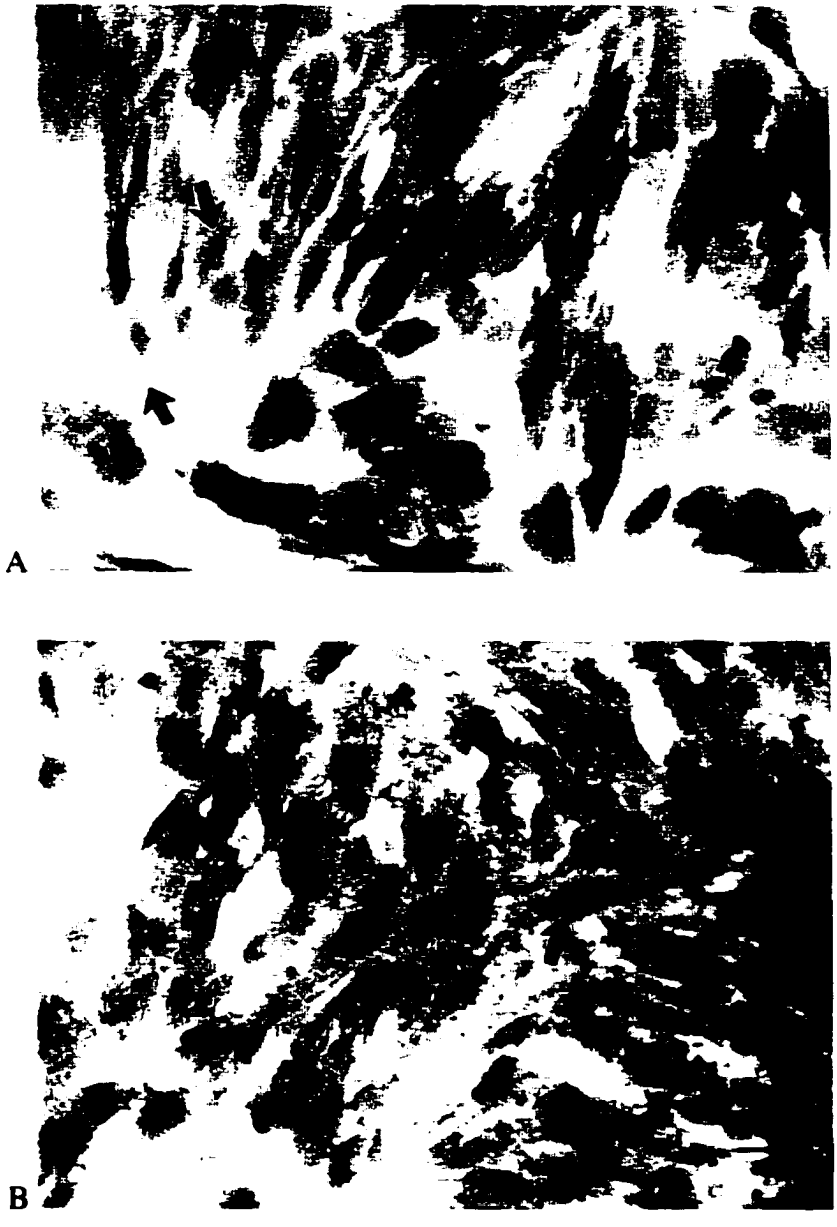

Figure 15b. Cytology of cells from the *in vitro* study evaluating the effect of sodium morrhuate on the transduction efficiency of Ad-LacZ. (A) Ad-LacZ was incubated with sodium morrhuate ($1:10^4$ dilution) for 2 hours prior to incubation with cells and (B) Ad-LacZ positive control. Although the transduction efficiency was 100% for both groups, there were more light blue cells when the Ad-LacZ was incubated with sodium morrhuate (arrow Figure (A)) and more dark blue cells in the Ad-LacZ control group (arrow Figure (B)). The importance of this finding is unknown.

Discussion

There are several advantages of the model used in this study. Firstly the rabbit was chosen as a model for economical reasons, ease of housing and care, their large size, and the fact that rabbits have Haversian bone. The use of the sclerosing agent on the ends of the fracture fragments caused some bone necrosis as indicated histologically by the presence of empty lacunae, pycnotic nuclei, and the presence of necrotic bone associated with infection. Early histological sections also indicated an acellular and avascular region. The avascularity was confirmed by the use of nuclear scintigraphy (Chapter 4), and bone lysis was slow to develop which is most likely a reflection of the poor blood supply early in the study. The non-infected rabbits had very little periosteal response associated with the fracture. The model was developed for evaluating gene therapy for enhancing healing of complicated fractures and hence is a severe model and probably adequate for that purpose. The sclerosing agent did not appear to affect the adenoviral vector at low concentrations. Although the concentration of sodium morrhuate in the defect at the time of injection of the Ad-BMP-2 is unknown, based on the 48-hour duration it was probably low. The infection rate in our study was >90% and there were few rabbits in the control groups with fracture healing; therefore, the proposed model is a reliable infected non-union model.

There were also several limitations with our model. While a baseline-mortality, from systemic illness, such as hemorrhagic enteritis, of approximately 20% is expected for rabbits in experimental studies (Dr D. Maul, CSU Laboratory Animal Resources, Personal Communication), the mortality associated with *S. aureus* inoculation of rabbits in the infected groups was high.

There were several changes made to the model developed in Pilot Study 1. The two major problems identified with the infected non-union model in this pilot study were bone-implant failure in the first two weeks after surgery, and radiographic union with resolution of the osteomyelitis at 12 weeks. Radiographic union and resolution of the osteomyelitis occurred only in the rabbits inoculated with the lower doses of *S. aureus* (10^5 and 10^6 cfu/mL); therefore, a dose of 10^7 cfu/mL of *S. aureus* was chosen.

To overcome surgical failure due to fracture propagation through the screw holes the size of the rabbits was increased and the size of the cortical screws and bone plate was decreased. We also used a burr instead of an oscillating bone saw to create the defect, because it was thought that this would be less traumatic and cause less iatrogenic destruction of the bone matrix.

Using a similar femoral fracture defect and with plate and screw fixation model, our collaborators demonstrated minimal bone healing and periosteal proliferation.[33,41] Inoculating the defect with *S. aureus* appeared to increase radiographic signs of bone proliferation and healing compared to our collaborator's study. Inoculation of the fracture site with *S. aureus* may have stimulated a greater healing response compared to the non-union model. Therefore, to reduce this response and to promote the development of an infected non-union, older rabbits were used, and a more thorough lavage of the surgical and more aggressive curettage of the endosteum was performed. A sclerosing agent (sodium morrhuate) was also placed on the proximal and distal bone fragments adjacent to the defect to both reduce the proliferative response and increase the development of osteomyelitis.

There was a large accumulation of purulent material at the fracture site. A smaller volume (0.5 mL) of *S. aureus* was used in an attempt to reduce the accumulation of purulent material in the soft tissues, which may cause false positive bone cultures because of gross contamination of the bone tissue.

The major limitation identified in the second pilot study was bone-implant failure with rabbits fracturing the limb through the screw holes. Therefore, it was concluded that the cerclage wire was critical for a favorable outcome. Additional modifications included: (1) the use of a longer bone plate and more screws (4 screws proximal and 4 screws distal to the fracture defect) to prevent fracture at the proximal and distal aspect of the plate, (2) the screws were angled cranially and caudally during placement to prevent fracture through the screw holes, and (3) the defect was created initially and then the plate applied to prevent trauma associated with repeated screw insertion and removal.

The higher inoculation dose of *S. aureus* was chosen to cause infection for the 16-week duration of the larger study. While rabbits tolerated the higher dose initially, when a blood sample was collected the rabbits began to develop severe signs of sepsis leading to death or requiring euthanasia. Therefore, the 0.5×10^7 cfu/mL dose of *S. aureus* appears to be the absolute maximum dose that can be administered to rabbits in this more complicated model.

Other studies have also found a high mortality associated with *S. aureus* in rabbits,[44,49,51] and doses higher than 10^8 cfu are almost invariably fatal.[49] Norden and Kennedy[51] reported a mortality from sepsis of 30% (19/64) following inoculation of rabbits with 3×10^6 cfu of *S. aureus*, and more recently Schulz and coworkers[61] reported a "relatively low" mortality of 25% following inoculation with 3×10^5 cfu. Similarly,

inoculation of sheep with 4 x 10^8 cfu of *S. aureus* resulted in fatal sepsis.[46] In these studies the only procedures performed were creating a drill hole in a long-bone, and not the extensive surgical procedures required for creation of an infected non-union. In the latter study,[46] treatment with a single dose of penicillin/streptomycin prevented death. Antimicrobials were not used in our study because the rabbits appeared to tolerate the inoculation dose based on Pilot Study 2, the development of fatal enterocolitis is associated with antimicrobial use in rabbits,[49] and we had not evaluated the effects of antimicrobial use on the infected non-union model in Pilot Studies 1 and 2. In future studies, rabbits should be treated aggressively with supportive therapy and a single dose of an antimicrobial, and a maximum inoculation dose of 0.5 x 10^7 cfu of *S. aureus* used. Unfortunately, as reported in other studies, the lower doses of *S. aureus* in Pilot Study 1 resulted in early resolution of the infection and defect ossification.

Interestingly, a recent infected non-union model in rats demonstrated a 100% infection rate and no mortality, as well as no lameness, weight-loss, or drainage when rats were inoculated with 10^5 cfu *S. aureus* following creation of a segmental defect stabilized with a polyacetyl plate and threaded Kirschner wires.[57] Although there were no signs of lameness, cortical fracture did occur with deformation of the limb and collapse of the fragments into the defect, which would have possibly affected the results of the study. Despite their small size and plexiform rather than Haversian bone, rats may be a more suitable model for evaluating infected non-unions because of the high infection rate and low mortality associated with inoculation. Other studies, however, evaluating the use of recombinant proteins in a non-union model in rats, reported a mortality of 20% (9/45) from general anesthesia, infection, and fixation failure.[14]

Staphylococcus aureus was chosen because it is a common cause of osteomyelitis in human[58] and veterinary[59] surgery, is commonly used in models of osteomyelitis, and has several virulence factors that facilitate formation of osteomyelitis.[62,63] Bacterial toxins as well as localized ischemia cause bone necrosis which leads to the formation of chronic osteomyelitis.[64] While the virulence of *S. aureus* was responsible for the high incidence of infection in our study, it was also responsible for the high mortality with rabbits showing signs consistent with sepsis which often resulted in death or euthanasia.

It has also been shown previously, however, that a low dose of a *S. aureus* strain that is not highly virulent will not establish infection, as found in our first pilot study. There is very little difference between the dose that will cause infection and the dose that will cause mortality in an infected non-union model. This was demonstrated in the study by Rodeheaver and coworkers[52] where a dose of 10^5 cfu resulted in an infection rate of only 81%, but a dose of 10^6 cfu caused a 75% mortality within 14 days of inoculation. There is also a wide variation in virulence of *S. aureus*; Andriole and coworkers[49] showed that 10^8 cfu of a particular strain of *S. aureus* caused almost 100% mortality, and the same dose of another strain did not appear to affect the rabbits while causing a high infection rate. The *S. aureus* strain used in our study was actually of relatively low virulence compared to some other strains.

The presence of skeletal implants is reported to increase the incidence of bone infection.[65,66] Stainless steel implants reduced the infective dose (ID50) from 1.7×10^8 cfu of *S. aureus* in control animals to 2.4×10^5 cfu of *S. aureus* in animals with a stainless steel implant.[66] The infection rate also increased from 21% in control animals to 67% in animals with stainless steel implants.[66] The results of the latter study would suggest that

the rabbits in our study inoculated with 10^5 cfu of *S. aureus* should have developed a persistent infection, however that study was performed in dogs, only 67% of animals developed infection, the duration of the study was 15 days, and there were low numbers of animals in our study which could explain the conflicting results. However, we had a combination of implants as well as a sclerosing agent which, based on yet other reports in rabbits,[61] should have resulted in infection with an inoculation dose of 10^5 cfu/mL of *S. aureus*. In Pilot Study 1 we did not use a sclerosing agent, therefore further studies with lower doses of *S. aureus* and a sclerosing agent should be performed prior to future studies using this model.

Other causes of rabbit loss in our study were bone-implant failure and lumbar vertebra fracture. A 38% incidence of bone-implant failure was reported in another study where a 20-mm femoral defect was created in rabbits, and stabilized with bone plates and screws, an intramedullary pin, and cerclage wire.[67] As mentioned previously, bone-implant failure was reduced by using larger rabbits, smaller but longer bone plates and smaller cortical screws, more cortical screws proximally and distally, angling the cortical screws during placement, creating the defect with a burr rather than an oscillating bone saw, creating the defect prior to plate and screw placement, use of cerclage wire, and sedation during recovery from general anesthesia and transport. While other authors[29] have found that the cerclage wire is not important for fracture stabilization in rats, rabbits are larger and have greater forces on their hindlimbs, and hence the use of cerclage wire is recommended.

Lumbar vertebra fracture was a common cause of loss in our study. The rabbits underwent several procedures including radiography, nuclear scintigraphy, and blood

collection during the course of this study. Sedation of rabbits prior to transportation and the use of an induction chamber to induce anesthesia appeared to reduce losses associated with lumbar vertebra fracture. Rabbit loss from general anesthesia was relatively uncommon in our study, which may have been a result of the extensive monitoring and treatment.

Based on our pilot studies we decided to use a longer bone plate to prevent fracture at the proximal and distal aspects. However, as a result of dissection adjacent to the femorotibial joint, several of the rabbits developed septic arthritis, which caused severe lameness. To avoid this complication, the plate was moved slightly proximal and there was less dissection of the soft tissues near the joint, and the incidence of infection was reduced. The development of septic arthritis from a hematogenous route has been reported as a complication in other rabbit models of osteomyelitis;[44] however, while infection may have been a result of septicemia in our study, it was most likely a result of direct extension from the surgical site because it was only observed in the femorotibial joint of the operated limb.

There was a lack of ossification within the defect following treatment with Ad-BMP-2 and rabbits in the Ad-BMP-2 treated groups healed by a large callus formation in both the non-infected and infected groups (Chapter 3). The major difference, other than the use of different plates and screws, between our model and previous models that showed defect ossification with Ad-BMP-2 treatment,[33,41] was the use of a sodium morrhuate on the bone fragments adjacent to the defect. Sodium morrhuate is a detergent sclerosant that causes cell damage by protein-theft denaturation. An aggregation of detergent molecules forms a lipid bilayer in the form of a sheet, a cylinder, or a micelle,

and then disrupts the cell surface membrane, and removes essential proteins from the cell membrane surface.[60] Sodium morrhuate also results in an inflammatory response and fibrosis.[60] The cell damage caused an acellular and avascular region in the defect area. The lack of defect ossification was, therefore, either a result of damage to the adenoviral vector during handling and transportation, a lack of cells in the fracture defect region for the adenoviral vector to transduce, reduced vascularity which would diminish cell migration to the defect, or damage to the adenoviral vector from the sclerosing agent.

The fact that injection of Ad-BMP-2 into the quadriceps muscles of nude rats produced bone in all animals indicates that the adenoviral vector was not damaged during handling and transportation. However, injection of Ad-BMP-2 48-hours after injection of sodium morrhuate reduced or eliminated bone production. This was either caused by the sodium morrhuate attenuating the adenoviral vector, or causing cell death at the site of injection resulting in no cells for the adenovirus to transduce. The differentiation of these two causes of reduced bone formation are important because severe soft tissue, vascular, and bone damage associated with some long-bone fractures results in a relatively acellular and avascular fracture site, therefore *in vivo* gene transfer may not be useful in these cases. If the sodium morrhuate attenuated the adenoviral vector, this would be important for the proposed infected non-union model. However, because sodium morrhuate is not used in clinical cases its effect on the adenoviral vector would not be important for clinical application. Therefore, an *in vitro* study was performed to further evaluate the effect of sodium morrhuate on the adenoviral vector.

The results of the *in vitro* study demonstrated that sodium morrhuate is very cytotoxic even at low concentrations ($1:2x10^3$ dilution). At low concentrations ($1:10^4$),

however, the sodium morrhuate does not appear to affect the transduction efficiency of the adenoviral vector. The concentration of sodium morrhuate at the fracture site at the time of injection of Ad-BMP-2 is unknown, but is presumed to be low based on dilution and a non-specific immune response. Another factor supporting the lack of effect of sodium morrhuate on the adenoviral vector is that it did not kill the *S. aureus* organisms. The *S. aureus* organisms were placed in the proximal and distal fragments adjacent to the defect, which was exactly the same location as the sodium morrhuate. The *S. aureus* were placed in the defect at a lower concentration (10^7 cfu) than the adenovirus (10^8 pfu); however, the *S. aureus* were able to replicate and the adenoviral vector was replication-incompetent. Although the bacteria were capable of replication, loss of bacteria, as a result of damage from the sodium morrhuate, would have in essence reduced the inoculation dose. Based on previous studies as well as our pilot studies, a lower inoculation dose of *S. aureus* would not have caused infection in 100% of the animals. This supports the conclusion that the sodium morrhuate did not damage the *S. aureus* or the adenoviral vector.

The lack of transduction of the Ad-LacZ with sodium morrhuate at a 1:10 dilution is most likely a result of cell death; however, the role of cell death versus damage to the adenoviral vector could not be determined in this study. When the cells were incubated with sodium morrhuate and evaluated with a viability stain, there appeared to be a large number of cells in the 1:10 dilution group that were viable. However, in this study, only some of the cells were detached and detachment occurred slowly. In the study evaluating the effect of the 1:10 dilution of sodium morrhuate on Ad-LacZ function, all of the cells rapidly detached; hence, it is difficult to determine whether these cells were viable or not.

Future *in vitro* studies, where the adenoviral vector is purified following incubation with sodium morrhuate, are required to evaluate the effect of sodium morrhuate on adenoviral vectors.

An alternative to the use of a sclerosing agent would have been to use liquid nitrogen on the proximal and distal fragments to cause necrosis.[68] This is likely to have a similar effect as the sclerosing agent and would not affect the adenoviral vector; however, is technically more difficult particularly with the small size of the rabbits, requires more equipment, and the freeze-thaw cycles need to be carefully controlled.

Histologically, rabbits had a high percentage of soft tissue in the fracture defect. Rabbits in both non-infected and infected groups, euthanized prior to 4 weeks, had muscle and fat in the defect, whereas rabbits in the non-infected group, euthanized at 16 weeks had predominantly fat. Initially it was difficult to determine whether the source of fat was the bone marrow or the surrounding soft tissue; however, the presence of muscle in the defect at 2 and 4 weeks suggests that the encroachment of soft tissue into the defect was the major source of fat. Other authors using a similar model[33,41] did not report muscle and fat in the defect. It is possible that the avascularity of the defect, which could have resulted from the sclerosing agent, may have induced the surrounding soft tissue to revascularize the defect region, which subsequently inhibited bone formation in the defect. Alternatively, bone formation in the defect may have been delayed, and more rapidly proliferating soft tissue filled the defect as a consequence of the slow rate of bone formation. A non-union model caused by interposition of soft tissue in the fracture defect has been described previously.[69] Soft tissue interposition in fracture defects is an important cause of non-unions in humans,[70] and may have contributed to failure of defect

ossification in our study. The consistency of soft tissue interposition in our model requires further investigation. Rabbits in the infected groups had significantly less fat in the defect compared to rabbits in the non-infected group, which was most likely a result of the *S. aureus* and inflammatory response causing soft tissue necrosis and production of fibrous tissue.

There were three rabbits in the control groups in the larger study evaluating Ad-BMP-2 for enhancing healing of infected non-unions that healed the fracture defect either by defect ossification or bridging-callus. Fracture healing occurred despite the use of a high dose of *S. aureus*, a sclerosing agent, a large (10-mm) defect, as well as removal of the periosteum, endosteum, marrow, and soft tissues. The defect ossification in the control animals may have been a result of osteogenic tissue remaining in the defect at the time of surgery, variation in injection of the sclerosing agent on the bone fragments, or a biological effect of BMP-2 expression in the adjacent soft tissue (Chapter 3). Although it was disappointing that there were rabbits in the control groups that healed the defect, there were only a very low percentage, and we concluded that the model was an adequate infected non-union model to evaluate the use of gene transfer of growth factors for enhancing fracture healing.

Future studies with euthanasia of rabbits at earlier time periods, and histological, immunohistochemical, and molecular biological analysis of the tissue in the defect region, are required to further define the infected non-union model. Similar studies should be performed on tissue obtained from the target species during surgical procedures or at euthanasia and compared to the model, to ascertain the similarities between the model and clinical cases.

References

1. Praemer A, Furner S, Rice DP. Musculoskeletal conditions in the United States. In: The American Academy of Orthopaedic surgeons. Park Ridge, Illinois, 1992, p85-124
2. Nixon AJ. Equine Fracture Repair. WB Saunders Co, Philadelphia, 1997.
3. Jingushi S, Heydemann A, Kana SK, Macey LR, Bolander ME. Acidic fibroblast growth factor (aFGF) injection stimulates cartilage enlargement and inhibits cartilage gene expression in rat fracture healing. J Orthop Res 1990; 8:364-371.
4. Joyce ME, Heydemann A, Bolander ME. Platelet-derived growth factor regulates the initiation of fracture repair. Orthop Trans 1990; 14:363.
5. Joyce MC, Jingushi S, Bolander ME. Transforming growth factor-β in the regulation of fracture repair. Orthop Clin N Am 1990; 21:199-209.
6. Lind M, Schumacker B, Soballe K, Keller J, Melsen F, Bunger C. Transforming growth factor-ß enhances fracture healing in rabbit tibiae. Acta Orthop Scand 1993; 64:553-556.
7. Nielsen HM, Andreassen TT, Ledet T, Oxlund H. Local injection of TGF-ß increases the strength of tibial fractures in the rat. Acta Orthop Scand 1994; 65:37-41.
8. Heckman JD, Boyan DB, Aufdemorte TB, Abbott JT. The use of bone morphogenetic protein in the treatment of nonunion in a canine model. J Bone Joint Surg 1991; 73A:750-764.
9. Heckman JD, Ehler W, Brooks BP, Aufdemorte TB, Lohmann CH, Morgan T, Boyan BD. Bone morphogenetic protein but not transforming growth factor-beta enhances

bone formation in canine diaphyseal nonunions implanted with a biodegradable composite polymer. 1999; 81A:1717-1729.

10. Zegzula HD, Buck DC, Brekke J, Wozney JM, Hollinger JO. Bone formation with use of rhBMP-2 (recombinant human bone morphogenetic protein-2). J Bone Joint Surg 1997; 79A:1778-1790.
11. Blokhuis TJ, den Boer FC, Bramer JAM, Jenner JMG, Bakker FC, Patka P, Haarman HJThM. Biomechanical and histological aspects of fracture healing stimulated with osteogenic protein–1. Biomater 2001; 22:725-730.
12. Ohura K, Hamanishi C, Tanaka S, Matsuda N. Healing of segmental bone defects in rats induced by a β-TCP-MCPM cement combined with rhBMP-2. J Biomed Mater Res 1999; 44:168-175.
13. Bostrom M, Lane JM, Tomin E, Browne M, Berberian W, Turek T, Smith J, Wozney J, Schildhauer T. Use of bone morphogenetic protein-2 in the rabbit ulna nonunion model. Clin Orthop Rel Res 1996; 327:272-282.
14. Yasko AW, Lane JM, Fellinger EJ, Rosen V, Wozney JM, Wang EA. The healing of segmental bone defects induced by recombinant human bone morphogenetic protein (rhBMP-2). J Bone Joint Surg 1992; 74A:659-670.
15. Cook SD, Baffes GC, Wolfe MW, Sampath TK, Rueger DC, Whitecloud TS. The effect of recombinant human osteogenic protein-1 on healing of large segmental bone defects. J Bone Joint Surg 1994; 76A:827-838.
16. Cook SD, Baffe SGC, Wolfe MW, Sampath TK, Rueger DC. Recombinant human bone morphogenetic protein-7 induces healing in a canine long-bone segmental defect model. Clin Orthop Rel Res 1994; 301:302-312.

17. Cook SD, Wolfe MW, Salkeld SL, Rueger DC. Effect of recombinant human osteogenic protein-1 on healing of segmental defects in non-human primates. J Bone Joint Surg 1995; 77A:734-750.

18. Welch RD, Jones AL, Bucholz RW, Reinert CM, Tjia JS, Pierce WA, Wozney JM, Li XJ. Effect of recombinant human bone morphogenetic protein-2 on fracture healing in a goat tibial fracture model. J Bone Min Res 1998; 13:1483-1490.

19. Nilsson OS, Urist MR, Dawson EG, Schmalzried TP, Finerman GAM. Bone repair induced by bone morphogenetic protein in ulnar defects in dogs. J Bone Joint Surg 1986; 68B:635-642.

20. Geehart TN, Kirker-Head CA, Kriz MJ, Holtrop ME, Hennig GE, Hipp J, Schelling SH, Wang E. Healing segmental femoral defects in sheep using recombinant human bone morphogenetic protein. Clin Orthop Rel Res 1993; 293:317-326.

21. Kirker-Head CA, Gerhart TN, Schelling SH, Hennig GE, Wang E, Holtrop ME. Long-term healing of bone using recombinant human bone morphogenetic protein 2. Clin Orthop Rel Res 1995; 318:222-230.

22. Zellin G, Linde A. Treatment of segmental defects in long bones using osteopromotive membranes and recombinant human bone morphogenetic protein-2. Scand J Plast Reconstr Hand Surg 1997;31:97-104.

23. Linde A, Hedner E. Recombinant bone morphogenetic protein-2 enhances bone healing, guided by osteopromotive e-PTFE membranes: An experimental study in rats. Calcif Tissue Int 1995; 56:549-553.

24. Bax BE, Wozney JM, Ashhurst DE. Bone morphogenetic protein-2 increases the rate of callus formation after fracture of the rabbit tibia. Calcif Tissue Int 1999; 65:83-89.

25. Lee FY, Hazan EJ, Trahan C, Snyder B, Gebhardt MC, Mankin HJ. Bone morphogenetic protein (BMP-2) can initiate and the conduct repair process at the allograft osteotomy site in an animal experimental model. Proc 45th Ann Mtg Orthop Res Soc 1999; p 620.

26. Chen X, Kidder LS, Lew WD. Osteogenic protein-1 induced bone formation in an infected segmental defect in the rat femur. J Orthop Res 2002; 20:142-150.

27. Johnson EE, Urist MR. One-stage lengthening of femoral nonunion augmented with human bone morphogenetic protein. Clin Orthop Rel Res 1998; 347:105-116.

28. Johnson EE, Urist MR, Finerman AM. Resistant non-union and partial or complete segmental defects of long bones. Clin Orthop Rel Res 1992; 277:229-237.

29. Johnson EE, Urist MR, Finerman AM. Distal metaphyseal tibial nonunion. Clin Orthop Rel Res 1990; 250:234-240.

30. Bulstra SK, Geesink RGT, Hoefnagels NHM. Osteogenic activity of OP-1, bone morphogenetic protein-7 (BMP-7), in a human fibular defect model. Proc 45th Ann Mtg Orthop Res Soc 1999; p 62.

31. Meng-Hai B, Xing-Yan L, Bao-Feng G, Chao Y, Dong-An C. An implant of a composite of bovine bone morphogenetic protein and plaster of Paris for treatment of femoral shaft nonunions. Int Surg 1996; 81:390-392.

32. Jain KK. Gene therapy for diseases of bones and joints. In Jain (Ed) Textbook of Gene Therapy. Hogrefe & Huber Publishers, Seattle, 1998; p 281-284.

33. Baltzer AWA, Lattermann C, Whalen JD, Braunstein S, Robbins PD, Evans CH. A gene therapy approach to accelerating bone healing. Knee Surg, Sports Traumatol, Arthrosc 1999; 7:197-202.

34. Musgrave DS, Bosch P, Ghivizzani S, Robbins PD, Evans CH, Huard J. Adenovirus-mediated direct gene therapy with bone morphogenetic protein-2 produces bone. Bone 1999; 24:541-547.

35. Spector JA, Mehrara BJ, Luchs JS, Geenwald JA, Fagenholz PJ, Saadeh PB, Steinbrech DS, Longaker MT. Expression of adenovirally delivered gene products in healing osseus tissues. Ann Plast Surg 2000; 44:522-528.

36. Lou J, Xu F, Merkel K, Manske P. Gene therapy: Adenovirus-mediated human bone morphogenetic protein-2 gene transfer induces mesenchymal progenitor cell proliferation and differentiation in vitro and bone formation *in vivo*. J Orthop Res 1999; 17:43-50.

37. Alden TD, Pittman DD, Hankins GR, Beres EJ, Engh JA, Das S, Hudson SB, Kerns KM, Kallmes DF, Helm GA. *In vivo* endochondral bone formation using a bone morphogenetic protein-2 adenoviral vector. Human Gene Ther 1999; 10:2245-2253.

38. Laurencin CT, Attawia MA, Lu LQ, Borden MD, Lu HH, Gorum WJ, Lieberman JR. Poly (lactide-co-glycolide)/hydroxyapatite delivery of BMP-2-producing cells: a regional gene therapy approach to bone regeneration. Biomater 2001; 22:1271-1277.

39. Fang J, Zhu Y-Y, Smiley E, Bonadio J, Rouleau JP, Goldstein SA, McCauley LK, Davidson BL, Roessler BJ. Stimulation of new bone formation by direct transfer of osteogenic plasmid genes. Natl Acad Sci USA 1996; 93:5753-5758.

40. Lieberman JR, Daluiski A, Stevenson S, Wu L, McAllister P, Lee YP, Kabo JM, Finerman GAM, Berk A, Witte ON. Regional gene therapy with a BMP-2 producing murine stromal cell line induces heterotopic and orthotopic bone formation in rodents. J Orthop Res 1998; 16:330-339.

41. Baltzer AWA, Lattermann C, Whalen JD, Wooley P, Weiss K, Grimm M, Ghivizzani SC, Robbins PD, Evans CH. Genetic enhancement of fracture repair: Evaluation of Ad-BMP-2 in a lapine femoral defect model. Gene Ther 2000; 7:734-739.

42. Gazit D, Tugeman G, Kelley P, Wang E, Jalenak M, Zilberman Y, Moutsatsos I. Engineered pluripotent mesenchymal cells integrate and differentiate in regenerating bone: A novel cell-mediated gene therapy. J Gene Med 1999; 1:121-133.

43. Mehrara BJ, Saadeh PB, Steinbrech DS, Dudziak M, Spector JA, Greenwald JA, Gittes GK, Longaker MT. Adenovirus-mediated gene therapy of osteoblasts *in vitro* and *in vivo*. J Bone Min Res 1999; 14:1290-1301.

44. Mader JT. Animal Models of Osteomyelitis. Am J Med 1985; 78:213-217.

45. Rissing JP. Animal Models of Osteomyelitis. Infectious Disease Clin N Am 1990; 4:377-390.

46. Kaarsemaker S, Walenkamp GHIM, vd Bogaard AEJ. New model for chronic osteomyelitis with Staphylococcus aureus in sheep. Clin Orthop Rel Res 1997; 339:246-252.

47. Eerenberg JP, Patka P, Haarman HJTHM. A new model for posttraumatic osteomyelitis in rabbits 1994; 7:453-465.

48. Smeltzer MS, Thomas JR, Hickmon SG, Skinner RA, Nelson CL, Griffith D, Parr TR, Evans RP. Characterization of a rabbit model of Staphylococcal osteomyelitis. J Orthop Res 1997; 15:414-421.

49. Andriole VT, Nagel DA, Southwick WO. Chronic Staphylococcal osteomyelitis: An experimental mode. Yale J Biol Med 1974; 1:33-39.

50. Worlock P, Slack R, Harvey L, Mawhinney R. An experimental model of post-traumatic osteomyelitis in rabbits. Br J Exp Pathol 1988; 69:235-244.

51. Norden, CW. Experimental osteomyelitis. I. A description of the model. J Infect Dis 1970; 122:410-418.

52. Rodeheaver GT, Rukstalis D, Bono M, Bellamy WA. A new model of bone infection used to evaluate the efficacy of antibiotic-impregnated polymethylmethacrylate cement. Clin Orthop Rel Res 1983; 178:303-311.

53. Philipov JP, Pascalev MD, Aminkov BY, Grosev CD. Changes in serum carboxyterminal telopeptide of type I collagen in an experimental model of canine osteomyelitis. Calcif Tissue Int 1995; 57:152-154.

54. Jacob E, Arendt DM, Brook I, Durham LC, Falk MC, Schaberg SJ. Enzyme-linked immunosorbent assay for detection of antibodies to Staphylococcus aureus cell walls in experimental osteomyelitis. J Clin Microbiol 1985; 22:547-552.

55. Hill PF, Watkins PE, Clasper JA, Parker SJ. Intramedullary nailing of a contaminated fracture in an experimental model. Proc 45th Ann Mtg Orthop Res Soc 1999; p 497.

56. Passl R, Muller C, Kielinski CC. A model of experimental post-traumatic osteomyelitis in guinea pigs. J Trauma 1984; 24:323

57. Chen X, Kidder LS, Lew WD. Osteogenic protein-1 induced bone formation in an infected segmental defect in the rat femur. J Orthop Res 2002; 20:142-150.

58. Tsukayama DT. Pathophysiology of posttraumatic osteomyelitis. Clin Orthop Rel Res 1999; 360:22-29.

59. Moore RM, Schneider RK, Kowalski J, Bramlage LR, Mecklenberg LM, Kohn CW. Antimicrobial susceptibility of bacterial isolates from 233 horses with musculoskeletal infection during 1979-1989. Equine Vet J 1992; 24:450-456.

60. Feied CF. Mechanism of action of sclerosing agents and rationale for selection of a sclerosing solution. American Vein Institute (www.veins.com) 2001; p 1-8.

61. Schulz S, Steinhart H, Mutters R. Chronic osteomyelitis in a new rabbit model. J Invest Surg 2001; 14:121-131.

62. Murray PR, Rosenthal KS, Kobayashi GS. Chapter 22: Staphylococcus and Related Organisms. In Murray PR, Rosenthal KS, Kobayashi GS (Ed): Medical Microbiology, 3rd Ed, Mosby, St Louis MO, 1998; p 175-188.

63. Tally FP, Barg NL. Chapter 11: Staphylococci: Abscesses and Other Diseases. In Schaechter M, Engleberg NC, Eisenstein B, Medoff G (Eds): Mechanics of Microbial Disease, 3rd Ed, Lipincott, Philadelphia, PA, 1999; p 135-142.

64. Woodard JC, Riser WH. Morphology of fracture nonunion and osteomyelitis. Vet Clin N Am Sm Anim Pract 1991; 21:813-844.

65. Petty W, Spanier S, Shuster JJ, Silverthorne C. The influence of skeletal implants on incidence of infection. J Bone Joint Surg 1985; 67:1263-1234.

66. Grewe SR, Stephens BO, Perlino C, Riggins RS. Influence of internal fixation of wound infections. J Trauma 1987; 27:1051-1054

67. Crigel MH, Balligand M. Development of an experimental critical size defect model on the femur in rabbits. Proc 2nd Ann Orthop Anim Models Symp, Cambridge Healthtech Institute, Washington DC, 2000.

68. Markel MD. Bogdanske JJ, Xiang Z, Klohnen A. Atrophic nonunion can be predicted with dual energy x-ray absorptiometry in a canine ostectomy model. J Orthop Res 1995; 13:869-875.

69. Fujita M. Matsui N. Tsunoda M. Saura R. Establishment of a non-union model using muscle interposition without osteotomy in rats. Kobe J Med Sci 1998; 44:217-233.

70. Milgram JW. Nonunion and pseudoarthrosis of fracture healing. Clin Orthop Rel Res 1991; 268:203-213.

CHAPTER 3

EVALUATION OF AD-BMP-2 FOR ENHANCING FRACTURE HEALING IN AN INFECTED NON-UNION MODEL

Abstract

Objective: The objective of this study was to evaluate the use of adenoviral transfer of the BMP-2 gene (Ad-BMP-2) for enhancing healing in infected non-unions. Our hypothesis was that Ad-BMP-2 would enhance fracture healing in the infected non-union model.

Materials and Methods: Sixty-four skeletally mature New Zealand White rabbits were used. A femoral defect stabilized with plates and screws was the basic model. Experimental groups were: (1) non-infected Ad-Luciferase (LUC) control, (2) non-infected Ad-BMP-2 treated, (3) infected Ad-LUC control, and (4) infected Ad-BMP-2 treated. Rabbits in the infected groups were inoculated with *Staphylococcus aureus*. A sclerosing agent was used on the ends of the bone at surgery to facilitate the development of osteomyelitis and to inhibit fracture healing. Fracture healing was evaluated radiographically, using dual-energy x-ray absorptiometry (DEXA), and histologically. Data were analyzed using an ANOVA. The level of significance was $p<0.05$.

Results: Radiographically, rabbits treated with Ad-BMP-2 had an earlier initial- and bridging-callus formation, and a higher overall external callus grade compared to rabbits in the Ad-LUC groups. Rabbits in the Ad-LUC groups had more defect ossification compared to rabbits in the Ad-BMP-2 groups. Based on DEXA analysis, there was no difference in the bone mineral density in the defect between the Ad-LUC and Ad-BMP-2 groups. Histological analysis revealed that there was no effect of treatment on the amount of new bone formation at 16 weeks; however, rabbits in the Ad-BMP-2 group that were euthanized at 2 and 4 weeks after surgery had more bone and cartilage compared to rabbits in the Ad-LUC group.

Conclusion: The results of this study suggest that Ad-BMP-2 may be useful to enhance healing of infected non-unions. The results of our study were not as favorable as previous studies because animals healed by a large bridging-callus and not by defect ossification. This could have been a result of the sclerosing agent, which may have caused damage to the cells in the defect leaving inadequate cells for the adenovirus to transduce. While Ad-BMP-2 appears to be effective in the presence of infection, *in vivo* gene transfer may not be ideal in fractures associated with severe tissue and cell damage.

Introduction

Non-union and infected non-union are devastating clinical complications following fracture repair in both veterinary and human medicine.[1-7] Characteristics associated with some long-bone fractures that may lead to complications with healing include: poor vascularity and minimal soft tissue support of the distal limb, high-energy trauma and subsequent massive bone, vascular, and soft tissue damage, and heavy contamination at the time of injury or during prolonged surgical procedures that often results in infection. In addition, the body weight and temperament of the horse, the necessity for early weight bearing on the affected limb, and the contaminated environment in which they are housed, predispose the horse to complications associated with fracture healing.[8] Therefore, novel methods to enhance healing of complicated fractures, particularly infected non-unions, are needed.

Growth factors have been shown to enhance fracture healing,[9-37] and are usually delivered to the fracture site as recombinant proteins in a carrier matrix.[9-37] Recombinant proteins that have been evaluated include acidic fibroblastic growth factor,[9] platelet-derived growth factor,[10] transforming growth factor-β (TGF-β),[11-13] and the bone morphogenetic proteins (BMPs).[14-37] Most of these growth factors have complicated biological activities and sometimes actually inhibit intramembranous and endochondral ossification depending on the stage of healing, the combination of growth factors, and the dose.[9,38-41] Bone morphogenetic proteins, on the other hand, are members of the TGF-β superfamily, and are currently the most studied proteins associated with fracture healing. The BMPs are the most potent osteoinductive proteins and the only growth factors capable of *de novo* bone formation *in vivo*.[43-46] The BMPs are expressed in normal

bone.[47,48] and by cells at the fracture site,[49] particularly during the stages of differentiation and early matrix production.[44] The BMPs are primarily responsible for differentiation of mesenchymal cells into osteoblasts or chondrocytes, and maintenance of an osteoblastic phenotype.[44,45,48] Because of their potent osteoinductive properties, their ability to induce *de novo* bone formation, and lack of a pleotrophic effect *in vivo* with different concentrations, cell types, and the presence of other growth factors, the BMPs are ideal proteins for enhancing healing of complicated fractures.

Recombinant human BMPs (rhBMP) combined with a carrier matrix have been shown to induce both endochondral and intramembranous ossification in several non-union models,[14-32] as well as in human and veterinary cases.[33-37] Recently, rhBMP-7 was shown to enhance fracture healing in an infected non-union rat model[32] and BMP-2 was shown to form *de novo* bone in irradiated tissue.[50] These studies suggest that BMPs may be useful for enhancing healing in more complicated fractures. There are several limitations, however, with the use of recombinant proteins. Recombinant proteins have a short biological half-life because they are rapidly resorbed and redistributed from the fracture site, they are technically difficult to synthesize and purify, they require large doses to be effective because they are an exogenous source of protein, and at these high doses they are expensive and potentially toxic.[51] Because of their rapid resorption, multiple treatments or a carrier matrix is required to obtain sustained concentrations of BMP at the fracture site. Multiple treatments are inconvenient and may increase the risk of infection, and a carrier matrix may induce a foreign body reaction and can inhibit fracture healing.[30] Therefore, alternate methods of BMP delivery may be preferable.

The use of gene therapy has overcome many of the limitations associated with recombinant protein delivery.[51-64] Gene therapy allows sustained release of the proteins at the fracture site, there is a reduction in protein synthesis and purification problems, and it is more economical and easier compared to the use of recombinant proteins. Further, endogenous growth factor production by the cells at the fracture site is more efficient than exogenous delivery of recombinant proteins,[51] as indicated by the smaller dose required to stimulate healing.[61]

Gene therapy involves the delivery of the gene of interest to the fracture site using a vector; the gene is then expressed by the cells at the fracture site.[52] The vector may be non-viral or viral.[52] Replication-incompetent adenoviruses have a high transduction rate and are capable of transducing both dividing and non-dividing cells.[52] Gene expression is transient (4 to 8 weeks) because of the immune response induced by the adenovirus.[53] Transduction may be *in vivo* or *ex vivo*. *In vivo* transduction involves simply injecting a solution of the virus containing the gene into the fracture site; however, it is dependent on viable cells being present at the site of injection. While *ex vivo* transduction provides viable cells to the fracture site, it is technically more difficult and involves transduction of the cells in the laboratory and then injection of the transduced cells into the fracture. Previous studies[53-58] have shown that the adenoviral vector is capable of transducing cells from skeletal tissue with the BMP-2 gene *in vitro* and *in vivo*, and that the transduced cells are capable of expressing a biologically active BMP-2 protein. Enhancement of fracture healing using *ex vivo* and *in vivo* transfer of the BMP-2 gene has been demonstrated using non-union models.[59-64] There have been no studies evaluating the used of Ad-BMP-2 for enhancing fracture healing in an infected non-union model.

The purpose of this study was to evaluate the use of Ad-BMP-2 for enhancing fracture healing in an infected non-union rabbit model. Our hypothesis was that fracture healing in the infected non-union rabbit model would be enhanced by treatment with Ad-BMP-2.

Materials and Methods

Animal Model

Sixty-four female, skeletally mature (9-10 month-old) New Zealand white rabbits were used in the study. Rabbits in the control groups were treated with a vector containing the firefly luciferase marker gene (Ad-LUC), and rabbits in the treatment groups were treated with a vector containing the gene for BMP-2 (Ad-BMP-2). Rabbits were randomly assigned to one of four treatment groups: (1) non-infected Ad-LUC control, (2) non-infected Ad-BMP-2 treated, (3) infected Ad-LUC control, and (4) infected Ad-BMP-2 treated. All procedures were approved by the Colorado State University Animal Care and Use Committee.

Enrofloxacin (10 mg/kg intramuscularly, IM) was administered pre-operatively only. Analgesia consisted of preoperative morphine epidurally (0.1 mg/kg) and subcutaneously (SQ; 0.5 mg/kg), fentanyl administered as a constant rate infusion during surgery, and flunixin meglumine (0.5 mg/kg SQ) every 12 hours for 72 hours after surgery. Butorphanol (0.4 mg/kg SQ) was administered as needed postoperatively. Acepromazine (0.3 to 0.5 mg/kg IM) was administered postoperatively to avoid self-trauma to the fracture fixation.

Following induction of general anesthesia using isoflurane in oxygen, a routine lateral approach to the femur, between the *vastus lateralis* and *biceps femoris*, was made. The soft tissue and periosteum were excised from the diaphysis of the femur. A 10 mm mid-diaphyseal femoral defect was surgically created using a side-cutting carbide burr (MicroAire Surgical Instruments, Charlottesville, VA). The endosteum and bone marrow were removed and the wound thoroughly lavaged to remove any bone debris. The femur was stabilized using two 2.0-mm cuttable bone plates and 2.0 mm cortical screws, with cerclage wire proximally and distally to prevent fracture through the screw holes (Chapter 2). A sclerosing agent (sodium morrhuate) was used on the end of the proximal and distal fragments to prevent defect ossification and to facilitate development and persistence of infection in rabbits in the infected groups (Chapter 2). The muscle, subcutaneous tissue, and skin were routinely apposed.

Rabbits were inoculated percutaneously with 0.5×10^7 colony-forming units (cfu)/0.5mL *Staphylococcus aureus* (S. Schaefler 1428, ATCC # 25923) 48 hours after surgery under general anesthesia with isofluorane in oxygen (Chapter 2). Rabbits were monitored for signs of lameness and systemic illness.

Gene Therapy

Gene therapy was direct, *in vivo*, using an Adenoviral vector. Rabbits were treated with either Ad-LUC or Ad-BMP-2 at the time of inoculation with *S. aureus*. Engineering of the Adenoviral vector was performed, as previously described by Baltzer and coworkers,[53] at the Department of Molecular Genetics and Biochemistry, University of Pittsburgh School of Medicine, Pittsburgh, PA. Briefly, a complimentary DNA encoding

human BMP-2 (Genetics Institute, Cambridge MA) was inserted into the E1 region of a serotype-5 Adenovirus deleted in the E1 and E3 regions of the genome, using cre-lox recombination. A human cytomegalovirus early promoter was used to drive gene expression. A similar vector containing the luciferase marker gene was generated using the same technique. Recombinant virus was propagated in the permissive cell line 293 and purified by standard cesium chloride banding techniques. Viral titers were determined by optical density (1 unit = 10^{12} virions/mL). Viral vectors encoding BMP-2 were diluted with sterile saline solution (Gey's Balanced Salt Solution, Sigma Chemical Co. St. Louis, MO) and injected directly into the gap percutaneously at a concentration of $7x10^{10}$ particles/0.5mL.[62]

Radiographic Evaluation

Qualitative Radiographic Analysis: Rabbits were evaluated radiographically (craniocaudal and lateral views) postoperatively at time 0, and at 4, 8, 12, and 16 weeks after surgery. Radiographs were evaluated objectively and subjectively in collaboration with a Board Certified Radiologist (Richard Park, DVM) who was unaware of the experimental group assignment. Radiographs were objectively evaluated for initial- and bridging-callus formation. Initial-callus formation was defined as any bone formation adjacent to the defect that was beginning to form callus, and bridging-callus formation was defined as bone uniting the proximal and distal fragments. New bone formation was classified as external callus (soft tissue and periosteal callus) or defect ossification (medullary callus). Radiographs were graded subjectively from 0 to 4 (0=none, 1=slight, 2=mild, 3=moderate, and 4=marked) for proliferation, soft tissue callus, and periosteal

callus formation. An overall external callus/proliferation grade was calculated from the average of the individual grades (Figure 1). Proliferation was any bone formation along the diaphysis or metaphysis of the femur, soft tissue callus was bone formation in the soft tissues adjacent to the defect, and periosteal callus was bone formation in the periosteum adjacent to the defect. The percentage of defect ossification or medullary callus was estimated.

Radiographs were also evaluated subjectively for changes consistent with infection. Radiographs were graded 0 to 4 for bone lysis and 0 to 1 (0=none 1= present) for sequestration. Bone lysis was considered slight (grade-1) if it was associated with the bone adjacent to a single screw or confined to the bone immediately adjacent to the defect, mild (grade-2) if it was associated with the bone adjacent to multiple screws, the defect, or the bone plate, moderate (grade-3) if it was associated with the bone in between the screws but was not extensive, and severe (grade-4) if it was associated with the entire bone. Sequestration was defined as mixed areas of sclerosis and lysis.

The defect length and bone length were measured on the lateral radiographic view immediately after surgery (time 0). The defect length was expressed as a percentage of the bone length.

Quantitative Radiographic Analysis: Following euthanasia at 16 weeks, the excised femur was imaged radiographically using a Faxitron X-Ray Corporation Cabinet X-Ray System (Faxitron X-Ray Corporation, Wheeling, IL) and Kodak Scientific Imaging Film (X-OMAT LS, Kodak Corporation, Rochester, NY) at an exposure of 2 minutes and 20 seconds and 44kVp. The craniocaudal view only was used, because the bone plate obliterated the bone on the lateromedial view. The thicker emulsion on the

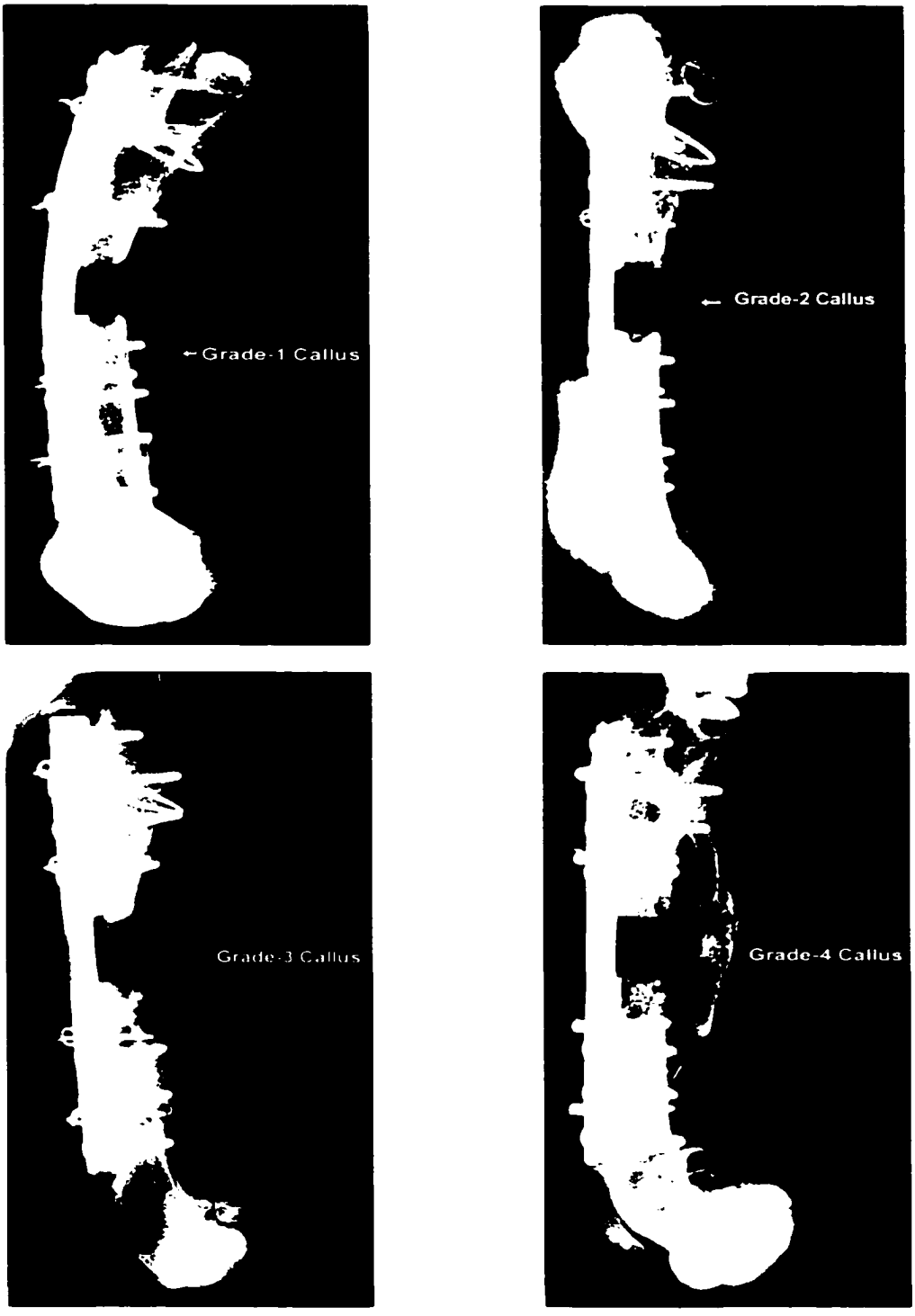

Figure 1. Craniocaudal radiographic views of operated femurs at 16 weeks, illustrating examples of overall radiographic external callus/proliferation grades. Grade-1 callus was defined by callus that was only slight; grade-2 was mild callus formation, not bridging the defect, and subjectively low bone density; grade-3 was a moderate amount of callus, that was not bridging the defect, and moderate bone density; and callus was graded as 4 if it was a large, bridging callus, with moderate to marked bone density.

film provided greater contrast between the bone and soft tissue; therefore the external callus and ossification in the defect could be more accurately measured. The radiographs were scanned into an imaging program (Bioquant Computer Software Program, BQ-TCW98 V3.50.6. R&M Biometrics Inc. Nashville. TN) for analysis.

There were two regions of interest (ROI) used for analysis of the external (periosteal and soft tissue) callus: (1) the whole bone ROI was defined as the region between the most proximal and most distal screws (Figure 2), and (2) the defect ROI from the screw proximal and distal to the defect (Figure 3).

The area of the external callus was calculated by measuring the area of the total bone (old bone + callus) and subtracting the area of the old bone ((old bone + callus) – old bone) because it was easier to measure the total bone area than the external callus area only and histomorphometric analysis was also performed by measuring the total bone area and subtracting the old bone area. There were two control markers of known area that were imaged concurrently with each sample (Figures 2 and 3). The old bone and external callus areas were standardized to these markers:

Old bone area (cm^2) = (old bone area/control marker area) x control marker area (cm^2)

External callus area (cm^2) = (external callus area /control marker area) x control marker area (cm^2)

The areas were standardized to the markers firstly for calculation of the area in centimeters squared (cm^2) and secondly to control for alterations in image size associated with scanning and importing. There were variations in image size associated with

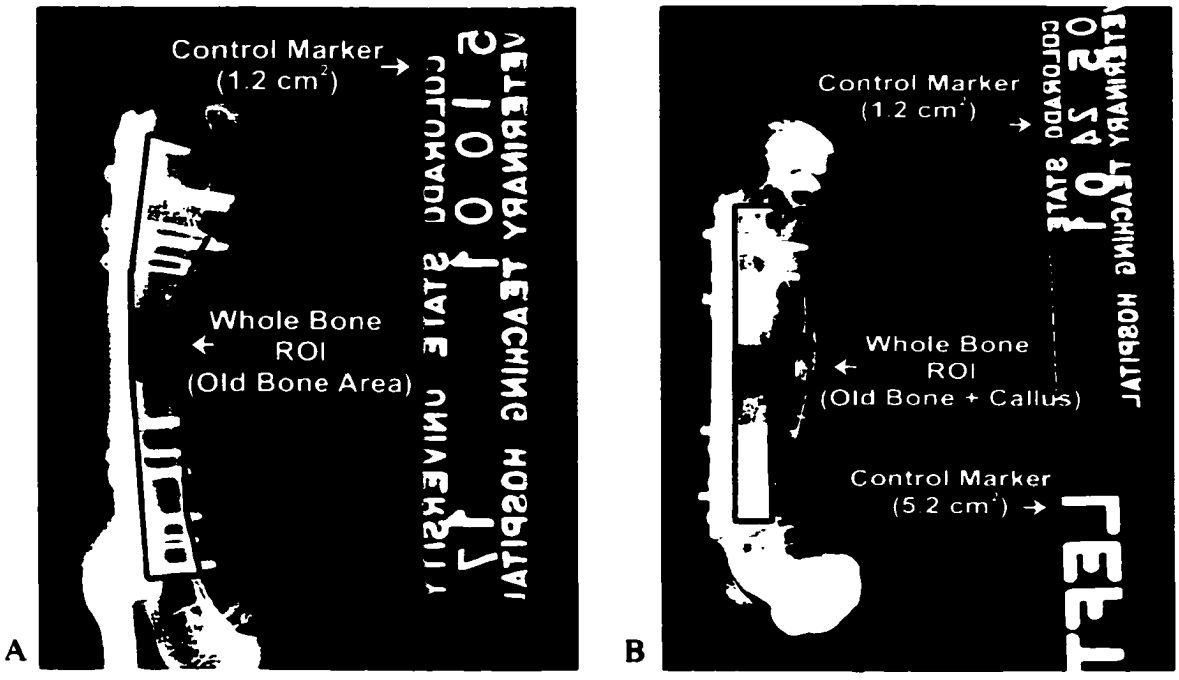

Figure 2. Quantitative evaluation of external callus formation based on craniocaudal radiographic views at 16 weeks after surgery. The whole bone region of interest (ROI) was defined as the region between the most proximal and distal screws. The external callus area for each ROI was calculated by subtracting the old bone area (A) from the total bone area (old bone +callus, B). The old bone and external callus areas were standardized to control markers of known area, to give areas in cm^2. If there were two control markers, the average value was used. The external callus area for the two ROIs was expressed as a percentage of the old bone area: (Callus Area/Old Bone Area) x 100 to account for magnification associated with soft tissue and positioning.

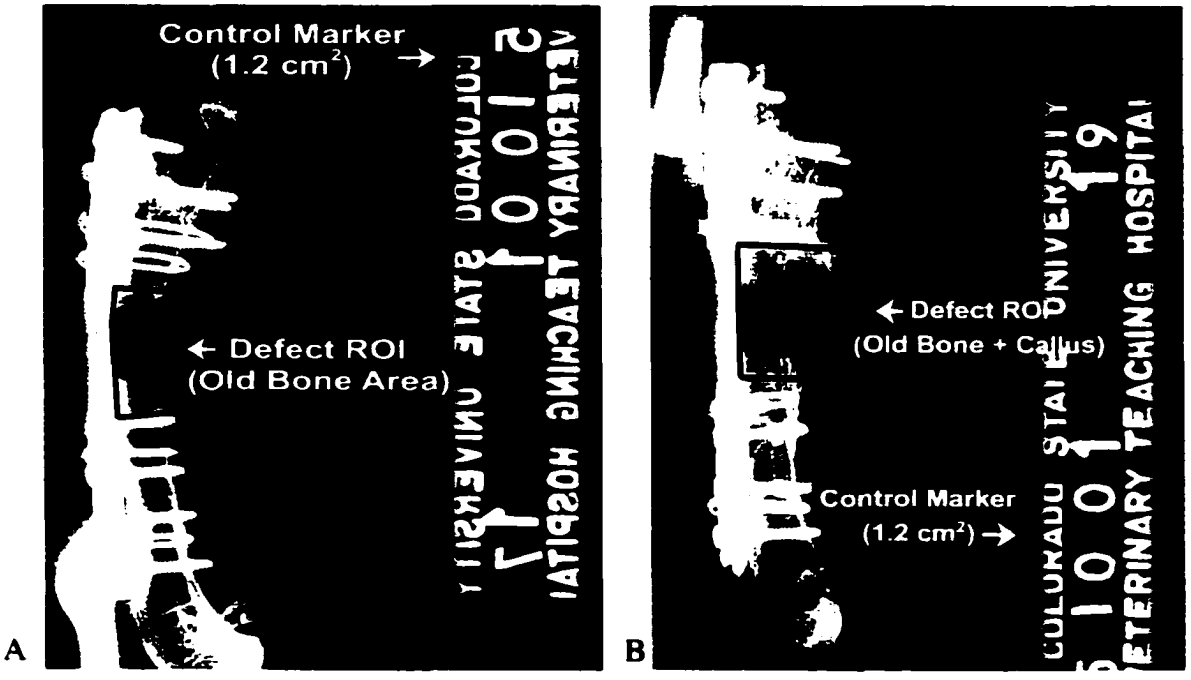

Figure 3. Quantitative evaluation of external callus formation based on craniocaudal radiographic views at 16 weeks after surgery. The defect region of interest (ROI) was defined as the region between the two screw holes adjacent to the defect. The external callus area for each ROI was calculated by subtracting the old bone area (A) from the total bone area (old bone +callus, B). The old bone and external callus areas were standardized to control markers of known area, to give areas in cm^2. If there were two control markers, the average value was used. The external callus area for the two ROIs was expressed as a percentage of the old bone area: (Callus Area/Old Bone Area) x 100 to account for magnification associated with soft tissue and positioning.

scanning and importing because there was variation in the distance between the marker and bone: therefore, the image size was adjusted to include the markers. When both control markers were visible on the image the area was standardized to each marker and the average value calculated and used for analysis. The external callus area was also expressed as a percentage of the old bone area to control for magnification associated with positioning of the bone on the film, and variation in the amount of soft tissue interposition between the actual bone and film.

Defect ossification, or medullary callus, was also quantitatively measured (Figure 4). The area of the defect was measured as the area between the cut ends of the old bone. The amount of ossification or new bone formation in the defect was measured. The area of the defect and the area of the new bone in the defect were standardized to control markers of known size. The area of new bone was expressed as a percentage of the area of the defect. The area of the defect was also expressed as a percentage of the whole bone area. Each image was analyzed by the same individual, in duplicate, and the average value was used.

Overview of Necropsy Procedure and Evaluation

Sixteen weeks after surgery, the rabbits were humanely euthanized (pentobarbital 88 mg/kg intravenously). Radiographs were performed immediately following euthanasia. The skin on the lateral aspect of the left thigh region was routinely clipped, prepared with alcohol, draped, and an incision was made aseptically over the femur. Signs of gross infection (accumulation of purulent material and necrotic bone) and bone union were recorded. Soft tissue (0.5-1 gram) and a cortical screw adjacent to the defect

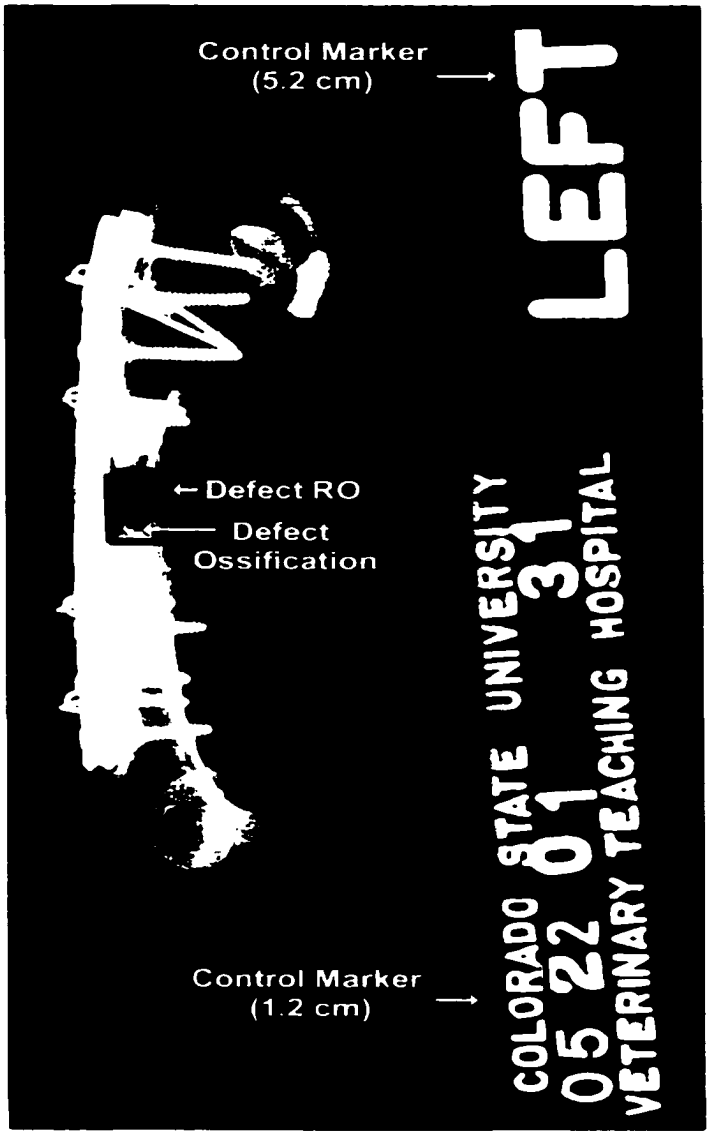

Figure 4. Quantitative evaluation of the percentage of defect ossification. The defect area was between the two ends of the old bone. The amount of ossification in the defect was measured. The areas were standardized to control markers of known area, to areas in cm^2. The amount of defect ossification was expressed as a percentage of the defect area.

were collected, placed in 5-mL thioglycollate (BBL 221741), and vortexed. Quantitative aerobic culture was routinely performed at the CSU Diagnostic Laboratory. Infection was defined as $>10^4$ cfu per gram of tissue. Following collection of the soft tissue and a screw for culture, the femur was excised, imaged radiographically with the soft tissue removed, DEXA was performed, and the femur sectioned for histomorphometry.

Dual Energy X-Ray Absorptiometry

Dual energy x-ray absorptiometry (DEXA; Hologic QDR 1000-W, Hologic Co, Waltham, MA) was used to measure the bone mineral content (BMC; grams) and bone area (cm^2) of the tissue in the defect. Analysis was performed in the Spine Subregion with Metal Removal mode (Figure 5). The bone mineral density (BMD; grams/cm^2) was calculated from the BMC and bone area. The BMD in a region of interest (ROI) within the fracture defect (R1; 0.5-cm^2), a similar sized area distal and proximal to the fracture defect (R2 and R3; 0.5-cm^2), and an area adjacent to the defect and adjacent to the proximal femur (R4 and R5; 0.5-cm^2) was calculated (Figure 5). The same ROIs were measured on the control limb. The BMD ratio R1/R2, R1/R3, and R1 Experimental (E)/ R1 Control (C) were calculated to measure the amount of bone in the defect, R2E/R2C and R3E/R3C were calculated to measure the density of bone in the femur adjacent to the defect, and the R4E/R4C and R5E/R5C were calculated to measure the amount of bone in the soft tissue adjacent to the defect.

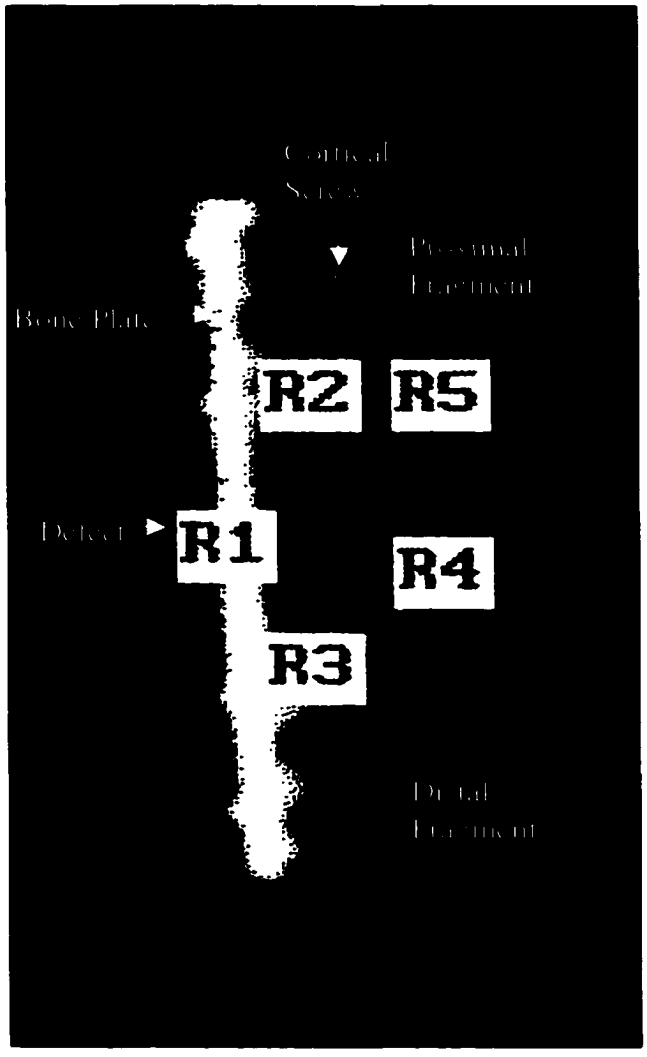

Figure 5. An image illustrating the use of dual energy x-ray absorptiometry for measuring the bone mineral density (BMD) of the tissue in the defect. The bone mineral content and bone area were measured for the regions of interest (ROI) and the BMD was calculated. The ROI were R1 (defect), R2 (proximal to the defect), R3 (distal to the defect), R4 (soft tissue adjacent to the defect), and R5 (soft tissue adjacent to the proximal fragment). The same ROIs were measured on the control femur and the ratio of the experimental to the control limb calculated.

Histomorphometry

Following DEXA analysis, the samples were placed in 10% neutral buffered formalin, sectioned frontally through the plate, screws, and cerclage wire using an Exakt diamond blade band saw (Model 310 CPV, Exakt Technologies Incorporated, Oklahoma City, OK). The femur was sectioned transversely proximally and distally at the level of the third and sixth screw, and then sectioned frontally. One half of the bone was decalcified and the other half remained undecalcified.

Decalcified Sections: The section to be decalcified was further fixed in 10% neutral buffered formalin for 48 hours and decalcified in an EDTA solution containing HCl for 20 hours (Decalcifying Solution, Stephens Scientific Division of Cornwall Corporation, Riverdale, NJ). Complete decalcification was determined using the 5% ammonium oxalate/ 5% ammonium hydroxide reaction; if decalcification was incomplete, the calcium oxalate precipitated. If there was any question regarding the completeness of decalcification radiographs were taken of the specimens. Following decalcification, the samples were cut into sections and stained with hematoxylin and eosin (H&E).

The decalcified sections, which were stained with H&E, were analyzed subjectively (Figure 6a). The defect was defined as the tissue between the screw holes adjacent to the defect. The distance between the screw holes was 18 mm, and the widest tissue sample was 18 mm, therefore the defect was defined by an 18 x 18-mm section. Tissue samples were graded from 0 to 4 for inflammation, necrosis, vascularity, and new bone formation (0=none, 1=slight, 2=mild, 3=moderate, 4=marked). The percentage of fat, fibrous tissue, necrosis, cartilage, and new bone in the defect was subjectively

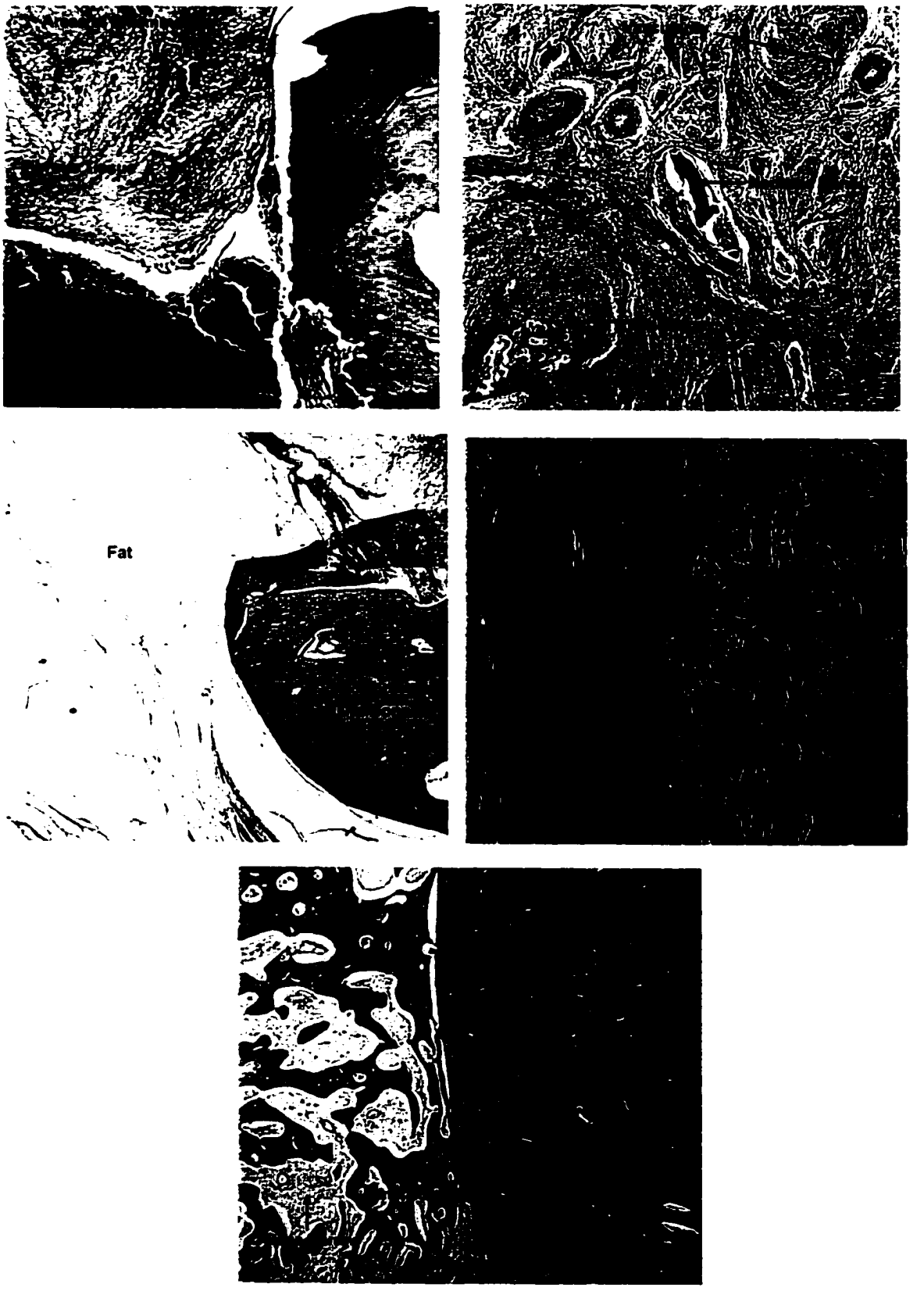

Figure 6a. See figure legend on next page

Figure 6a. Histological Section of rabbit femur at 16 weeks illustrating subjective histological grading of decalcified sections. Sections were stained with hematoxylin and eosin (H&E). A subjective grade for vascularity, inflammation, necrosis, and new bone formation was given to each section (0=none, 1=slight, 2=mild, 3=moderate, 4=severe). The percentage of fat, fibrous tissue, cartilage, and new bone; as well as the percentage of total bone that was necrotic was estimated. The ratio of the amount of new bone to old bone, and the ratio of mineralized new bone to bone marrow, were also estimated. Magnification 20X.

estimated. The percentage necrotic bone of the total bone, the ratio of new bone to old bone, and the ratio of mineralized new bone to new bone marrow was also subjectively estimated. Necrotic bone was defined as acellular tissue, with no soft tissue attached, and surrounded by necrosis and inflammation. Old bone was defined as pale, acellular bone with distinct cut edges. Samples were analyzed in duplicate, and any sample that had a difference in grade more than 1.5 or a difference in percentage more than 15% were reanalyzed. The average of the 2 values that were similar was taken; if the difference between all three values was <15% or 1.0, then the average of the three values was used.

Undecalcified Sections: The undecalcified sections were further fixed in 70% ethyl alcohol (ETOH) for 1 week, and then dehydrated in graded solutions of ETOH (70%, 95%, 100%) over approximately 3 weeks, with increasing concentrations of embedding resin (Technovit 7200, Exakt Technologies). The final solution contained 100% of the embedding resin and was polymerized using light activation. The sections were cut from the specimen block with an Exakt diamond blade band saw (Model 310 CPV, Exakt Technologies). All sections were ground using an Exakt microgrinder (Model 400 CS, Exakt Technologies) to 30-50 μm thickness and stained with a modified van Giesson bone stain for quantitative analysis of the amount of new bone formation.

The undecalcified sections were analyzed quantitatively using the Image ProPlus system (Media Cybernetics, Silver Spring, MD; Figure 6b). A ROI between the two screw holes adjacent to the defect was used. The distance between the screw holes was 18 mm, and the widest tissue sample was 30 mm, therefore the defect was defined by an 18 x 30-mm section. Sections were given a subjective grade (0 to 4) for new bone formation as described in the section on "Decalcified Sections". The total amount of tissue in the

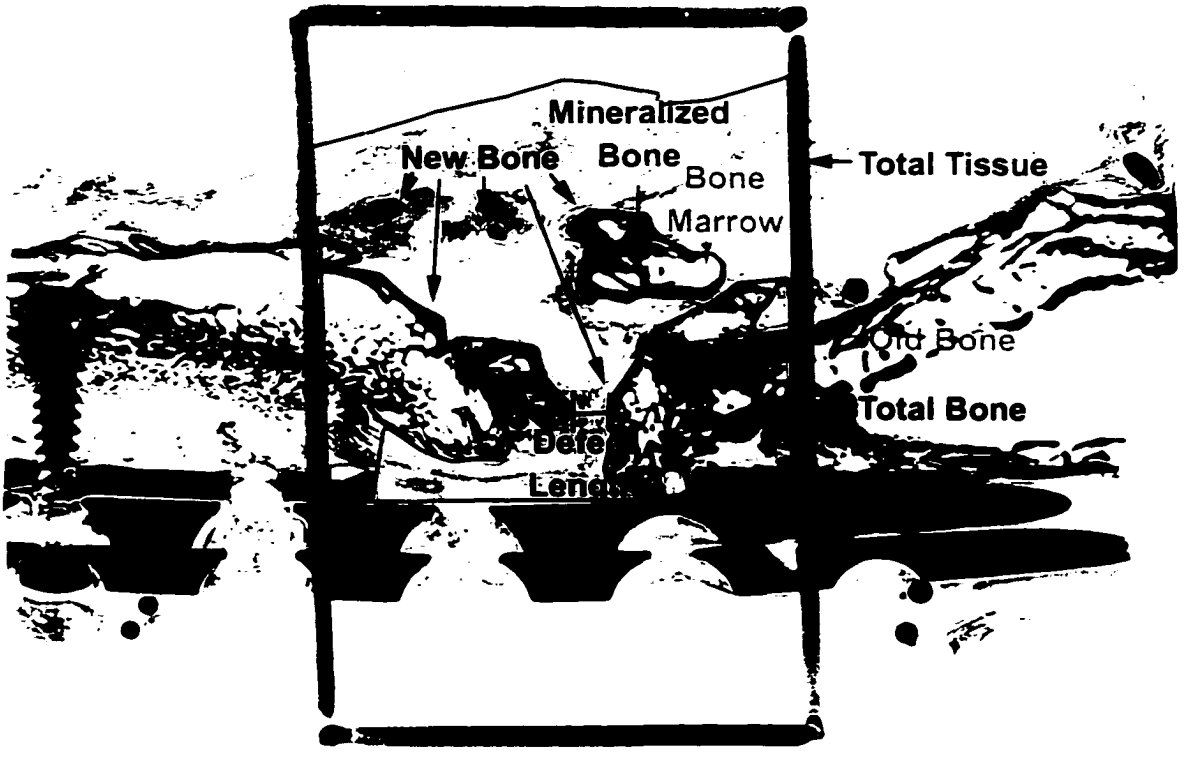

Figure 6b. Histological section of a rabbit femur at 16 weeks illustrating the method for quantitative histomorphometric analysis of undecalcified sections. Sections were stained with van Giesson bone stain. The 20 x 30-mm region of interest (ROI) is outlined in black. The total tissue, total bone, and old bone were measured. The amount of new bone was calculated from subtracting the amount of old bone from the total bone. Mineralized bone is pink and bone marrow is white. The amount of total and old bone that was mineralized was measured, and the amount of new bone that was mineralized was calculated. Values were expressed as a percentage of the ROI and a percentage of the total tissue. The length between two adjacent areas of bone was measured as the remaining defect length and was used as a measure of bone healing. Magnification 1X.

region, total bone, and old bone were measured. Bone included both mineralized bone and bone marrow, therefore the amount of mineralized total bone and mineralized old bone was measured. The amount of new bone, the percentage of new and old bone of the total tissue, the ratio of new to old bone, and the percentage of new bone that was mineralized were calculated. The length between two adjacent areas of bone was measured as the remaining defect length and was used as a measure of healing.

Statistical Analysis

Categorical data were analyzed using a Fisher's Exact test (PROC FREQ, SAS Institute, Cary, NC). Continuous data were analyzed using an ANOVA (PROC MIXED, SAS Institute). Rabbit, time (0, 4, 8, 12, 16 weeks), treatment (BMP, LUC), and infection (Infected, Non-infected) were used as class variables. Rabbit nested within treatment and infection groups was used as the random variable. Data were analyzed using several models to evaluate the association between dependent variables (radiographic, DEXA, and histological measurements) and fixed effects (time, treatment, infection, and interactions). Data are represented as the least squares mean (LSM) +/- standard error of the mean (SEM). The level of significance was $p<0.05$.

Results

Animal Model

Rabbits in the non-infected group had no morbidity. The major complications associated with the model were signs of systemic illness (fever, inappetence, and weight-loss) and lameness associated with infection (Chapter 2). Systemic illness was monitored

at the time of sample collection, and lameness was graded 0-4. Overall there were 42 rabbits completing the 16-week study (non-infected BMP-2 n=11; Non-infected LUC n=14; Infected BMP-2 n=10, Infected LUC n=7). Therefore, 22 rabbits were euthanized for humane reasons, based on the severity of the systemic illness or lameness, before the completion of the study (Chapter 2). Eight rabbits were euthanized after week-4; therefore, data from these rabbits were included until the time of euthanasia.

Rabbits were classified as infected or non-infected initially whether they were inoculated with *S. aureus* at 48 hours or not inoculated. Infection was further classified as whether there was accumulation of purulent material on gross examination, a positive culture, and radiographic lysis at 16 weeks (non-infected = lysis grade of 0.5 or less; infected = lysis grade of 1 or greater). There were only three rabbits that did not meet all three requirements for being infected or non-infected. There was one rabbit in the infected group that had no signs of infection grossly, a negative culture, and no radiographic lysis at 16 weeks, and on further examination of this rabbit's record the culture of the inoculation was negative; therefore, this rabbit was considered to be in the non-infected group. All other rabbits in the infected group had established infection. There was one rabbit in the non-infected group that had a small amount of inspissated purulent material at the fracture site; however, this was sterile on culture of the tissue and screw, and the rabbit was considered in the non-infected group. There was one rabbit in the infected group that did not have signs of infection at the fracture site; however, this rabbit had severe infection of the femorotibial joint, and was therefore considered in the infected group.

Radiographic Evaluation

Qualitative Radiographic Analysis: Rabbits in the Ad-BMP-2 treated groups had initial- and bridging-callus formation at earlier time periods compared to rabbits in the Ad-LUC control groups and there were a higher percentage of rabbits in the Ad-BMP-2 treated groups with bridging-callus formation compared to rabbits in the Ad-LUC control groups (Figure 7a and b). Rabbits in the Ad-BMP-2 treated groups also had a higher grade for proliferation, soft tissue callus, periosteal callus, and overall external callus/proliferation ($p<0.001$; Figure 8a and b). There was a significant interaction between treatment and time ($p=0.01$); rabbits in the Ad-BMP-2 treated groups formed external callus more rapidly than rabbits in the Ad-LUC control groups. There were no interactions between treatment and infection groups. There was no association between infection and proliferation, soft tissue callus, periosteal callus, and overall external callus/proliferation grades. There was an interaction between infection and time for periosteal callus formation ($p=0.02$); periosteal callus formation increased with time in infected rabbits more rapidly than in non-infected rabbits. There was a trend for rabbits in the Ad-LUC control group to have a higher percentage defect ossification compared to rabbits in the Ad-BMP-2 treated groups ($p=0.09$; Figure 9).

Rabbits in the infected groups had a higher lysis grade compared to rabbits in the non-infected groups ($p<0.001$) and a higher percentage of rabbits in the infected groups had sequestration at 12 and 16 weeks ($p=0.01$ and $p=0.04$, respectively). There was also a trend for rabbits in the Ad-LUC control group to have a higher lysis grade compared to rabbits in the Ad-BMP-2 groups and this was significant at 16 weeks (Figure 10).

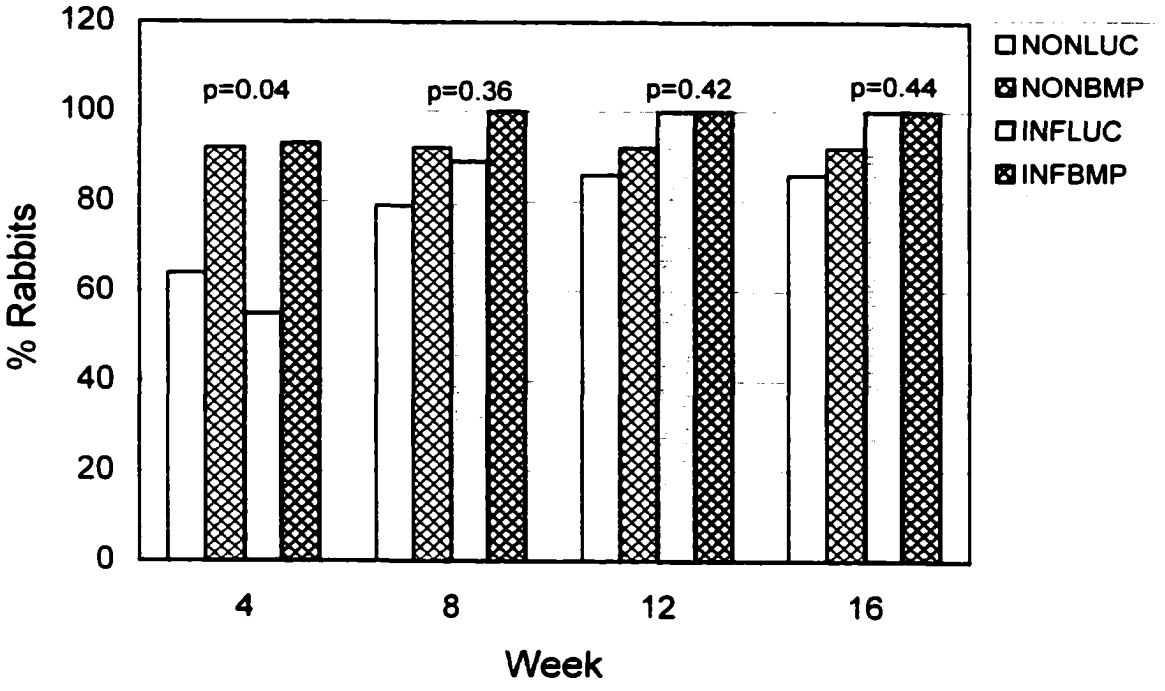

Figure 7a. A plot showing the percentage of rabbits with initial callus formation in the different experimental groups. The percentage of rabbits is shown on the y-axis and the week postoperatively is shown on the x-axis. Rabbits treated with BMP-2 (NONBMP and INFBMP) had earlier initial callus formation compared to control rabbits (NONLUC and INFLUC). The p-value is comparing the difference between the four experimental groups using a Fisher's Exact test. The level of significance was $p<0.05$. There was a significant difference between experimental groups at 4 weeks.

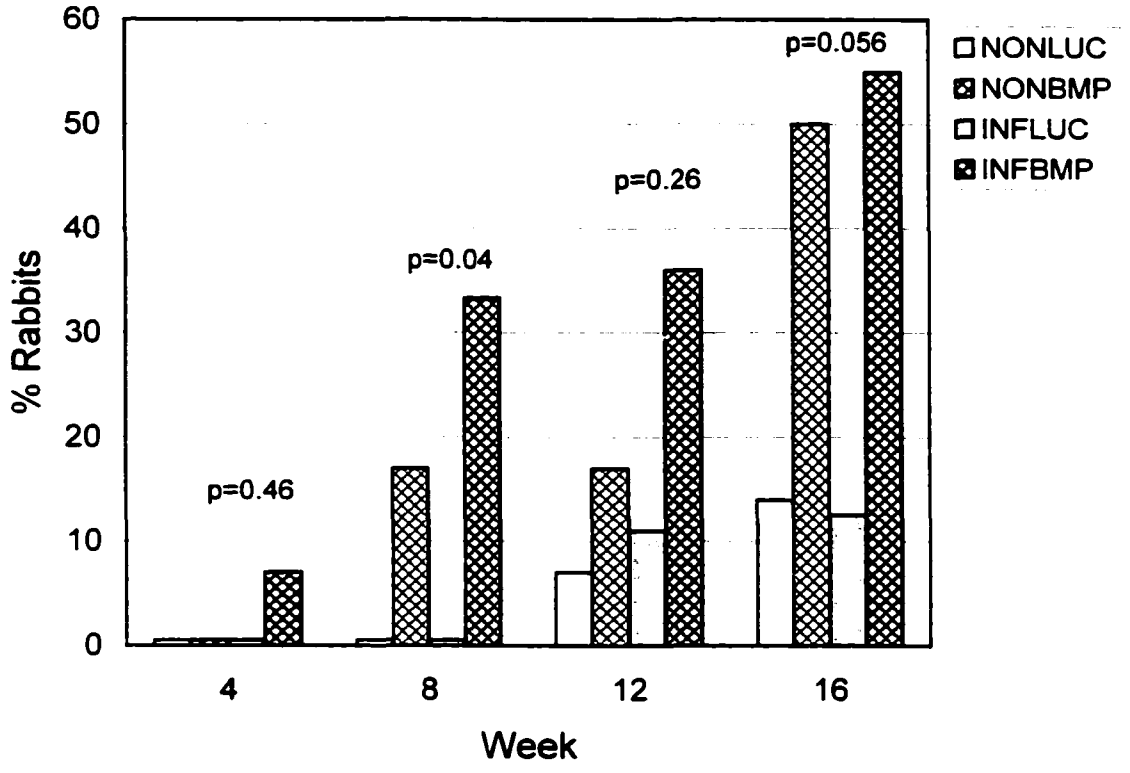

Figure 7b. A plot showing the percentage of rabbits with bridging callus formation in the different experimental groups. The percentage of rabbits is shown on the y-axis and the week postoperatively is shown on the x-axis. Rabbits treated with BMP-2 (NONBMP and INFBMP) had earlier bridging callus formation compared to control rabbits (NONLUC and INFLUC) and there were a higher percentage of rabbits in the BMP-2 treated groups with bridging callus compared to the LUC control groups. The p-value is comparing the difference between the four experimental groups using a Fisher's Exact test. The level of significance was $p<0.05$. There was a significant difference between experimental groups at 8 weeks and a trend at 16 weeks.

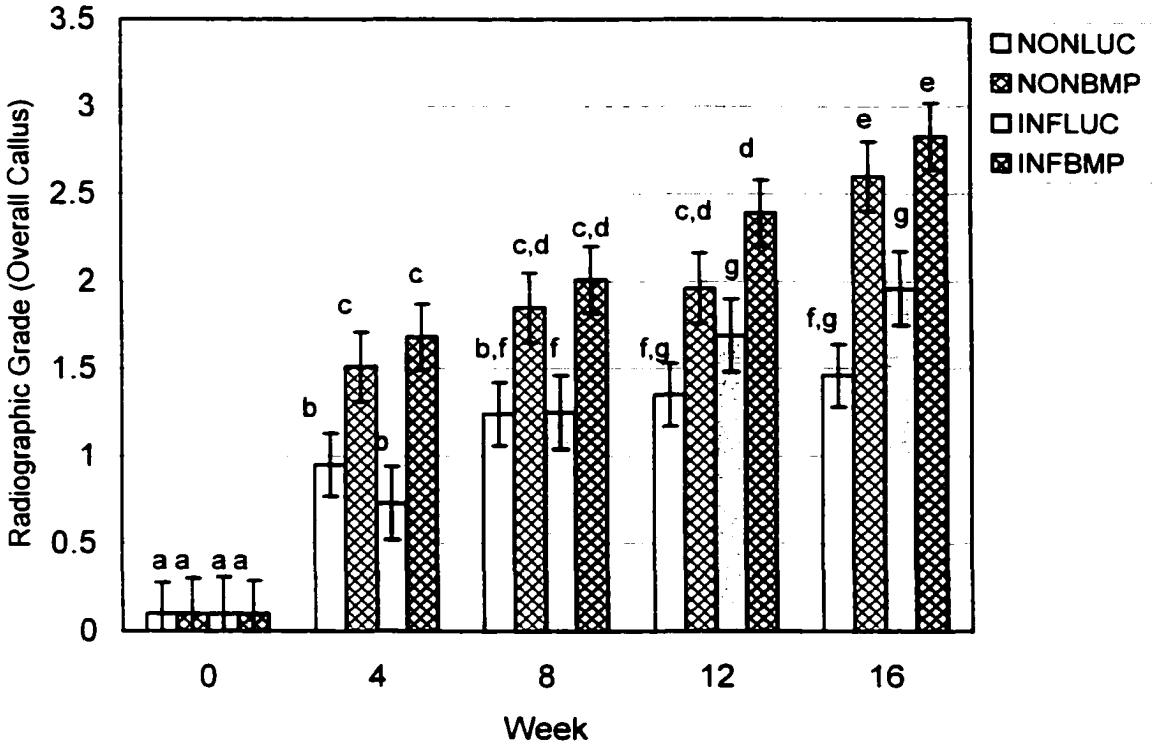

Figure 8a. A plot showing the association between treatment group and radiographic external callus/proliferation grade. External callus/ proliferation grade is shown on the y-axis and week after surgery is shown on the x-axis. Rabbits in the Ad-BMP-2 treated groups (NONBMP and INFBMP) had a higher callus grade compared to control rabbits (NONLUC and INFLUC). Data are represented as least squared means (LSM) +/- standard error (SE); different letters represent statistically significant differences.

Non-infected Ad-LUC Control

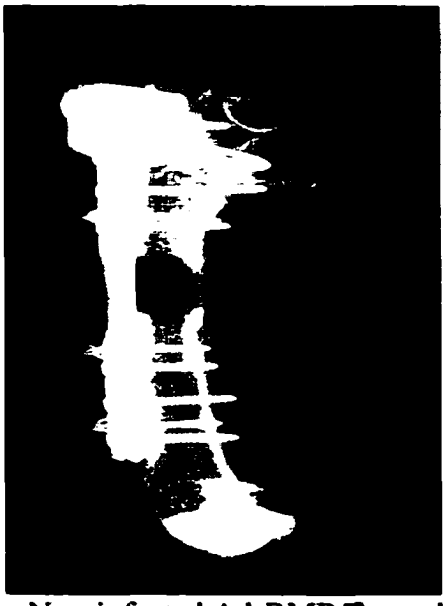

Non-infected Ad-BMP Treated

Infected Ad-LUC Control

Infected Ad-BMP Treated

Figure 8b. Examples of craniocaudal radiographic views of rabbits with non-infected and infected non-union at 16 weeks. Rabbits treated with Ad-BMP-2 had more callus formation compared to control groups. Rabbits in the non-infected and infected Ad-BMP-2 treated groups had a similar pattern of bone formation.

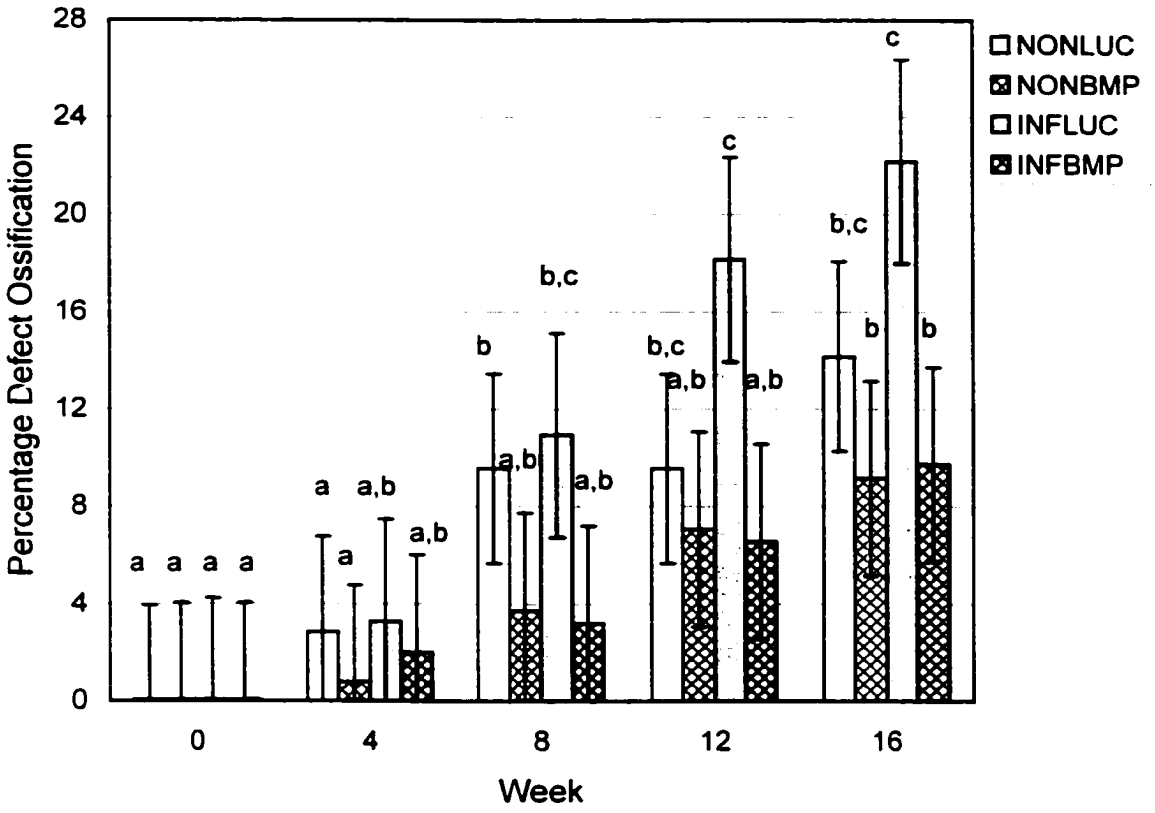

Figure 9. A plot showing the association between treatment group and radiographic percentage of defect ossification. The percentage of defect ossification is shown on the y-axis and week after surgery is shown on the x-axis. There was a trend for rabbits in the Ad-LUC control groups (NONLUC and INFLUC) to have a higher percentage of defect ossification compared to rabbits in the Ad-BMP-2 treated groups (NONBMP and INFBMP) . Data are represented as least squared means (LSM) +/- standard error (SE); different letters represent statistically significant differences.

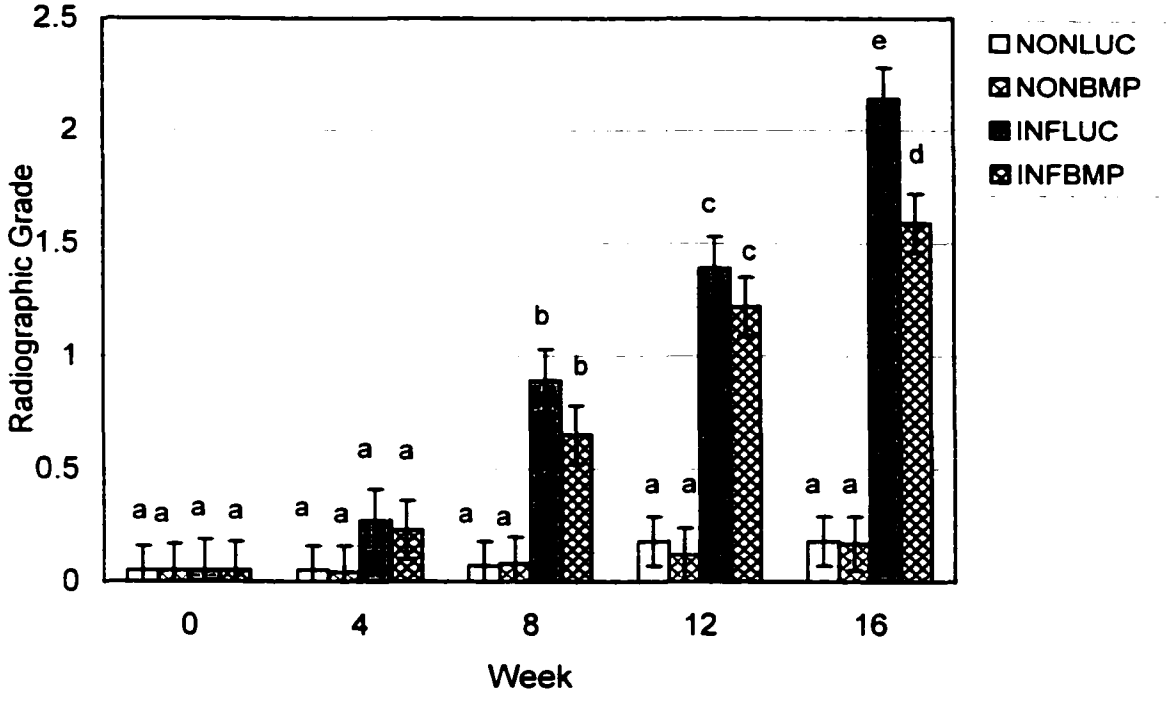

Figure 10. A plot showing the association between treatment group and radiographic lysis grade. Lysis grade is shown on the y-axis and week after surgery is shown on the x-axis. Rabbits in the infected groups (INFLUC and INFBMP) had a higher lysis grade compared to non-infected rabbits (NONLUC and NONBMP). There was also a trend for rabbits in the INFLUC control group to have a higher lysis grade than rabbits in the INFBMP treated group. Data are represented as least squared means (LSM) +/- standard error (SE); different letters represent statistically significant differences.

Quantitative Radiographic Analysis: Rabbits in the Ad-BMP-2 treated groups had more external callus (soft tissue and periosteal callus) in the defect ($p=0.07$; Figure 11a and b) and whole bone ($p=0.13$; Figure 11c) ROI at 16 weeks compared to rabbits in the Ad-LUC control groups; however, this did not reach statistical significance. There was no association between infection and external callus formation and no interaction between treatment and infection groups. Rabbits in the Ad-LUC control groups had a higher percentage of new bone in the defect area, or defect ossification (medullary callus), compared to rabbits in the control groups ($p=0.03$), and infected rabbits had a higher percentage of defect ossification compared to non-infected rabbits ($p=0.03$; Figure 12).

There was a good positive correlation between the qualitative and quantitative measurement of external callus ($p<0.0001$ and $r^2=0.74$) and the qualitative and quantitative amount of defect ossification ($p<0.0001$ and $r^2=0.71$). There was no correlation between defect ossification and callus formation ($p=0.28$, $r^2=0.03$).

Defect Length and Area: The mean defect length measured at time 0 on the lateral radiographic view was 11.1 mm (9-12mm), the mean bone length was 104.6mm (98-113 mm) and, therefore, the mean percent defect length was 10.6% (8.1-12.2%). The mean defect area measured at week-16 on the craniocaudal radiographic view (Figure 4) was 0.67 (0.4-1) cm^2, the mean bone area was 6.4 (5.5 to 7.3) cm^2, and the mean percent defect area was 10.4% (5-13.5%). The radiographic defect length was used for further analysis. When the defect length was the dependent variable, there was a trend for rabbits in the Ad-LUC control groups to have a smaller defect length ($p=0.09$). There was no association between defect length and infection group. There was no association between defect length (fixed effect) and defect ossification ($p=0.5$) or callus formation ($p=0.9$;

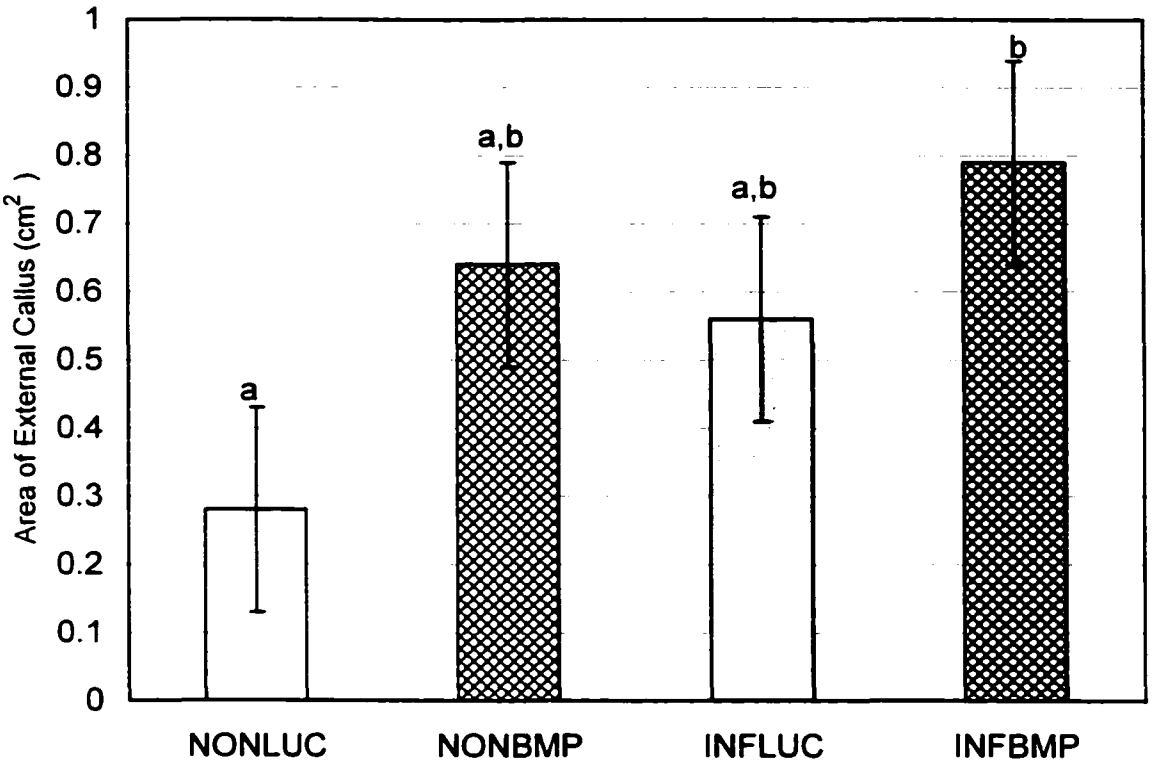

Figure 11a. A plot showing the association between treatment group and the quantitative amount of radiographic external callus formation in the defect region of interest. The amount of callus formation is shown on the y-axis and the treatment groups are shown on the x-axis. There was a trend for rabbits in the Ad-BMP-2 treated groups (NONBMP and INFBMP) to have a higher amount of callus formation compared to rabbits in the Ad-LUC control groups (NONLUC and INFLUC); however, this was only statistically significant for NONLUC and INFBMP. Data are represented as least squared means (LSM) +/- standard error (SE); different letters represent statistically significant differences.

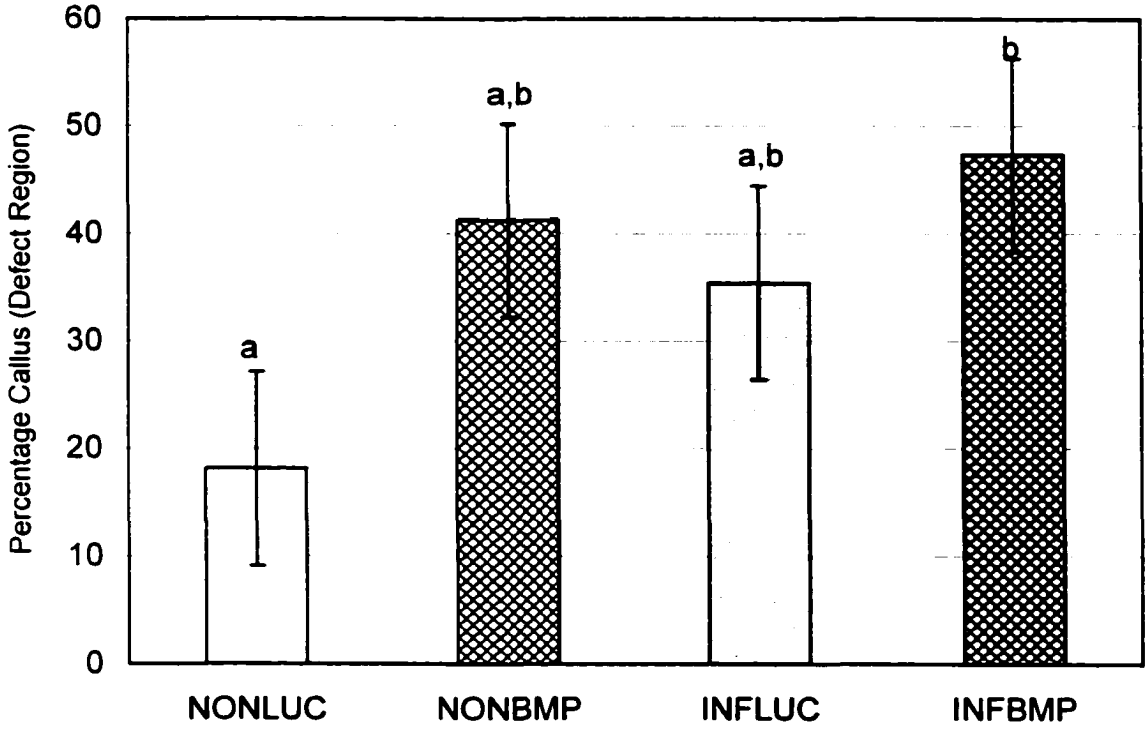

Figure 11b. A plot showing the association between treatment group and quantitative radiographic percentage external callus formation in the defect region. The percentage callus formation is shown on the y-axis and the treatment groups are shown on the x-axis. There was a trend for rabbits in the Ad-BMP-2 treated groups (NONBMP and INFBMP) to have a higher percentage callus formation compared to rabbits in the Ad-LUC control groups (NONLUC and INFLUC); however, this was only statistically significant for NONLUC and INFBMP. Data are represented as least squared means (LSM) +/- standard error (SE); different letters represent statistically significant differences.

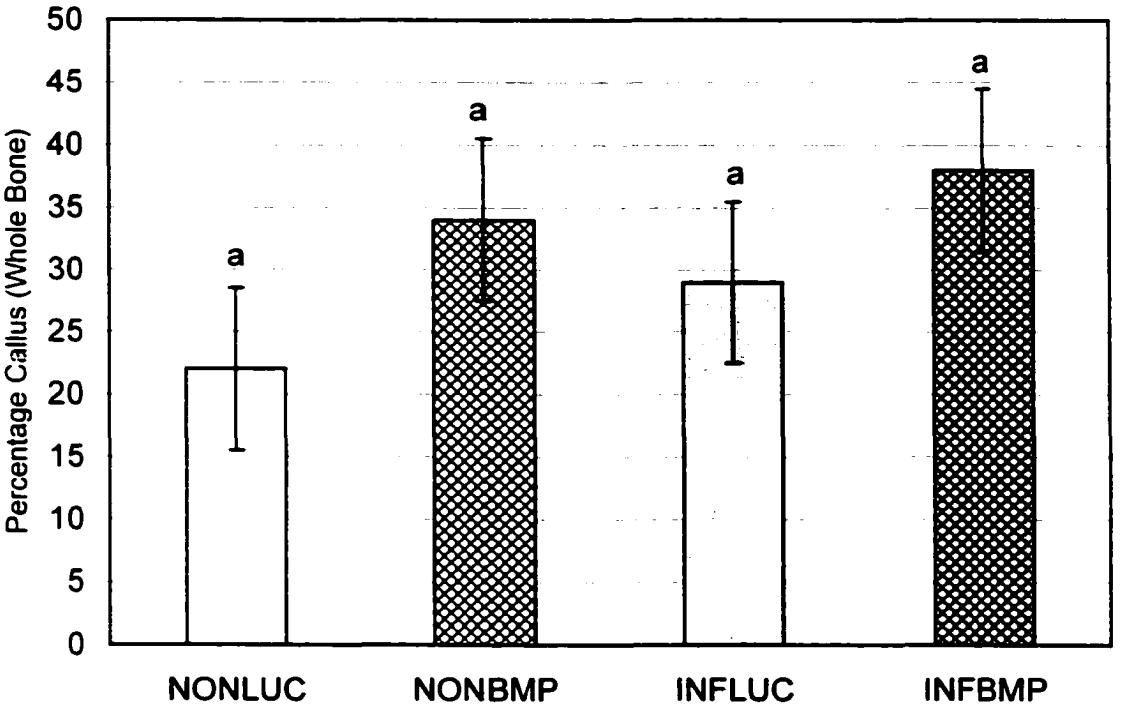

Figure 11c. A plot showing the association between treatment group and quantitative radiographic percentage external callus formation in the whole bone region of interest. The percentage callus formation is shown on the y-axis and the treatment groups are shown on the x-axis. There was a trend for rabbits in the Ad-BMP-2 treated groups (NONBMP and INFBMP) to have a higher percentage callus formation compared to rabbits in the Ad-LUC control groups (NONLUC and INFLUC). Data are represented as least squared means (LSM) +/- standard error (SE); different letters represent statistically significant differences.

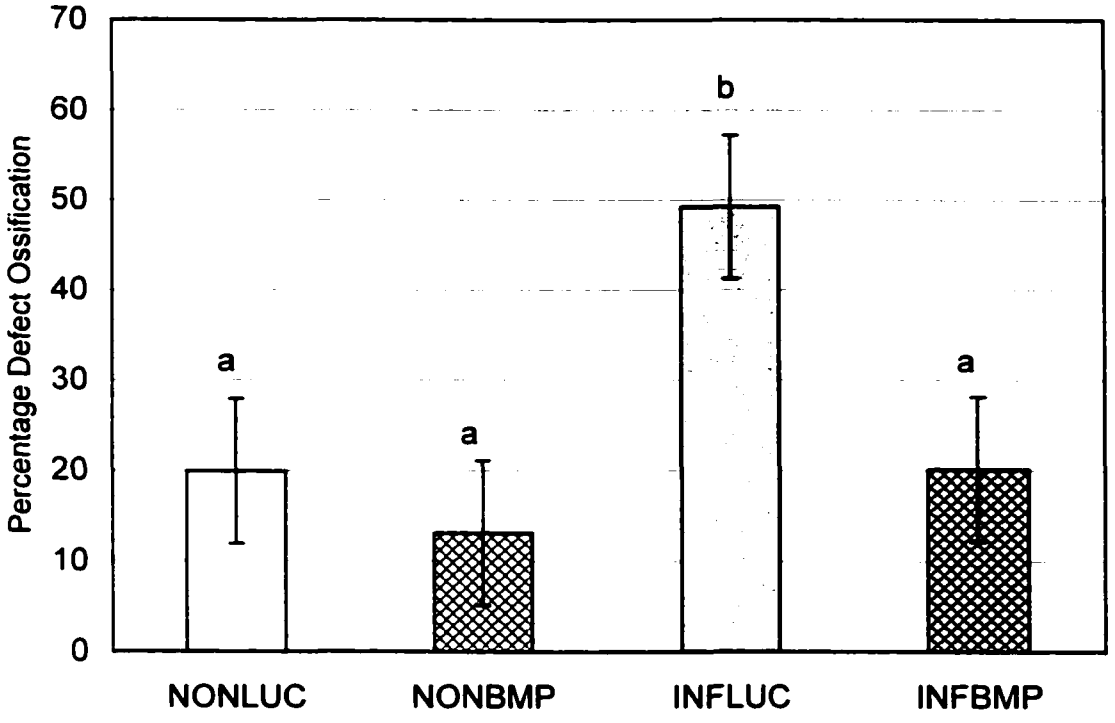

Figure 12. A plot showing the association between treatment group and quantitative radiographic percentage of defect ossification. The percentage of defect ossification is shown on the y-axis and the treatment groups are shown on the x-axis. There was a trend for rabbits in the Ad-LUC control groups (NONLUC and INFLUC) to have a higher percentage of defect ossification compared to rabbits in the Ad-BMP-2 treated groups (NONBMP and INFBMP) . Data are represented as least squared means (LSM) +/- standard error (SE); different letters represent statistically significant differences.

dependent variables) at 16 weeks. There was no correlation between defect length or area and the percentage ossification or callus grade. Therefore, although there was variability in defect length and area, the defect length or area overall did not appear to have a significant effect on defect ossification or callus formation.

Plate Bending: There were seven rabbits (17%) with plates subjectively observed to be bent adjacent to the defect at 16 weeks. Although the plates were bent at surgery to conform to the proximal femur, they were not bent adjacent to the defect. Radiographically, there were no rabbits with bent plates that had bridging-callus, whereas 40% of the rabbits without plate bending had bridging-callus at 16 weeks ($p=0.04$). Rabbits with bent plates had significantly less external callus formation ($p<0.001$; Figure 13) compared to rabbits without plate bending. There was also a trend for rabbits with bent plates to have less defect ossification ($p=0.07$).

Dual Energy X-Ray Absorptiometry

There was no association between treatment group and BMD of the defect ($p=0.6$); however, infected rabbits had higher BMD of the defect compared to non-infected rabbits ($p=0.04$; Figure 14). There was a trend for rabbits treated with Ad-BMP-2 to have a higher BMD in the proximal fragment ($p=0.1$) compared to rabbits in the Ad-LUC groups, and for infected rabbits to have a higher BMD in the proximal fragment ($p=0.1$; Figure 15) compared to non-infected rabbits. There was no association between treatment or infection group and BMD in the distal fragment. (Figure 15). There was a trend for rabbits treated with Ad-BMP-2 to have a higher BMD in the ROI adjacent to the defect compared to rabbits in the Ad-LUC group ($p=0.1$; Figure 16a), and for rabbits in

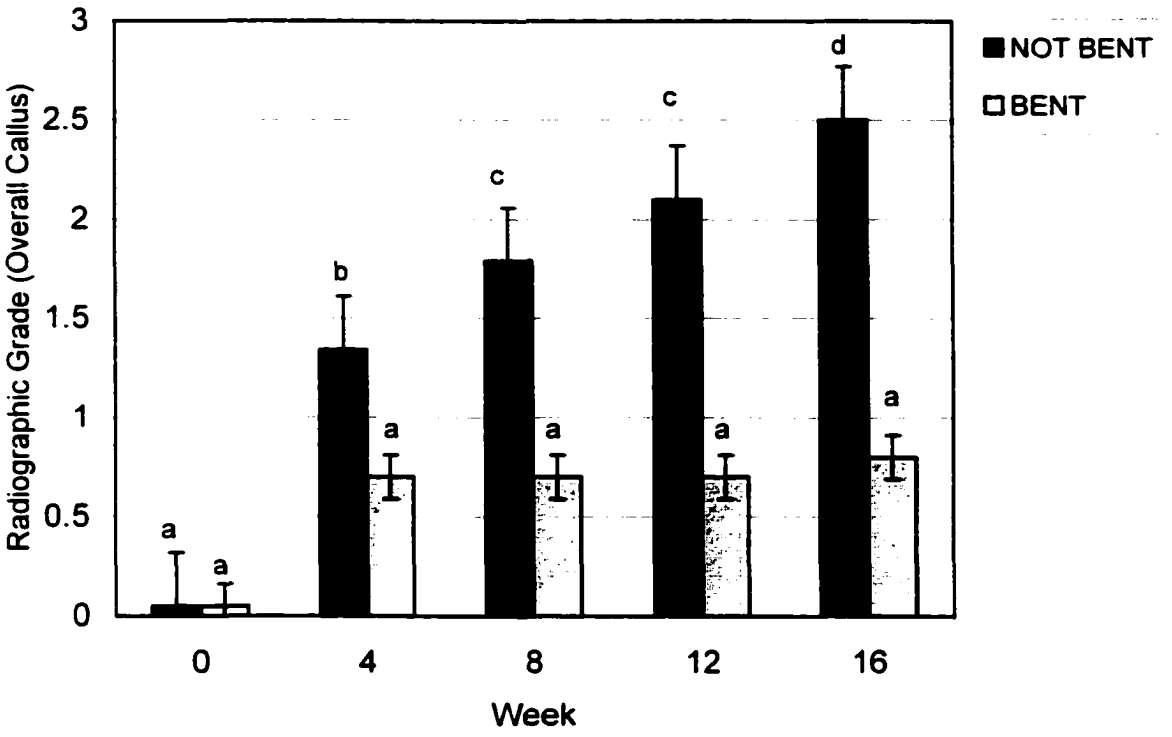

Figure 13. A plot showing the association between plate bending and radiographic callus grade. The radiographic callus grade is shown on the y-axis and week after surgery is shown on the x-axis. Rabbits with a bent plate had significantly less callus formation compared to rabbits without a bent plate. Data are represented as least squared means (LSM) +/- standard error (SE): different letters represent statistically significant differences.

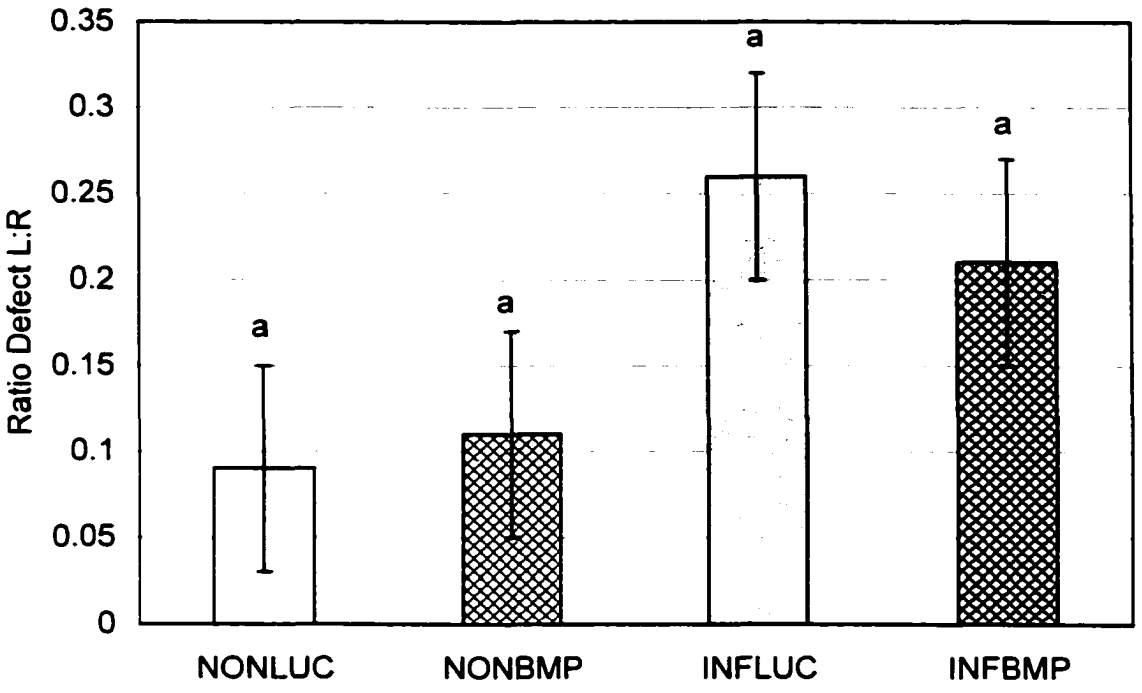

Figure 14. A plot showing the association between the ratio of the bone mineral density (BMD) in the left (L) : right (R) defect region and treatment group. The L:R BMD of the defect is shown on the y-axis and the treatment group is shown on the x-axis. There was a trend for rabbits in the infected groups (INFLUC and INFBMP) to have a higher L:R BMD of the defect compared to rabbits in the non-infected groups (NONLUC and NONBMP) . Data are represented as least squared means (LSM) +/- standard error (SE); different letters represent statistically significant differences.

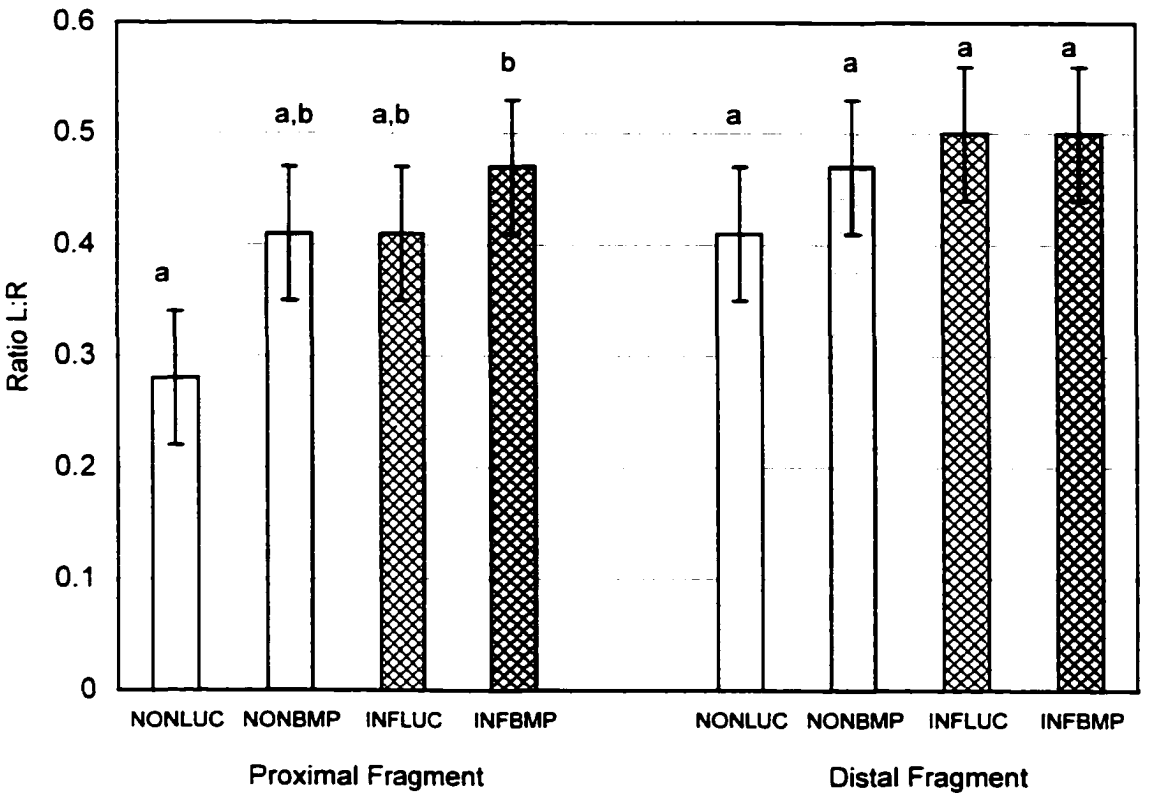

Figure 15. A plot showing the association between the ratio of the bone mineral density (BMD) in the left (L) : right (R) proximal and distal fragment and treatment group. The L:R BMD is shown on the y-axis and the treatment group is shown on the x-axis. There was a trend for rabbits in the Ad-BMP-2 treated groups (NONBMP and INFBMP) to have a higher L:R BMD of the proximal fragment compared to rabbits in the Ad-LUC control groups (NONLUC and INFLUC) . Data are represented as least squared means (LSM) +/- standard error (SE); different letters represent statistically significant differences.

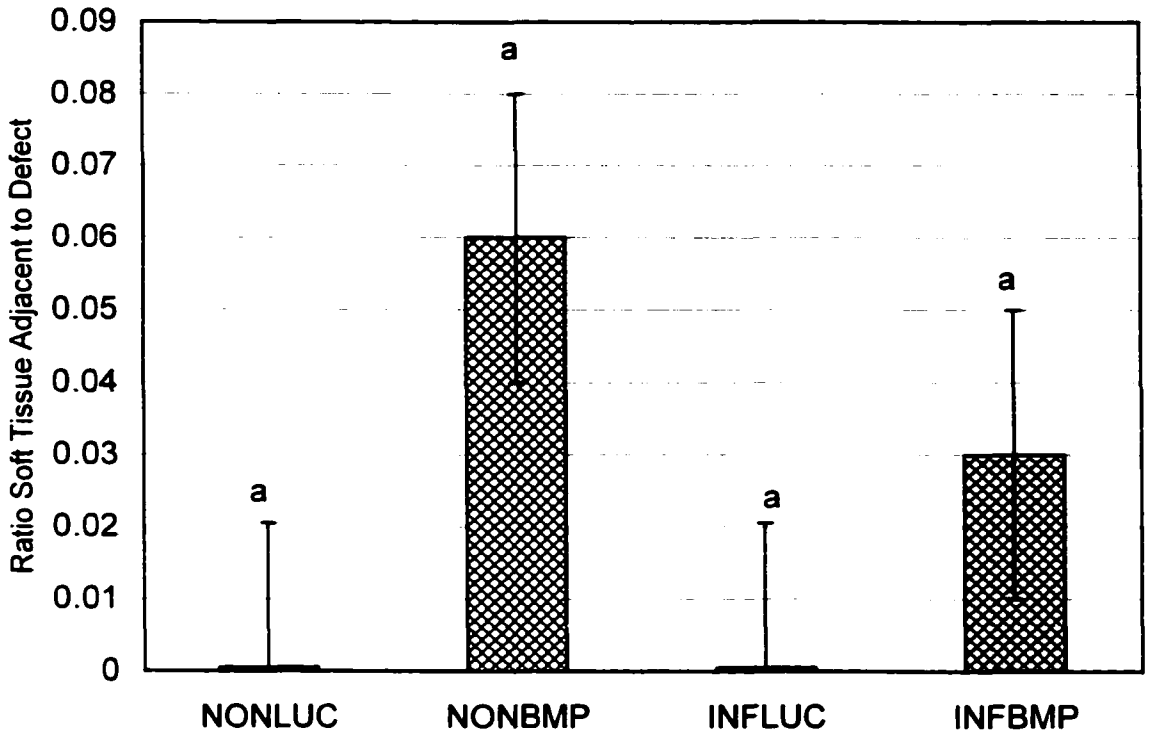

Figure 16a. A plot showing the association between the ratio of the bone mineral density (BMD) in the left (L) : right (R) soft tissue adjacent to the defect and treatment group. The L:R BMD is shown on the y-axis and the treatment group is shown on the x-axis. There was a trend for rabbits in the Ad-BMP-2 treated groups (NONBMP and INFBMP) to have a higher L:R BMD of the soft tissue adjacent to the defect compared to rabbits in the Ad-LUC control groups (NONLUC and INFLUC) . Data are represented as least squared means (LSM) +/- standard error (SE); different letters represent statistically significant differences.

the infected groups to have a higher BMD in the ROI adjacent to the proximal fragment compared to rabbits in the non-infected groups ($p=0.1$; Figure 16b). There was no correlation between callus formation and BMD ($p=0.09$; $r^2=0.07$), BMC ($p=0.005$; $r^2=0.18$), or area ($p=0.0002$, $r^2=0.3$). There was no correlation between defect ossification and BMD ($p=0.004$, $r^2=0.19$), BMC ($p=0.0007$, $r^2=0.26$), or area ($p=0.0005$, $r^2=0.27$).

Histomorphometry

Decalcified Sections: At 16 weeks there was no difference between treatment groups for new bone grade, percentage new bone, or the ratio between new and old bone ($p>0.6$). Rabbits in the infected groups, however, had a higher new bone grade, higher percentage new bone, and a higher ratio between new and old bone ($p<0.01$; Figure 17). There was no difference between groups in the ratio of mineralized new bone to bone marrow. The new bone in both groups was predominantly mature bone (lamellar bone with bone marrow). The surface of the new bone was covered with osteoblasts and there were no osteoclasts seen, despite the presence of numerous Howship's Lacunae. There was a trend for rabbits in the Ad-LUC control group to have a higher percentage of cartilage ($p=0.14$; Figure 17) compared to Ad-BMP-2 treated rabbits, and for non-infected rabbits to have a higher percentage of cartilage compared to infected rabbits ($p=0.16$). There was no difference between treatment groups for the percentage of fibrous tissue ($p=0.5$); however, infected rabbits had a higher percentage of fibrous tissue compared to non-infected rabbits ($p<0.0001$; Figure 17). Rabbits in the non-infected groups had significantly more fat compared to infected rabbits ($p<0.0001$) and rabbits in

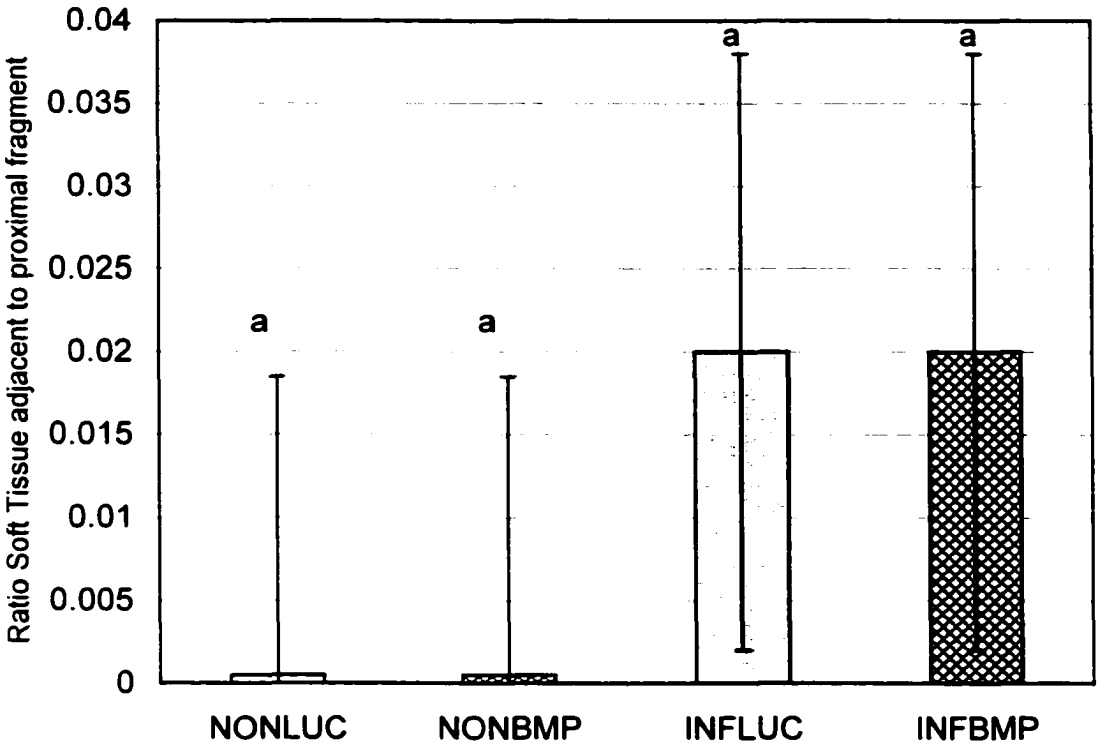

Figure 16b. A plot showing the association between the ratio of the bone mineral density (BMD) in the left (L) : right (R) soft tissue adjacent to the proximal fragment and treatment group. The L:R BMD is shown on the y-axis and the treatment group is shown on the x-axis. There was a trend for rabbits in the infected groups (INFLUC and INFBMP) to have a higher L:R BMD of the soft tissue adjacent to the proximal fragment compared to rabbits in the non-infected groups (NONLUC and NONBMP) . Data are represented as least squared means (LSM) +/- standard error (SE); different letters represent statistically significant differences.

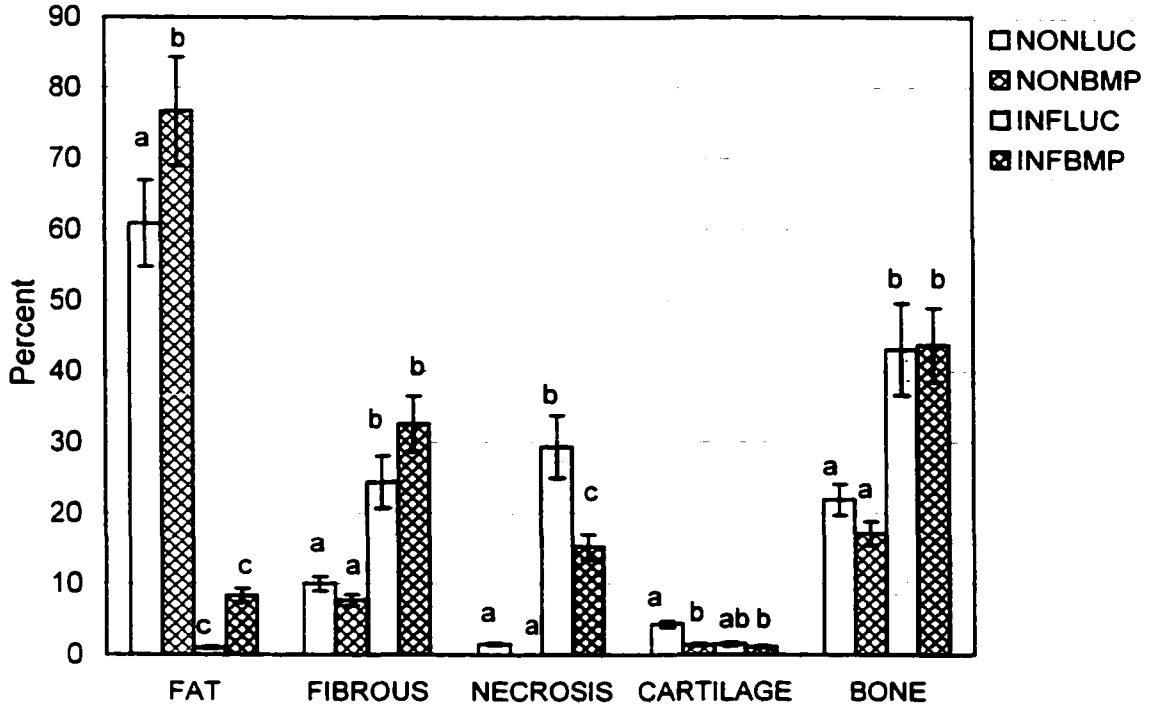

Figure 17. A plot showing the association between the percentage of fat, fibrous tissue, necrotic tissue, fibrocartilage, and bone in the defect region of interest and treatment group. The percentage of tissue is shown on the y-axis and the tissue type and treatment group is shown on the x-axis. Rabbits in the non-infected groups had more fat and less fibrous tissue, necrosis, and new bone. Rabbits in the Ad-BMP-2 treated groups had more fat, less necrosis, and less fibrocartilage. Data are represented as least squared means (LSM) +/- standard error (SE); different letters represent statistically significant differences.

the Ad-BMP-2 treated groups had significantly more fat in the defect than rabbits in the Ad-LUC control groups ($p=0.04$; Figure 17).

Rabbits in the infected groups had significantly higher grade for vascularity, inflammation, and necrosis, and a higher percentage of necrotic bone compared to non-infected rabbits ($p<0.0001$). There was a trend for rabbits in the Ad-LUC control groups to have a higher grade for inflammation ($p=0.14$), necrosis ($p=0.11$), and necrotic bone ($p=0.1$) compared to Ad-BMP-2 treated rabbits (Figure 18). The data for inflammation and necrosis were analyzed categorically and there was no association between treatment group and inflammation or necrosis grade ($p>0.5$).

There was a negative correlation between the percentage of bone and fat ($r^2= -0.52$, $p<0.0001$), the percentage of fibrous tissue and fat ($r^2= -0.58$, $p<0.0001$), and vascularity and fat ($r^2= -0.42$, $p<0.0001$). There was no correlation between the percentage of fibrous tissue and new bone ($r^2= 0.02$, $p=0.32$).

Subjective histological evaluation was performed on 16 rabbits euthanized before the completion of the study. There were only 2 rabbits from each treatment group that were non-infected; therefore, infected and non-infected rabbits were combined for analysis. There was a trend for rabbits in the Ad-BMP-2 treated groups to have a higher grade for new bone formation at 2 and 4 weeks ($p=0.11$; Figure 19a and b). Rabbits treated with Ad-BMP-2 at 2 and 4 weeks were found to have some cartilage (Figure 19b). There were no rabbits in the Ad-LUC group that had cartilage. Fat and muscle were observed in the defect ROI as early as 1 week after surgery in both treatment groups. The amount of fibrous tissue grade increased with time. There was no difference between

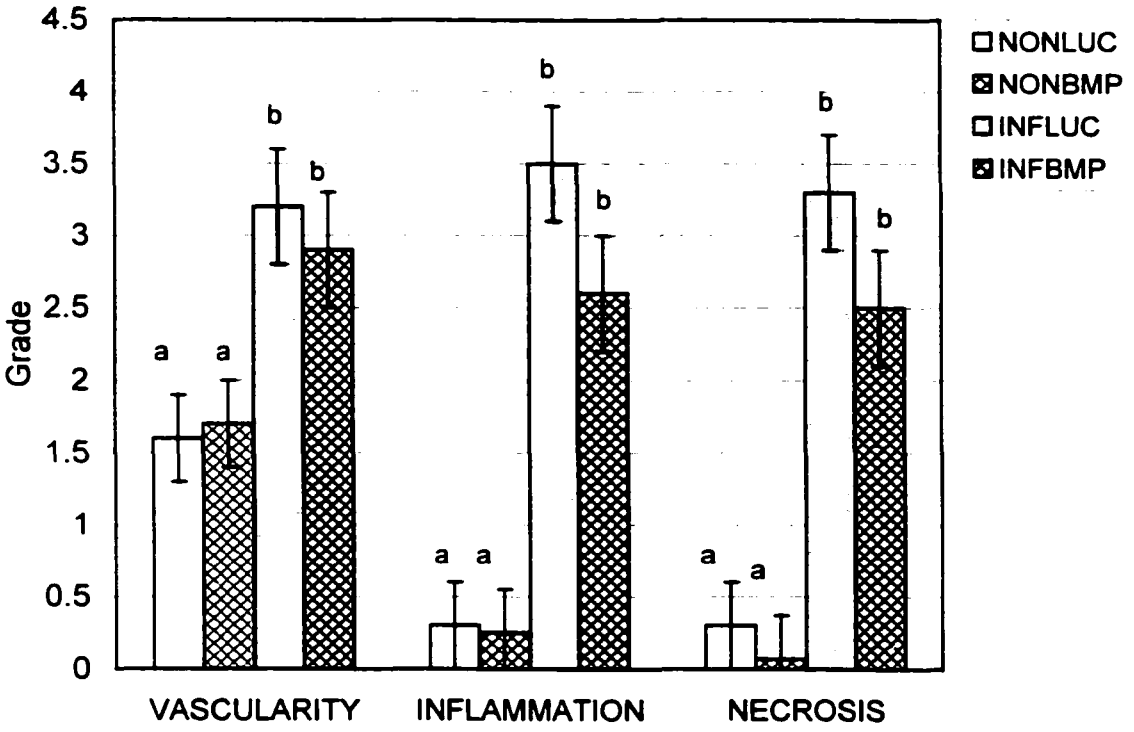

Figure 18. A plot showing the association between the histological grade for vascularity, inflammation, and necrosis and treatment group. The histological grade is shown on the y-axis and the tissue type and treatment group is shown on the x-axis. Rabbits in the infected groups had a higher grade for vascularity, inflammation, and necrosis compared to non-infected rabbits. There was a trend for rabbits in the infected Ad-LUC control group to have a higher grade for inflammation and necrosis compared to the infected Ad-BMP-2 treated group. Data are represented as least squared means (LSM) +/- standard error (SE); different letters represent statistically significant differences.

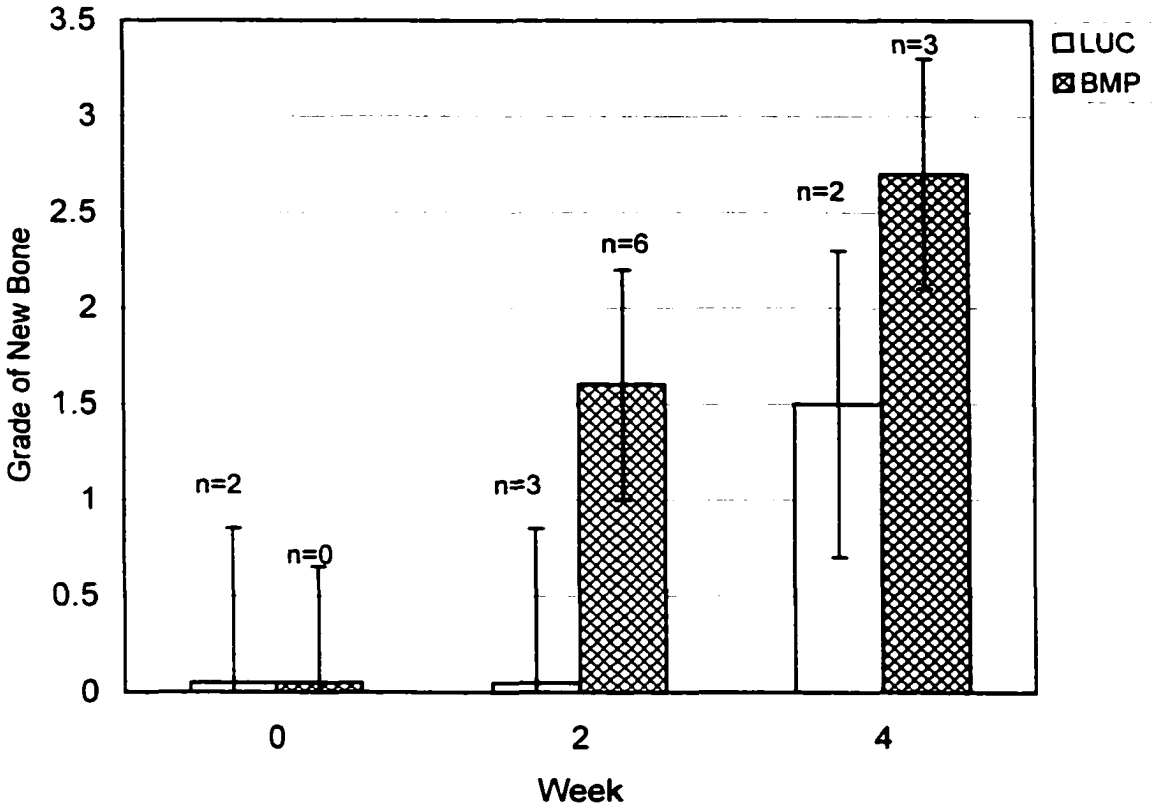

Figure 19a. A plot showing the association between the histological grade for new bone formation and treatment group. The grade for new bone formation is shown on the y-axis and the week after surgery and treatment group is shown on the x-axis. There was a trend for rabbits in the Ad-BMP-2 treated groups (BMP) to have a higher grade for new bone formation compared to rabbits in the Ad-LUC control groups (LUC). Data are represented as least squared means (LSM) +/- standard error (SE).

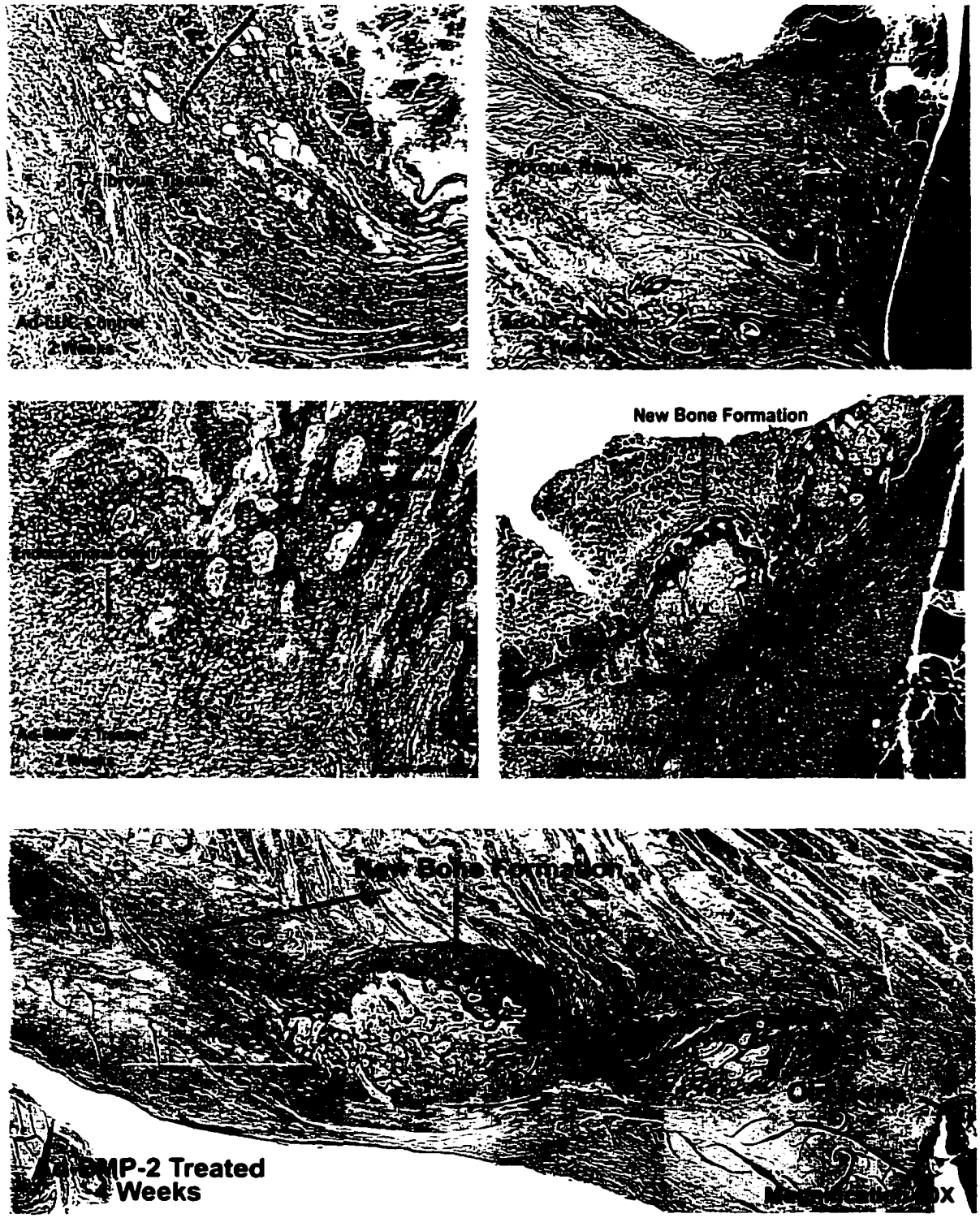

Figure 19b. Histological sections of rabbit femoral defects at 2 and 4 weeks after surgery. Sections are stained with hematoxylin and eosin. Rabbits treated with Ad-BMP-2 had more bone formation and endochondral ossification at 2 and 4 weeks compared to rabbits in the Ad-LUC control groups.

treatment group and fibrous tissue formation. There was no association between treatment group and inflammation, necrosis, or vascularity prior to 16 weeks; however, there was an increase in inflammation and vascularity with time.

Undecalcified Sections: Quantitative histomorphometry showed there was no association between treatment groups and the subjective grade for new bone formation ($p=0.18$); however, rabbits in the non-infected group treated with Ad-BMP-2 had a higher grade for new bone formation compared to non-infected rabbits in the Ad-LUC control group ($p=0.05$; Figure 20). Infected rabbits had a significantly higher grade for new bone formation compared to non-infected rabbits ($p=0.01$).

When the total tissue in the 20 x 30 mm ROI was measured (Figure 6b), there was a significant interaction between infection and time ($p=0.03$). Rabbits in the non-infected Ad-LUC group and in the infected Ad-BMP-2 treated groups had less tissue. This was most likely a result of tissue sectioning because there were some sections that the tissue was minimal and if these sections were excluded the results were not different.

Rabbits in the infected groups had significantly less old bone in the ROI than rabbits in the non-infected groups ($p=0.04$), but the difference was only significant for the non-infected Ad-LUC control groups. When the old bone was expressed as a percentage of the total tissue in the defect, although similar trends were observed, the association with infection was not significant. This may suggest that this is a result of the section or may be a real finding in that the old bone was resorbed in the infected rabbits.

There was no association between treatment group and the amount of new bone in the ROI, the percentage new bone of total tissue (Figure 21), or the amount of

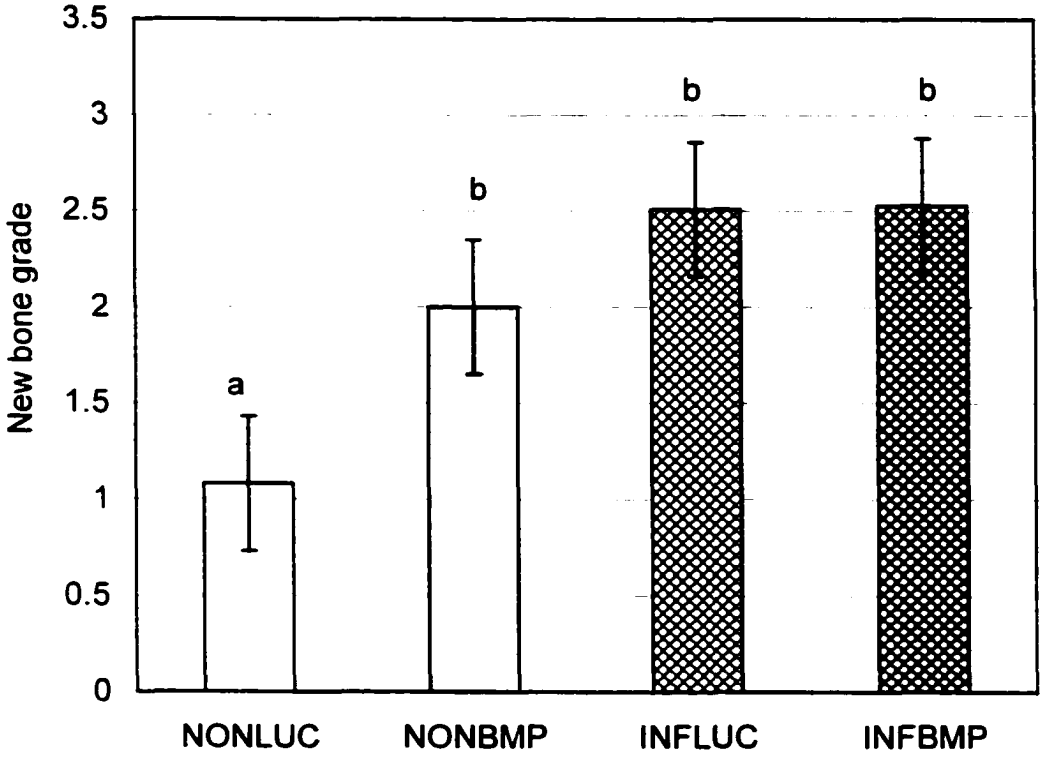

Figure 20. A plot showing the association between the histological new bone formation grade at 16 weeks and treatment group. The new bone grade is shown on the y-axis and the treatment group is shown on the x-axis. Rabbits in the non-infected Ad-LUC control group had less bone formation compared to rabbits in the other groups. Data are represented as least squared means (LSM) +/- standard error (SE); different letters represent statistically significant differences.

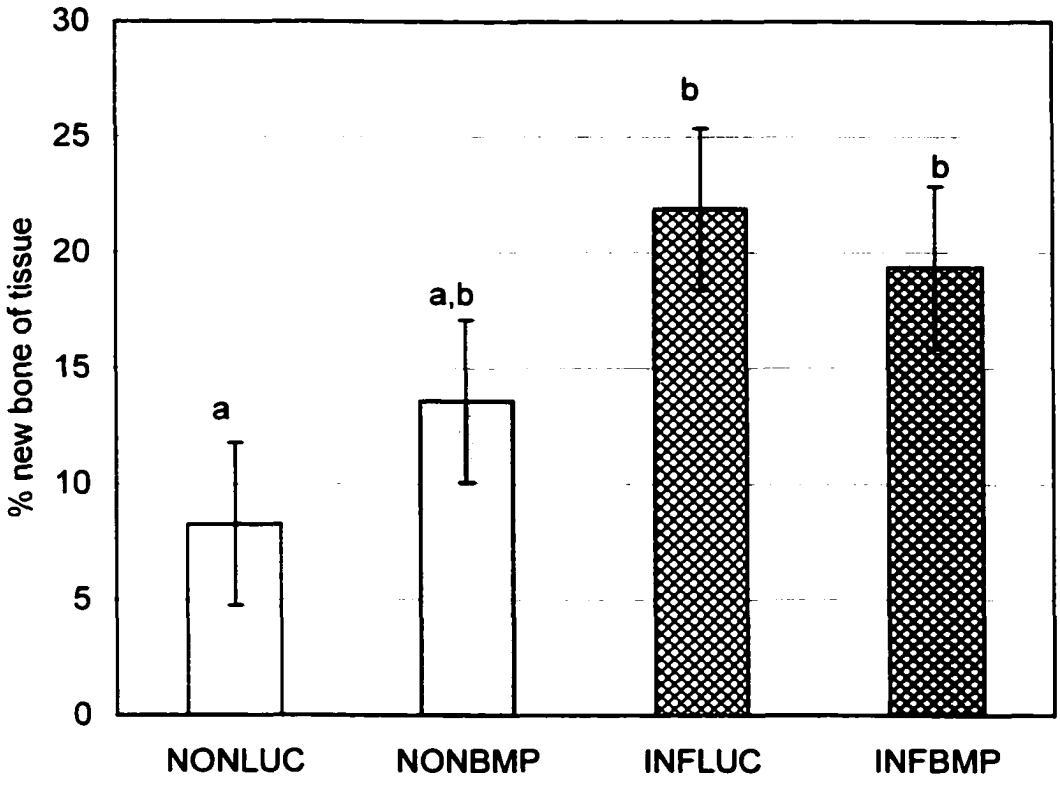

Figure 21. A plot showing the association between the quantitative histomorphometric percentage of new bone at 16 weeks and treatment group. The percentage of new bone is shown on the y-axis and the treatment group is shown on the x-axis. Rabbits in the non-infected Ad-LUC control group had less bone formation compared to rabbits in the other groups. Data are represented as least squared means (LSM) +/- standard error (SE): different letters represent statistically significant differences.

mineralized new bone in the ROI. However, there was a significant association between infection and the percentage new bone of total tissue (p=0.01: Figure 21). There was a trend for rabbits in the Ad-BMP-2 treated groups to have a higher percentage of new bone that was mineralized (p=0.08; Figure 22). Although it appeared that rabbits in the Ad-BMP-2 treated groups had a higher ratio of new bone to old bone, this did not reach statistical significance (Figure 23; p=0.2). Rabbits in the infected group had a significantly higher ratio of new bone to old bone compared to non-infected rabbits (p=0.03). There was no associated between treatment or infection group and defect length, which was the distance between adjacent areas of new bone.

Discussion

The results of this study suggest that *in vivo* adenoviral transfer of the BMP-2 gene may be useful for enhancing fracture healing in infected non-unions. There was no difference between infected and non-infected rabbits in initial- and bridging-callus formation or radiographic callus grade, and rabbits in both of the Ad-BMP-2 treated groups had earlier initial- and bridging-callus formation and higher radiographic external callus grades compared to rabbits in the Ad-LUC control groups. Further, rabbits in the Ad-BMP-2 treated groups had more cartilage and new bone formation early in the study, based on histological evaluation, compared to rabbits in the Ad-LUC control groups. Our results, however, were not as favorable as previous studies because rabbits did not heal by defect ossification and not all of the rabbits treated with Ad-BMP-2 healed the fracture.

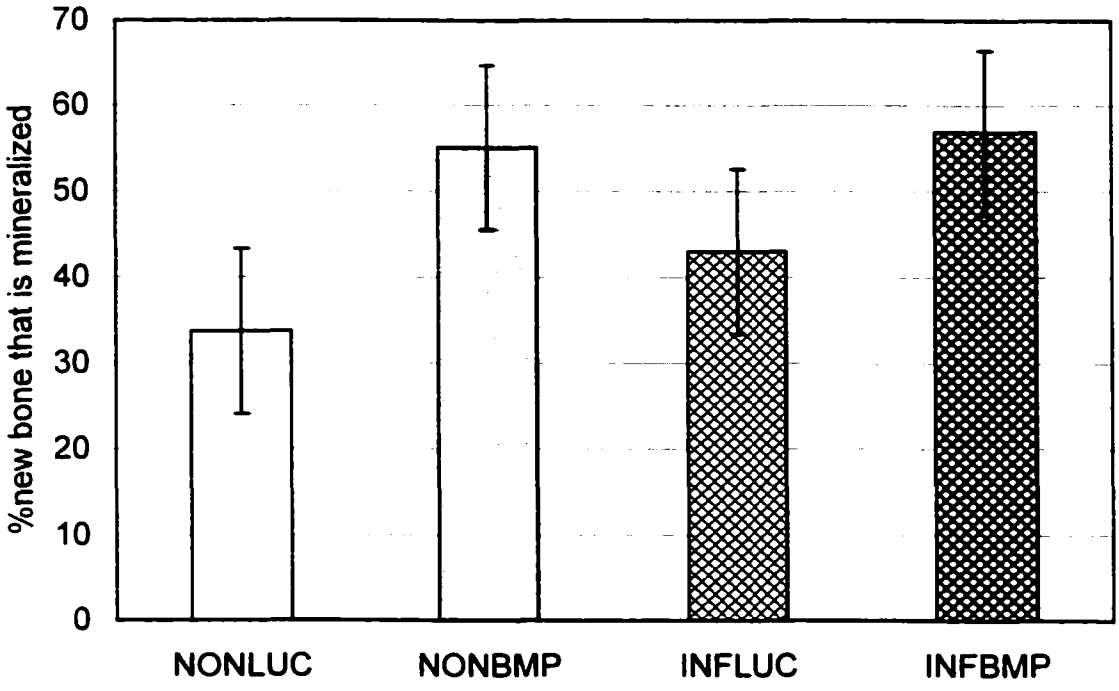

Figure 22. A plot showing the association between the quantitative histomorphometric percentage of new bone that was mineralized at 16 weeks and treatment group. The percentage of new bone that was mineralized is shown on the y-axis and the treatment group is shown on the x-axis. There was a trend for rabbits in the Ad-LUC control groups (NONLUC and INFLUC) to have a lower percentage of new bone that was mineralized compared to rabbits in the Ad-BMP-2 treated groups (NONBMP and INFBMP). Data are represented as least squared means (LSM) +/- standard error (SE); different letters represent statistically significant differences.

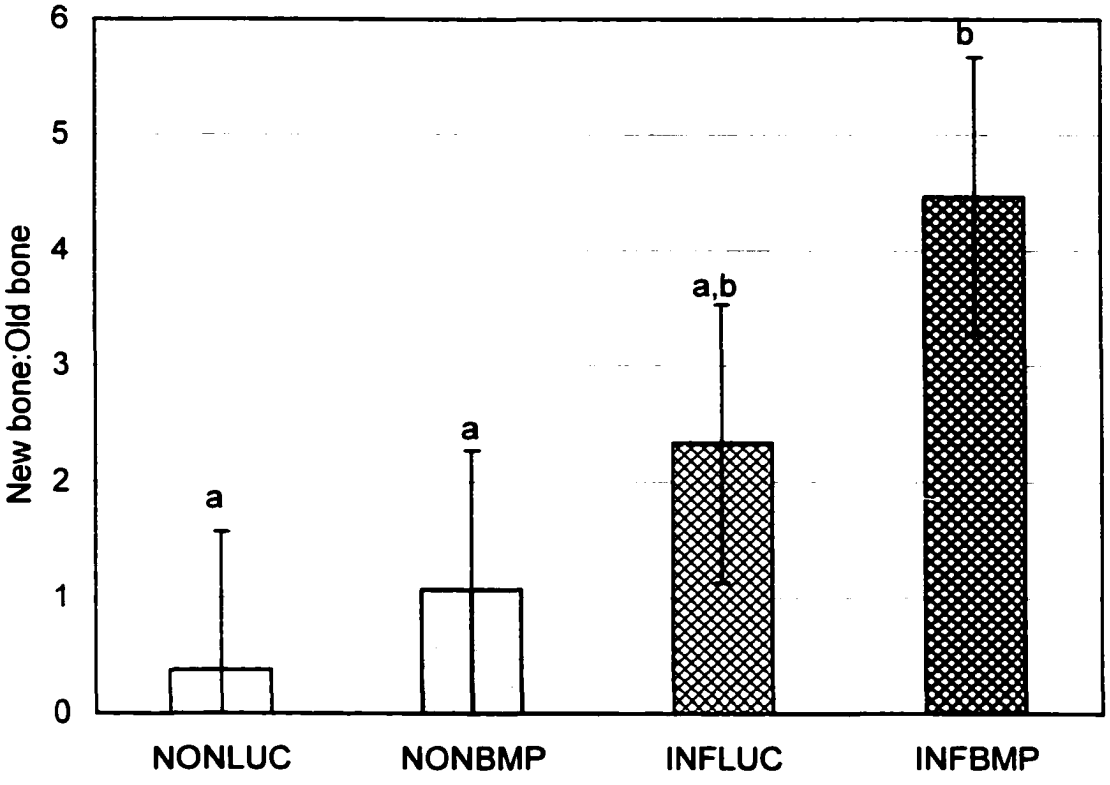

Figure 23. A plot showing the association between the quantitative histomorphometric ratio of new bone to old bone at 16 weeks and treatment group. The ratio of new bone to old bone is shown on the y-axis and the treatment group is shown on the x-axis. There was a trend for rabbits in the Ad-BMP-2 treated groups (NONBMP and INFBMP) to have a higher ratio of new bone to old bone compared to rabbits in theAd-LUC control groups (NONLUC and INFLUC). Data are represented as least squared means (LSM) +/- standard error (SE); different letters represent statistically significant differences.

The lack of defect ossification may have been a consequence of the use of the sclerosing agent that was used on the proximal and distal bone fragments. The sclerosing agent acts by disrupting cell membranes and causing cell death, which was confirmed histologically by a large number of empty lacunae in the bone as well as acellular and avascular tissue in the defect in the rabbits euthanized prior to 16 weeks. The poor vascularity of the defect early in the study was also confirmed by the pool phase scan of the nuclear scintigraphy study (Chapter 4). Therefore, the model in this study was particularly severe compared to previously used models.[62,63]

The sclerosing agent was used because in a pilot study rabbits inoculated with *S. aureus* healed the defect and resolved the infection despite the presence of a large defect and metallic implants. Because this was the first study evaluating the use of Ad-BMP-2 for enhancing healing in infected fractures, a non-union model was chosen to more definitively determine whether Ad-BMP-2 had a favorable response. An infected fracture model could have been chosen, where a sclerosing agent was not used, and the control defects were allowed to heal.

It is unknown whether the sclerosing agent actually damaged the adenoviral vector. The sclerosing agent was used 48-hours prior to treatment with Ad-BMP-2 to try to avoid vector damage. Alternatively, in addition to reducing the number of osteoprogenitor cells and blood vessels in the defect region, the sclerosing agent may have caused enough cell damage in the defect region that there were no cells for the virus to transduce. The latter explanation may be a limitation associated with *in vivo* gene transfer for treatment of fractures with severe tissue damage. This problem was

summarized by Stevenson and coworkers[65] in that "successful induction of bone requires at least one instructive inducer, a permissive substratum, and a population of responder cells." *Ex vivo* gene transfer would provide both BMP-2 as well as cells at the fracture site. The transduced cells would express BMP-2 and provide a source of osteoprogenitor cells. Researches using recombinant human BMPs have also recognized the benefits of treating fractures with either determined or inducible osteoprogenitor cells as well as BMP.[66]

An *in vivo* study in nude rats was performed to evaluate the effect of sodium morrhuate on ectopic bone formation following injection with Ad-BMP-2. The sodium morrhuate attenuated bone production by Ad-BMP-2 (Chapter 2). The results of the latter study did confirm that the Ad-BMP-2 was capable of producing an active protein and that the less than impressive results of the current study were not a result of damage to the adenoviral vector during transportation and handling. An *in vitro* study evaluating the effect of sodium morrhuate on the transduction efficiency of Ad-LacZ showed that transduction efficiency was not reduced following incubation of the adenoviral vector with sodium morrhuate. This suggested that cell loss was the most likely cause of the attenuated results (Chapter 2). Therefore, we propose that there were inadequate cells in the defect for the adenovirus to transduce, but the cells in the soft tissue adjacent to the defect were transduced and callus was formed predominantly adjacent to the defect.

The periosteum, endosteum, and marrow immediately adjacent to the fracture site are important sources of both growth factors and cells for fracture healing, and were removed in both our study and the study by Baltzer and coworkers.[42,53,62] Baltzer and coworkers[42] reported that the cells in the ends of the bone fragments adjacent to the

defect were transduced by the adenoviral vector. However, in that study,[42] a sclerosing agent was not used. The sclerosing agent damaged the tissue and cells on the end of the bone, removing a source of bone regeneration as well as cells for adenoviral transduction. The duration of expression of BMP-2 by cells in the ends of the bone fragments was 6 weeks, whereas cells in the soft tissue expressed the protein for only 3 weeks. The shorter duration of expression by the cells in the soft tissue adjacent to the defect may be one factor accounting for the less favorable response seen in our study compared to previous studies. In many clinical cases the bone ends adjacent to the fracture site are often damaged, therefore this may simulate some severe clinical cases.

The lack of vascularity most likely contributed to the lack of defect ossification. Vascularity and angiogenesis are essential for fracture healing. There is an intimate association between blood vessels and osteoblasts in both endochondral and intramembranous ossification and outlined in Chapter 1. Additionally, antiangiogenic agents have been shown to reversibly inhibit the biological activity of BMP-2.[67] The mechanism of inhibition was thought to be associated with a lack of angiogenesis impeding migration of both vessels and associated undifferentiated mesenchymal cells to the site of implantation, or direct inhibition of undifferentiated mesenchymal cells by the antiangiogenic agent.[67] While a direct comparison between the two studies is not possible, because the latter study inhibited neoangiogenesis of a collagen pellet containing rhBMP-2 and in our study there was no inhibition of neoangiogenesis but damage to the vessels by a sclerosing agent prior to treatment with Ad-BMP-2, the principle of inhibition of bone formation may be similar.

Despite the early avascularity, at 16 weeks the defect was well vascularized, particularly in infected rabbits, suggesting that between the time of early histological analysis and euthanasia at 16 weeks an extensive amount of neovascularization occurred. By this time, however, soft tissue had occupied the defect region and over expression of BMP-2 by the transduced cells would have ceased. The implications of these findings suggest that complicated fractures, with excessive bone, soft tissue, and vascular damage, may require a second treatment with Ad-BMP-2 or initial treatment with an angiogenic growth factor, such as vascular endothelial growth factor (VEGF), as well as BMP-2. There is a close relationship between VEGF and the BMPs, which is reflected in the intimate association between osteoblasts and vessels in fracture healing. Bone morphogenetic protein-7 was actually found to increase expression of VEGF *in vitro*, and inhibition of VEGF prevented the osteoinductive effects of BMP-7.[68] Therefore, use of the combination of BMP-2 and VEGF may further increase fracture healing.

Osteomyelitis causes resorption and necrosis of bone as outlined in Chapter 1; and recently, extracts of *S. aureus* and *S. epidermis* were found to cause a decrease in bone matrix formation *in vitro*.[69] While this may explain, in part, the lack of defect ossification in infected rabbits, it does not account for the lack of ossification in non-infected rabbits.

In other studies,[60-62] animals were treated with Ad-BMP-2 at the completion of surgery. In the current study, the rabbits were treated 48 hours after surgery, which may have not been the optimum time for treatment. Other studies using the recombinant human protein, however, have shown enhanced healing even in chronic fractures.[15] Therefore, the delay in treatment is not likely to be the cause of the attenuated response to Ad-BMP-2.

Biomechanical factors may have been important in the distribution of bone in this study.[30] Other studies have reported that Ad-BMP-2 enhances callus formation rather than defect ossification in unstable fractures, and that there was no increase in healing in stable fractures with treatment with BMP-2.[30] The fracture in our study was not rigid as indicated by the fact that several rabbits that did not form callus had plate bending. The most likely explanation for this is that these rabbits did not form adequate callus to stabilize the fracture, and, therefore, cycled the plate resulting in bending. The callus may have been laid down on the medial aspect because that was the site at which they were injected with Ad-BMP-2 or because that was the region requiring the most callus to stabilize the fracture. Yasko and coworkers[20] also reported eccentrically formed bone opposite to the plate and proposed that this was a result of either settling of the implant material in this location or was related to the mechanical environment of the defect-plate construct.

In a recent study by Chen and coworkers[32] evaluating the use of recombinant human BMP-7 for treatment of infected non-unions in rats, there was a large amount of external callus in the area opposite to the plate radiographically, and there was also less bone in the defect compared to adjacent to the defect. While the reasons for this were not addressed by the authors, it is possible that there was mechanical instability leading to more external callus formation than defect ossification. Alternatively, the carrier matrix may have actually inhibited defect healing as suggested by yet other authors.[30]

There was variability in the amount of callus formation in rabbits treated with Ad-BMP-2. While this may be a reflection of variability in injection technique because injections were performed percutaneously 48 hours after surgery, it may also be a

reflection of inherent variability between rabbits. Leiberman and coworkers[61] also reported that some rabbits did not heal the defect and that these rabbits were found to have less BMP-2 production compared to rabbits that did heal the defect, suggesting variability in BMP-2 protein production.

Other studies[17,23,30] have also found that while treatment with BMP-2 did not actually increase the amount of bone and cartilage, the rate of development of cortical union (bridging-callus) was accelerated. Similarly, in our study the actual amount of bone formation did not increase significantly based on radiography and histomorphology at 16 weeks, but rabbits treated with Ad-BMP-2 had earlier radiographic initial- and bridging-callus formation. Further, studies have shown that most of the response to BMP-2 occurs early in fracture healing.[17] Our study supports this previous finding in that there was no difference in histological analysis at 16 weeks; however, there was a trend for rabbits treated with Ad-BMP-2 to have more cartilage and new bone formation at 2 and 4 weeks after surgery compared to rabbits in the Ad-LUC control groups.

Rabbits in the Ad-LUC control groups appeared to have more defect ossification compared to rabbits in the Ad-BMP-2 treated groups. Although this may have been a random response based on a few outliers in the Ad-LUC control groups, it seems unlikely because similar trends were observed in both non-infected and infected rabbits. The explanation for this is difficult. The results may be real and reflect either biological or biomechanical events occurring at the fracture site. Possible causes include: (1) the adenovirus with the luciferase gene could have stimulated defect healing through the presence of a foreign protein causing bone proliferation, (2) rabbits in the Ad-LUC groups had less external callus formation and therefore a less stable fracture which may

have resulted in more defect ossification, or (3) the difference between groups may have been related to the smaller defect size at time 0 in the Ad-LUC control group. The variation in defect size at time 0 was not expected. Defects were maintained during surgery using a bone plate; however, angulation and tightening of the screws and weight-bearing may have caused a slight alteration in defect size. The effect of defect size on healing was evaluated and found not to be statistically significant.

It has been suggested that the increase in callus formation in response to treatment with BMP-2 is a result of an increase in the number of osteoprogenitor cells, because treatment with BMP-2 did not increase in mineral apposition or bone formation rate.[27] Because the cells in the soft tissue adjacent to the defect are transduced,[52,55,70] it is also possible that the BMP-2 may have caused chemotaxis of osteoprogenitor cells to the soft tissue adjacent to the defect and therefore there were fewer bone producing cells in the defect region for baseline bone production as observed in the Ad-LUC control rabbits. Therefore, the rabbits in the Ad-BMP-2 groups had more external callus and the rabbits in the Ad-LUC groups more defect ossification.

Our model is best described as a delayed- or non-union rather than a critical sized defect (CSD) model, because several rabbits in the control groups healed the defect, there was more than 10% ossification in the defect in many animals, the periosteum, endosteum, and marrow were removed, and a sclerosing agent was used on the ends of the bone to prevent healing (Chapter 1). While a CSD may have reduced the variability in bone healing and prevented rabbits in the Ad-LUC control groups from healing the defect, the use of true CSD in the current study would most likely result in an increase in the number of rabbits with bone-implant failure.

Skeletally mature animals were used because of the improved ability of young animals to heal. Although the rabbits in our study were skeletally mature, based on growth plate closure rather than body weight; the results of serum bone marker concentration suggest that the rabbits may have been somewhat immature (Chapter 5). This may have accounted for variability in fracture healing, and defect healing by animals in the Ad-LUC groups. Using more mature rabbits, however, may have resulted in the bone fracturing through the screw holes.

Although radiographic evaluation suggests that rabbits treated with Ad-BMP-2 had increased external callus healing, this was not supported by histomorphometric analysis. The plate was left in place during section preparation and as a result the sections were difficult to cut, and grinding was uneven resulting in considerable loss of tissue adjacent to the defect (Figure 24). As a result, histomorphometric analysis was a measure of the bone in the defect and close to the bone plate rather than the soft tissue callus. Further, histomorphometric analysis was performed at 16 weeks only. Rabbits that were euthanized prior to completion of the study (2 and 4 weeks) were also evaluated histologically, and there was a trend for rabbits treated with Ad-BMP-2 to have a higher grade for new bone formation and cartilage at these earlier time points suggesting, as expected from previous studies, that the main effect of BMP-2 was early in the course of fracture healing. Further, radiographic evaluation considered the amount of bone as well as the density and the direction of bone formation (bridging versus not bridging), whereas the other methods evaluated only the presence and amount of bone. For example, rabbits with a grade-4 callus not only had a lot of callus formation but the callus was dense and bridging the defect. Finally, the difference between infected Ad-LUC control and Ad-

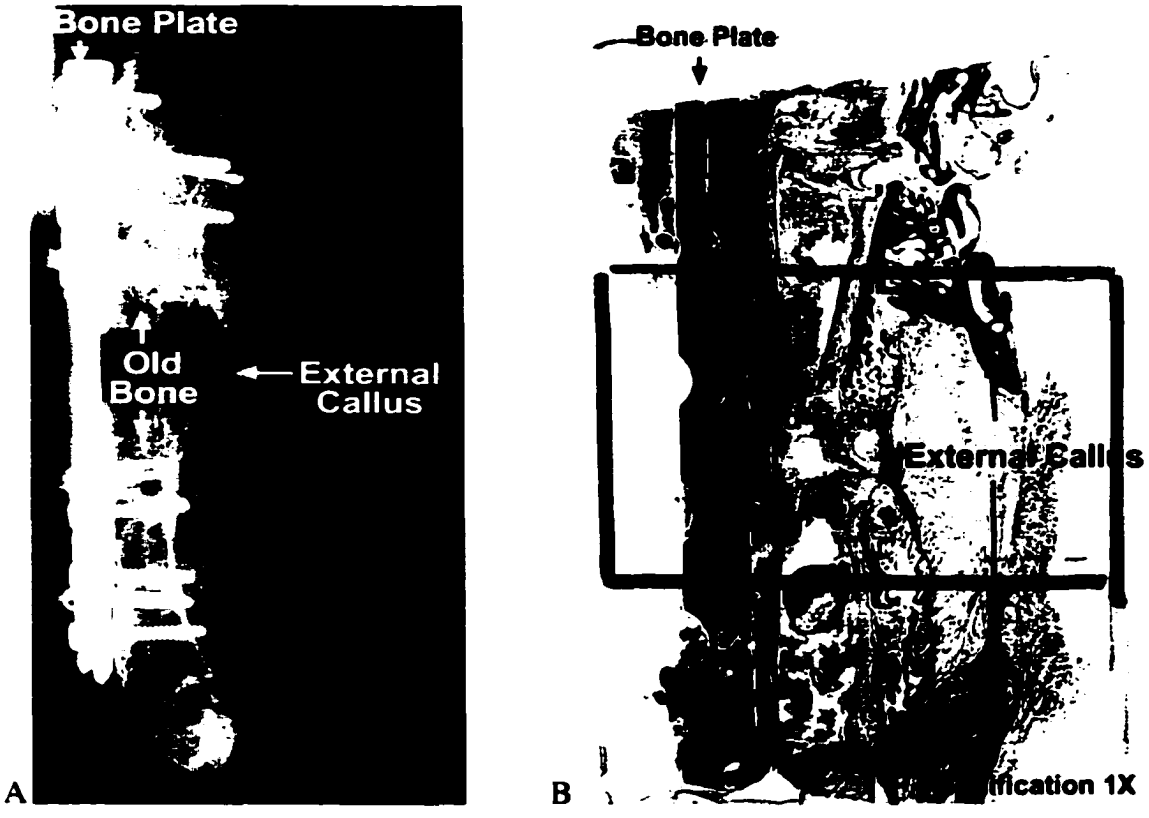

Figure 24. A craniocaudal radiograph (A) and undecalcified histological section (B) at 16 weeks illustrating the disparity between radiographs and histological sections with regard to external callus (soft tissue and periosteal callus). The soft tissue callus was lost during grinding of the sections because of the plate was more difficult to grind than the tissue, therefore grinding was uneven.

BMP-2 treated was difficult to distinguish based on the amount of new bone only, because of the large proliferative response generated by the presence of infection. Therefore, the location and direction of external callus formation was only taken into consideration in the radiographic grades.

There is also considerable variability between previous studies[16,17] in the type of tissue in the fracture defect following treatment with BMPs. This has been attributed to the dose of BMP, the type of BMP, and the stage of healing at which the tissue was evaluated. Therefore, the lack of difference histologically between groups in our study at 16 weeks is most likely a result of the stage of healing, because the Ad-BMP-2 treated rabbits had more cartilage and new bone formation earlier compared to rabbits in the Ad-LUC control groups.

Using DEXA analysis, BMD was only detected in the region adjacent to the defect in the Ad-BMP-2 treated rabbits, which supports the radiographic findings of an increase in soft tissue and periosteal callus formation in the Ad-BMP-2 treated rabbits. Rabbits in the infected groups had an increase in BMD in the defect ROI which was most likely a result of the proliferative response in infected rabbits as well as almost complete defect ossification in a few rabbits in the infected Ad-LUC control group.

Biomechanical testing was not performed in this study because a large number of rabbits were euthanized and the rabbits in the non-infected and infected groups did not heal the fracture defect as anticipated, therefore it was decided to perform histological analyses only. Other studies,[23] however, have found that while animals in the control groups may heal the fracture, the animals in the BMP treated groups had a stronger repair because of an increase in the maturity of the newly formed bone. In future studies

evaluating fracture healing in infected non-unions, biomechanical testing should be performed.

Interestingly, previous studies[54,57] have reported an attenuation of bone formation in immunocompetent animals. The inflammatory response and the non-specific immunity at the fracture site may have also resulted in an early neutralization of the adenoviral vector and an attenuation of the BMP-2 response in our model. The sclerosing agent, the presence of dead tissue, and bacteria may have all contributed to an increase in inflammation. However, the histological inflammatory grade in non-infected rabbits was minimal at 16 weeks and there were only three non-infected rabbits euthanized at 2 and 4 weeks and only one of these rabbits had an inflammation grade above 0 (2/4). Therefore, while inflammation in the infected rabbits could have limited the expression of BMP-2, the role of inflammation in the non-infected rabbits was difficult to determine from this study.

Rabbits in the non-infected Ad-LUC control group had significantly more cartilage at 16 weeks compared to rabbits in the other groups. These rabbits also had the least amount of new bone formation. Therefore, the presence of cartilage may have been an indication of the immaturity of the healing response.

Rabbits in the infected Ad-LUC control group had a higher radiographic lysis grade at 16 weeks. The higher lysis grade was also supported by Ad-BMP-2 treated rabbits having a trend for a higher BMD in the proximal fragment, and Ad-LUC control rabbits having more necrosis and inflammation histologically compared to rabbits in the Ad-BMP-2 treated group. This may have been a result of the BMP-2 increasing vascularity and forming new bone, which replaced the old bone. The increase in

vascularity may be supported by an increase in uptake ratio of the femur with the Tc-CIPRO scan despite there being no increase in uptake ratio in the pool phase scan (Chapter 4) in rabbits treated with Ad-BMP-2. One study[15] evaluating the effect of rhBMP in a carrier matrix on fracture healing found that the presence of BMP resulted in less inflammation compared to controls. The mechanism of the reduced inflammation is unknown, but may be a result of an increase in angiogenesis early in fracture healing. While one author[71] has suggested that one of the target cells for the BMPs are pericytes and that BMPs are angiogenic, others authors have not supported this suggestion.[20] It was difficult to assess the role of angiogenesis in our study because there were inadequate measurements early in the study. Interestingly, rabbits in the infected Ad-BMP-2 treated group had a higher concentration of deoxypyridinoline crosslinks (DPYR) at 4 weeks compared to rabbits in the Ad-LUC control groups, and then the DPYR concentration decreased in the infected Ad-BMP-2 group compared to the infected Ad-LUC group (Chapter 5). Although the explanation for this is unknown, it is possible that there was a greater blood flow to the femur of the rabbits in the infected Ad-BMP-2 group compared to the infected Ad-LUC control group earlier in the course of fracture healing, and the increase in blood flow caused both an increase in the release of DPYR into the circulation as well as removal of the necrotic tissue and degraded bone. However, there was only a slight and insignificant increase in the markers of bone formation (osteocalcin and bone-specific alkaline phosphatase) in the Ad-BMP-2 treated rabbits (Chapter 5). One study[72] also reported an increase in bone resorption associated with BMP-2 through direct stimulation of osteoclast formation and activation. In our study, BMP-2 may have stimulated an early resorption of damaged bone followed by new bone formation, which

accounted for the increase in DPYR at 4 weeks and lower grade for radiographic bone lysis at 16 weeks.

Non-infected rabbits in the Ad-BMP-2 treated group had significantly more fat in the defect compared to Ad-BMP-2 control rabbits and a similar trend was observed in the infected rabbits. There was also a negative correlation between the amount of fat and the amount of new bone. Although this was initially thought to be an random finding attributable to chance, other studies[73-75] have found that BMP-2 causes some mesenchymal cell lines (3T3-F442A and C3H10T1/2) to differentiate into both adipocytes and osteoblasts. Some authors[73] concluded that this effect of BMP-2 may explain the inverse correlation between trabecular bone volume and fat volume in the bone marrow cavity, hence supporting our findings. Further, low concentrations of BMP-2 were found to favor differentiation into adipocytes and high concentrations into chondrocytes and osteoblasts.[74] We propose that there may have been a lower concentration of BMP-2 in the fracture defect as a result of a reduced transduction rate and that this may be one reason for the lack of defect ossification and the higher percentage of fat in Ad-BMP-2 treated rabbits. This may have important implications for use of Ad-BMP-2 for enhancing healing of complicated fractures and requires further investigation. In contradiction to this theory, another study[76] found that human fat cells were capable of being transduced with the BMP-2 gene and produced bone at a faster rate than bone marrow cells. While the latter study suggests that Ad-BMP-2 may be useful for treatment of non-unions associated with soft tissue interposition in the fracture defect, this would require a second treatment with Ad-BMP-2. Coordination of the concentration

of BMP-2 and type of cells or tissue in the defect is obviously important to prevent the formation of a non-union associated with soft tissue interposition.

A recent report has found that sonic hedgehog, which is an upstream regulator of BMP-2 and capable of *de novo* bone formation through its effects on BMP-2, may actually suppress the expression of the BMP-2 induced fat-cell phenotype and promote the osteoblastic phenotype.[75] Such proteins may be an alternative to the use of BMPs in fracture healing.

The presence of soft tissue in the defect is an important cause of non-union in human patients,[77,78] and the presence of soft tissue between the fracture fragments has been shown experimentally to produce a non-union.[78] Interposition of muscle and formation of fat may have been the cause of failure of defect ossification in our study. Several (5/13) rabbits euthanized prior to 16 weeks had muscle and fat at the fracture site as early as 3 weeks after surgery. Rabbits with soft tissue in the defect were both infected and non-infected as well as rabbits in Ad-BMP-2 treated and Ad-LUC control groups. It was difficult to ascertain using the 16-week samples whether the fat was encroaching into the defect from the muscle or from the bone marrow, but the early samples (less than 4 weeks) showed muscle in the defect suggesting that the source of the fat was from the surrounding soft tissue. Studies[28,29,79-82] have clearly demonstrated that the use of a porous polymeric membrane enhances fracture healing in non-union models, the hypothesis being that it prevents soft tissue interposition in the fracture defect and optimizes the association between the surrounding soft tissue and the fracture site. Other studies using gene therapy to enhance fracture healing have not reported complications

associated with soft tissue interposition in the defect and the role of gene therapy in this area of impaired fracture healing requires further investigation.

The ability of cells to differentiate into osteo- and chondroprogenitor cells is species dependent, with marrow stromal cells, muscle-derived pericytes, and embryonic myoblasts being capable of differentiation in rodents, and marrow stromal cells being more inducible in non-human primates.[83] The ability of various mammalian species to heal fractures is also proportional to their location on the phylogenetic scale.[71] Therefore, while initial pilot studies should be performed in lower vertebrates the variation in fracture healing and slower healing in higher vertebrates emphasize the importance of performing studies in the target species.

In conclusion, the results of this study indicate that Ad-BMP-2 may be useful for enhancing healing in the presence of infection; however, the use of *in vivo* transduction of Ad-BMP-2 may have limitations in complicated fractures when there is a large amount of damage to the soft tissue, vasculature, and bone. Further studies comparing *in vivo* and *ex vivo* transduction as well as other growth factors such as vascular endothelial growth factor are required.

References

1. Auer JA. Watkins JP. Treatment of radial fractures in adult horses: An analysis of 15 clinical cases. Equine Vet J 1987; 19: 103-110.
2. Sanders-Shamis M. Bramlage LR. Gable AA. Radius fractures in the horse: A retrospective study of 47 cases. Equine Vet J 1986; 18:432-437.
3. Crawford WH. Fretz PB. Long bone fractures in large animals. A retrospective study. Vet Surg 1985; 14:295-302.
4. Hance SR. Bramlage LR. Schneider RK. Embertson RM. Retrospective study of 38 cases of femur fractures in horses less than one year of age. Equine Vet J 1992; 24:357-363.
5. Yelin E. Callahan LF. The economic cost and social and psychological impact of musculoskeletal conditions. Arthritis Rheum 1995; 38:1351-1362.
6. Praemer A. Furner S. Rice DP. Musculoskeletal conditions in the United States. Park Ridge IL. Am Acad Orthop Surg 1992. p85-124.
7. Johnson EE. Urist MR. Finerman AM. Resistant nonunion and partial or complete segmental defects of long bones. Clin Orthop Rel Res 1992; 277:229-237.
8. Ducharme NG. Nixon AJ. Delayed Union. Non-Union. and Malunion. In Nixon AJ: Equine Fracture Repair. Philadelphia. WB Saunders Co.. 1996. p 354-358.
9. Jingushi S. Hydemann A. Kana SK. Macey LR. Bolander ME. Acidic fibroblast growth factor (aFGF) injection stimulates cartilage enlargement and inhibits cartilage gene expression in rat fracture healing. J Orthop Res 1990; 8:364-371.
10. Joyce ME. Heydemann A. Bolander ME. Platelet-derived growth factor regulates the initiation of fracture repair. Orthop Trans 1990; 14:363.

11. Joyce MC, Jingushi S, Bolander ME. Transforming growth factor-B in the regulation of fracture repair. Orthop Clin N Am 1990; 21:199-209.

12. Lind M, Schumacker B, Soballe K, Keller J, Melsen F, Bunger C. Transforming growth factor-ß enhances fracture healing in rabbit tibiae. Acta Orthop Scand 1993; 64:553-556.

13. Nielsen HM, Andreassen TT, Ledet T, Oxlund H. Local injection of TGF-ß increases the strength of tibial fractures in the rat. Acta Orthop Scand 1994; 65:37-41.

14. Heckman JD, Boyan DB, Aufdemorte TB, Abbott JT. The use of bone morphogenetic protein in the treatment of nonunion in a canine model. J Bone Joint Surg 1991; 73A:750-764.

15. Heckman JD, Ehler W, Brooks BP, Aufdemorte TB, Lohmann CH, Morgan T, Boyan BD. Bone morhpogenetic protein but not transforming growth factor-beta enhances bone formation in canine diaphyseal nonunions implanted with a biodegradable composite polymer. 1999; 81A:1717-1729.

16. Zegzula HD, Buck DC, Brekke J, Wozney JM, Holllinger JO. Bone formation with use of rhBMP-2 (recombinant human bone morphogenetic protein-2). J Bone Joint Surg 1997; 79A:1778-1790.

17. Blokhuis TJ, den Boer FC, Bramer JAM, Jenner JMG, Bakker FC, Patka P, Haarman HJThM. Biomechanical and histological aspects of fracture healing stimulated with osteogenic protein –1. Biomaterials 2001; 22:725-730.

18. Ohura K, Hamanishi C, Tanaka S, Matsuda N. Healing of segmental bone defects in rats induced by a β-TCP-MCPM cement combined with rhBMP-2. J Biomed Mater Res 1999; 44:168-175.

19. Bostrom M, Lane JM, Tomin E, Browne M, Berberian W, Turek T, Smith J, Wozney J, Schildhauer T. Use of bone morphogenetic protein-2 in the rabbit ulna nonunion model. Clin Orthop Rel Res 1996; 327:272-282.

20. Yasko AW, Lane JM, Fellinger EJ, Rosen V, Wozney JM, Wang EA. The healing of segmental bone defects induced by recombinant human bone morphogenetic protein (rhBMP-2). J Bone Joint Surg 1992; 74A:659-670.

21. Cook SD, Baffes GC, Wolfe MW, Sampath TK, Rueger DC, Whitecloud TS. The effect of recombinant human osteogenic protein-1 on healing of large segmental bone defects. J Bone Joint Surg 1994; 76A:827-838.

22. Cook SD, Baffe SGC, Wolfe MW, Sampath TK, Rueger DC. Recombinant human bone morphogenetic protein-7 induces healing in a canine long-bone segmental defect model. Clin Orthop Rel Res 1994; 301:302-312.

23. Cook SD, Wolfe MW, Salkeld SL, Rueger DC. Effect of recombinant human osteogenic protein-1 on healing of segmental defects in non-human primates. J Bone Joint Surg 1995; 77A:734-750.

24. Welch RD, Jones AL, Bucholz RW, Reinert CM, Tjia JS, Pierce WA, Wozney JM, Li XJ. Effect of recombinant human bone morphogenetic protein-2 on fracture healing in a goat tibial fracture model. J Bone Min Res 1998; 13:1483-1490.

25. Nilsson OS, Urist MR, Dawson EG, Schmalzried TP, Finerman GAM. Bone repair induced by bone morphogenetic protein in ulnar defects in dogs. J Bone Joint Surg 1986; 68B:635-642.

26. Geehart TN, Kirker-Head CA, Kriz MJ, Holtrop ME, Hennig GE, Hipp J, Schelling SH, Wang E. Healing segmental femoral defects in sheep using recombinant human bone morphogenetic protein. Clin Orthop Rel Res 1993; 293:317-326.

27. Kirker-Head CA, Gerhart TN, Schelling SH, Hennig GE, Wang E, Holtrop ME. Long-term healing of bone using recombinant human bone morphogenetic protein 2. Clin Orthop Rel Res 1995; 318:222-230.

28. Zellin G, Linde A. Treatment of segmental defects in long bones using osteopromotive membranes and recombinant human bone morphogenetic protein-2. Scand J Plast Reconstr Hand Surg 1997;31:97-104.

29. Linde A, Hedner E. Recombinant bone morphogenetic protein-2 enhances bone healing, guided by osteopromotive e-PTFE membranes: An experimental study in rats. Calcif Tissue Int 1995; 56:549-553.

30. Bax BE, Wozney JM, Ashhurst DE. Bone morphogenetic protein-2 increases the rate of callus formation after fracture of the rabbit tibia. Calcif Tissue Int 1999; 65:83-89.

31. Lee FY, Hazan EJ, Trahan C, Snyder B, Gebhardt MC, Mankin HJ. Bone morphogenetic protein (BMP-2) can initiate and the conduct repair process at the allograft osteotomy site in an animal experimental model. Proc 45th Ann Mtg Orthop Res Soc 1999; p 620.

32. Chen X, Kidder LS, Lew WD. Osteogenic protein-1 induced bone formation in an infected segmental defect in the rat femur. J Orthop Res 2002; 20:142-150.

33. Johnson EE, Urist MR. One-stage lengthening of femoral nonunion augmented with human bone morphogenetic protein. Clin Orthop Rel Res 1998; 347:105-116.

34. Johnson EE, Urist MR, Finerman AM. Resistant non-union and partial or complete segmental defects of long bones. Clin Orthop Rel Res 1992; 277:229-237.

35. Johnson EE, Urist MR, Finerman AM. Distal metaphyseal tibial nonunion. Clin Orthop Rel Res 1990; 250:234-240.

36. Bulstra SK, Geesink RGT, Hoefnagels NHM. Osteogenic activity of OP-1, bone morphogenetic protein-7 (BMP-7), in a human fibular defect model. Proc 45th Ann Mtg Orthop Res Soc 1999; p 62.

37. Meng-Hai B, Xing-Yan L, Bao-Feng G, Chao Y, Dong-An C. An implant of a composite of bovine bone morphogenetic protein and plaster of Paris for treatment of femoral shaft nonunions. Int Surg 1996; 81:390-392.

38. Kasperek C, Wergedal JE, Mohan S. Interaction of growth factors present in bone matrix and bone cells: effects of DNA synthesis and alkaline phosphatase. Growth Factors 1990; 3:147-155.

39. Bonewald LF, Mundy GR. Role of transforming growth factor-beta in bone remodeling. Clin Orthop Rel Res 1990; 250:261-276.

40. Canalis E, McCarthy TL, Centrella M. Effects of platelet-derived growth factor on bone formation in vitro. J Cell Physiol 1989; 140:530-537.

41. Canalis E, Centrella M, McCarthy T. Effects of basic fibroblast growth factor on bone formation in vitro. J Clin Invest 1988; 81:1572-1577.

42. Baltzer AWA, Latterman C, Whalen JD, Ghivizzani S, Wooley P, Krauspe R, Robbins PD, Evans CH. Potential role of direct adenoviral gene transfer in enhancing fracture repair. Clin Orthop Rel Res 2000; 379S:S120-S125.

43. Wang EA, Rosen V, D'Alessandro JS, Bauduy M, Cordes P, Harada T, Isael DI, Hewick RM, Kerns KM, LaPan P, Luxenberg DP, McQuaidD, Moutsatsos IK, Nove J, Wozney JM. Recombinant human bone morphogenetic protein induces bone formation. Proc Natl Acad Sci USA 1990; 87:2220-2224.

44. Bostrom MPG, Lane JM, Berberian WS, Missri AA, Tomin E, Weiland A, Doty SB, Glaser D, Rosen VM. Immunolocalization and expression of bone morphogenetic proteins 2 and 4 in fracture healing. J Orthop Res 1995; 13:357-367.

45. Kirker-Head CA. Recombinant bone morphogenetic proteins: Novel substances for enhancing bone healing. Vet Surg 24:8-419, 1995.

46. Schmitt JM, Hwang K, Winn SR, Hollinger JO. Bone Morphogenetic Proteins: An update on basic biology and clinical relevance. J Orthop Res 1999; 17:269-278.

47. Yan J, Lianjia Y, White FH. An immunocytochemical study of bone morphogenetic protein in experimental fracture healing of the rabbit mandible. Chin Med Sci J 1994; 9:91-95.

48. Lianjia Y, Yan J. Immunohistochemical observations on the bone morphogenetic protein in normal and abnormal conditions. Clin Orthop Rel Res 1990; 257:249-256.

49. Si XH, Jin Y, Yang LJ, Tipoe GL, White FH. Expression of BMP-2 and TGF-B1 mRNA during healing of the rabbit mandible. Eur J Oral Sci 1997; 105:325-330.

50. Howard BK, Brown KR, Leach JL, Chang CH, Rosenthal DI. Osteoinduction using bone morphogenic protein in irradiated tissue. Arch Otolaryngol Head Neck Surg 1998; 124:985-988.

51. Jain KK. Gene therapy for diseases of bones and joints. In Jain (Ed) Textbook of Gene Therapy. Hogrefe & Huber Publishers, Seattle, 1998; p 281-284.

52. Sandell LJ. Genes and gene expression. Clin Orthop Rel Res 2000; 379S:S9-S16.

53. Baltzer AWA, Lattermann C, Whalen JD, Braunstein S, Robbins PD, Evans CH. A gene therapy approach to accelerating bone healing. Knee Surg, Sports Traumatol, Arthrosc 1999; 7:197-202.

54. Musgrave DS, Bosch P, Ghivizzani S, Robbins PD, Evans CH, Huard J. Adenovirus-mediated direct gene therapy with bone morphogenetic protein-2 produces bone. Bone 1999; 24:541-547.

55. Spector JA, Mehrara BJ, Luchs JS, Geenwald JA, Fagenholz PJ, Saadeh PB, Steinbrech DS, Longaker MT. Expression of adenovirally delivered gene products in healing osseus tissues. Ann Plast Surg 2000; 44:522-528.

56. Lou J, Xu F, Merkel K, Manske P. Gene therapy: Adenovirus-mediated human bone morphogenetic protein-2 gene transfer induces mesenchymal progenitor cell

proliferation and differentiation in vitro and bone formation *in vivo*. J Orthop Res 1999; 17:43-50.

57. Alden TD, Pittman DD, Hankins GR, Beres EJ, Engh JA, Das S, Hudson SB, Kerns KM, Kallmes DF, Helm GA. *In vivo* endochondral bone formation using a bone morphogenetic protein 2 adenoviral vector. Human Gene Ther 1999; 10:2245-2253.

58. Laurencin CT, Attawia MA, Lu LQ, Borden MD, Lu HH, Gorum WJ, Lieberman JR. Poly (lactide-co-glycolide)/hydroxyapatite delivery of BMP-2-producing cells: a regional gene therapy approach to bone regeneration. Biomater 2001; 22:1271-1277.

59. Goldstein SA, Bonadio J. Potential role for direct gene transfer in the enhancement of fracture healing. Clin Orthop Rel Res 1998; 355S:S154-S162.

60. Fang J, Zhu Y-Y, Smiley E, Bonadio J, Rouleau JP, Goldstein SA, McCauley LK, Davidson BL, Roessler BJ. Stimulation of new bone formation by direct transfer of osteogenic plasmid genes. Natl Acad Sci USA 1996; 93:5753-5758.

61. Lieberman JR, Daluiski A, Stevenson S, Wu L, McAllister P, Lee YP, Kabo JM, Finerman GAM, Berk A, Witte ON. Regional gene therapy with a BMP-2 producing murine stromal cell line induces heterotopic and orthotopic bone formation in rodents. J Orthop Res 1998; 16:330-339.

62. Baltzer AWA, Lattermann C, Whalen JD, Wooley P, Weiss K, Grimm M, Ghivizzani SC, Robbins PD, Evans CH. Genetic enhancement of fracture repair: Evaluation of Ad-BMP-2 in a lapine femoral defect model. Gene Ther 2000; 7:734-739.

63. Niyibizi C, Baltzer A, Lattermann C, Oyama M, Whalen JD, Robbins PD, Evans CH. Fracture Healing Enhancement: Potential role for gene therapy in the enhancement of fracture healing. Clin Orthop Rel Res 1998; 355S:S148-153.

64. Gazit D, Tugeman G, Kelley P, Wang E, Jalenak M, Zilberman Y, Moutsatsos I. Engineered pluripotent mesenchymal cells integrate and differentiate in regenerating bone: A novel cell-mediated gene therapy. J Gene Med 1999; 1:121-133.

65. Stevenson S, Cunningham N, Toth J, Davy D, Reddi AH. The effect of osteogenin (a bone morphogenetic protein) on the formation of bone in orthotopic segmental defects in rats. J Bone Joint Surg 1994; 76A:1676-1687.

66. Kirker-Head CA. Recombinant bone morphogenetic proteins: Novel substances for enhancing fracture healing. Vet Surg 1995; 24:408-419.

67. Mori S, Yshikawa H, Hashimoto J, Ueda T, Funai H, Kato M, Takaoka K. Antiangiogenic agent (TNP-470) inhibition of ectopic bone formation induced by bone morphogenetic protein-2. Bone 1998; 22:99-105.

68. Yeh LC, Lee JC. Osteogenic protein-1 increases gene expression of vascular endothelial growth factor in primary cultures of fetal rat calvaria cells. Molecular Cellular Endocrin 1999; 153:113-124.

69. Lerner UH, Sundqvist G, Ohlin A, Rosenquist JB. Bacteria inhibit biosynthesis of bone matrix proteins in human osteoblasts. Clin Orthop Rel Res 1998; 346:244-254.

70. Mehrara BJ, Saadeh PB, Steinbrech DS, Dudziak M, Spector JA, Greenwald JA, Gittes GK, Longaker MT. Adenovirus-mediated gene therapy of osteoblasts in vitro and in vivo. J Bone Min Res 1999; 14:1290-1301.

71. Urist MR. Bone morphogenetic protein, bone regeneration, heterotopic ossification and the bone-bone marrow consortium. In Peck WA (Ed): Bone and Mineral Research Annual. No 6. Amsterdam, Elsevier, 1989, p 57-112.

72. Kanatani M, Sugimoto T, Kaji H, Kobayashi T, Nishiyama K, Fukase M, Kumegawa M, Chihara K. Stimulatory effect of bone morphogenetic protein-2 on osteoclast-like cell formation and bone-resorbing activity. J Bone Min Res 1995; 10:1681-1690.

73. Ji X, Chen D, Xu C, Harris SE, Mundy GR, Yoneda T. Patterns of gene expression associated with BMP-2-induced osteoblast and adipocyte differentiation of mesenchymal progenitor cell 3T3-F442A. J Bone Min Metab 2000; 18:132-139.

74. Wang EA, Isreal DI, Kelly S, Luxenberg DP. Bone morphogenetic protein-2 causes commitment and differentiation in C3H10T1/2 and 3T3 cells. Growth Factors 1993; 9:57-71.

75. Zehentner BK, Leser U, Burtscher H. BMP-2 and sonic hedgehog have contrary effects on adipocyte-like differentiation of C3H10T1/2 cells. DNA & Cell Biol 2000; 19:275-281.

76. Dragoo JL, Lieberman JR, Choi J, Zuk PA, Zhang J, Hedrick MH, Huang J, Benhaim P. Bone induction of genetically manipulated stem cells derived from human fat. Proc 48th Ann Mtg Orthop Res Soc 2002; p 0021.

77. Milgram JW. Nonunion and pseudoarthrosis of fracture healing. Clin Orthop 1991; 268:203-213.

78. Fujita M. Matsui N. Tsunoda M. Saura R. Establishment of a non-union model using muscle interposition without osteotomy in rats. Kobe J Med Sci 1998; 44:217-233.

79. Shibi L. Zijun Z. Jifang W. Guided bone regeneration in long bone. An experimental study. Chinese Med J 1996; 109:551-554.

80. Gugala Z. Gogolewski S. Regeneration of segmental diaphyseal defects in sheep tibiae using resorbable polymeric membranes: A preliminary study. J Orthop Trauma 1999; 13:187-195.

81. Meinig RP. Rahn B. Perren S. Gogolwski S. Bone regeneration with resorbable polymeric membranes: Treatment of diaphyseal bone defects in the rabbit radius with poly (l-lactide) membrane. A pilot study. J Orthop Trauma 1996; 10:178-190.

82. Pineda LM. Büsing M. Meinig RP. Gogolewski S. Bone regeneration with resorbable polymeric membranes. III. Effect of poly (l-lactide) pore size on the bone healing process in large defects. J Biomed Mater Res 1996; 31:385-394.

83. Lindholm TS. Urist MR. A quantitative analysis of new bone formation by induction in composite grafts of bone marrow and bone matrix. Clin Orthop Rel Res 1980; 150:288-300.

CHAPTER 4

EVALUATION OF NUCLEAR SCINTIGRAPHY FOR EARLY DIAGNOSIS OF NON-UNION AND INFECTED NON-UNION

Abstract

Objective: The objective of this study was to evaluate the use of nuclear scintigraphy using technetium-labeled phosphate (Tc-PO) and ciprofloxacin (Tc-CIPRO) for assessing fracture healing and for early diagnosis of osteomyelitis. Our hypothesis was that the uptake ratio for the Tc-CIPRO scan would be higher in infected compared to non-infected rabbits, and that the uptake ratio for the Tc-PO scan would be higher for rabbits that healed compared to rabbits that developed a non-union.

Materials and Methods: Thirty-two skeletally mature New Zealand White rabbits were used. This study was part of a study evaluating the use of adenoviral transfer of the bone morphogenetic-2 gene (Ad-BMP-2) for enhancing fracture healing in an infected non-union model. A rabbit femoral fracture defect stabilized with bone plates and cortical screws was used. Experimental groups were: (1) non-union Ad-Luciferase (LUC) control, (2) non-union Ad-BMP-2 treated, (3) infected non-union Ad-LUC control, and (4) infected non-union Ad-BMP-2 treated. Nuclear scintigraphy was performed 4, 8, 12, and 16 weeks after surgery. The Tc-CIPRO scan was performed 48 hours after the Tc-PO scan. The uptake ratio of the experimental limb to normal bone was calculated using multiple regions of interest. Radiographic external callus and lysis grade at 16 weeks were used in the analysis. Data were analyzed using an ANOVA and Pearson's Correlation. The level of significance was $p<0.05$.

Results: Overall infected rabbits had a higher uptake ratio for both Tc-PO and Tc-CIPRO scans compared to non-infected rabbits. Tc-PO was able to differentiate infected from non-infected fractures late in healing. Although Tc-CIPRO was better than Tc-PO at identifying infection, there was a high incidence of false positive and negative results.

There was an association between Tc-PO uptake ratio and callus formation and a correlation between Tc-PO uptake ratio and defect ossification after 4 weeks.

Conclusions: Nuclear scintigraphy (Tc-PO and –CIPRO) may be useful to diagnose postoperative osteomyelitis late in fracture healing; however, false positive and false negative results occur frequently. The use of Tc-PO may be useful for evaluating fracture healing. Serial scans will most likely be more useful than a single scan at one point in the healing process. Future clinical studies, with evaluation earlier in the course of fracture healing, are needed to further evaluate these imaging modalities.

Introduction

Non-union and infected non-union are devastating complications following fracture repair in both veterinary[1-4] and human[5-7] medicine. Early treatment may lead to a favorable outcome; however, early diagnosis of impaired fracture healing and osteomyelitis is critical for early treatment intervention. Methods that are used to diagnose impaired healing and osteomyelitis include history, physical, and laboratory findings, radiography, ultrasonography, computerized tomography (CT), and magnetic resonance imaging (MRI). History, physical examination, and laboratory findings are not sensitive or specific for assessing healing and diagnosing osteomyelitis[8] and imaging techniques are, therefore, used.

Radiography is the most commonly used imaging modality for evaluating fracture healing and osteomyelitis, but it is not sensitive.[9,10] Ultrasound can be used to diagnose osteomyelitis by detecting abnormal fluid accumulation immediately adjacent to the bone, but these changes are not specific for osteomyelitis associated with fracture and surgical repair.[10] While CT is sensitive for early diagnosis of acute hematogenous osteomyelitis,[10] anatomical alterations associated with fracture and surgery reduce the specificity, and metallic implants create artifact that may obscure the fracture site.[10] Magnetic resonance imaging provides good soft tissue images but does not provide adequate detail of cortical bone,[11] and because of the strong magnetic field MRI should not be used with metallic implants. Both CT and MRI are expensive, currently require general anesthesia for veterinary patients, and not readily available for large animal applications. While these techniques provide high quality anatomical information, trauma, surgery, and implants alter the normal anatomy, making interpretation difficult.

Nuclear scintigraphy, which evaluates physiological rather than anatomical changes,[12] may be better than these techniques for assessing fracture healing.

While nuclear scintigraphy has been used in the assessment of bone diseases for over thirty years, the traditionally used radionuclides had limitations that prohibited their routine clinical use. [13-22] The use of technetium-99m labeled phosphates (Tc-PO) has overcome many of these limitations. Technetium-PO accumulates in areas of rapid bone turnover,[25,26] has a high sensitivity for bone disease, good image quality, is inexpensive, simple to prepare, and widely available.[10] Technetium has a short half-life and does not emit beta radiation, resulting in a low level of radiation delivered to the patient and allows for a higher dose of Tc. The higher allowed dose and the decay characteristics (monochromatic gamma rays) produce a good quality image. Technetium is not protein bound resulting in faster blood clearance. Patients can therefore be scanned 2 to 3 hours postinjection.[22-24] Technetium-PO has been shown to be useful for evaluating fracture healing in a limited number of studies.[27,28]

Nuclear scintigraphy can be used to detect osteomyelitis several months before radiography can.[29] Technetium-PO bone scanning is commonly used to diagnose osteomyelitis,[30] and is useful for differentiating infected bone from soft tissue.[9,31-36] However, because it will accumulate in any area of rapid bone turnover, it has a low specificity for infection. Gallium-67 citrate and indium-111 labeled leukocytes also have a low specificity for infection, because of an increase in radionuclide uptake with any cause of inflammation[37-51] and image quality is poor.[10]

Technetium-labeled ciprofloxacin (Infecton; Tc-CIPRO) is one method that can distinguish infection from other causes of inflammation.[52-56] Ciprofloxacin binds to

bacterial DNA gyrase. Advantages of Tc-CIPRO over other methods of nuclear scintigraphy for detecting infection include the high specificity, handling of blood is not required, and there is minimal time, technical skills, and laboratory equipment needed for radionuclide preparation and scanning. There have been no controlled studies evaluating the use of Tc-CIPRO for differentiation of infected and non-infected fractures.

The purpose of this study was to evaluate the use of Tc-PO for assessing fracture healing, and Tc-PO and Tc-CIPRO for early diagnosis of osteomyelitis in a rabbit model. Our hypotheses were that there would be a difference in uptake ratio with Tc-PO between animals that healed and animals that did not heal and that there would be a significant difference in uptake ratio of Tc-PO and Tc-CIPRO in infected compared to non-infected animals.

Materials and Methods

Animal Model

Thirty-two skeletally mature female New Zealand White rabbits were used to evaluate the use of Tc-PO and Tc-CIPRO for evaluating fracture healing and infection. This study was performed as part of another study evaluating the use of adenoviral transfer of the bone morphogenetic–2 gene (Ad-BMP-2) for enhancing healing of non-unions and infected non-unions (Chapter 3). Therefore there were 4 groups (1) non-infected Ad-Luciferase (LUC) control, (2) non-infected Ad-BMP-2 treated, (3) infected Ad-LUC control, and (4) infected Ad-BMP-2.

A non-union and infected non-union model was created using a 10-mm mid-diaphyseal femoral fracture defect stabilized with a plate and screws and cerclage wire

(Chapter 2). The soft tissues, periosteum, endosteum, and bone marrow were removed to create a non-union. In addition, a sclerosing agent (sodium morrhuate) was used on the ends of the bone to prevent fracture healing as a result of the proliferation associated with the infection (Chapter 2).

Enrofloxacin (10mg/kg) was administered pre-operatively only. Perioperative analgesia consisted of preoperative morphine epidurally (0.1mg/kg) and subcutaneously (SQ: 0.5mg/kg), fentanyl administered as a constant rate infusion during surgery, and flunixin meglumine (0.5 mg/kg SQ) every 12 hours for 3 days. Butorphanol (0.4 mg/kg SQ) was also administered as needed postoperatively. Acepromazine (0.3 to 0.5 mg/kg) was administered intramuscularly to avoid self-trauma to the fracture during recovery from general anesthesia.

Rabbits in the infected groups were inoculated percutaneously in the defect from the medial aspect of the limb with *Staphylococcus aureus* ($0.5x10^7$ colony-forming units (cfu)/0.5mL) 48 hours after surgery. At the same time rabbits were injected in the fracture defect with either Ad-LUC or Ad-BMP-2. Rabbits were euthanized 16 weeks after surgery. Quantitative aerobic culture (QAC) was performed following euthanasia at 16 weeks, and a QAC greater than 10^4 cfu/gram of tissue was used to define infection.

Radiographic Evaluation

Rabbits were evaluated radiographically (craniocaudal and lateromedial views) postoperatively at time 0, and at 4, 8, 12, and 16 weeks after surgery. Radiographic evaluation is outlined in Chapter 3. The radiographic lysis grade, percentage ossification,

overall external callus/proliferation grade at 16 weeks, as well as the presence of bridging callus, were used for analysis in this study.

Nuclear Scintigraphy

Rabbits were evaluated using nuclear scintigraphy at 4, 8, 12, and 16 weeks after surgery. Rabbits were injected with Tc-PO (Oxidronate, Technescan-HDP, Mallinckrodt Medical, St. Louis MO: 1 mCi), and 48 hours later Tc-CIPRO (Infecton, IV Direct Ltd., London, England: 1 mCi/kg). A one minute pool-phase image was obtained immediately post injection and three minute planar images were made 2 hours postinjection using a 20-inch by 14.5-inch rectangular field of view imaging system with a general purpose collimator (Vari-Cam, General Electric Medical Systems, Waukesha, WI). Additional scans were made one hour later in four rabbits to evaluate any difference between 2-hour and 3-hour scans.

Images were analyzed using the XPert Software program (Version 5.13, General Electric Medical Systems). Lateromedial and craniocaudal views were used (Figure 1). The rabbits were held in position by the same person for each scan. All data was expressed as a ratio of experimental bone: normal bone. The average radionuclide uptake was measured for each region of interest (ROI). Regions of interest for the experimental limb (numerator: left limb: L) were the defect (1-cm), 3- and 5-cm adjacent to the defect, the whole bone, the proximal fragment, and the distal fragment. Regions of interest for the normal bone (denominator) were the identical areas of the contralateral femur (right limb: R), the left and right tibia, the left and right tuber ischii, and the first lumbar vertebra. The uptake in the heart was also measured and the ratio of whole bone: heart

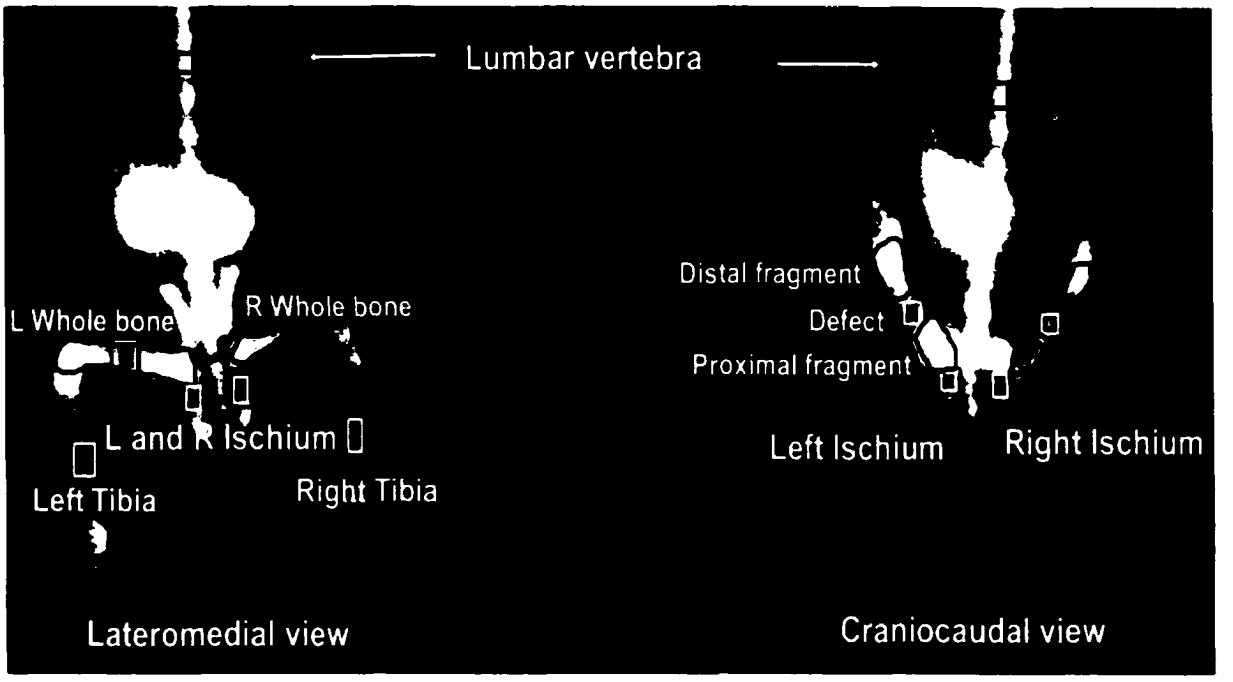

Figure 1. Lateromedial and craniocaudal views of a delayed-phase scan using technetium-labeled phosphate (Tc-PO). The regions of interest (ROI) on the experimental bone (left (L): numerator) and normal bone (right (R): denominator) are illustrated. The same ROIs were used on the Tc-PO and Tc-CIPRO scans. The ROIs that were used were the same on both views, except the tibia could not be seen on the craniocaudal view. The ROIs on the experimental (left, L) were the defect (1-cm), 3- and 5-cm adjacent to the defect, proximal and distal fragment, and the whole bone. The ROIs on the control bone were the same ROIs on the contralateral femur (right, R), the lumbar vertebra, the left and right tibia, and the left and right ischium. The radionuclide uptake was expressed as a ratio of experimental: normal bone.

calculated for rabbits with Tc-CIPRO. This was to control for any radionuclide remaining in the circulation.

The whole bone, proximal fragment, and distal fragment ROI were defined as the area of increased uptake, and were not consistent between rabbits and time periods. Therefore the area of radionuclide uptake was evaluated and expressed as a ratio of experimental: normal (L:R) femur. The areas of the other ROIs were kept consistent.

The craniocaudal views on the Tc-CIPRO scans were evaluated subjectively by a Board Certified Radiologist (Dr Philip Steyn) to determining whether the experimental femur was infected or non-infected.

Statistical Analysis

Continuous data were analyzed using a mixed model ANOVA (PROC MIXED, Statistical Analysis System, SAS Institute, Cary, NC). The class variables were rabbit, time (4, 8, 12, and 16 weeks), treatment (BMP, LUC), and infection (infected, non-infected). The random variable was rabbit nested within infection and treatment groups. Data were analyzed using three models to evaluate the association between uptake ratio (dependent variable) and the fixed effects: (1) time, treatment, infection, and interactions, (2) radiographic lysis grade (0 to 3), time, and interactions, and (3) radiographic callus grade, time and interactions (fixed effects). The dependent variables for both Tc-PO and –CIPRO were the defect L:R, 3-cm L:R, 5-cm L:R, whole bone L:R, the ratios of defect: L tibia, defect: R tibia, defect: L ischium, defect: R ischium, whole bone: lumbar vertebra, whole bone: L tibia, whole bone: R tibia, whole bone: L ischium, whole bone: R ischium, and whole bone: heart. Data from both the craniocaudal and lateromedial views

were analyzed separately. The ratio of whole bone and area for the pool-phase scans were used as the dependent variables. A plot of the predicted versus the residual values was performed, and if an increase in variance with increase in uptake ratio was observed a log transformation of the data was performed, and the data was reanalyzed.

A Pearson's correlation (PROC CORR, SAS Institute) was used to evaluate the correlation between each dependent variable and the callus and lysis grade (continuous data), as well as the correlation between Tc-PO and Tc-CIPRO. There was no correlation if $r^2<0.3$, a weak correlation was $r^2=0.3$ to 0.4, a moderate correlation was $r^2=0.5$ to 0.6, and a good correlation was $r^2>0.6$. A significant correlation was $r^2>0.3$.

The probability of the various ROIs being able to predict whether an animal was infected or not, or had bridging callus at 16 weeks, was also determined (PROC PROBIT, SAS Institute), and the accuracy, true positive (sensitivity), true negative (specificity), positive predictive value, and negative predictive value calculated (PROC FREQ, SAS Institute). Level of significance was $p<0.05$. All data are expressed as the least squared means (LSM) of the nuclide uptake ratio.

The coefficient of variation (CV) was determined by measuring the radionuclide uptake in 40 assigned ROIs three times, calculating the standard deviation and mean of the three measurements, and then dividing the standard deviation by the mean. This was performed to determine the amount of variability associated with measuring the radionuclide uptake. The CV was expressed as a percentage value. The median, minimum, and maximum CV for the assigned ROIs was reported.

Results

Animal Model

There were 20 rabbits completing the 16-week study (non-infected BMP-2 n=5; non-infected LUC n=6; infected BMP-2 n=3; infected LUC n=6). Therefore, 12 rabbits were euthanized for humane reasons prior to completion of the study (Chapter 2). Three rabbits were euthanized after week-4 of the study; therefore, data from these rabbits were included until the time of euthanasia.

Rabbits were classified as infected or non-infected initially whether they were inoculated with *S. aureus* at 48 hours or not inoculated. Infection was further classified as whether there was accumulation of purulent material on gross examination, positive culture, and radiographic lysis (non-infected = 0.5 or less and infected = 1 or greater) at 16 weeks. There was one rabbit in the infected group that had no signs of infection grossly, a negative culture, and no radiographic lysis at 16 weeks. Further examination of this rabbit's record revealed that the culture of the inoculum was negative. Therefore, it was decided pre-analysis that this rabbit was included in the non-infected group. All other rabbits in the infected group had established infection, and non-infected rabbits did not have signs of infection.

Nuclear Scintigraphy

Tc-99m-PO: There were higher variance estimates seen with high radionuclide uptake ratios; therefore a log transformation was performed to normalize the data. All data for Tc-PO uptake ratios were analyzed as log values and are presented as least squared means of the log values. Data for the defect and whole bone numerator ROI are

presented unless there were differences between trends in the other ROIs. The median CV for the Tc-PO scans was 3.5% (range 1 to 10.4%), based on the 40 assigned ROIs. There was a significant association between infection and uptake ratio. Infected rabbits had a higher uptake ratio using all views and ROIs. The association between uptake ratio and infection was significant at all time periods except for week-4 (Table 1). There was no difference between the lateromedial and craniocaudal views; therefore the data for the lateromedial view only is shown. The use of uptake ratio to determine the probability of rabbits being infected or not infected is shown in Table 2. Generally the accuracy was good (>80%) after 4 weeks using the whole bone or proximal ROI and the craniocaudal view.

There was a significant association between the L:R ratio of the areas of the whole bone ROI on the lateral view and time. The ratio of the L:R area increased in infected rabbits and decreased in non-infected rabbits with time. Infected rabbits had a significantly higher ratio of the L:R area than non-infected rabbits at 12 and 16 weeks. There was no association between L:R ratio of the area and time or infection on the craniocaudal view. The L:R ratio of the area of the whole bone ROI on the pool-phase was higher in infected rabbits at 8, 12, and 16 weeks, and the ratio in non-infected rabbits decreased with time.

Table 1. The statistical association between the uptake ratio for the technetium-labeled phosphate scan and the presence of infection.

ROI	View	4 wk	8 wk	12 wk	16 wk
Defect L:R	Lateromedial	-	+	+	+
Defect:R Tibia	Lateromedial	-	+	+	+
Defect:L Tibia	Lateromedial	-	+	+	+
Defect:R Ischium	Lateromedial	-	+/-	+	+
Defect:L Ischium	Lateromedial	-	-	+	+
Proximal L:R	Lateromedial	-	+	+	+
Distal L:R	Lateromedial	+/-	+/-	+	-
Bone L:R	Lateromedial	-	+	+	+
Bone: Lumbar	Lateromedial	-	+	+	+
Bone:R Tibia	Lateromedial	-	+	+	+
Bone:L Tibia	Lateromedial	-	+	+	+
Bone:R Ischium	Lateromedial	-	+	+	+
Bone:L Ischium	Lateromedial	-	+	+	+

+ Significant difference between infected versus non-infect ($p<0.05$)
- No significant difference between infected versus non-infected ($p>0.1$)
+/- Trend for difference between infected versus non-infected ($p\leq 0.1$)

Table 2. Accuracy of the use of technetium-labeled phosphate for detecting infection.

ROI[1]	View[2]	WK[3]	Ratio[4]	Sens[5]	Spec[6]	Pos Pred Value[7]	Neg Pred Value[8]	Accuracy
Defect L:R	LAT	4	3.8	10	92	50	57	57
		8	3	56	83	71	71	71
		12*	3.5	63	83	71	77	75
		16*	5.4	50	92	80	75	75
	CC	4	3.6	20	92	67	60	61
		8	2.9	56	83	71	71	71
		12*	4.2	63	92	83	79	80
		16*	5.0	63	92	83	79	80
Prox L:R	LAT	4	3.7	40	92	80	67	70
		8**	3.1	44	92	80	67	71
		12*	2.8	75	92	86	85	85
		16*	2.8	75	92	86	85	85
	CC	4*	2.7	60	85	75	73	74
		8*	2.5	67	100	100	80	86
		12*	2.6	88	92	88	92	90
		16*	3.3	75	92	86	85	85
Bone L:R	LAT	4	>3.7	0	100	0	100	57
		8*	2.9	56	92	83	73	76
		12*	2.6	75	83	75	83	80
		16*	2.9	88	92	88	92	90
	CC	4	2.6	50	77	63	67	65
		8*	2.2	89	100	100	92	95
		12*	2.4	100	100	100	100	100
		16*	2.4	88	92	88	92	90
Bone: Lumb	LAT	4	2.8	30	85	60	61	61
		8*	2.7	67	92	86	79	81
		12*	1.2	100	100	100	100	100
		16*	2.6	75	92	86	85	85
	CC	4	1.5	20	85	50	58	57
		8*	1.3	78	83	78	83	81
		12*	1.1	88	92	92	88	90
		16*	1.4	75	92	86	85	85

*$p<0.05$ **$p\leq 0.1$: 1. ROI=Region of interest, prox=proximal, lumb=lumbar vertebra, 2. LAT=Lateral, CC=Craniocaudal, 3. WK=weeks after surgery, 4. infected rabbits have a ratio equal to or greater than the given ratio, 5. sensitivity or true positive rate, 6. specificity or true negative rate, 7. positive predictive value, 8. negative predictive value.

There was a significant association between uptake ratio and time; however, the association was different depending on the ROI. The interaction between infection and time was significant for all views and ROIs. The change in uptake ratio with time varied depending on the denominator ROI that was used; the uptake ratio in infected rabbits increased or did not change with time and the uptake ratio for non-infected rabbits decreased or did not change with time (Figure 2a, b, c). Therefore, the relationship between the different denominator ROIs changed with time.

Because of the variability between uptake ratios with the different denominator ROIs, this was further investigated using the lateromedial view. The lateromedial view only was used because there appeared to be the same trends observed with the two views and the tibia ROIs were only visible on the lateromedial view (Figure 1). The ratio of the lumbar vertebra to the control whole bone and the ratios of the left and right tibia and left and right ischium were evaluated.

The ratio of the lumbar vertebra to the control femur increased with time; therefore there was either an increase in uptake in the lumbar vertebra and/or a decrease in uptake in the right femur with time in both infected and non-infected rabbits. Because the change in relationship could be associated with either a change in blood flow and/or a change in bone metabolism, the pool-phase was evaluated. The pool-phase showed that infected rabbits had a lower ratio than non-infected rabbits, and that there was no change with time. This means that infected rabbits had either a reduced blood flow to the lumbar vertebra or increase to the control femur; as well as an increase in bone metabolism in the lumbar vertebra or a decrease in the control femur with time.

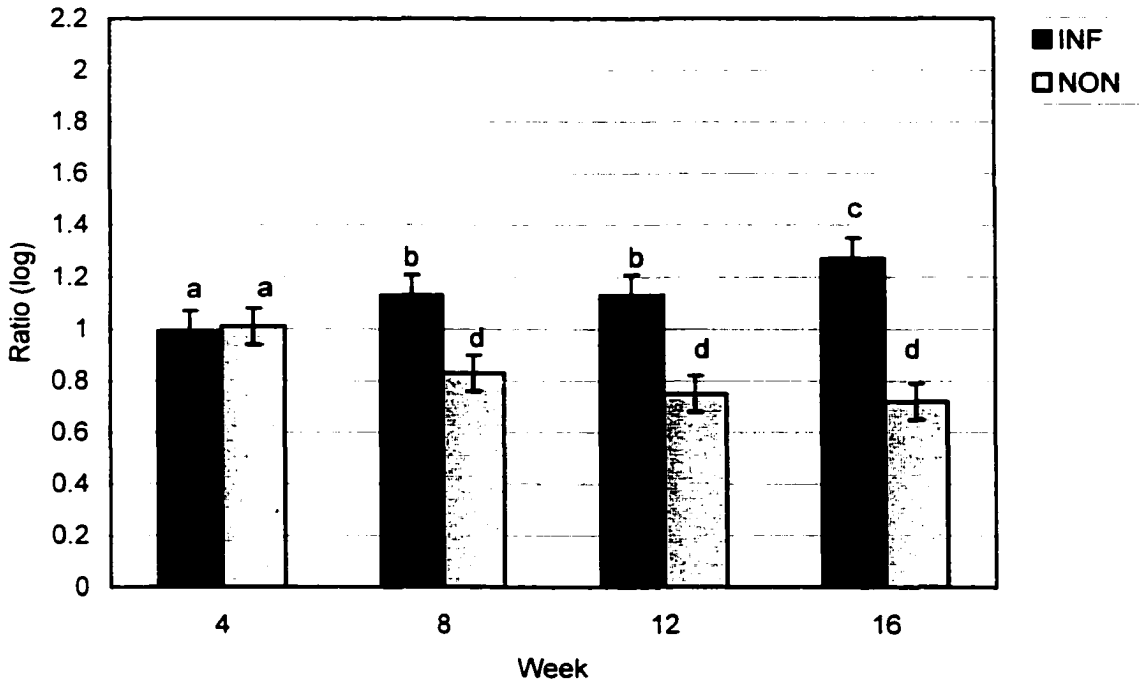

Figure 2A. A plot illustrating the association between infection and delayed-phase technetium-labeled phosphate (Tc-PO) uptake ratio of the whole bone L:R region of interest (ROI) on the lateromedial view. The log of the uptake ratio is shown on the y-axis, the time after surgery is shown on the x-axis, and infected rabbits are represented with black bars and non-infected rabbits with gray bars. Data are presented as least squared means of the log of the uptake ratio +/- the standard error of the mean. Different letters represent statistically significant differences.

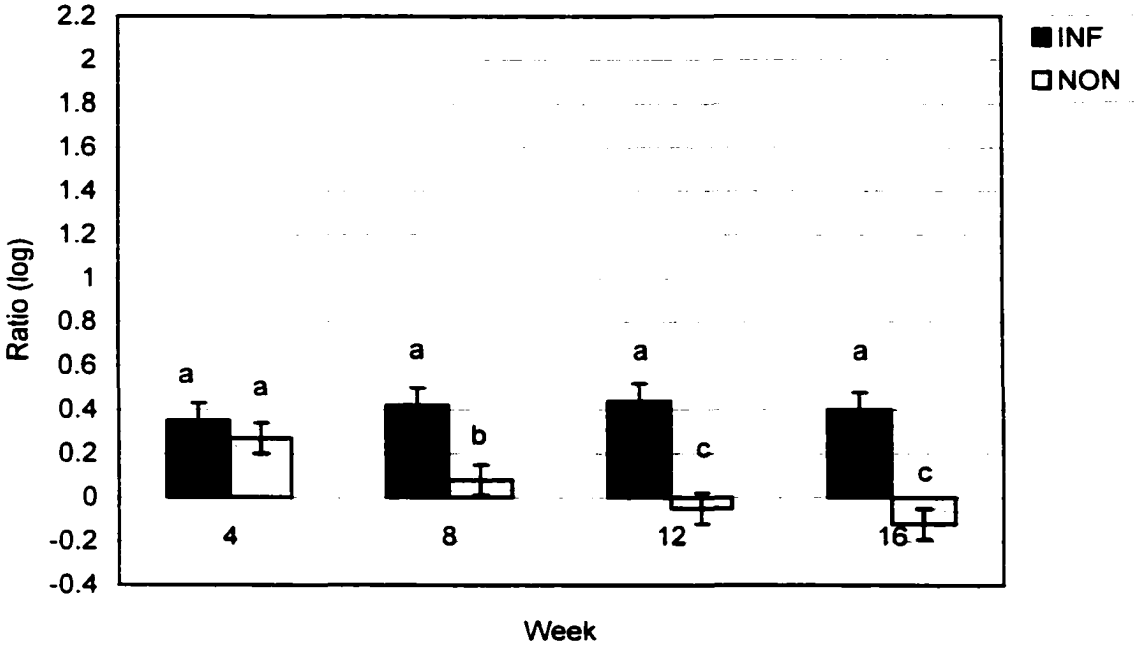

Figure 2B. A plot illustrating the association between infection and delayed-phase technetium-labeled phosphate (Tc-PO) uptake ratio of the whole bone: lumbar vertebra region of interest (ROI) on the lateromedial view. The log of the uptake ratio is shown on the y-axis, the time after surgery is shown on the x-axis, and infected rabbits are represented with black bars and non-infected rabbits with gray bars. Data are presented as least squared means of the log of the uptake ratio +/- the standard error of the mean. Different letters represent statistically significant differences.

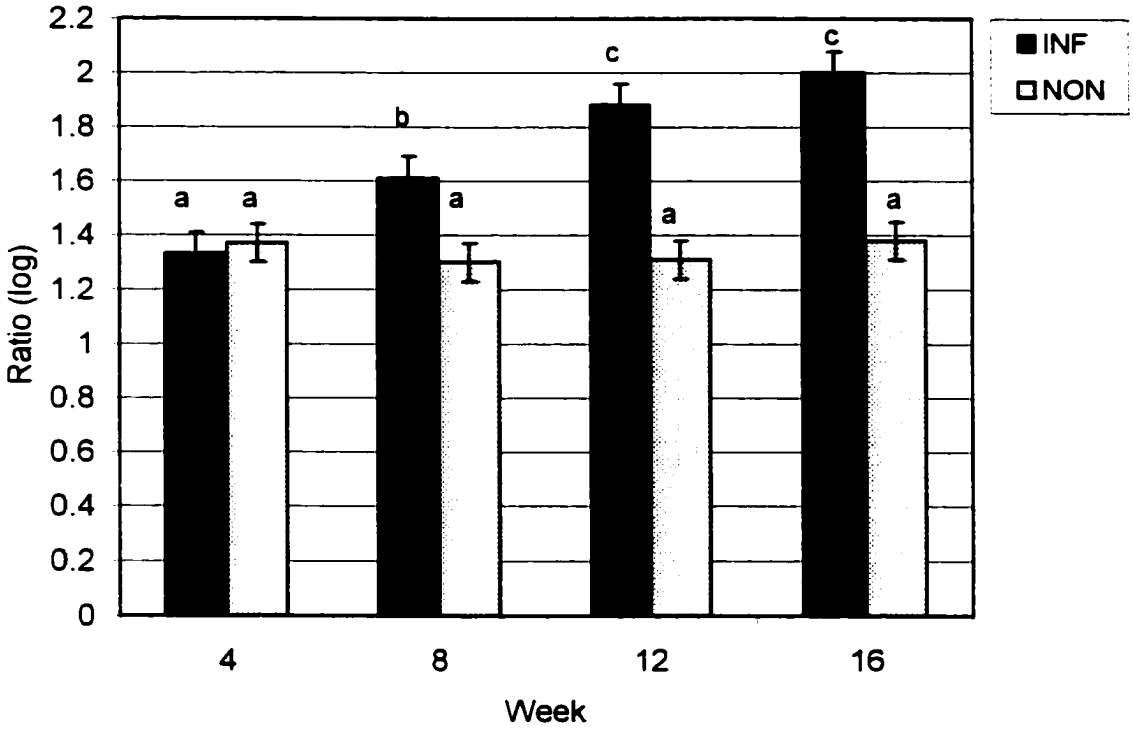

Figure 2C. A plot illustrating the association between infection and delayed-phase technetium-labeled phosphate (Tc-PO) uptake ratio of the whole bone: left tibia region of interest (ROI) on the lateromedial view. The log of the uptake ratio is shown on the y-axis, the time after surgery is shown on the x-axis, and infected rabbits are represented with black bars and non-infected rabbits with gray bars. Data are presented as least squared means of the log of the uptake ratio +/- the standard error of the mean. Different letters represent statistically significant differences.

The uptake ratio of the L:R tibia decreased with time in both infected and non-infected rabbits, and was higher in infected than non-infected rabbits. This means that the uptake in the left tibia decreased and/or the right tibia increased with time in both infected and non-infected rabbits, and that infected rabbits had a higher uptake in the left tibia and/or lower uptake in the right tibia compared to non-infected rabbits. There was no association between infection and time on the pool-phase scans. The ratio of the right femur: tibia was higher in infected rabbits, and there was a trend for this ratio to be higher in the pool-phase.

There was also a decrease in uptake ratio of the L:R ischium with time, and a trend for infected rabbits to have a higher ratio. Therefore, the uptake in the left ischium decreased or the right ischium increased with time and infected rabbits had either a higher uptake in the left or lower uptake in the right ischium. The pool-phase followed a similar pattern.

The defect L:R, whole bone L:R, and whole bone: lumbar vertebra ratios were used to evaluate the association between uptake ratio and radiographic lysis grade. There was a good correlation between uptake ratio of the both the whole bone L:R as well as the whole bone: lumbar vertebra ROIs and lysis grade at 8, 12, and 16 weeks (r^2=0.7). There was also a significant association between the uptake ratio of the defect and whole bone L:R ROI and the interaction between lysis grade and time. With the whole bone L:R at 4 weeks rabbits with a higher lysis grade appeared to have a lower uptake ratio although this was not statistically significant. There was a decrease in uptake ratio over time in rabbits with no lysis, rabbits with mild lysis (grade 1) had no change, and rabbits

with moderate to marked lysis (grades 2 and 3) had an increase in uptake ratio over time (Figure 3).

The defect L:R, whole bone L:R, and whole bone: lumbar vertebra ratios were used to evaluate the association between uptake ratio and defect ossification. There was a statistically significant correlation between the percentage defect ossification and uptake ratio of the defect L:R on both the lateromedial and craniocaudal views. There was no correlation at 4 weeks (r^2=0.1), the correlation peaked at 8 and 12 weeks (r^2=0.6), and then decreased at 16 weeks (r^2=0.5). There was no correlation between defect ossification and uptake ratio for whole bone L:R or whole bone: lumbar ROI.

The defect L:R, whole bone L:R, and whole bone: lumbar vertebra uptake ratios were used to evaluate the association between uptake ratio and radiographic external callus grade. When the data were analyzed continuously, there was no correlation between uptake ratio and callus grade. However, when the data were analyzed categorically, there was a significant association between uptake ratio of the defect L:R ROI and the interaction between callus grade and time on both the lateromedial and craniocaudal views. Rabbits with bridging callus (grade-4) had a consistently high uptake ratio, rabbits with minimal callus (grade 1) had a consistently low uptake ratio, and rabbits with callus formation that was not bridging (grade 2 and 3) had an increase in uptake ratio over time (Figure 4). The uptake ratio of the defect L:R ROI on the lateral view at 4 weeks was useful for determining the probability of rabbits developing bridging callus with a sensitivity of 57%, specificity of 88%, and overall accuracy of 78%. A ratio of 2.9 was used to differentiate rabbits that would develop bridging callus from those that would not. There was no association between callus and uptake ratio for whole bone L:R

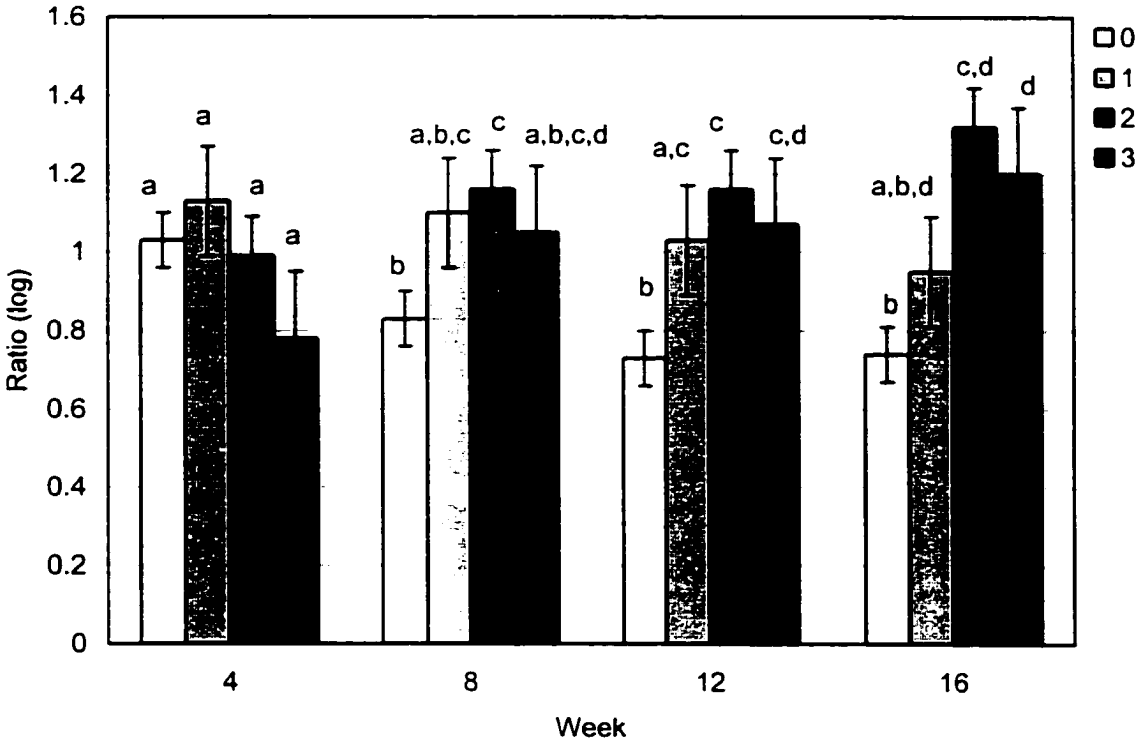

Figure 3. A plot illustrating the association between lysis grade and the delayed-phase technetium-labeled phosphate (Tc-PO) uptake ratio of the whole bone L:R ROI on the lateromedial view. The log of the uptake ratio is shown on the y-axis, the time after surgery is shown on the x-axis, and the lysis grades (0=none, 1=slight, 2=mild, 3=moderate) are represented by white, light gray, dark gray, and black bars. Data are presented as least squared means of the log of the uptake ratio +/- standard error of the mean. Different letters represent statistically significant differences.

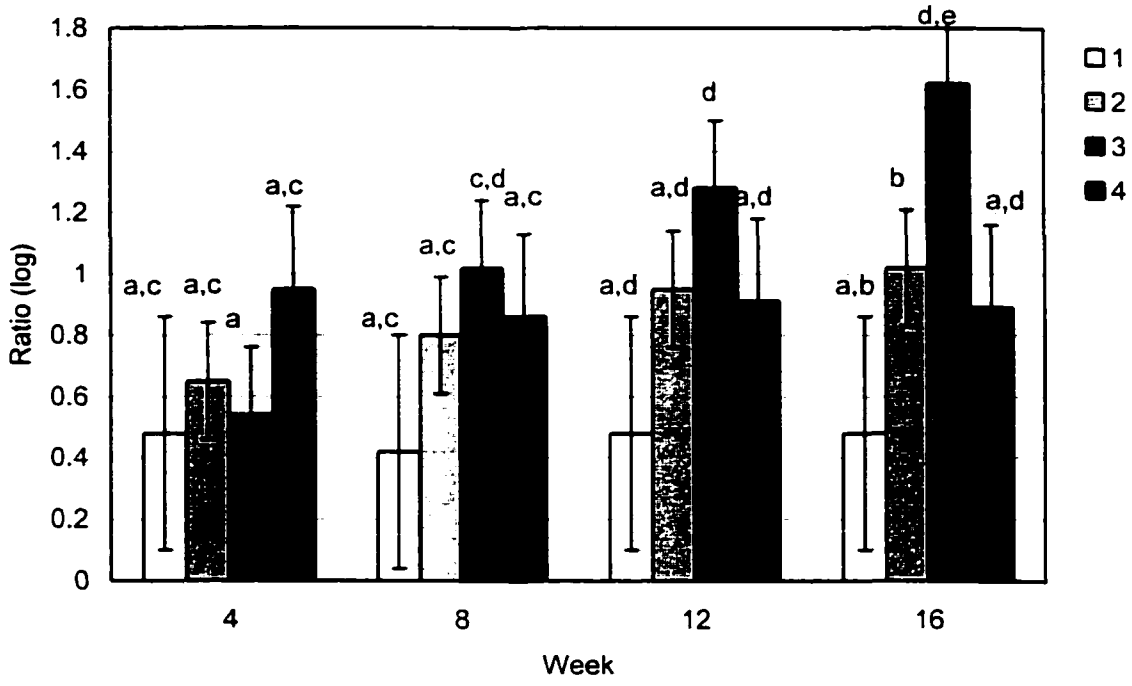

Figure 4. A plot illustrating the association between external callus grade and the delayed-phase technetium-labeled phosphate (Tc-PO) uptake ratio of the defect L:R ROI on the lateromedial view. The log of the uptake ratio is shown on the y-axis, the time after surgery is shown on the x-axis, and the external callus grades (1=slight, 2=mild, 3=moderate, 4=severe) are represented by white, light gray, dark gray, and black bars. Data are presented as least squared means of the log of the uptake ratio +/- standard error of the mean. Different letters represent statistically significant differences.

or whole bone: lumbar ROI. There was no association between callus grade and pool-phase ratios or area ratios. There was no association between treatment group and uptake ratio.

Overall there was a significant correlation between the Tc-PO and –CIPRO scans for the uptake ratio of the defect and whole bone ROI. The correlation was higher on the lateromedial than the craniocaudal view, and was weak at 4 weeks and increased with time.

Tc-99m-CIPRO: Based on the plot of residual versus predicted values the data appeared to be normal and was not transformed. The uptake ratios for the defect and whole bone numerator ROI will be presented unless there are any important differences in trends for the other ROIs. The ischium denominator ROI was not used because the region was difficult to identify and there was superimposition with the left femur. The median CV for the Tc-CIPRO scans was 1.4% (range 0 to 6.4%) based on 40 assigned ROIs.

There was a significant association between the uptake ratio for Tc-CIPRO and infection and a significant interaction between infection and time. The uptake ratio of rabbits in the infected group increased or did not change with time, and the ratio of the rabbits in the non-infected groups decreased or did not change with time, depending on the view and ROI. Similar trends were observed on the craniocaudal and lateromedial views. There was no association between uptake ratio and infection at 4 weeks using the L:R defect ROI (Table 3; Figure 5a). However, using the L:R whole bone or proximal fragment ROI, the results were significant; the craniocaudal view showed a significant difference more frequently than the lateromedial view (Table 3; Figure 5b-d). Non-

Table 3. The statistical association between the uptake ratio for the technetium-labeled ciprofloxacin scan and the presence of infection.

ROI	View	4 wk	8 wk	12 wk	16 wk
Defect L:R	Lateral	-	+	+	+
	Craniocaudal	-	-	+	+
Defect:R Tibia	Lateral	-	+	+	+
Defect:L Tibia	Lateral	-	+	+	+
Proximal L:R	Lateral	+	+	+	+
	Craniocaudal	+	+	+	+
Distal L:R	Lateral	-	+	+	+
	Craniocaudal	+	-	-	+
Bone L:R	Lateral	+/-	+	+	+
	Craniocaudal	+	+	+	+
Bone:Lumbar	Lateral	+	+	+	+
	Craniocaudal	+	+	+	+
Bone:R Tibia	Lateral	-	+	+	+
Bone:L Tibia	Lateral	+	+	+	+
Bone:Heart	Lateral	-	+	+	+
	Craniocaudal	-	+	+	+

+ Significant difference between infected versus non-infect ($p<0.05$)
- No significant difference between infected versus non-infected ($p>0.1$)
+/- Trend for difference between infected versus non-infected ($p\leq 0.1$) [52-56]

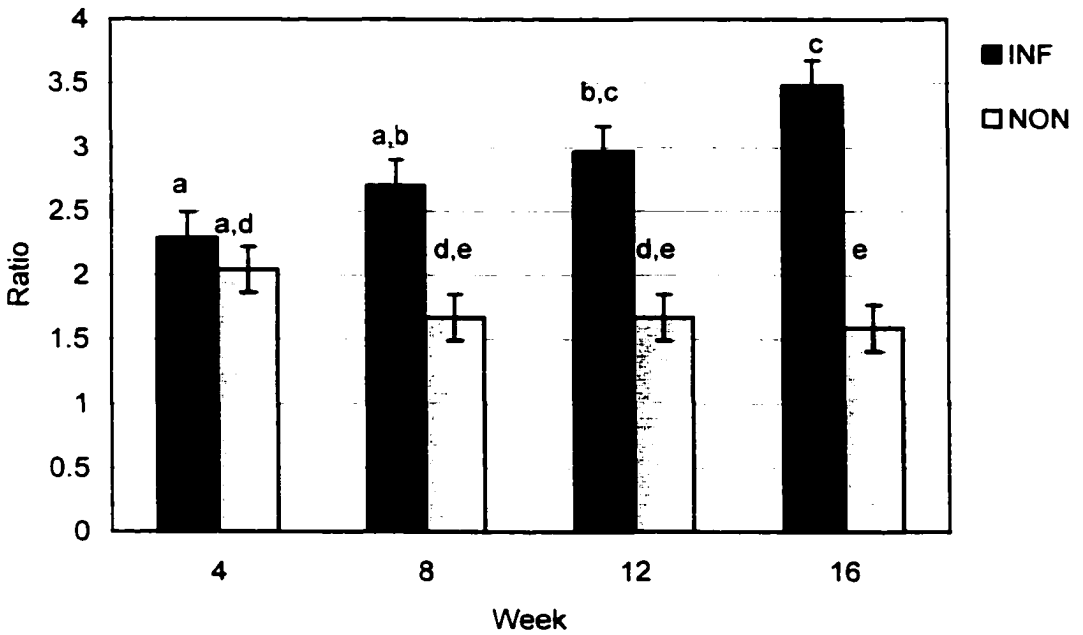

Figure 5A. A plot illustrating the association between infection and delayed-phase technetium-labeled ciprofloxacin (Tc-CIPRO) uptake ratio of the defect L:R region of interest (ROI) on the lateromedial view. The uptake ratio is shown on the y-axis, the time after surgery is shown on the x-axis, and infected rabbits are represented with black bars and non-infected rabbits with gray bars. Data are presented as least squared means of the uptake ratio +/- standard error of the mean. Different letters represent statistically significant differences.

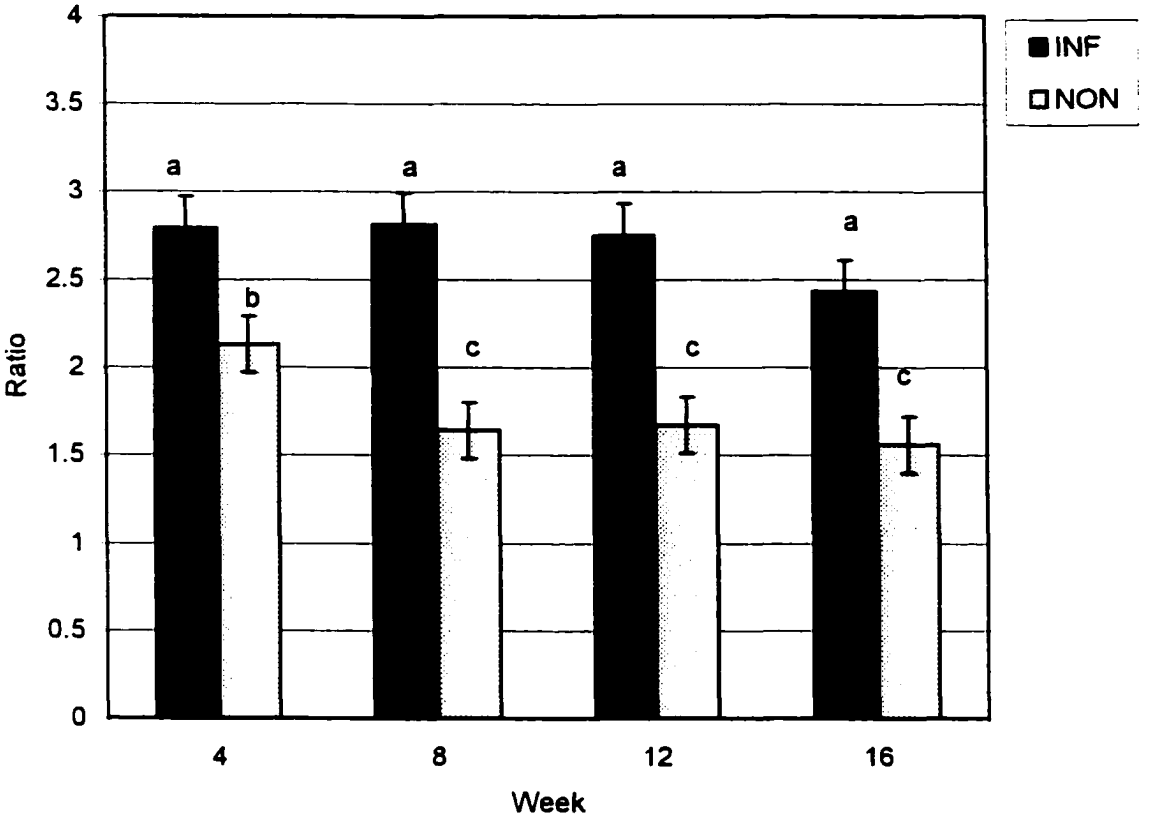

Figure 5B. A plot illustrating the association between infection and delayed-phase technetium-labeled ciprofloxacin (Tc-CIPRO) uptake ratio of the proximal fragment L:R region of interest (ROI) on the lateromedial view. The uptake ratio is shown on the y-axis, the time after surgery is shown on the x-axis, and infected rabbits are represented with black bars and non-infected rabbits with gray bars. Data are presented as least squared means of the uptake ratio +/- standard error of the mean. Different letters represent statistically significant differences.

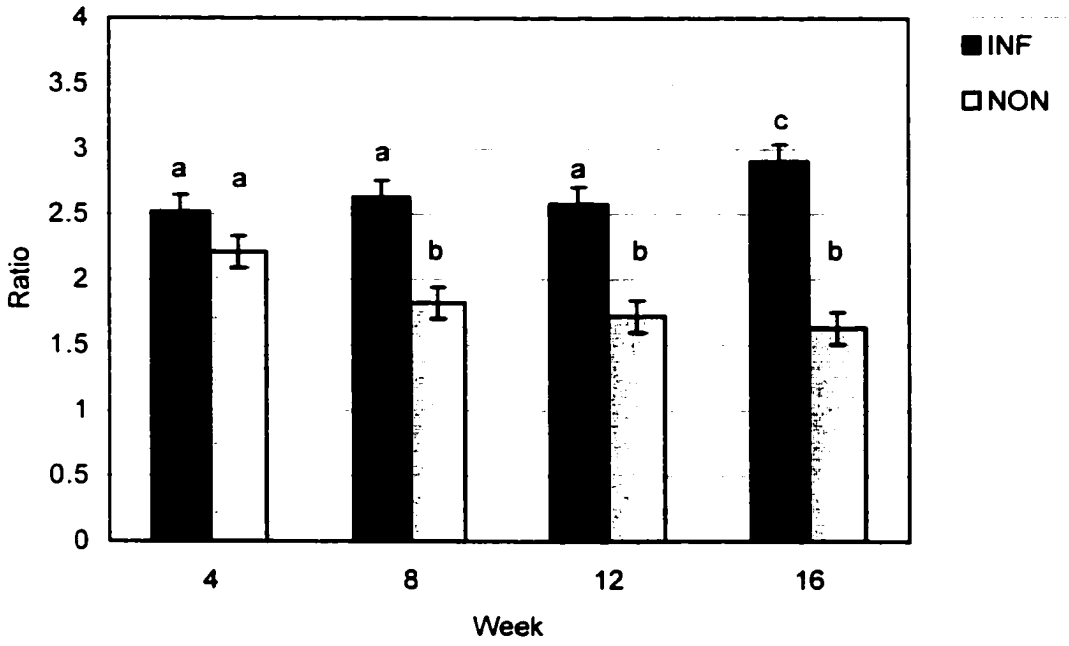

Figure 5C. A plot illustrating the association between infection and delayed-phase technetium-labeled ciprofloxacin (Tc-CIPRO) uptake ratio of the whole bone L:R region of interest (ROI) on the lateromedial view. The uptake ratio is shown on the y-axis, the time after surgery is shown on the x-axis, and infected rabbits are represented with black bars and non-infected rabbits with gray bars. Data are presented as least squared means of the uptake ratio +/- standard error of the mean. Different letters represent statistically significant differences.

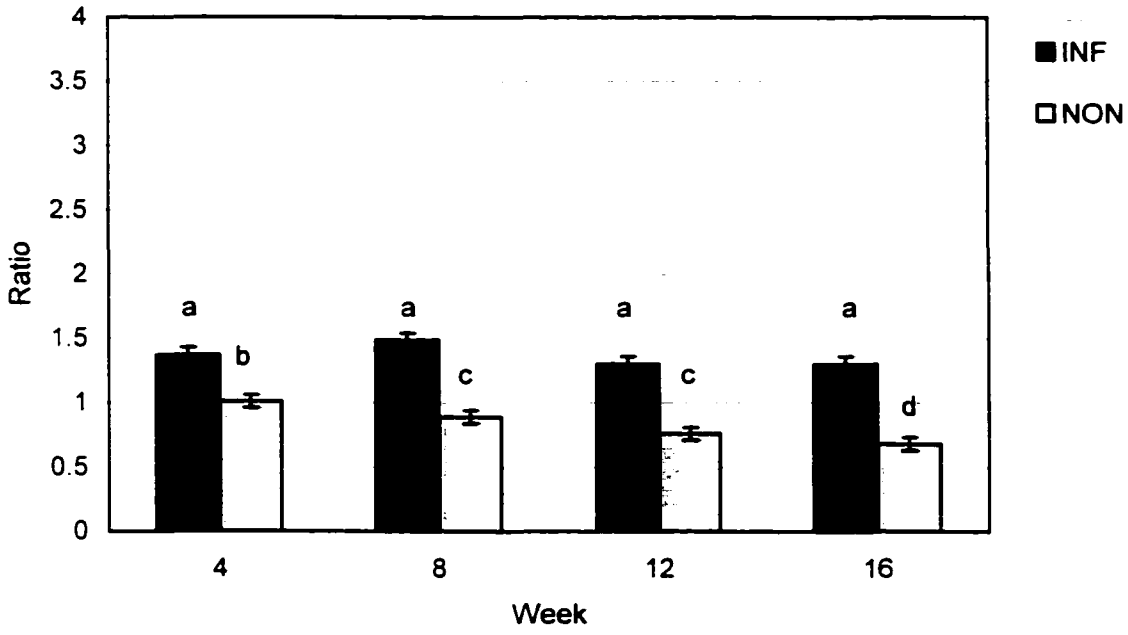

Figure 5D. A plot illustrating the association between infection and delayed-phase technetium-labeled ciprofloxacin (Tc-CIPRO) uptake ratio of the whole bone: lumbar vertebra region of interest (ROI) on the lateromedial view. The uptake ratio is shown on the y-axis, the time after surgery is shown on the x-axis, and infected rabbits are represented with black bars and non-infected rabbits with gray bars. Data are presented as least squared means of the uptake ratio +/- standard error of the mean. Different letters represent statistically significant differences.

infected rabbits had a decrease in uptake ratio with time, and infected rabbits did not change with time, except with the defect ROI where there was an increase in uptake ratio with time. The use of Tc-CIPRO for determining the probability of a rabbit being infected or non-infected is shown in Table 4. The whole bone and proximal numerator ROI and the craniocaudal view were the best for differentiating infected from non-infected rabbits.

Subjective analysis revealed a relatively low specificity and high sensitivity for detecting infection with the Tc-CIPRO scans. Overall, the true positive (sensitivity) was 94% (33/35) and true negative (specificity) was 73% (35/48), with an overall accuracy of 82% (68/83). There appeared to be the most difficulty differentiating infected from non-infected rabbits at 4 weeks using the objective analysis; at 4 weeks using subjective analysis the true positive (sensitivity) was 80% (10/12) and true negative (specificity) was 85% (11/13), with an overall accuracy of 83% (19/23). The overall accuracy was similar to that obtained using objective analysis on the whole bone L:R and proximal L:R ROI at 4 weeks (78% and 83%, respectively; Table 4). The rabbits that were incorrectly classified as infected on the subjective analysis were different to those incorrectly classified based on the objective analysis, and the specificity was high on the objective analysis and the sensitivity low. The observer randomly re-evaluated nine images, and the repeatability was 89% (8/9). Figure 6 illustrates a non-infected and infected rabbit at 4 and 16 weeks; the uptake in the non-infected rabbit decreased with time, whereas the uptake in the infected rabbit did not change or increased.

Table 4. Accuracy of technetium-labeled ciprofloxacin for detecting infection.

ROI[1]	View[2]	WK[3]	Ratio[4]	Sens[5]	Spec[6]	Pos Pred Value[7]	Neg Pred Value[8]	Accuracy
Defect L:R	LAT	4	2.5	40	77	57	63	61
		8*	2.2	67	83	75	77	76
		12*	2.5	75	83	75	83	80
		16*	3.1	75	92	86	85	85
	CC	4	2.4	40	85	67	65	65
		8	2.3	33	83	60	63	62
		12*	2.1	63	92	83	79	80
		16*	2.5	75	83	75	83	80
Prox L:R	LAT	4*	2.6	60	100	100	76	83
		8*	2.5	78	100	100	86	90
		12*	2.3	100	100	100	100	100
		16*	2.1	75	100	100	86	90
	CC	4*	1.9	60	100	100	76	83
		8*	1.6	89	100	100	92	95
		12**	1.6	63	100	100	80	85
		16*	1.8	75	92	86	85	85
Bone L:R	LAT	4**	2.7	50	85	71	69	70
		8*	2.3	89	100	100	92	95
		12*	2.3	100	92	89	100	95
		16*	2.5	88	100	100	92	95
	CC	4*	1.8	70	85	78	79	78
		8*	1.7	89	92	89	92	90
		12*	1.8	63	92	83	79	80
		16*	1.8	88	100	100	92.3	95
Bone: Lumb	LAT	4	1.2	50	77	63	67	65
		8*	1.0	100	100	100	100	100
		12*	1.0	100	100	100	100	100
		16*	1.1	88	100	100	92	95
	CC	4*	1.2	80	85	80	85	83
		8*	1.2	100	100	100	100	100
		12*	1.0	100	100	100	100	100
		16*	1.0	75	92	86	85	85

* $p<0.05$ **$p\leq0.1$; 1. ROI=Region of interest, prox=proximal, lumb=lumbar vertebra, 2. LAT=Lateral, CC=Craniocaudal, 3. WK= weeks after surgery, 4. infected rabbits have a ratio equal to or greater than the given ratio, 5. sensitivity or true positive rate 6. specificity or true negative rate, 7. positive predictive value, 8. negative predictive value.

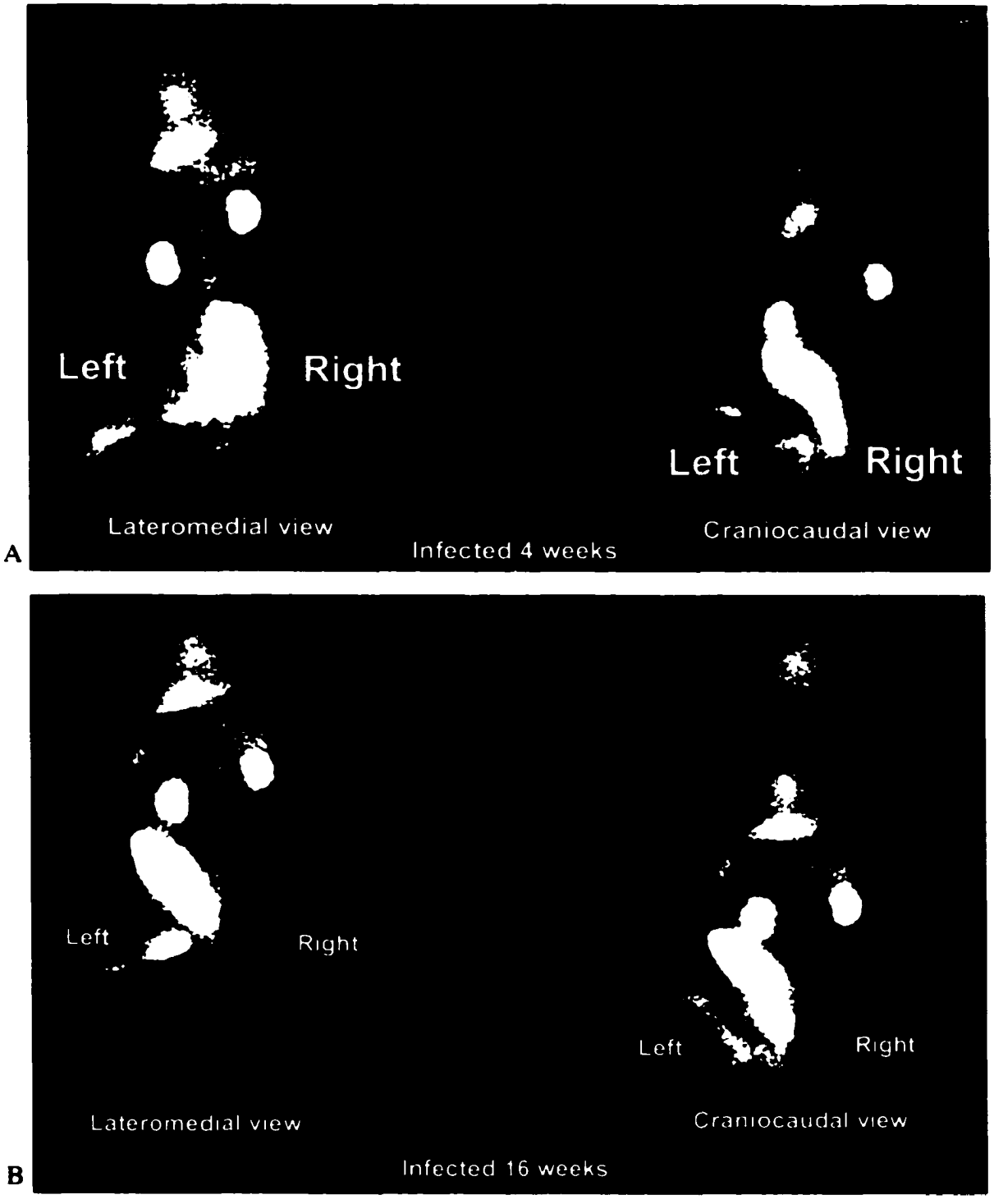

Figure 6. Lateromedial and craniocaudal views of delayed-phase scan using technetium-labeled ciprofloxacin (Tc-CIPRO). (A) Infected rabbit at 4 weeks and (B) Infected rabbit at 16 weeks. The uptake ratio of Tc-CIPRO in the infected rabbits either did not change or increased over time.

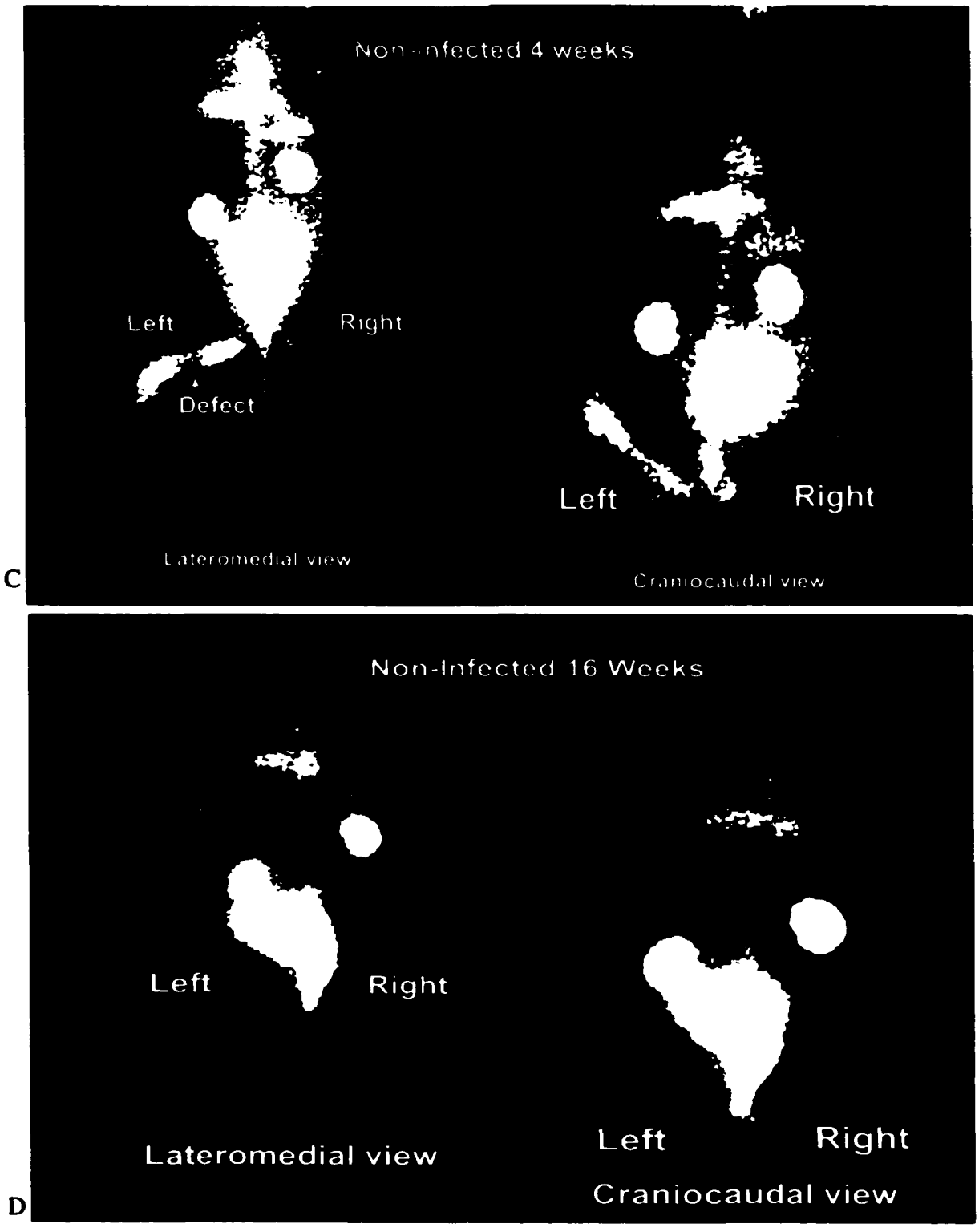

Figure 6. Lateromedial and craniocaudal views of delayed-phase scan using technetium-labeled ciprofloxacin (Tc-CIPRO). (C) Non-Infected rabbit at 4 weeks and (D) Non-Infected rabbit at 16 weeks. The uptake ratio of Tc-CIPRO in the non-infected rabbits was high early in the study (4 weeks), resulting in false positive findings, and decreased over time

Blood flow was evaluated with the pool-phase scan. There was a significant association between infection, time, and the interaction between infection and time and the uptake ratio of the whole bone L:R ROI on the pool-phase (Figure 7). There was no difference between infected and non-infected rabbits at 4 weeks; the uptake ratio in the non-infected rabbits decreased with time whereas in infected rabbits it did not change with time (Figure 7, 8 a,b,c). The rabbits were inoculated in the defect; however, the Tc-CIPRO uptake ratio in the defect L:R ROI was not statistically significantly different between infected and non-infected rabbits at 4 weeks. The cause of the lack of significance is demonstrated by the pool-phase, which shows photopenia in the defect region, indicating a relative lack of blood flow to this area (Figure 8). Further, the infected rabbits had areas of photopenia and areas of increased uptake associated with abscessation and this is shown in both the pool and delayed-phase on the Tc-CIPRO scan (Figure 8 and 9). Therefore, non-infected rabbits had an increase in blood flow to the experimental limb at 4 weeks, which may have contributed to the false positive results, and there was a relative photopenic area on the pool-phase suggesting a decrease in distribution of Tc-CIPRO to the defect area also contributing to the lack of significance early in fracture healing.

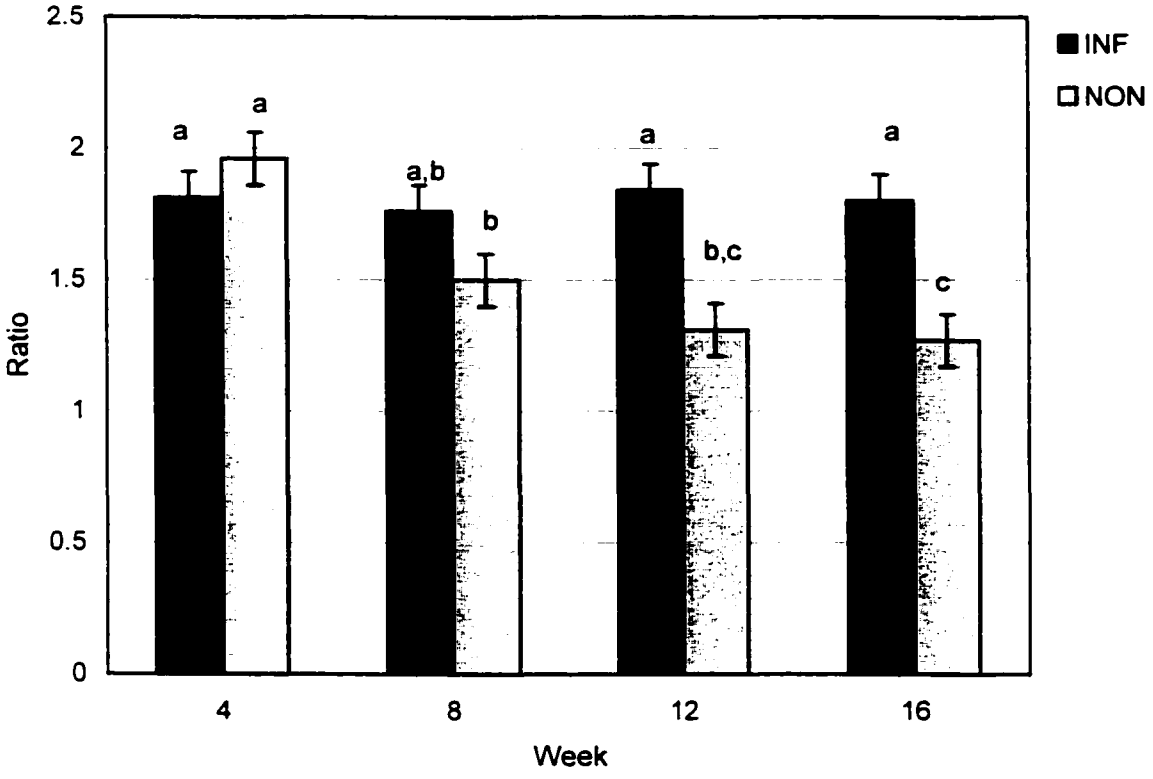

Figure 7. A plot illustrating the association between infection and pool-phase technetium-labeled ciprofloxacin (Tc-CIPRO) uptake ratio of the whole bone L:R on the lateromedial view. The uptake ratio is shown on the y-axis, the time after surgery is shown on the x-axis, and infected rabbits are represented with black bars and non-infected rabbits with gray bars. Data are presented as least squared means of the uptake ratio +/- standard error of the mean. Different letters represent statistically significant differences.

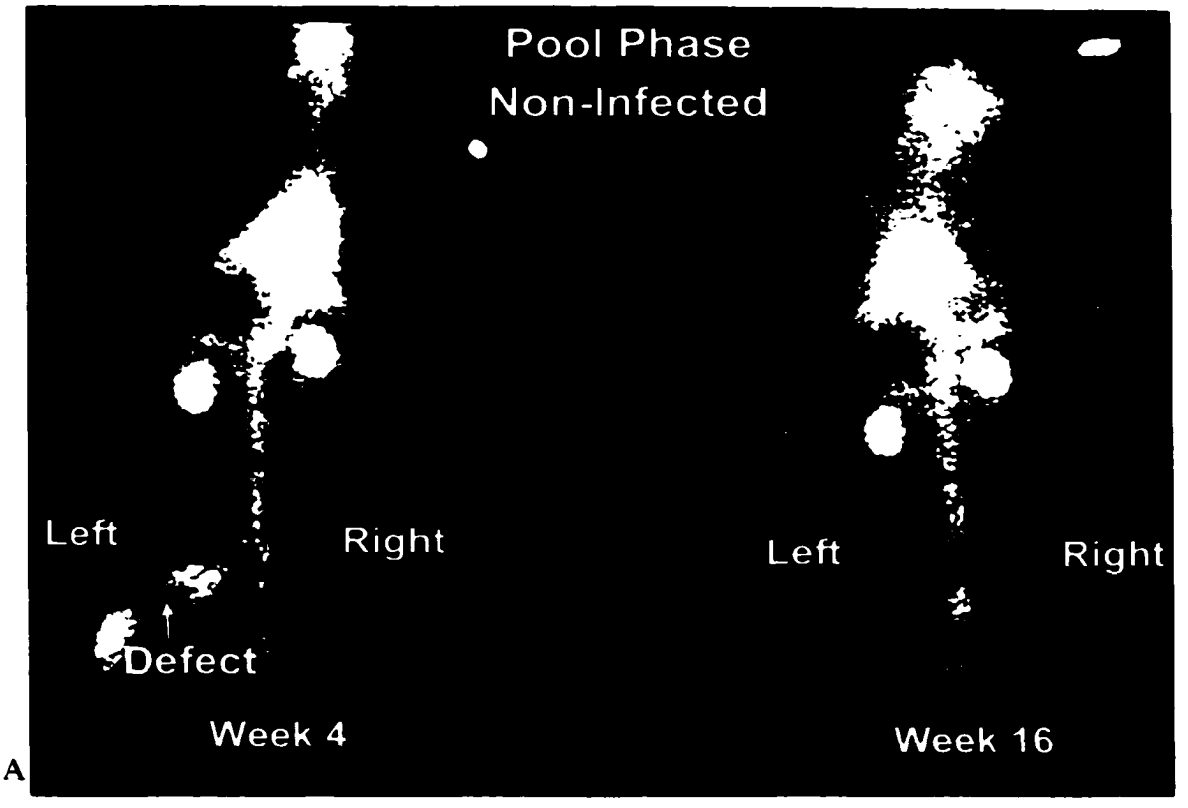

Figure 8. Lateromedial views of pool-phase scan using technetium-labeled ciprofloxacin (Tc-CIPRO) at 4 (left) and 8 (right) weeks after surgery. (A) Non-infected rabbits. There was an increase in blood flow in non-infected rabbits at 4 weeks that decreased over time. There was also less blood flow to the defect region compared to the proximal and distal fragments.

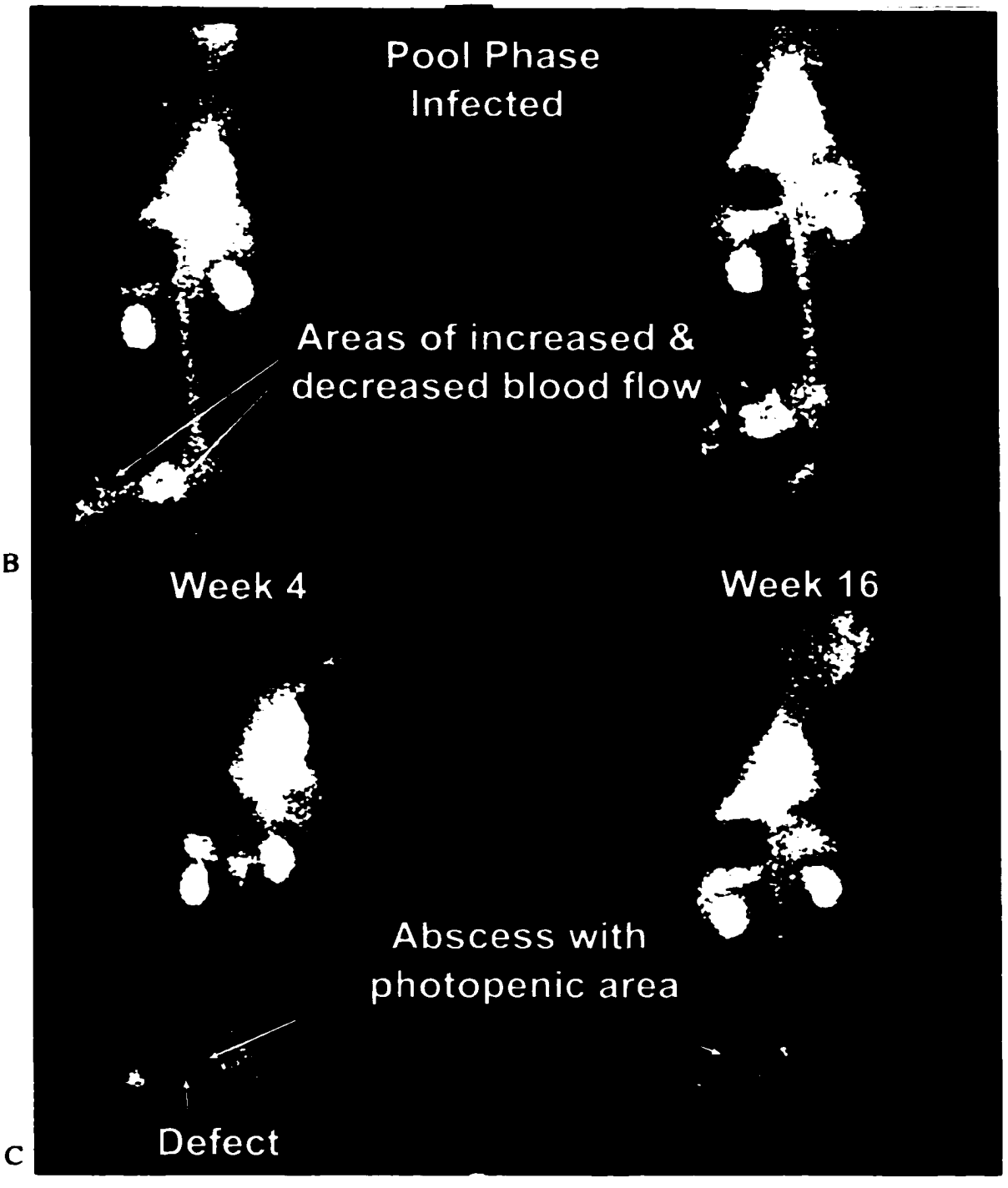

Figure 8. Lateromedial views of pool-phase scan using technetium-labeled ciprofloxacin (Tc-CIPRO) at 4 (left) and 16 (right) weeks after surgery. B and C are infected rabbits. There was mixed areas of increased and decreased blood flow in infected rabbits. Although Tc-CIPRO penetrates abscesses, they appeared as photopenic areas on the scan. The defect ROI had a decrease in blood flow and therefore there was no increase in Tc-CIPRO uptake ratio in infected rabbits.

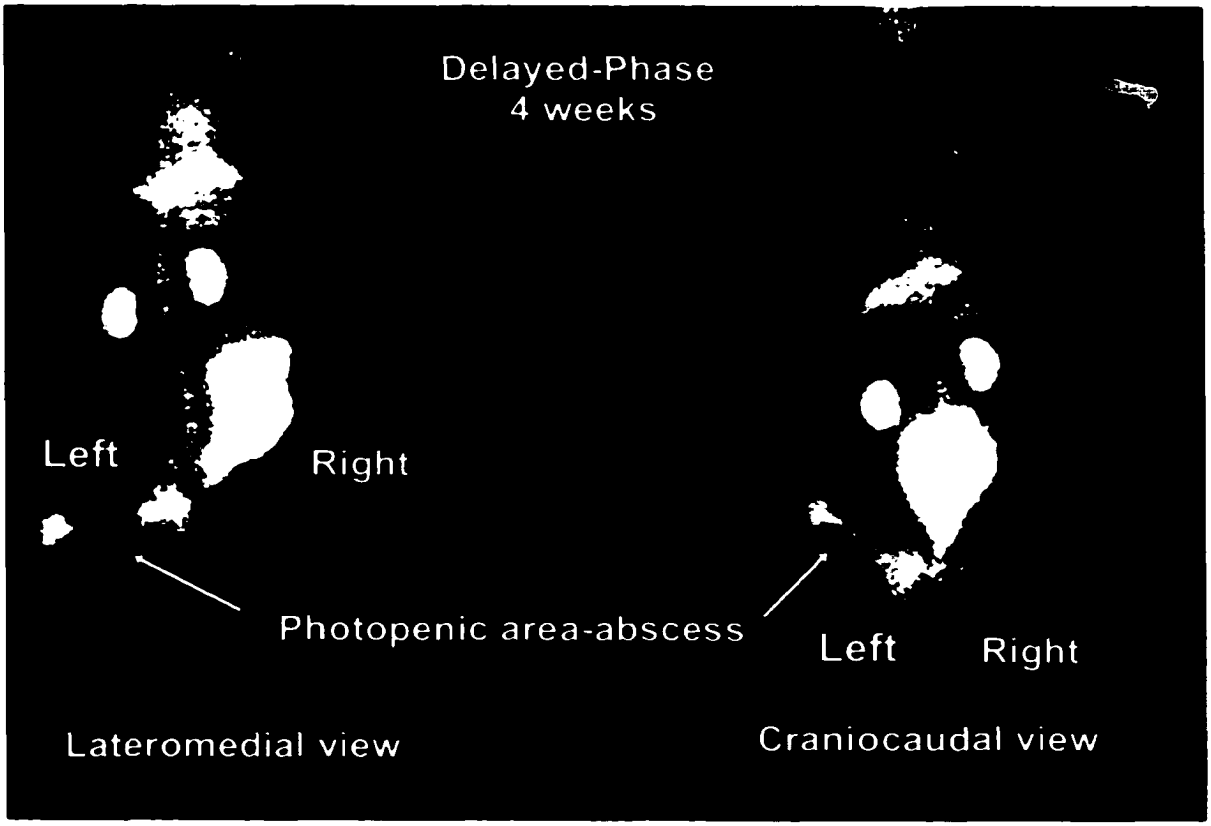

Figure 9. Lateromedial and craniocaudal views of delayed-phase scan using technetium-labeled ciprofloxacin (Tc-CIPRO) of an infected rabbit (Figure 8c) 4 weeks after surgery. There is a photopenic area in the defect ROI, which is most likely a result of decreased blood flow associated with abscessation.

The results were then re-analyzed using the whole bone L:R ROI by subtracting the pool-phase ratio from the delayed-phase ratio. and by dividing the delayed-phase ratio by the pool-phase ratio. The difference between infected and non-infected rabbits did not change at 4 weeks (Figure 10a,b). The ratio of delayed- to pool-phase for non-infected rabbits was greater than one. and the difference between delayed- and pool-phase for non-infected rabbits was greater than zero. This means that although an increase in blood flow was a contributing factor. it was not the only reason for an increase in uptake ratio of Tc-CIPRO at 4 weeks in non-infected rabbits.

The change in significance with time may be a result of a true increase in uptake in the numerator ROI in infected rabbits or a decrease in non-infected rabbits. a decrease or increase in uptake in the denominator ROI. or a change in the area of the ROI. The ratio of the lumbar vertebra to the control femur increased with time; therefore there was either an increase in uptake in the lumbar vertebra and/or a decrease in uptake ratio in the right femur with time in both infected and non-infected rabbits. The ratio of the lumbar vertebra to control femur was lower in infected rabbits at 8. 12. and 16 weeks; therefore infected rabbits had a higher uptake in the contralateral femur or lower uptake in the lumber vertebra than non-infected rabbits. However, the results were similar using the contralateral femur and the lumbar vertebra as the denominator ROI. There was no change with time or infection with the ratio of the left to right tibia.

There was a significant association between the ratio of the area of the whole bone L:R and time and infection. Infected rabbits had a greater ratio at all time periods on the lateromedial view and at 12 weeks on the craniocaudal view. The ratio of whole bone L:R area decreased with time on both views. Because of the variation in area, this may

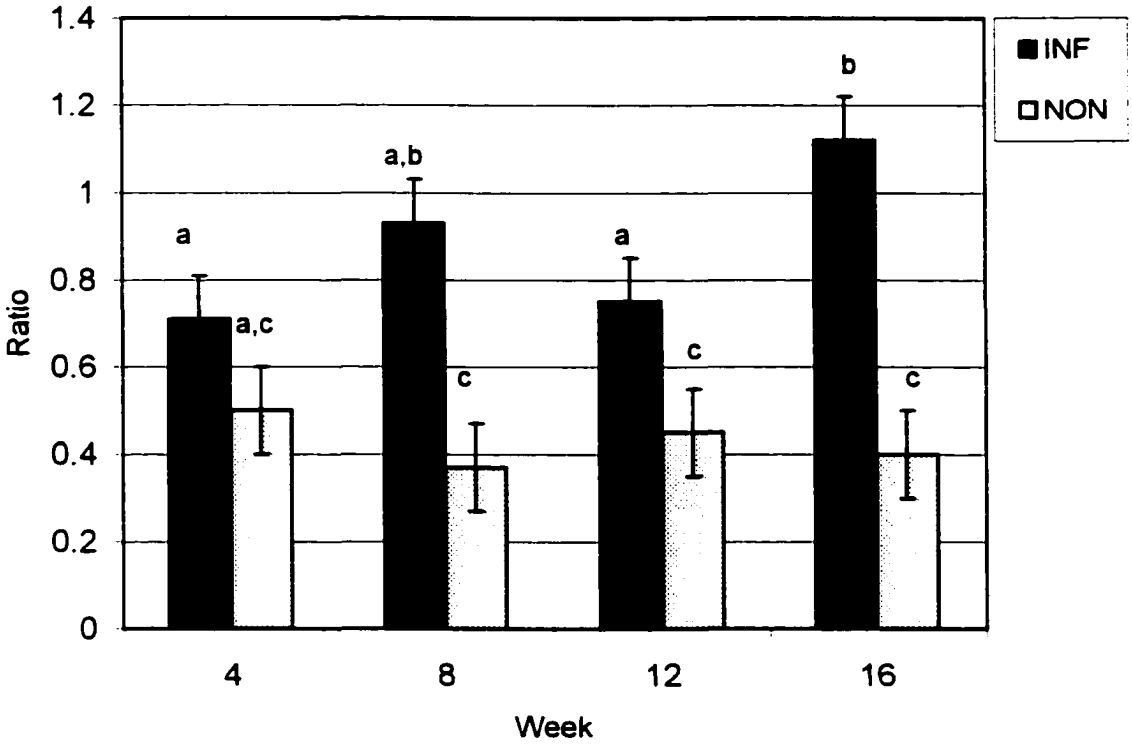

Figure 10A. A plot illustrating the association between infection and pool-phase subtracted from the delayed-phase technetium-labeled ciprofloxacin (Tc-CIPRO) uptake ratio for the whole bone L:R ROI on the lateromedial view. The uptake ratio is shown on the y-axis, the time after surgery is shown on the x-axis, and infected rabbits are represented with black bars and non-infected rabbits with gray bars. Data are presented as least squared means of the uptake ratio +/- standard error of the mean. Different letters represent statistically significant differences.

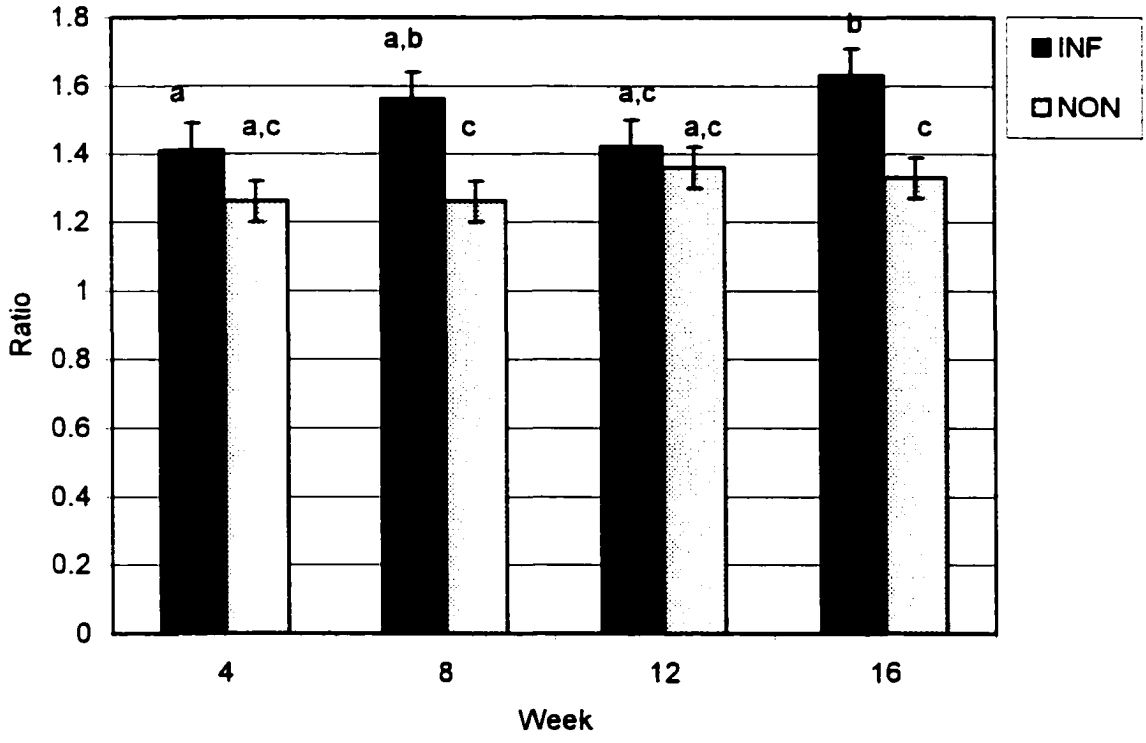

Figure 10B. A plot illustrating the association between infection and the delayed-phase divided by the pool-phase technetium-labeled ciprofloxacin (Tc-CIPRO) uptake ratio for the whole bone L:R ROI on the lateromedial view. The uptake ratio is shown on the y-axis, the time after surgery is shown on the x-axis, and infected rabbits are represented with black bars and non-infected rabbits with gray bars. Data are presented as least squared means of the uptake ratio +/- standard error of the mean. Different letters represent statistically significant differences.

have altered the average uptake values; therefore the maximum and minimum values were for the whole bone L:R and defect L:R were analyzed. There was no difference in the ratios between infected and non-infected rabbits in the maximum or minimum value at 4 weeks in the defect L:R ROI on either view. The maximum and minimum values in the infected rabbits increased with time and the non-infected rabbits decreased with time, and the results became significant after 4 weeks. Using the whole bone L:R ROI, infected rabbits had a higher maximum value at all time periods on both views; however, the minimum value was only higher in infected rabbits on the lateromedial view at 16 weeks. The maximum value decreased over time in the non-infected rabbits on the lateromedial view only.

Overall, there was a significant correlation between lysis grade and uptake ratio for Tc-CIPRO. The correlation was higher for the whole bone numerator ROI, and higher for the lateromedial than the craniocaudal view (r^2=0.7). There was no correlation at 4 weeks and the correlation increased with time. There was a significant association between lysis grade uptake ratio of Tc-CIPRO (Figure 11a,b). The uptake ratio in the whole bone L:R ROI decreased in rabbits with no radiographic lysis and increased with time in rabbits with lysis grades 2 and 3.

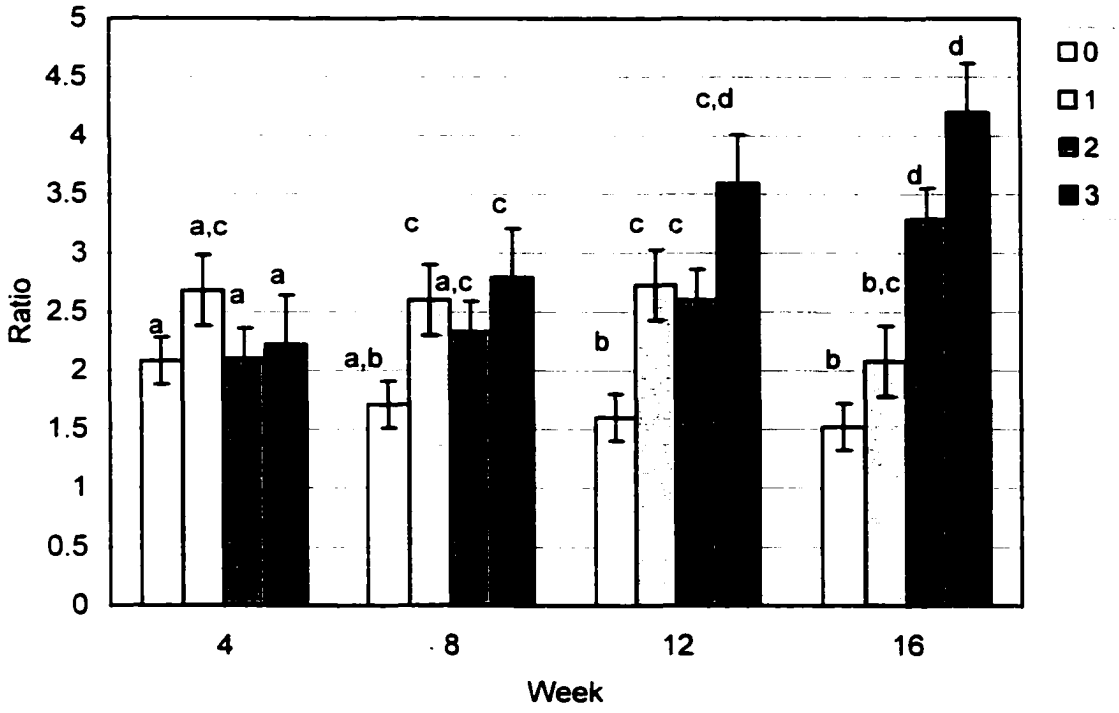

Figure 11A. A plot illustrating the association between lysis grade and the delayed-phase technetium-labeled ciprofloxacin uptake ratio of the defect L:R region of interest (ROI) on the lateromedial view. The uptake ratio is shown on the y-axis, the time after surgery is shown on the x-axis, and the lysis grades (0=none, 1=slight, 2=mild, 3=moderate) is represented by white, light gray, dark gray, and black bars. Data are presented as least squared means of the uptake ratio +/- standard error of the mean. Different letters represent statistically significant differences.

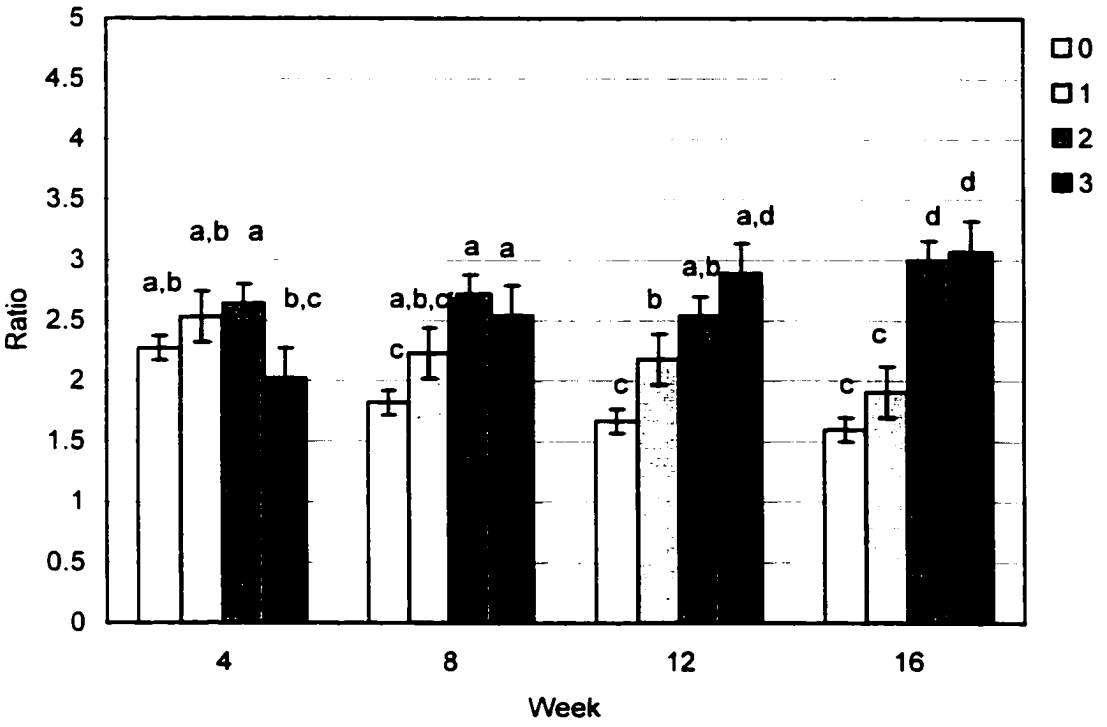

Figure 11B. A plot illustrating the association between lysis grade and the delayed-phase technetium-labeled ciprofloxacin uptake ratio of the whole bone L:R region of interest (ROI) on the lateromedial view. The uptake ratio is shown on the y-axis, the time after surgery is shown on the x-axis, and the lysis grades (0=none, 1=slight, 2=mild, 3=moderate) is represented by white, light gray, dark gray, and black bars. Data are presented as least squared means of the uptake ratio +/- standard error of the mean. Different letters represent statistically significant differences.

There was no correlation or association between uptake ratio and defect ossification or callus formation. There was no overall association between treatment group and Tc-CIPRO uptake ratios, except on the craniocaudal views there was an interaction between treatment group and time; rabbits in the BMP treated group had a significantly higher uptake ratio at 16 weeks on the defect L:R ROI, and at 4 and 16 weeks on the whole bone and proximal L:R ROI. The three rabbits that were euthanized after week 4 were in the BMP treated group; therefore the change over time may have been a result of the loss of these rabbits. However, when these rabbits were excluded from the analysis the results were still significant. There was no three-way interaction between infection, treatment, and time; hence these findings were not a result of an interaction with infection. Therefore this was most likely a result of an increase in blood flow in the BMP treated rabbits; the pool-phase was performed on the lateromedial view only and there was only a slight trend for BMP treated rabbits to have a higher ratio, consequently this assumption could not be confirmed.

Because of the concern with blood pool-phase not having been cleared at 2 hours, three rabbits were rescanned 3 hours after injection to determine if there was a difference between the 2- and 3-hour scans. Subjectively the images appeared identical, and this was supported by the uptake ratios of the defect L:R and whole bone L:R (Table 5). The CV for the difference between 2 and 3 hours is within the CV range for the Tc-CIPRO scan.

Table 5. Ratios of the defect L:R and whole bone L:R regions of interest at 2 and 3 hours after injection with the technetium-labeled ciprofloxacin.

Group	Time (hours)	Defect L:R	Coefficient of Variation	Bone L:R	Coefficient of Variation
NONLUC	2	2.19	1.0	2.67	6.9
	3	2.16		2.42	
INFLUC	2	1.71	3.8	2	3.6
	3	1.62		1.90	
INFBMP	2	1.81	4.9	2.08	4.6
	3	1.94		2.22	

Discussion

The results of this study showed that Tc-PO was able to differentiate infected from non-infected fractures in the late phase of fracture healing. Although Tc-CIPRO was better than Tc-PO at identifying the presence of infection, there was a high incidence of false positive results and when the defect, which was the site of inoculation, was evaluated there was no difference between infected and non-infected rabbits at 4 weeks. Technetium-PO could only be used to predict bridging callus formation at 4 weeks and although the specificity was high, the sensitivity was low; this may be explained by the small number of animals with bridging callus. There was only a correlation between Tc-PO uptake ratio and defect ossification after 4 weeks. As expected there was no association between Tc-CIPRO and defect ossification or callus formation.

The lack of association between the presence or absence of infection and the uptake ratio on the Tc-PO scan at 4 weeks may be explained by a relative lack of bone formation in infected rabbits at 4 weeks. Serum bone marker concentrations were measured concurrently with nuclear scintigraphy imaging and at 4 weeks there was a decrease in the concentration of markers of bone formation (osteocalcin (OC) and bone-specific alkaline phosphatase (BS-ALP)) in infected rabbits (Chapter 5). The increase in uptake ratio with Tc-PO in the late phase of fracture healing is supported by the OC concentration being higher in infected rabbits at 16 weeks (Chapter 5). Although it was not statistically significant, there was a decrease in Tc-PO uptake ratio with increase in lysis grade at 4 weeks. Similarly, there was a decrease in BS-ALP concentration with increase in lysis grade at 4 weeks (Chapter 5). In addition to the decreased bone formation in infected rabbits, there was an increase in bone metabolism and blood flow in

non-infected rabbits during the early phase of fracture healing. The uptake of Tc-PO is dependent on blood flow as well as bone metabolism and there was an increase in blood flow (pool-phase) in both the infected and non-infected fractures early in fracture healing resulting in a higher uptake ratio in the delayed-phase of the Tc-PO scan. It could also be argued that the low serum marker concentration in infected rabbits at 4 weeks was a result of a relative decrease in blood flow to the area in infected rabbits. However, the marker of bone resorption (deoxypyridinoline crosslinks) was increased in infected rabbits and there was no difference between infected and non-infected rabbits in the pool-phase uptake ratio. Therefore, Tc-PO is useful for diagnosing osteomyelitis in the late phase of fracture healing but not in the early phase.

Other studies have also found that Tc-PO is beneficial for diagnosing osteomyelitis in late infection. Spinelli et al[57] found that Tc-PO could be used to diagnose infection following total hip arthroplasty 6 to 8 months after surgery, however prior to 6 to 8 months surgical trauma and thermal necrosis of the bone resulted in an increase in uptake ratio in non-infected arthroplasties. Most authors have concluded, however, that a negative Tc-PO scan can be used to rule-out infection.[57-59] As in our study, patients with infection in previous studies had an increase in uptake ratio with time whereas non-infected patients had a decrease in uptake ratio with time.[26,57] Some studies have reported that a focal area of increased uptake was more consistent with infection[57] whereas other studies reported that a diffuse uptake is consistent with infection and a focal uptake is consistent with aseptic loosening of the prosthesis.[58] However, other studies have reported that aseptic loosening and fracture adjacent to the prosthetic are indistinguishable from infection using Tc-PO scans.[57,58] Despite the lack of specificity,

Tc-PO could identify infected arthroplasties prior to radiographic signs.[26] In our study, lysis was identified in some rabbits at 4 weeks; however, the mean lysis grade was not greater than 1 (slight) until 12 weeks (Chapter 3). The differentiation of soft tissue from bone infection is also important in postoperative evaluation of fractures. The use of the delayed-phase of the Tc-PO scan to differentiate cellulitis from osteomyelitis has been previously reported.[9,31-36] Although further evaluation of the use of Tc-PO to differentiate soft tissue infection from osteomyelitis after fracture repair is needed, this could not be evaluated in the current study because all of the infected rabbits had both soft tissue infection and osteomyelitis.

Although the lack of specificity for the Tc-PO scan was expected, the lack of specificity early in fracture healing with the Tc-CIPRO is difficult to explain. Ciprofloxacin should bind specifically to the bacterial DNA gyrase of living bacteria and both technetium and ciprofloxacin have low protein binding; therefore the blood-pool phase should be rapidly cleared[60] resulting in a high uptake ratio in infected rabbits only.

While the overall accuracy was similar for objective and subjective analyses, the rabbits that were incorrectly classified as infected on the subjective analysis were different from those incorrectly classified based on the objective analysis, and the specificity was high on the objective analysis and the sensitivity low. This appeared to be because the ratio that was used to define infection for the objective analysis was high because of the high values for the non-infected rabbits.

Previous studies[52-56] have reported a high specificity (greater than 90%) and sensitivity (70 to 84%) for diagnosing infection with Tc-CIPRO. The specificity and sensitivity in our study, at 4 weeks, was lower than previously reported. [52-56] There were

several limitations, however, with these previous studies. [52-56] Firstly, the definition of infection was not well defined;[52,54] for example, one study had human patients with a negative culture classified as infected if they were treated as infected by the attending physician and the criteria used by the attending physician were not described. Secondly, the specificity and sensitivity for diagnosing infection in patients with osteomyelitis at a fracture site could not be determined from these studies because all cases of osteomyelitis were classified together, and one study did report false positive results in patients with fracture.[53] Finally, the specificity and sensitivity are dependent on the number of animals with or without the disease and the high specificity in other studies may be due to higher numbers of animals with the disease.[47]

The false positive results obtained early in fracture healing in our study may have been a result of several factors. Surgery and in particular the use of a sclerosing agent caused inflammation. Infection and inflammation both result in vasodilation, increase in vascular permeability, expansion of the extracellular space, and an increase in leukocyte accumulation, all of which may result in an increase in non-specific accumulation of Tc-CIPRO. The uptake ratio in the pool-phase was not different between infected and non-infected rabbits at 4 weeks: therefore this may have contributed to the false positive results in the non-infected rabbits. Similar studies have reported an increase in uptake with an increase in blood flow using other Tc-labeled pharmaceuticals. Thrall et al[61] reported an extended pattern with Tc-PO in which the increase in uptake extended beyond the lesion, and the cause was though to be increase in blood flow to the region. Other authors have emphasized the importance of bone blood flow in determining the uptake patterns for technetium–labeled agents[62] and that positive images reflect the

distribution of the radiolabel rather than the pharmaceutical to which it is attached.[30] However, when the pool-phase was subtracted from the delayed-phase Tc-CIPRO scan, the non-infected rabbits still had a ratio above zero and there was still no significant differences between infected and non-infected rabbits at 4 weeks. Therefore in addition to an increase in blood flow to the fracture site, which would have delivered more Tc-CIPRO, there was a decrease in elimination of the Tc-CIPRO from the fracture site.

The decrease in elimination may have been a result of decrease in venous and lymphatic drainage associated with inflammation and accumulation of Tc-CIPRO in edema fluid, or the Tc-CIPRO may have bound to something other than the bacteria. Using microradiography, studies evaluating radiolabeled IgG, which binds specifically to inflammatory cells, found non-specific uptake through increased vascular permeability and accumulation in edema fluid rather than specific uptake associated with inflammatory cells.[63] There may have been non-specific accumulation of Tc-CIPRO in the non-infected rabbits in our study and further evaluation of Tc-CIPRO accumulation using microradiography is required. Ciprofloxacin concentrates in bone and phagocytic cells.[59] therefore, may also accumulate in sterile inflammation of bone such as occurs with a fracture. Although accumulation of unassociated technetium may have also been the cause of the increase in uptake in non-infected rabbits this is unlikely because technetium is covalently bound the pharmaceutical and there is a low dissociation rate.

Using the whole bone ROI, there was an increase in maximum uptake in infected rabbits and infected rabbits had an increase in uptake ratio in the proximal fragment L:R ROI at all time periods. The pattern of uptake was different in infected and non-infected rabbits; infected rabbits had mixed areas of increased and decreased uptake whereas non-

infected rabbits had a more uniform uptake pattern. Therefore, if only the area of the highest uptake (such as the proximal fragment) is used rather than a defined region (such as the whole bone) then Tc-CIPRO may be useful for early diagnosis of infection. The use of colored scintigraphy[56] may be more useful to demonstrate a higher maximum value with infection. This means that the lack of significance in the whole bone L:R ROI at 4 weeks on the lateromedial view could be attributed to a greater area ROI, which resulted in inclusion of regions with a lower uptake. However, at 4 weeks there was no difference in the maximum and minimum uptake values between infected and non-infected rabbits in the defect ROI; this suggests that the lack of significant difference in the defect region was real and most likely attributed to a decrease in blood flow.

The delayed-phase scan was performed at 2 hours. Increasing the time from injection to scanning may have resulted in an increase in uptake ratio in infected rabbits and a decrease in uptake ratio in non-infected rabbits as a result of clearing of non-specifically bound Tc-CIPRO. Scanning was repeated at 3 hours and there was no difference between the 2- and 3-hour scans. Technetium has a short half-life (6 hours) and rapid urinary excretion therefore if scanning is delayed for 24 to 72 hours to allow for adequate clearance of the non-specifically bound Tc-CIPRO the radionuclide has decayed. In another study evaluating radiolabeled antibiotics, tetracycline was used to scan for abscesses because it has an affinity for necrotic cells and was labeled with iodine (I)-131 rather than technetium-99m because the longer half-life of I-131 would permit 72 hour imaging when the lesion to background ratio is higher.[64] A delayed-phase Tc-CIPRO scan has been performed successfully at 24 hours in horses for diagnosis of vertebral osteomyelitis; however, the amount of technetium administered to a horse is

large and therefore can still be detected with the gamma camera at 24 hours. Further, because of the large soft tissue mass in the horse, a longer time is required for soft tissue clearance of the unbound radionuclide. Therefore labeling antibiotics with a longer half-life would allow scanning to be performed at a later time when the soft tissue and blood are cleared of unbound ciprofloxacin.

Rabbits were inoculated in the defect and there was no difference in Tc-CIPRO uptake ratio between infected and non-infected rabbits at 4 weeks using the defect ROI; that is, when the defect L:R ROI was evaluated there were false negative results in the infected rabbits. This was associated with a decrease in blood flow to the defect region as shown on the pool-phase scan. Therefore, false negative results may occur from reduced blood flow. In our model the soft tissue, periosteum, endosteum, and bone marrow were removed from the bone during surgery, and a sclerosing agent was used in the defect to prevent healing, therefore a decreased blood flow to the defect would be expected. Additionally, there was abscess formation in and adjacent to the fracture defect in all infected rabbits, which may also have caused a decrease in uptake of Tc-CIPRO. Absessation, ischemia, and necrosis result in an area of relative photopenia.[33] Ciprofloxacin has good penetration into abscesses, however abscesses contain predominantly dead bacteria therefore Tc-CIPRO shows a diffuse increase in uptake around the abscess as seen in our study.[52]

Technetium-PO was useful for evaluating callus formation and defect ossification. The OC followed a similar trend to Tc-PO4 uptake ratios, in that the rabbits with the bridging callus (grade-4) had a higher OC concentration and Tc-PO uptake ratio during the early phase of fracture healing (4 weeks) and then a lower ratio compared to rabbits

with grade-2 and –3 callus thereafter because bridging callus had formed. Rabbits with grade-1 callus (non-union) had almost no radiographic signs of bone formation and a persistently low uptake of Tc-PO and rabbits with grade-2 and –3 callus had radiographic signs of proliferation without bridging callus and the uptake of Tc-PO continued to increase throughout the study in these rabbits. Our results were similar to other studies, in that the normal union reached a peak at 8-12 weeks and then declined, whereas rabbits in the delayed or non-union group remained elevated. The time scale with this study may be difficult to compare to clinical cases because of the severity of the model and the rabbits healed by bridging callus rather than defect ossification.

There was a change in the relationship between the denominator ROIs with time. This was attributed to either a change in bone metabolism or blood flow; the pool-phase scan was used to assess the amount of increased uptake that was associated with blood flow. Alterations in gait and activity may have caused changes in uptake in different parts of the skeleton, particularly the contralateral limb and lumbar vertebra, as a result of change in bone metabolism as well as change in blood flow. The decrease in uptake ratio of the L:R tibia with time was attributed to an increase in bone metabolism, because there was no change on the pool-phase scan. This could be a result of an increase in weight bearing on the right limb and a decrease in weight bearing the left limb; or an initial response in the left tibia to infection and fracture, which subsided with time. The higher uptake on the left tibia in infected rabbits may be associated with a bone response to infection. Further superimposition of the operated femur over the left ischium, blood flow to the operative limb, and a possible response of adjacent bones (ischium and tibia) to the operated femur may have also caused a change in uptake in the control bones with time.

The uptake ratio on the craniocaudal view was more significant for infection than the lateromedial view. Possible reasons for this were superimposition of the plate or abscess formation on the lateral aspect of the limb resulting in attenuation of the gamma rays: however. the ratios on the lateromedial view were higher than those on the craniocaudal view.

The results of this study underscore the challenge of assessing fracture healing and early diagnosis of osteomyelitis in postoperative fractures. Labeling of numerous other agents are currently being investigated,[65] and ultimately development of simultaneous dual radionuclide techniques incorporating computer subtraction may be most useful for diagnosing the presence of osteomyelitis in patients following fracture repair.[66]

References

1. Auer JA, Watkins JP. Treatment of radial fractures in adult horses: An analysis of 15 clinical cases. Equine Vet J 1987; 19: 103-110.
2. Sanders-Shamis M, Bramlage LR, Gable AA. Radius fractures in the horse: A retrospective study of 47 cases. Equine Vet J 1986; 18:432-437.
3. Crawford WH, Fretz PB. Long bone fractures in large animals. A retrospective study. Vet Surg 1985; 14:295-302.
4. Hance SR, Bramlage LR, Schneider RK, Embertson RM. Retrospective study of 38 cases of femur fractures in horses less than one year of age. Equine Vet J 1992; 24:357-363.
5. Yelin E, Callahan LF. The economic cost and social and psychological impact of musculoskeletal conditions. Arthritis Rheum 1995; 38:1351-1362.
6. Praemer A, Furner S, Rice DP. Musculoskeletal conditions in the United States. Park Ridge IL, Am Acad Orthop Surg, 1992, p85-124.
7. Johnson EE, Urist MR, Finerman AM. Resistant nonunion and partial or complete segmental defects of long bones. Clin Orthop Rel Res 1992; 277:229-237.
8. Spangehl MJ, Younger ASE, Masri BA, Duncan CP. Diagnosis of infection following total hip arthroplasty. J Bone Joint Surg 1997; 79A:1578-1588.
9. Letts RM, Afifi A, Sutherland JB. Technetium bone scanning as an aid in the diagnosis of atypical acute osteomyelitis in children. Surg Gynecol Obstet 1975; 140:899-902.
10. Munoz P, Bouza E. Acute and chronic adult osteomyelitis and prosthesis-related infections. Bailliere's Clinical Rheumatology 1999; 13:129-147.

11. Tiel-van Buul MMC, Roolker W, Verbeeten BWB, Broekhuizen AH. Magnetic resonance imaging versus bone scintigraphy in suspected scaphoid fracture. Eur J Nucl Med 1996; 23:971-975.

12. Buscombe J. The challenge of nuclear medicine. British J Hosp Med 1995; 54: 68-69.

13. Bauer GCH, Lindberg L, Naversten Y, Sjöstrand L-O. ^{85}Sr radionuclide scintimetry in infected total hip arthroplasty. Acta Orthop Scand 1973; 44:417-425.

14. Segmuller G, Cech O, Bekier AM. Diagnostic use of Sr-85 in the preoperative evaluation of non-union. Acta Orthop Scand 1970; 41:150.

15. Wendeberg B Mineral metabolism of fractures of the tibia in man studied with external counting of Sr85. Acta Orthop Scand 1961; S52:135.

16. Asnis SE, Shoji H, Bohne WHO. Scintimetric evaluation of complications after femoral neck fractures. Clin Orthop Rel Res 1976; 121:149-156.

17. Feith R, Slooff TJJH, Kazem I, van Rens TJG. Strontium 87m bone scanning for the evaluation of total hip replacement. J Bone Joint Surg 1976; 58B:79-83.

18. Muheim G. Assessment of fracture healing in man by serial 87mstrontium-scintimetry. Acta Orthop Scand 1973; 44: 621-627.

19. Johannsen A. Fracture healing controlled by 87m-Sr uptake. Acta Orthop Scand 1973; 44:628-639.

20. McGrail JW, Vulpetti AT, Shifrin LZ. 18F scintigraphy of non-neoplastic skeletal lesions. Clin Orthop Rel Res 1974; 101:292-298.

21. Fueger GF, Tscherne H, Schwarz G, Szyszkowitz R. Szintigraphische untersuchungen mit 87m-strontium-zitrat zur Beurteilung der Frakturheilung. In Glauner R (Ed): Angiologie und Szintigraphie bei Knochen- und Gelenkerkrankungen. Stuttgart, Georg Thieme Verlag, 1971; p133-143.

22. Hughes S. Radionuclides in orthopaedic Surgery. J Bone Joint Surg 1980; 62B:141-150.

23. Subramanian G, McAfee JG, Blair RJ, Kallfelz FA, Thomas FD. Technetium-99m-methylene diphosphonate-a superior agent for skeletal imaging: comparison with other technetium complexes. J Nucl Med 1975; 16:744-755.

24. Hendler A, Hershkop M. When to use bone scintigraphy. It can reveal things other studies cannot. Bone Scint 1998; 104:54-61.

25. Rosenthall L, Lisbona R, Hernandez M, Hadkipavlou A. 99mTc-PO4 and Ga-67 imaging following the insertion of orthopaedic devices. Radiol 1979; 133:717-721.

26. Tilden RL, Jackson J, Enneking WF, DeLand FH, McVey JT. 99mTc-polyphosphonate: Histological localization in human femurs by autoradiography. J Nucl Med 1973; 14:576.

27. Hadjipavlou A, Lisbona R, Rosenthall L. Difficulty of diagnosing infected hypertrophic pseudoarthrosis by radionuclide imaging. Clin Nucl Med 1983; 3:45-49.

28. Markel MD, Snyder JR, Hornof WJ, Meagher DM. Nuclear scintigraphic evaluation of third metacarpal and metatarsal bone fractures in three horses. J Am Vet Med Assoc 1987; 191:75-77.

29. Creutzig H. Bone imaging after total replacement arthroplasty of the hip joint. Eur J Nucl Med 1976; 1:177-180.

30. Peters AM. The use of nuclear medicine in infections. Br J Radiol 1998; 71: 252-261.

31. Lisbona R, Rosenthal L. Observations on the sequential use of 99m-Tc-phosphate complex and 67Ga imaging in osteomyelitis, cellulites, and septic arthritis. Radiol 1977; 123:123-129.

32. Gilday DL, Paul DJ, Paterson J. Diagnosis of osteomyelitis in children by combined blood pool and bone imaging. Radiol 1975; 117:331-335.

33. Treves S, Khettry J, Broker FH, Wilkinson RH, Watts H. Osteomyelitis: Early scintigraphic detection in children. Pediatrics 1976; 57: 173-186.

34. Gelfand MJ, Silberstein EB. Radionuclide Imaging. Use in diagnosis of osteomyelitis in children. J Am Med Assoc 1977; 237: 245-247.

35. Atcheson SG, Coleman RE, Ward JR. Septic arthritis mimicking cellulitis: Distinction using radionuclide bone imaging. Clin Nucl Med 1979; 4:79-81.

36. Lutzker LG, Koenigsberg M, Freeman LM. Focal bone pain. Infection or infarction? J Am Med Assoc 1976; 235:425-426.

37. Palestro CJ. The current role of gallium imaging in infection Semin Nucl Med 1994; 24:128-141.

38. Deysine M, Rafkin H, Russell R, Teicher I, Aufses AH. The detection of acute experimental osteomyelitis with 67Ga citrate scanning. Surg Gynecol Obstet 1975; 141:40-42.

39. Deysine M, Robinson R, Rafkin H, Teicher I, Silver L, Aufses AH. Clinical infections detected by 67Ga scanning. Ann Surg 1974; 180:897-901.

40. Deysine M, Rafkin H, Teicher I, Silver L, Robinson R, Manly J, Aufses AH. Diagnosis of chronic and postoperative osteomyelitis with gallium 67 citrate scans. Am J Surg 1975; 129:632-635.

41. Oyen WJG, Corstens FHM. Scintigraphic techniques for delineation of infection and inflammation. Br J Hosp Med 1995; 54:75-80.

42. Merkel KD, Brown ML, Dewanjee MK, Fitzgerald RH. Comparison of indium-labeled-leukocyte imaging with sequential technetium-gallium scanning in the diagnosis of low grade musculoskeletal sepsis. A prospective study. J Bone Joint Surg 1985; 67(A):465-76.

43. Seabold JE, Napola JV, Conrad GR, Marsh JL, Montgomery WJ, Bricker JA, Kirchner PT. Detection of osteomyelitis at fracture non union sites: comparison of two scintigraphy methods. Am J Roentenol 1989; 152: 1021-7.

44. Schauwecker DS. Osteomyelitis: Diagnosis with In-111-labeled leukocytes. Radiol 1989; 171: 141-146.

45. Datz FL. Indium-111 labeled leukocytes for the detection of infection: Current status. Semin Nucl Med 1994; 24:92-109.

46. Ali SA, Cesani F, Nusynowitz ML, Briscoe EG, Shirtliff ME, Mader JT. Skeletal scintigraphy with technetium-99m-tetraphenyl porphyrin sulfonate for the detection and determination of osteomyelitis in an animal model. J Nuclear Med 1997; 38:1999-2002.

47. Rüther W, Hotze A, Moller F, Böckisch A, Heitzmann P, Diersack HJ. Diagnosis of bone and joint infection by leucocyte scintigraphy. Arch Orthop Traum Surg 1990; 110:26-32.

48. Aktolun C, Ussov WY, Arka A, Glass D, Gunasekera RD, Peters AM. Technetium-99m and indium-111 double labeling of granulocytes for kinetic and clinical studies. Eur J Nucl Med 1995; 22:330-334.

49. Long CD, Galuppo LD, Waters NK, Hornof WJ. Scintigraphic detection of equine orthopedic infection using Tc-HMPAO labeled leukocytes in 14 horses. Vet Radiol Ultrasound 2000; 41:354-359.

50. Morrel EM, Tompkins RG, Fischman AJ, Wilkinson RA, Yarmush ML. Imaging infections with antibodies. J Immunol Methods 1990; 130:39-48.

51. Oyen WJG, Claessens AMJ, Van der Meer JWM, Rubin RH, Strauss HW, Corstens FHM. Indium-111 labeled human non-specific immunoglobulin G: a new radiopharmaceutical for imaging infectious and inflammatory foci. Clin Infect Dis 1992; 14:1110-1119.

52. Britton KE, Vinjamuri S, Hall AV, Solanki K, Siraj QH, Bomanji J, Das S. Clinical evaluation of technetium-99m infecton for the localisation of bacterial infection. Eur J Nucl Med 1997; 24:553-556.

53. Hall AV, Solanki KK, Vinjamuri S, Britton KE, Das SS. Evaluation of the efficacy of 99mTc-Infecton, a novel agent for detecting sites of infection. J Clin Pathol 1998; 51:215-219.

54. Jayaraman S, Al-Nahhas AM, Vivian G, Gilbert TJ, Hughes PM. Demonstration of spinal osteomyelitis with Ga-67 citrate, Tc-99m MDP, and Tc-99m

ciprofloxacin wit provisionally negative results of MRI. Clin Nucl Med 2000; 25:224-226.

55. Vinjamuri S, Hall AV, Solanki KK, Bomanji J, Siraj Q, O'Shaughnessy EO, Das SS, Britton KE. Comparison of 99mTc-infecton with radiolabeled white cell imaging the evaluation of bacterial infection. Lancet 1996; 347-233-5, 1996.
56. Amaral H, Morales B, Pruzzo R, Britton KE. Cold-hot mismatch between Tc-99m HMPAO-labeled leukocytes and Tc-99m ciprofloxacin in axial skeleton infections: a report of three cases. Clin Nucl Med 1999; 24:855-888.
57. Spinelli R. The role of scintigraphy in the diagnosis of late complications of total prosthesis of the hip. Italian J Orthop Traum 1975; 2:79-87.
58. Williamson BRJ, McLaughlin RE, Wang GJ, et al. Radionuclide bone imaging as a means of differentiating loosening and infection in patients with a painful total hip prosthesis. Radiol 1979; 133:723-725.
59. Williams ED, Tregonning RJ, Hurley PJ. 99Tcm-diphosphonate scanning as an aid to diagnosis of infection in total hip joint replacements. Br J Rad 1977; 50:562-566.
60. Beard LA: Ch 4.1 Principles of antimicrobial therapy. In Reed SM and Bayly WM. Equine Internal Medicine, Philadelphia, WB Saunders, 1998, p157-187.
61. Thrall JH, Geslien GE, Corcoron RJ, Johnson MC. Abnormal radionuclide deposition patterns adjacent to focal skeletal lesions. Radiol 1975; 115:659-663.
62. Genant HK, Bautocich GJ, Singh M, Lathrop KA, Harper PV. Bone-seeking radionuclides: and *in vivo* study of factors influencing skeletal uptake. Radiol 1974; 113:373-382.

63. Oyen WJG, Claessens RAMJ, Van der Meer JWM, Corstens FHM. Biodistribution and kinetics of radiolabeled proteins in rats with focal infection. J Nucl Med 1992; 33:388-394.

64. Hagan PL, Taylor A, Chauncey DM, Schelbert H. Comparison of 131I-tetracycline and 67Ga-citrate as abscess localizing agents. Nucl Medizin 1977; 16:76-78.

65. Oyen WJG, Corstens FHM. Scintigraphic techniques for delineation of infection and inflammation. Br J Hospital Med 1995; 54:75-80.

66. Sloboda RS. Subtraction of simultaneously acquired dual radionuclide images. Medical Physics 1986; 13:723-727.

CHAPTER 5

EVALUATION OF SERUM BONE MARKERS FOR EARLY DIAGNOSIS OF NON-UNION AND INFECTED NON-UNION

Abstract

Objective: The objective of this study was to evaluate the use of the serum bone markers, osteocalcin (OC), bone-specific alkaline phosphatase (BS-ALP), and deoxypyridinoline crosslinks (DPYR) for assessing fracture healing. Our hypothesis was that markers of bone formation (OC and BS-ALP) would be higher in rabbits that healed compared to rabbits that developed a non-union, and that the marker of bone resorption (DPYR) would be higher in infected compared to non-infected rabbits.

Materials and Methods: Thirty-two skeletally mature New Zealand White rabbits were used. This study was part of a larger study evaluating the use of adenoviral transfer of bone morphogenetic-2 gene (Ad-BMP-2) for enhancing fracture healing in an infected non-union model (Chapter 3). A rabbit femoral fracture defect stabilized with bone plates and cortical screws was the basic model. Experimental groups were: (1) non-union Ad-Luciferase (LUC) control, (2) non-union Ad-BMP-2 treated, (3) infected non-union Ad-LUC control, and (4) infected non-union Ad-BMP-2 treated. Serum was collected preoperatively, and 4, 8, 12, and 16 weeks postoperatively. Serum was analyzed for OC, BS-ALP, and DPYR using commercially available kits. Radiographic external callus and lysis grades at 16 weeks were used in the analysis. Data were analyzed using an ANOVA. The level of significance was $p<0.05$.

Results: Markers of bone formation (OC, BS-ALP) decreased significantly from time 0 to 4 weeks, peaked at 8 weeks and then decreased, whereas the marker of bone degradation (DPYR) peaked at 4 weeks and then decreased. Compared to non-infected rabbits, OC and BS-ALP were lower in infected rabbits at 4 weeks, OC was higher in infected rabbits at 16 weeks, and DPYR was higher in infected rabbits at 4, 8, and 16

weeks. Using this combination of bone markers at 4 weeks, infection could be predicted with an accuracy of 96%. There were weak associations between markers and external callus grade.

Conclusions: Serum bone markers could be useful for clinical evaluation of fracture healing and early diagnosis of osteomyelitis. The use of multiple markers at various time periods may be more useful that the use of a single bone marker.

Introduction

Non-union and infected non-union are devastating clinical complications following fracture repair in both human[1-3] and veterinary[4-7] medicine. In retrospective studies, success rates of less than 20% for repair of long-bone fractures in adult horses have been reported.[4-7] Impaired fracture healing (delayed- or non-union) and osteomyelitis (infected non-union) were the most common causes of failure of treatment of long-bone fractures in horses, with an occurrence rate of 30-40% following treatment.[4-7] Approximately 70-90% of horse that develop either impaired healing or osteomyelitis were euthanized.[4-7] Early diagnosis of impaired fracture healing and osteomyelitis is critical for successful treatment.

While history and physical examination findings may suggest a diagnosis of impaired healing or osteomyelitis, ancillary tests are usually performed to confirm the clinical diagnosis, ascertain whether the infection involves the soft tissue or the actual bone, and to estimate the prognosis. Radiography is used most commonly; however, it is limited by a lack of sensitivity.[8,9] Magnetic resonance imaging (MRI) and computerized tomography (CT) have limitations when metallic implants are used to stabilize the fracture, may be cost prohibitive for use in veterinary medicine, and are not commonly available. They also currently require general anesthesia, which is often contraindicated for horses with long-bone fractures because of the risk of damage to the repair during recovery. Nuclear scintigraphy is expensive, requires the use of radioactivity, and further evaluation of the accuracy of this imaging modality is required.[a] Ultrasound is reported to be accurate for diagnosing osteomyelitis by detection of a fluid immediately adjacent to the cortical bone;[10] however, there is a lack of specificity for postoperative osteomyelitis

because trauma and surgery can result in local fluid accumulation.[10] Therefore, novel methods for early diagnosis of non-union and infected non-union are required.

Serum and urinary bone markers have been evaluated in various diseases of altered bone metabolism,[11-15] including fracture healing.[16-46] The advantage of measuring markers of bone formation and resorption for detection of delayed healing and osteomyelitis are that it is specific for bone, easier, less invasive, more economical, and does not require general anesthesia or prolonged restraint compared to imaging techniques.[16] However, results from studies evaluating bone markers have been controversial.

Markers of bone formation include osteocalcin (OC) and bone-specific alkaline phosphatase (BS-ALP). Osteocalcin is a specific product of osteoblasts,[17] and is associated with bone mineralization.[18,19] A fraction of the OC molecule is released into the blood during incorporation of OC into bone during bone formation, and OC has been shown to increase following fracture.[22-27] In one study, human patients with delayed healing had lower OC postfracture compared to patients with normal healing;[20,28] and in another study patients with delayed healing had prolonged elevations in OC.[20] Bone-specific alkaline phosphatase is an osteoblast enzyme,[25] which is thought to play a role in the formation and mineralization of bone matrix.[32,33] It has been shown to increase after fracture.[20,25,26,36,37] and was lower in patients with delayed compared to normal fracture healing.[16,29] In dogs with experimental infected femoral fractures, the OC and BS-ALP were found to increase compared to preoperative values.[31] Markers of bone resorption include the deoxypyridinoline crosslinks (DPYR), which are specific for bone and dentine.[22] During bone resorption, collagen is degraded and DPYR are released into the

blood. An increase in serum and urinary DPYR has been reported after fracture,[22,27] but the DPYR have not been evaluated in patients with osteomyelitis. The results of these studies suggest that serum bone markers may be useful for assessing fracture healing and for early diagnosis of osteomyelitis following fracture repair.

There have been no studies evaluating serum bone marker concentrations in non-union or infected non-union animal models. The purpose of this study was to evaluate the use of serum bone markers for evaluating infected versus non-infected fractures and normal healing versus delayed- or non-union. Our hypothesis was that markers of bone formation (OC and BS-ALP) would be lower in animals with non-union compared to animals with normal healing, and markers of bone degradation (DPYR) higher in animals with infection compared to animals without infection.

Materials and Methods

Animal Model

This study was performed as a part of larger study evaluating the effect of adenoviral transfer of the bone morphogenetic-2 (Ad-BMP-2) gene on fracture healing in a non-union and an infected non-union rabbit femur model (Chapter 3). All procedures were approved by the Colorado State University Animal Care and Use Committee.

Thirty-two female, skeletally mature (9-10 month-old) New Zealand white rabbits were used in the study. Rabbits were assigned to one of four treatment groups: (1) non-infected Ad-BMP-2 treated, (2) non-infected Ad-Luciferase (LUC) control, (3) infected Ad-BMP-2 treated, and (4) infected Ad-LUC control.

Following induction of general anesthesia using isofluorane in oxygen, a routine lateral approach to the femur, between the *vastus lateralis* and *biceps femoris* was made. A 10-mm mid diaphyseal femoral defect was surgically created using a side cutting carbide burr (MicroAire Surgical Instruments, Charlottesville, VA). The periosteum, endosteum, and bone marrow were removed and the wound thoroughly lavaged to remove any bone debris. The femur was stabilized by stacking two 2.0-mm cuttable bone plates and 2.0 mm cortical screws, with cerclage wire proximally and distally to prevent fracture through the screw holes (Chapter 2). A sclerosing agent (sodium morrhuate) was used on the end of the proximal and distal fragments to prevent defect ossification in control rabbits and to facilitate development and persistence of infection in rabbits in the infected groups. The muscle, subcutaneous tissue, and skin were routinely apposed.

Enrofloxacin (10 mg/kg) was administered pre-operatively only. Perioperative analgesia consisted of preoperative morphine epidurally (0.1 mg/kg) and subcutaneously (SQ; 0.5 mg/kg), fentanyl administered as a constant rate infusion during surgery, and flunixin meglumine (0.5 mg/kg SQ) for 72- hours after surgery or as needed. Butorphanol (0.4 mg/kg SQ) was also administered as needed postoperatively. Acepromazine (0.3 to 0.5 mg/kg IM) was administered to avoid self-trauma to the fracture.

Rabbits were inoculated percutaneously with 0.5×10^7 colony-forming units (cfu)/0.5mL *Staphylococcus aureus* (S. Schaefler 1428, ATCC # 25923) 48 hours after surgery under general anesthesia with isofluorane in oxygen (Chapter 2). Treatment with either Ad-LUC or Ad-BMP-2 (10^{10} viral particles/0.5mL) was also administered percutaneously into the fracture defect at the time of inoculation with *S. aureus*. Rabbits were monitored for signs of lameness and systemic illness.

Sample Collection

Blood was collected preoperatively (time 0), and at 4, 8, 12, and 16 weeks after surgery. Samples were collected during the morning over a 1-2 hour period. Blood was collected in a 12-mL syringe via a 20-gauge catheter placed in the auricular artery, and was immediately transferred to a serum collection tube, placed on ice, and refrigerated (4°C). Following clot formation the samples were centrifuged at 4°C, the serum aliquoted and stored at –80°C. All samples were analyzed at the completion of the study. Because of variability between assay plates and our focus being the difference between normal union versus delayed- or non-union, and infected versus non-infected fractures, samples from each time period (0, 4, 8, 12, and 16 weeks) were analyzed in the same assay.

Measurement of Serum Bone Markers

All markers were measured using an enzyme-linked immunosorbant assay (ELISA, Quidel Corporation, Santa Clara, CA). Briefly, the immunoassay was a microtiter strip format.

The OC assay (Osteocalcin, Quidel Corporation) utilizes a competitive immunoassay with osteocalcin coated microtiter strips, a mouse anti-osteocalcin antibody, and an anti-mouse IgG-alkaline phosphatase (ALP) conjugate. P-nitrophenyl phosphate (p-NPP) was used as a substrate for ALP, and the reaction resulted in a yellow color, with the intensity inversely related to the concentration of OC in the sample. The OD for the standards, samples, and controls was measured at 405 nm (Dynex Revelation 3.2) and a 4-parameter calibration curve plotted from the standards (Metra Fit 1.1, Metra Biosystems, Inc, Mountain View, CA). The concentration of OC (ng/mL) for the samples

and controls was calculated from the 4-parameter calibration curve. The BS-ALP assay (Alkphase-B, Quidel Corporation) utilized a monoclonal antibody coated on the microtiter strip. The monoclonal antibody bound the BS-ALP in the serum sample. P-nitrophenyl phosphate was used as a substrate for the bound BS-ALP. The OD of the standards, samples, and controls was measured at 405 nm. A standard curve was generated from the standards, and the concentration (U/L) of BS-ALP in the control and samples calculated from the standard curve (Dynex Revelation 3.2). Total serum DPYR was measured using a competitive enzyme immunoassay (Total DPD and DPD, Quidel Corporation). The DPYR in the samples competes with ALP conjugated DPYR for binding to monoclonal anti-DPYR antibodies coated on the strip. The reaction is detected with p-NPP substrate, and the concentration of DPYR was calculated from 4-parameter standard curve (Metra Fit 1.1) following OD measurement of standards, samples and controls at 405 nm.

There was no correction for the OD of the zero-standard in any assay. Samples were analyzed by week (0, 4, 8, 12, and 16), in duplicate. If a value on the standard curve had a CV greater than 15% and appeared to be an outlier, the value was eliminated from the standard curve and the concentration of the controls and samples recalculated. Intraassay and interassay coefficient of variation (CV) were calculated for the samples. If the intraassay CV was greater than 15%, the sample was reanalyzed. An average value was used for samples analyzed twice with an intraassay CV less than 15%. An initial analysis to determine the required sample dilution was performed.

Radiography

Rabbits were evaluated radiographically (craniocaudal and lateral views) postoperatively at time 0, and at 4, 8, 12, and 16 weeks postoperatively. The methods for radiographic analysis are outlined in Chapter 3. The radiographic grades for external callus formation and bone lysis at 16 weeks were used in this study.

Nuclear Scintigraphy

Nuclear scintigraphy was performed as part of another study (Chapter 4). Nuclear scintigraphy was performed at week 4, 8, 12, and 16, using technetium-99m (Tc99m)-labeled oxidronate (Tc-PO) and Tc99m-labeled ciprofloxacin (Tc-CIPRO). The methods for nuclear scintigraphy are outlined in Chapter 4. The uptake ratio for the entire femur using the craniocaudal views for both Tc-PO and Tc-CIPRO were used in this study.

Statistical Analysis

Continuous data were analyzed using an ANOVA (PROC MIXED, SAS Institute, Cary, NC). Rabbit, time (0, 4, 8, 12, 16 weeks), treatment (BMP, LUC), and infection (Infected, Non-infected) were used as class variables. Rabbit nested within treatment and infection groups was used as the random variable. Data were analyzed using several models to evaluate the association between marker concentration (dependent variable) and fixed effects: (1) time, treatment, infection, and interactions, (2) radiographic lysis grade (1 to 4), time, and interactions, (3) radiographic external callus grade (1 to 4), time, and interactions, and (4) bridging-callus, time, and interactions (fixed effects). An overall analysis as well as analysis at each time period was performed. Data was analyzed for

normalcy using a plot of the predicted versus residual values; if the data did not appear normal a transformation was performed and the data reanalyzed. If there was an increase in variance with increase in concentration a log transformation of the data was performed. The difference in log value between time 0 and each subsequent time period was calculated, and represents the change in bone marker concentration. The association between the fixed effects and the change in bone marker concentration was analyzed. The association between preoperative body weight, body weight at euthanasia, change in body weight, and lameness were also evaluated with the previously evaluated models using an ANCOVA (PROC MIXED, SAS Institute). If there was a significant association between serum bone marker concentration and body weight or lameness grade, these data were included in the analysis. Data are presented as least squared means. The power was estimated by evaluating the confidence interval of the difference between fixed effect variables for each analysis.

Correlations between different marker concentrations and external callus grade, lysis grade, body weight, lameness, and nuclear scintigraphy findings were analyzed using Pearson's correlation coefficient (PROC CORR, SAS Institute). The probability of OC, BS-ALP, and DPYR concentrations being able to predict whether an animal was infected or not infected, or had bridging-callus at 16 weeks, was also determined (PROC PROBIT, SAS Institute), and the accuracy, true positive (sensitivity), true negative (specificity), positive predictive value, and negative predictive value calculated (PROC FREQ, SAS Institute). The level of significance was $p<0.05$.

Results

Animal Model

There were 20 rabbits completing the 16-week study (non-infected BMP-2 n=5; non-infected LUC n=7; infected BMP-2 n=3; infected LUC n=5). Twelve rabbits were euthanized for humane reasons prior to completion of the study (Chapter 2). Four rabbits were euthanized after week 4, and data from these rabbits were included until the time of euthanasia. Serum was collected at 16 weeks from an additional 24 rabbits that were part of another study (Chapter 3), and the results included in the 16-week analyses. Rabbits healed predominantly by external callus formation rather than defect healing; therefore external callus grade at 16 weeks rather than defect ossification was used as a measure of fracture healing.

Rabbits were classified as infected or non-infected initially whether they were inoculated with *S. aureus* at 48 hours or not inoculated. Infection was further classified as whether there was accumulation of purulent material on gross examination, positive culture, and radiographic lysis at 16 weeks. There was only one rabbit in the infected group that had no signs of infection grossly, a negative culture, and no radiographic lysis at 16 weeks. On further examination of this rabbit's record the culture of the inoculum was negative; therefore this rabbit was considered to be in the non-infected group. All other rabbits in the infected group had established infection. There was one rabbit in the non-infected group that had a small amount of purulent material at the fracture site; however, culture of the tissue and screw were negative, and there was no radiographic bone lysis. Therefore this rabbit was classified as non-infected.

Measurement of Serum Bone Markers:

Osteocalcin: The interassay CV for OC, based on 12 samples analyzed on 2 different plates, was 16.6% (1.6 to 33.9%) and the intraassay variability, based on all samples analyzed in duplicate, was 3.7% (0.1 to 12.3%). A dilution of 1:5 was required for analysis of samples. Control values for each assay were within the reference range. There was an increase in variance with increase in OC; therefore a log transformation of the data was performed. All data presented are transformed and analyses were performed on the transformed data.

There was a significant association between time and OC ($p<0.001$; Figure 1a). The OC significantly decreased, from time 0, at week 4. The OC then significantly increased at week 8, but was not significantly different from time 0. Then the OC decreased at weeks 12 and 16, which were not significantly different from week 4.

Overall there was no association between infection and OC (Figure 1a); however, there was a trend for an interaction between infection and time ($p=0.1$; Figure 1b). When data were analyzed at individual time periods there was a trend for infected rabbits to have lower OC at week 4 and higher OC at week 16 compared to non-infected rabbits ($p\leq 0.1$). When the change in OC from time 0 was evaluated, there was a significant association with infection at week-4 ($p=0.02$); infected rabbits had a greater decrease in OC than non-infected rabbits. There was an association between OC and preoperative body weight ($p=0.01$); when preoperative body weight was included in the analysis the interaction between infection and time was significant ($p=0.05$), and at 4 weeks there was

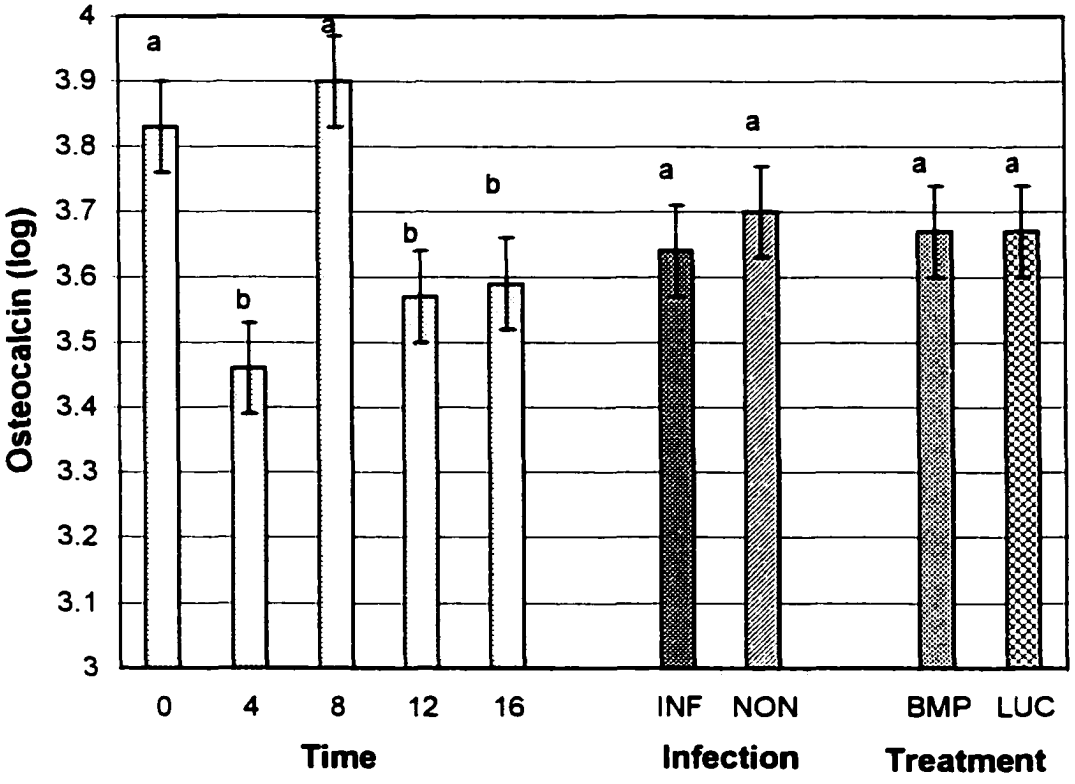

Figure 1A. A plot showing the association between the log values of osteocalcin concentration and the main fixed effects (time, infection, and treatment) averaged over all other variables. The sample at time 0 was collected preoperatively and the other samples 4, 8, 12, and 16 weeks after surgery. Data are expressed as least squared means +/- standard error of the mean. Different letters represent statistically significant differences. INF=infected, NON=non-infected, BMP=treated with adenoviral transfer of the BMP-2 gene, LUC=adenoviral transfer of the luciferase gene (control).

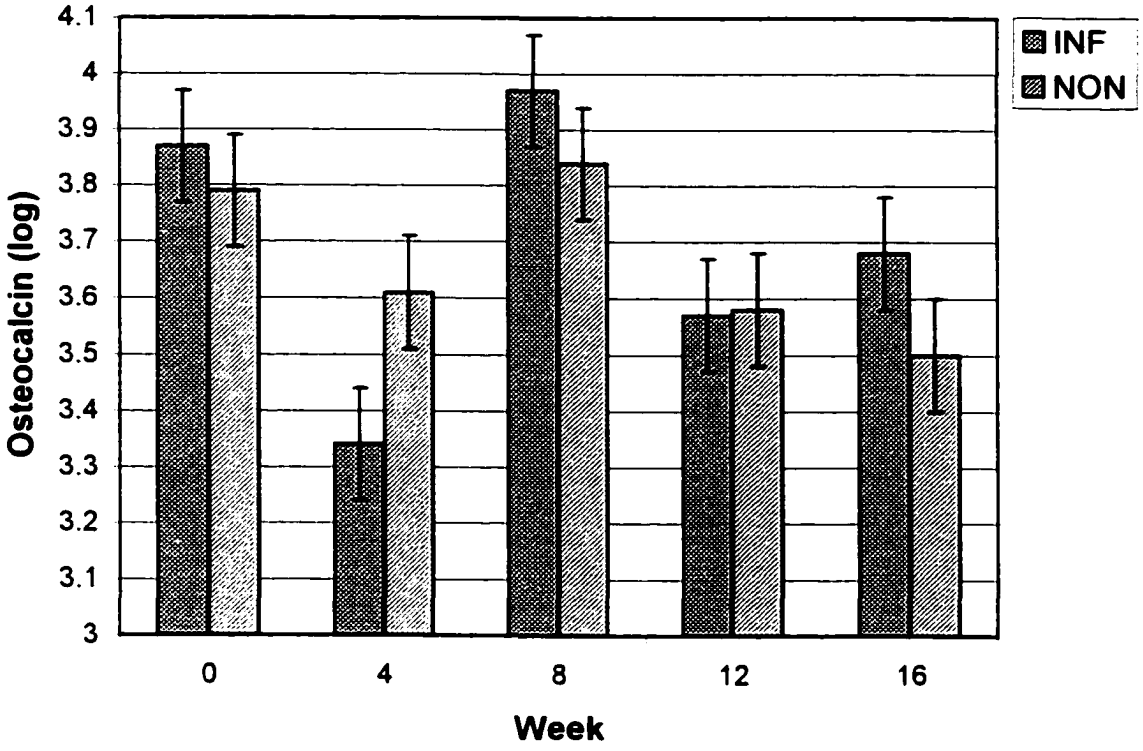

Figure 1B. A plot showing the association between osteocalcin concentration and the presence of infection, over time (0 to 16 weeks). The sample at time 0 was collected preoperatively and the other samples 4, 8, 12, and 16 weeks after surgery. Data are expressed as least squared means +/- standard error of the mean. INF=infected, NON=non-infected

a significant association between infection and OC (p=0.04) and change in OC (p=0.02). There was no correlation, however, between OC and preoperative body weight at any time period. There was no association between OC and postoperative weight, difference in weight, or lameness; therefore these variables were not analyzed further. The use of OC to predict infection is shown in Table 1. Overall OC was not useful for predicting infection compared to BS-ALP and DPYR; however, there were trends observed at week 4 and 16. There was no association or correlation between lysis grade and OC (Figure 1c).

Although rabbits in the Ad-BMP-2 treated groups appeared to have higher OC at 4 and 8 weeks (Figure 1d), there was no association between treatment and OC. However, given the difference between treatment groups is correct the power was low because of the wide CI compared to the difference; for example, the difference at 8 weeks was 0.09 (95% confidence interval (CI) -0.2 to 0.4). Rabbits with bridging-callus did not have a significantly different OC compared to rabbits that did not have bridging-callus. When comparing the change in OC from time 0, however, there was a trend at 16 weeks for rabbits with bridging-callus to have a lower OC than rabbits that did not have bridging-callus (p=0.08). The OC was not useful for differentiating rabbits with bridging-callus from those that did not have bridging-callus using logistic regression. Although it appeared that rabbits with a higher external callus grade had higher OC at week-8 and -12 (Figure 1e), there was no association between OC and external callus formation; however, the confidence limits were wide compared to the differences, and therefore, the power for this analysis was low. For example, the difference between grade-1 and –4 callus at 4 weeks was -0.5 (CI –1.1 to 0.1). There was no correlation between external

Table 1. Accuracy, sensitivity (true positive rate), specificity (true negative rate), and positive and negative predictive values for osteocalcin (OC), bone-specific alkaline phosphatase (BS-ALP), and deoxypyridinoline crosslinks (DPYR) for predicting the presence of infection.

Serum Bone Marker	Time (Weeks After Surgery)	Accuracy (%)	Sensitivity (%)	Specificity (%)	Pos Pred Value (%)	Neg Pred Value (%)
OC	4**	67	45	85	71	65
	8	48	33	58	38	54
	12	60	0	100	0	60
	16**	66	33	88	67	66
BS-ALP	4*	75	73	77	73	77
	8	62	11	100	100	60
	12	60	0	100	0	60
	16	59	0	100	0	60
DPYR	4*	75	64	85	78	73
	8 *	81	78	83	78	83
	12**	70	50	83	67	71
	16*	75	61	85	73	76
All	4*	96	91	100	100	93
	8**	71	67	75	67	75
	12*	75	50	92	80	73
	16*	75	61	85	73	76

* $p<0.05$ and ** $p\leq 0.1$ for infected versus non-infected

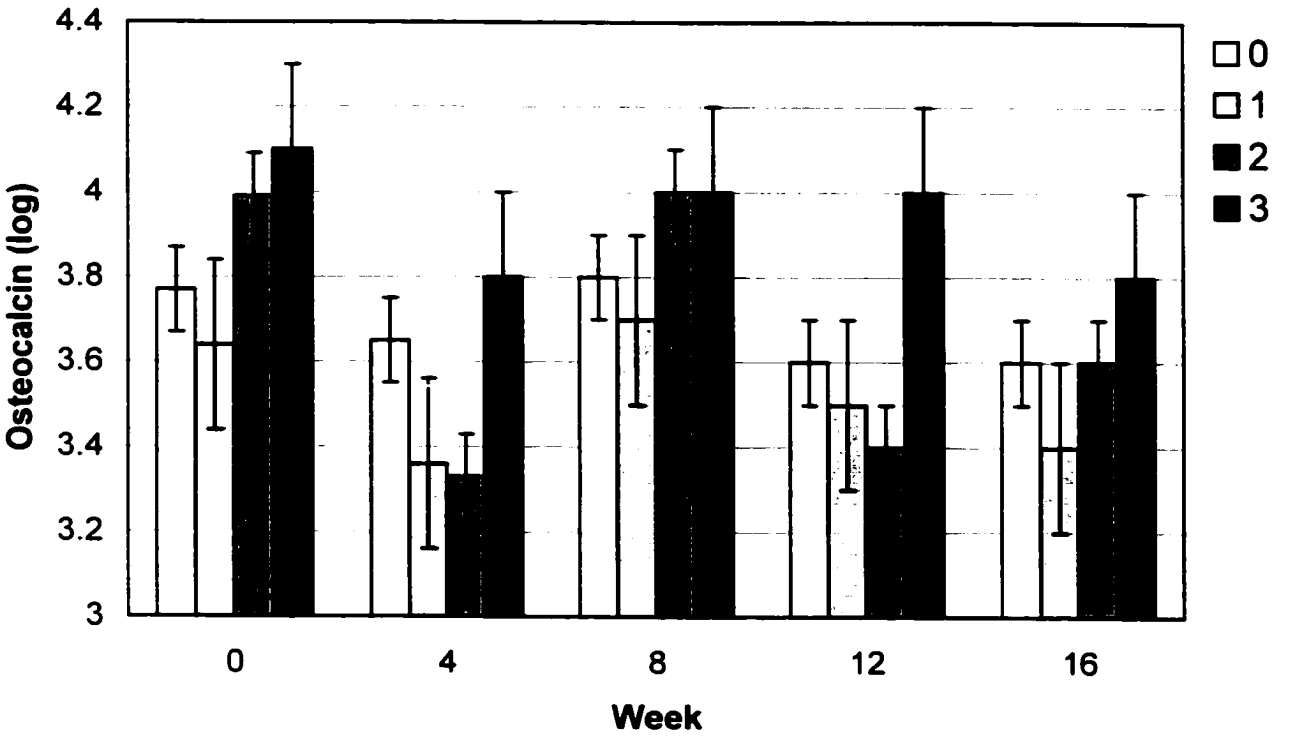

Figure 1C. A plot showing the association between osteocalcin concentration and radiographic lysis grade (0=none, 1=slight, 2=mild, 3=moderate). The sample at time 0 was collected preoperatively and the other samples 4, 8, 12, and 16 weeks after surgery. Data are expressed as least squared means +/- standard error of the mean.

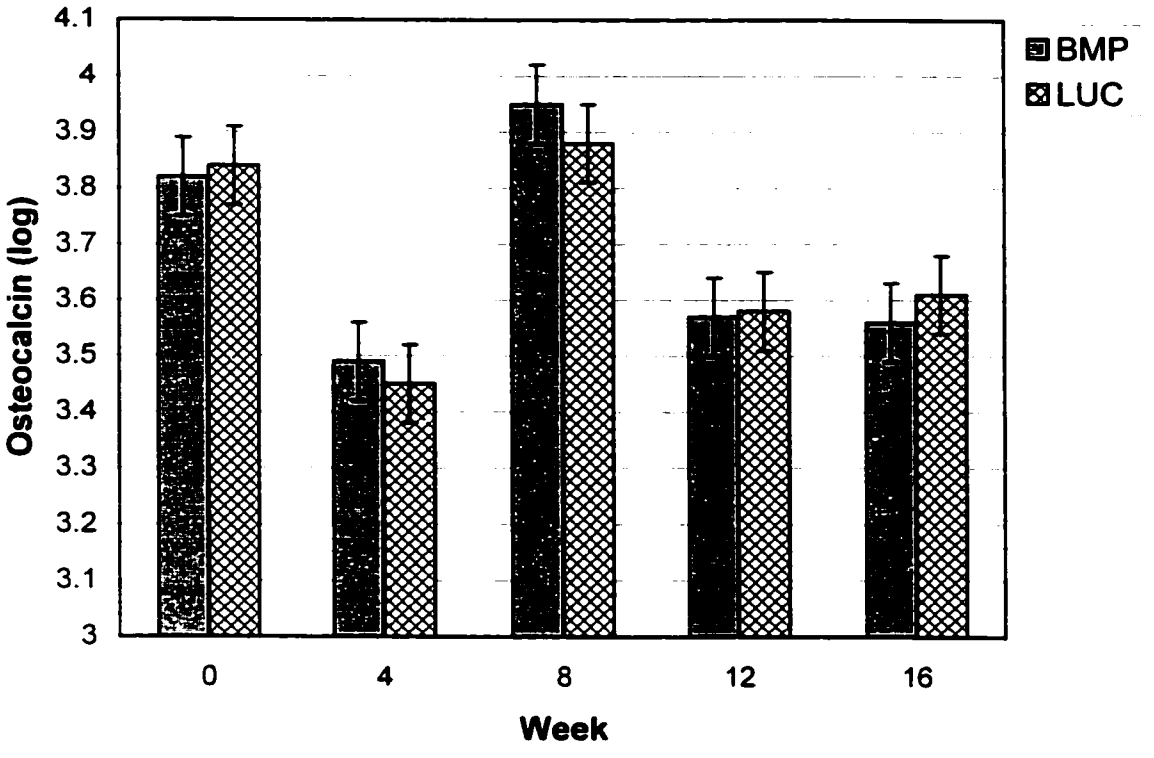

Figure 1D. A plot showing the association between osteocalcin concentration and treatment group over time. The sample at time 0 was collected preoperatively and the other samples 4, 8, 12, and 16 weeks after surgery. Data are expressed as least squared means +/- standard error of the mean. BMP=treated with adenoviral transfer of the BMP-2 gene. LUC=adenoviral transfer of the luciferase gene (control).

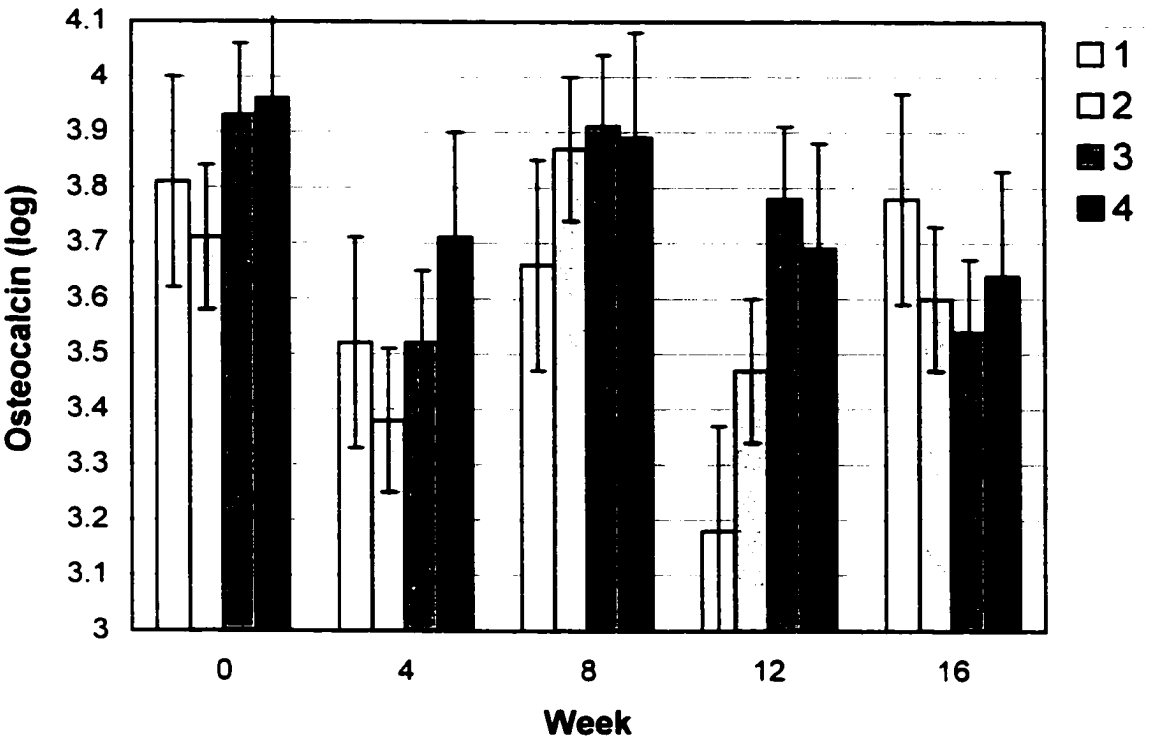

Figure 1E. A plot showing the association between osteocalcin concentration and radiographic external callus grade (1=slight, 2=mild, 3=moderate, and 4=marked). The sample at time 0 was collected preoperatively and the other samples 4, 8, 12, and 16 weeks after surgery. Data are expressed as least squared means +/- standard error of the mean.

callus grade and OC. All values for OC in the rabbits were higher than reference values for normal human subjects (3.7 to 10 ng/mL; Osteocalcin, Quidel Corporation).

There was no overall correlation between OC and nuclear scintigraphy findings; however, at 4 weeks there was a weak negative correlation between OC and the EXP: NORM femur using Tc-CIPRO (r^2= -0.27, p=0.01).

Bone-Specific Alkaline Phosphatase: The interassay CV for BS-ALP, based on 5 samples analyzed on 2 different plates, was 10.6% (3.4 to 16.4%) and the intraassay variability, based on all samples analyzed in duplicate, was 2.1% (0 to 11.9%). No dilution was required for analysis of samples. Control values for each assay were within the reference range. There was an increase in variance with increase in BS-ALP; therefore a log transformation of the data was performed. All data presented are transformed and analyses were performed on the transformed data.

There was an overall significant effect of time on BS-ALP (p=0.0001; Figure 2a). The BS-ALP significantly decreased, from time zero, at week 4. BS-ALP then increased at week 8 to a value that was significantly higher than that at week 4, but not different from time 0. The BS-ALP then decreased from week 8.

There was a significant association between infection and BS-ALP (p=0.04; Figure 2a) and a significant interaction between infection and time (p<0.0001). Rabbits in the infected groups had significantly lower BS-ALP at 4 weeks compared to rabbits in the non-infected groups (Figure 2b). The change in BS-ALP from time 0 was also significantly greater for rabbits in the infected group at 4 weeks (p=0.0002). There was no association between preoperative bodyweight, bodyweight at euthanasia, change in

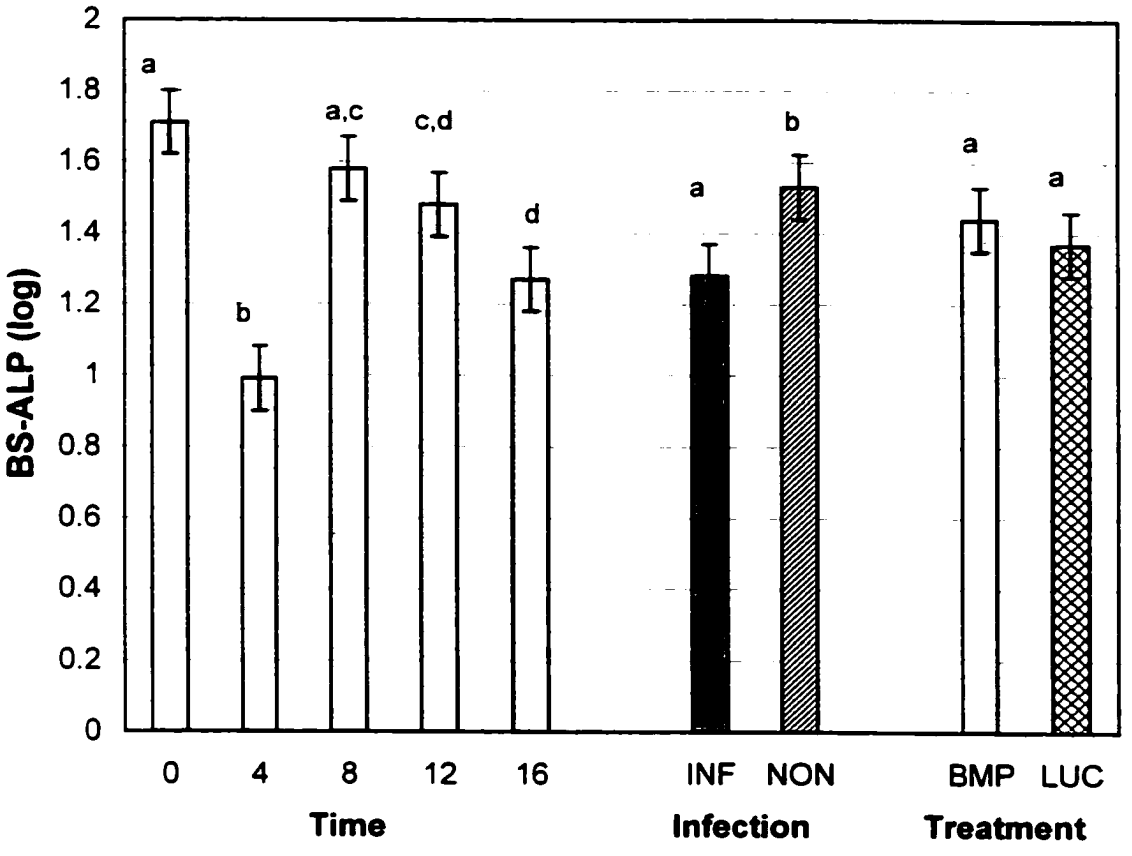

Figure 2A. A plot showing the association between log values of bone-specific alkaline phosphatase (BS-ALP) concentration and the main fixed effects (time, infection, and treatment) averaged over all other variables. The sample at time 0 was collected preoperatively and the other samples 4, 8, 12, and 16 weeks after surgery. Data are expressed as least squared means +/- standard error of the mean. Different letters represent statistically significant differences. INF=infected non-union, NON=non-union, BMP=rabbits treated with adenoviral transfer of the bone morphogenetic-2 gene (Ad-BMP-2), and LUC=adenoviral transfer of the Luciferase gene (control).

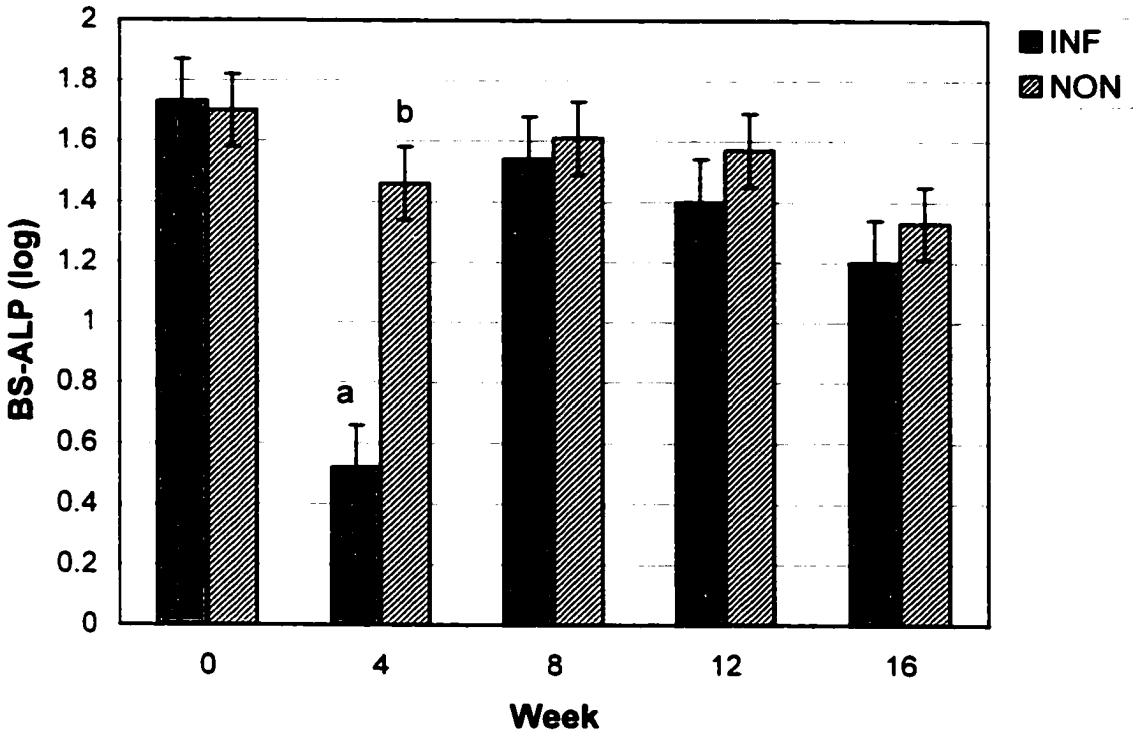

Figure 2B. A plot showing the association between log values of bone-specific alkaline phosphatase (BS-ALP) concentration and the presence of infection over time (0 to 16 weeks). Data are expressed as least squared means +/- standard error of the mean. Different letters represent statistically significant differences. INF=infected non-union, NON=non-union.

body weight or lameness examination and BS-ALP. However, when body weight at euthanasia or change in body weight were included in the model, rabbits with infection still had a lower BS-ALP compared to non-infected rabbits at 4 weeks, but the significance decreased (p=0.05). There was a moderate correlation between BS-ALP at 4 weeks and body weight at euthanasia (r^2=0.47, p=0.0008) as well as change in body weight (r^2=0.5, p=0.0005). Using logistic regression, the BS-ALP could differentiate infected from non-infected rabbits at 4 weeks, but not at other time periods (Table 1). For example, the median BS-ALP at 4 weeks for infected rabbits was 2.0 U/L (0.3 to 4.7 U/L) and non-infected rabbits 4.7 U/L (1.9 to 12.9 U/L). A concentration of 2.0 U/L was arbitrarily established to define infected from non-infected rabbits; 55% (6/11) of infected rabbits had a BS-ALP less than 2.0 U/L and 92% (12/13) of non-infected rabbits had a BS-ALP higher than 2.0 U/L. Therefore, the overall accuracy was 75% (18/24). There was a significant association between lysis grade and BS-ALP (p=0.005) as well as change in BS-ALP (p=0.007) at 4 weeks; rabbits with a higher lysis grade had a lower BS-ALP (Figure 2c). At 4 weeks there was also a moderate negative correlation between lysis grade and BS-ALP (r^2=-0.45, p=0.001) as well as change in BS-ALP (r^2=-0.48, p=0.0007).

Although rabbits in the Ad-BMP-2 treated group appeared to have a higher BS-ALP at 4, 8, and 12 weeks (Figure 2d), there was no association between BS-ALP and treatment group. However the CIs were large relative to the difference; therefore the power was low for the given difference. For example, the difference at 4 weeks was 0.2 (CI –0.2 to 0.6). There was no difference in BS-ALP between rabbits that had bridged the defect at 16 weeks and rabbits that had not bridged the defect, and BS-ALP

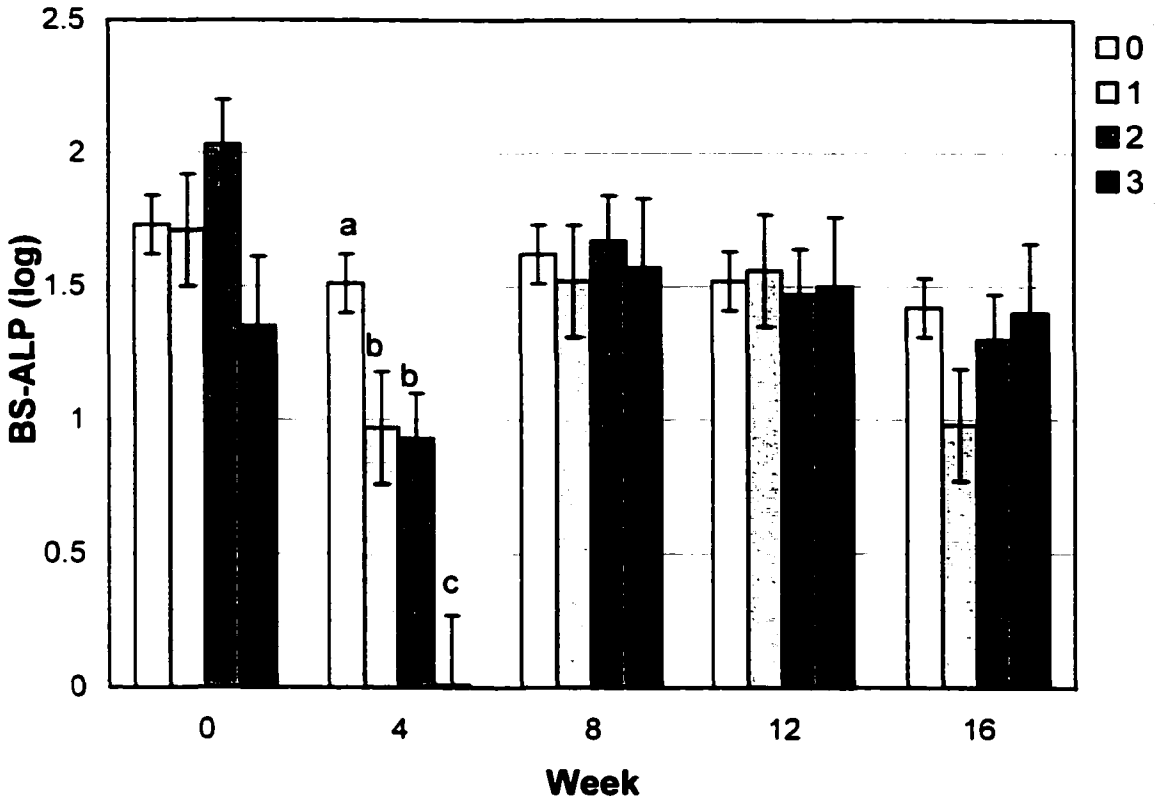

Figure 2C. A plot showing the association between log values of bone-specific alkaline phosphatase (BS-ALP) concentration and radiographic lysis grade at 16 weeks (0=none, 1=slight, 2=mild, 3=moderate).The sample at time 0 was collected preoperatively and the other samples 4, 8, 12, and 16 weeks after surgery. Data are expressed as least squared means +/- standard error of the mean. Different letters represent statistically significant differences.

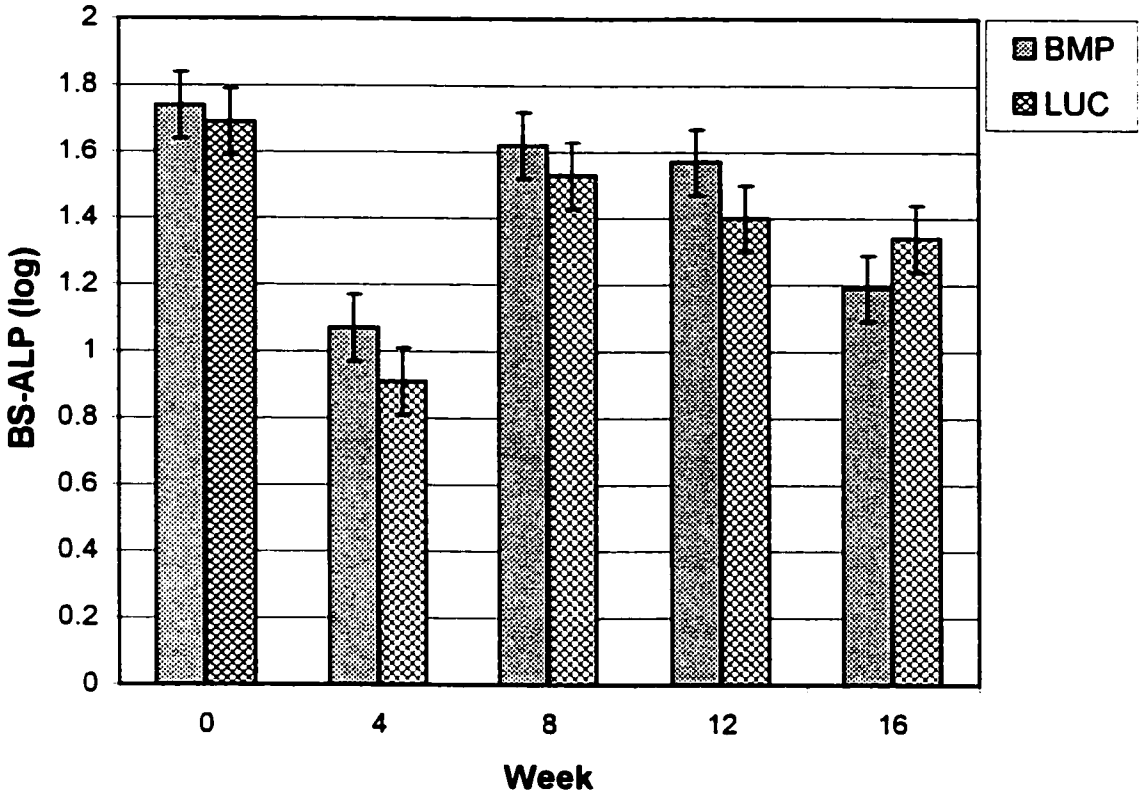

Figure 2D. A plot showing the association between log values of bone-specific alkaline phosphatase (BS-ALP) concentration and treatment group over time. The sample at time 0 was collected preoperatively and the other samples 4, 8, 12, and 16 weeks after surgery. Data are expressed as least squared means +/- standard error of the mean. BMP=rabbits treated with adenoviral transfer of the bone morphogenetic-2 gene (Ad-BMP-2), and LUC=rabbits treated with Ad-Luciferase control.

was not useful for predicting rabbits that had bridging-callus and rabbits that did not have bridging-callus using logistic regression. There was a significant overall association between radiographic external callus grade and BS-ALP ($p=0.05$; Figure 2e); rabbits with grade-4 external callus overall had a higher BS-ALP. There was no correlation, however, between external callus grade and BS-ALP. The values for BS-ALP in the rabbits are all less than reference ranges for normal human subjects (11.6 to 42 U/L; Alkphase-B. Quidel Corporation).

There was a weak negative correlation between BS-ALP and the ratio of EXP: NORM femur with Tc-CIPRO nuclear scintigraphy at 4 weeks ($r^2=-0.27$; $p=0.01$); however there was no correlation with Tc-PO.

Deoxypyridinoline Crosslinks: The interassay CV for DPYR, based on 31 samples analyzed on 2 different plates, was 20.2% (0.6 to 61.8%), and the average intraassay CV, based on all samples analyzed in duplicate, was 3.7% (0.1 to 14%). Control values for each assay were within the reference range. There was an increase in variance with increase in DPYR; therefore a log transformation of the data was performed. All data presented are transformed and analyses were performed on the transformed data.

There was a significant association between time and DPYR ($p<0.001$; Figure 3a). DPYR significantly increased from time 0 to peak at 4 weeks, then decreased, and was not significantly different from time 0 at week 12 and 16.

Overall, there was a significant association between infection and DPYR concentration ($p<0.001$; Figure 3a). Rabbits with infection had a significantly higher

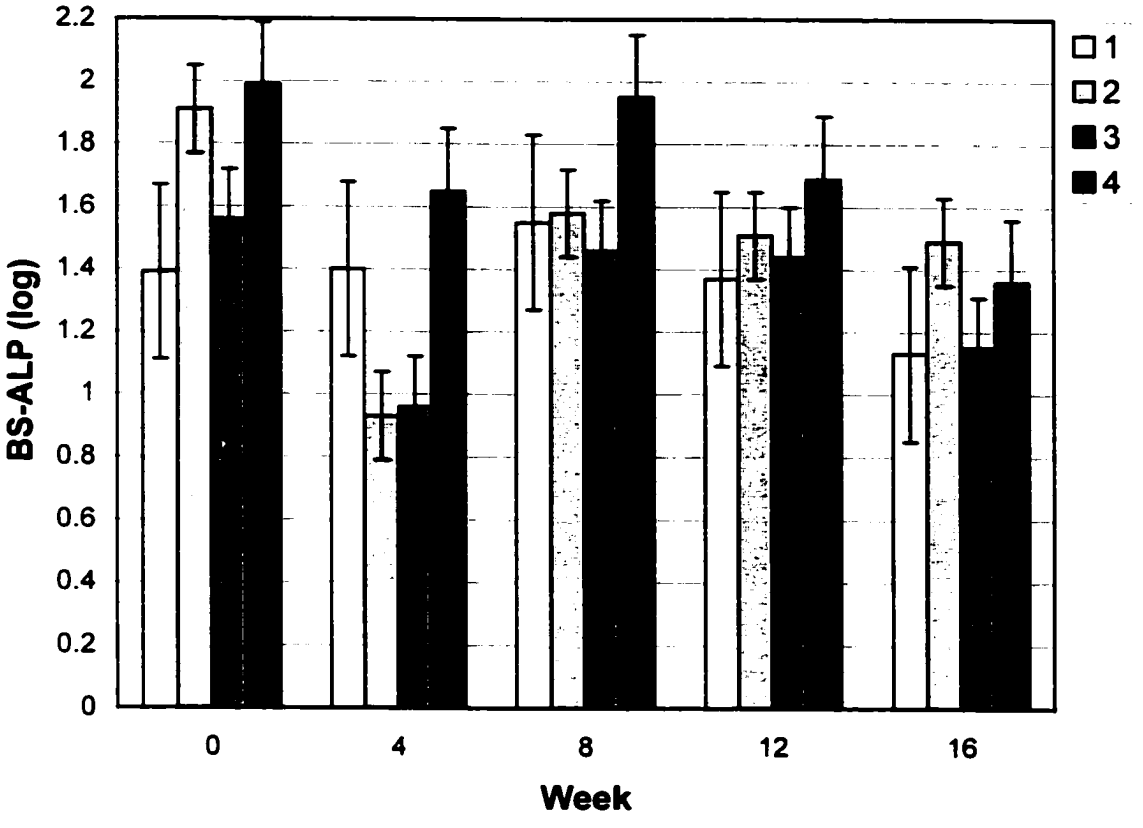

Figure 2E. A plot showing the association between log values of bone-specific alkaline phosphatase (BS-ALP) concentration and radiographic external callus grade at 16 weeks (1=slight, 2=mild, 3=moderate, and 4=marked). The sample at time 0 was collected preoperatively and the other samples 4, 8, 12, and 16 weeks after surgery. Data are expressed as least squared means +/- standard error of the mean.

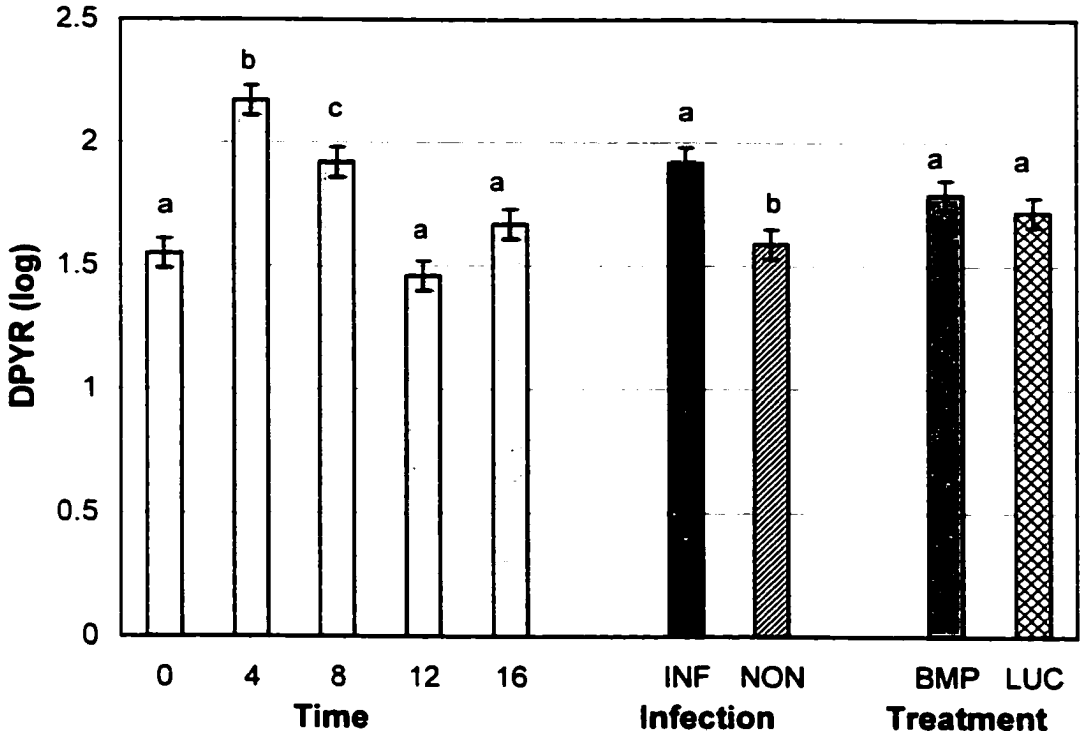

Figure 3A. A plot showing the association between log values of deoxypyridinoline crosslinks (DPYR) concentration and the main fixed effects (time, infection, and treatment) averaged over all other variables. The sample at time 0 was collected preoperatively and the other samples at 4, 8, 12, and 16 weeks after surgery. Data are expressed as least squared means +/- standard error of the mean. Different letters represent statistically significant differences. INF=infected, NON=non-infected, BMP=treated with adenoviral transfer of the BMP-2 gene, LUC=adenoviral transfer of the luciferase gene (control).

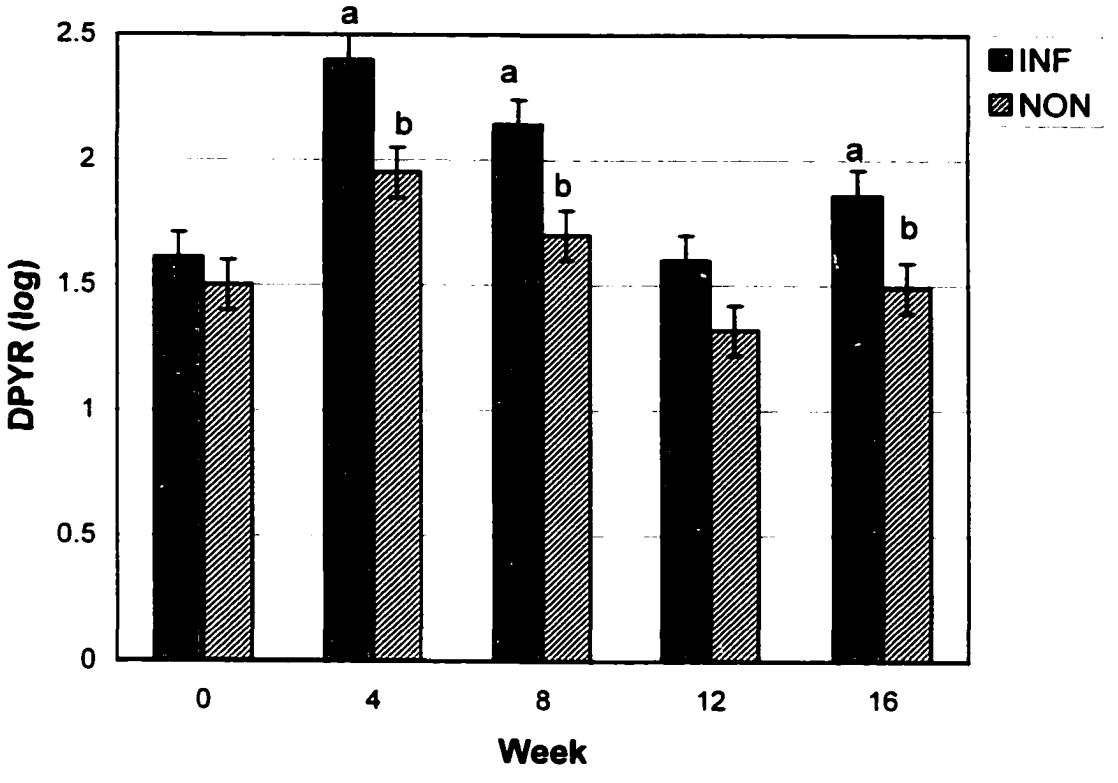

Figure 3B. A plot showing the association between log values of deoxypyridinoline crosslinks (DPYR) concentration and infection over time. The sample at time 0 was collected preoperatively and the other samples 4, 8, 12, and 16 weeks after surgery. Data are expressed as least squared means +/- standard error of the mean. Different letters represent statistically significant differences. INF=infected, NON=non-infected.

did not change the results of the analyses. However there was a good correlation between preoperative body weight and DPYR at time 0 (r^2 = 0.67; p<0.001). There was a significant association between infection and the change in DPYR at 4 weeks (p=0.03); however, when bodyweight at euthanasia was included in the analysis this was no longer significant (p=0.3). Although there was no correlation between DPYR and body weight at euthanasia, there was a negative correlation between change in DPYR and body weight at euthanasia at 8 and 12 weeks (r^2 = -0.3; p=0.01); rabbits with a greater increase in DPYR had a lower body weight at euthanasia.

The DPYR was the most useful serum bone marker for differentiating infected from non-infected rabbits (Table 1). For example, the median serum DPYR concentration at 4 weeks for infected rabbits was 11.3 nmol/L (7.8 to 18.1 nmol/L) and non-infected rabbits 6.5 nmol/L (4.2 to 14 nmol/L). A concentration of 7.7 nmol/L was arbitrarily established to define infected from non-infected rabbits. At 4 weeks all the infected rabbits (11/11) had a DPYR higher than 7.7 nmol/L and 77% (10/13) of the non-infected rabbits had a DPYR less than 7.7 nmol/L. Therefore, the overall accuracy was 88% (21/24). When a combination of serum bone markers was used to differentiate infected from non-infected rabbits at 4 weeks, the accuracy was 96% (Table 1). There was a significant association between radiographic lysis grade and DPYR concentration (p=0.001: Figure 3c); overall, rabbits with a higher lysis grade had a higher DPYR concentration. There was a correlation between lysis grade and DPYR concentration at week 4 (r^2 = 0.33, p=0.008), and only a weak correlation thereafter (r^2=0.24).

Although there was no association between treatment group and DPYR (Figure 3a), there was a significant three-way interaction between infection, treatment, and time

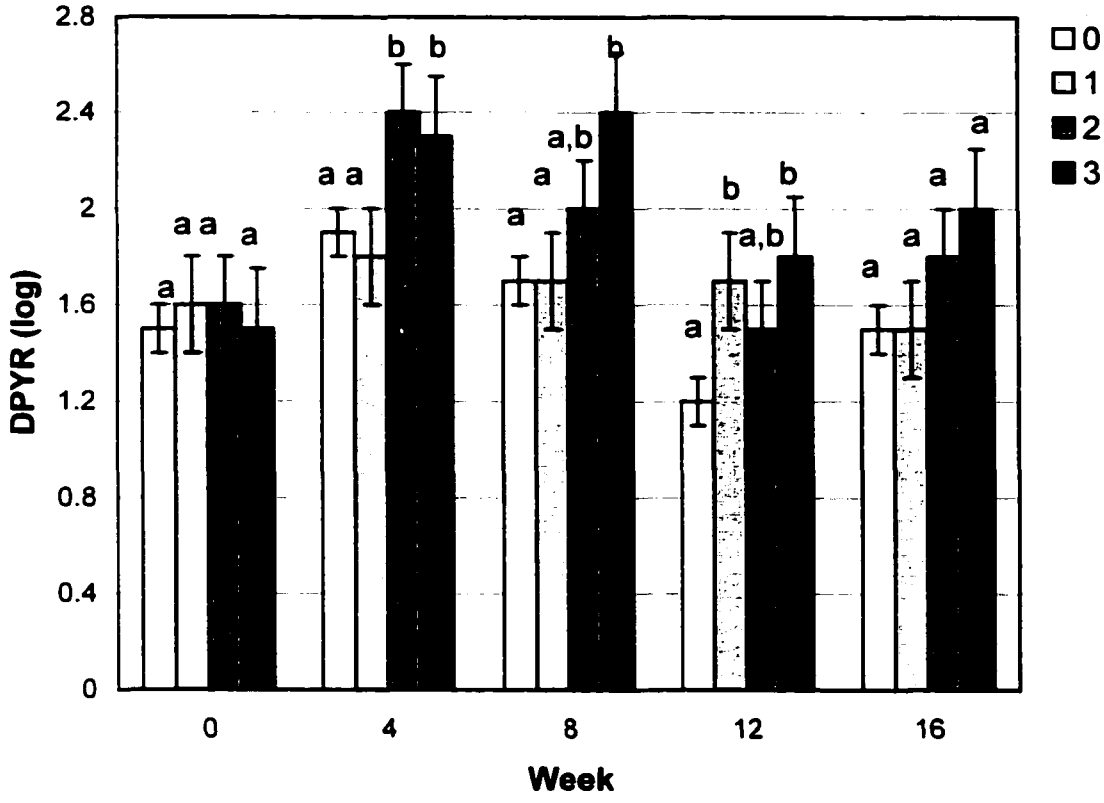

Figure 3C. A plot showing the association between log values of deoxypyridinoline crosslinks (DPYR) concentration and radiographic lysis grade at 16 weeks (0=none, 1=slight, 2=mild, 3=moderate). The sample at time 0 was collected preoperatively and the other samples 4, 8, 12, and 16 weeks after surgery. Data are expressed as least squared means +/- standard error of the mean. Different letters represent statistically significant differences.

(p=0.02; Figure 3d,e). Rabbits in the infected groups had an increase in DPYR, which remained elevated compared to non-infected rabbits, and rabbits in the BMP-treated groups also had an increase in DPYR, which then decreased after week 4. There was no difference in DPYR between rabbits with bridging-callus compared to rabbits without bridging-callus. The difference at 4 weeks was –0.05 (CI –0.4 to 0.3); therefore the power to detect statistical significance with this difference is low. The DPYR was not useful for differentiating rabbits with bridging-callus from those without bridging-callus using logistic regression. Rabbits with a higher external callus grade appeared to have a higher DPYR at 4 weeks, and rabbits with bridging-callus (grade-4) had an earlier decrease in DPYR; however, this was not significant (Figure 3f). The difference between grade-1 and –4 callus at 4 weeks was –0.54 (CI –1.2 to 0.13); therefore the power is low for detecting a difference with these values. There was no correlation between DPYR and external callus grade at any time period. The values for DPYR were higher than those for normal human subjects (2.2 to 4.8 nmol/L; Total DPD, Quidel Corporation).

Overall there was no correlation between DPYR and nuclear scintigraphy findings, however the correlation increased with and increase in time from surgery and there was a positive correlation between DPYR and the ratio EXP: NORM for both the Tc-CIPRO (r^2 = 0.35; p=0.006) and Tc-PO (r^2 = 0.5; p=0.001) nuclear scintigraphy at 16 weeks.

There was a weak positive correlation between OC and BS-ALP at 4 weeks (r^2 = 0.23, p=0.02), and a moderate correlation between the change in OC and BS-ALP from time 0 at 4 weeks (r^2=0.42, p=0.0006). There was no correlation between OC or BS-ALP and DPYR.

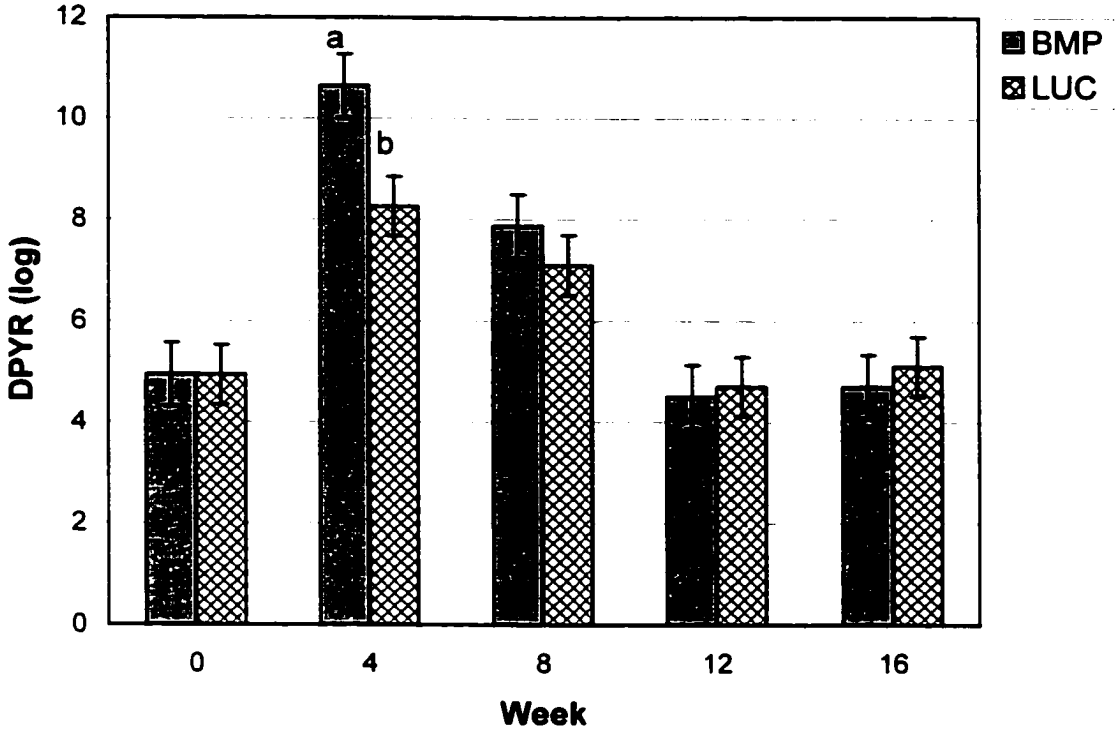

Figure 3 D. A plot showing the association between log values of deoxypyridinoline crosslinks (DPYR) concentration and treatment group over time. The sample at time 0 was collected preoperatively and the other samples 4, 8, 12, and 16 weeks after surgery. Data are expressed as least squared means +/- standard error of the mean. Different letters represent statistically significant differences. BMP=treated with adenoviral transfer of the BMP-2 gene, LUC=adenoviral transfer of the luciferase gene (control).

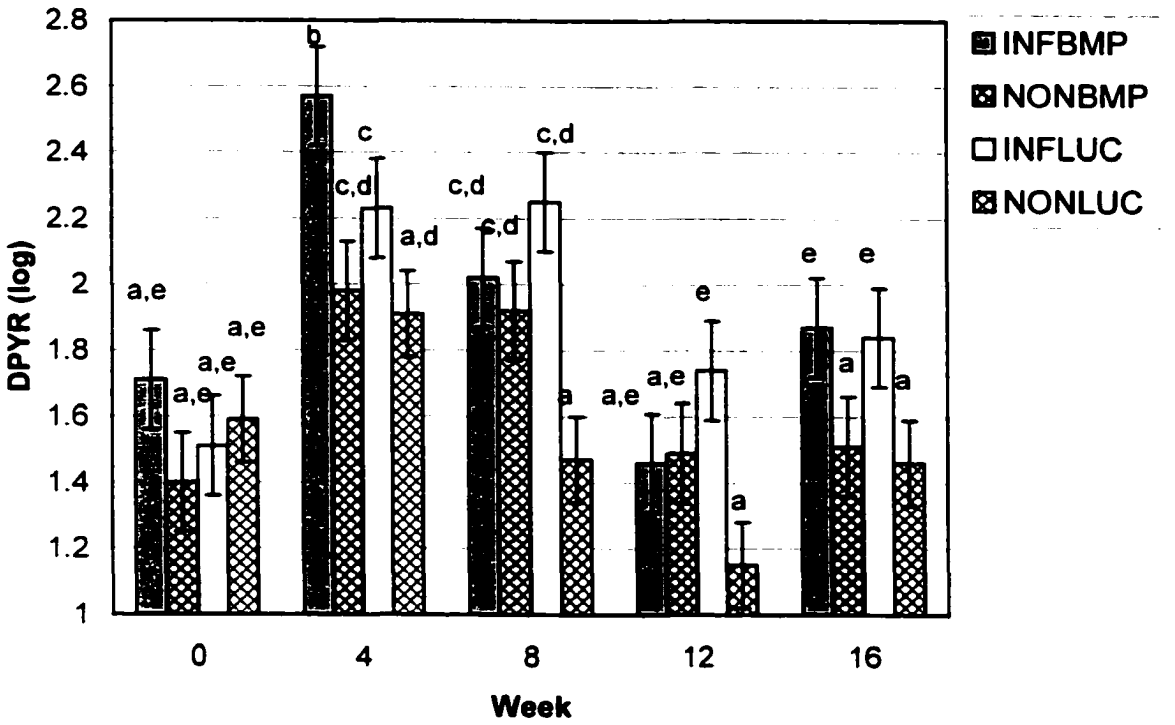

Figure 3E. A plot showing the association between log values of deoxypyridinoline crosslinks (DPYR) concentration and the interaction between infection and treatment groups over time. The sample at time 0 was collected preoperatively and the other samples 4, 8, 12, and 16 weeks after surgery. Data are expressed as least squared means +/- standard error of the mean. Different letters represent statistically significant differences. INF=infected, NON=non-infected, BMP=treated with adenoviral transfer of the BMP-2 gene, LUC=adenoviral transfer of the luciferase gene (control).

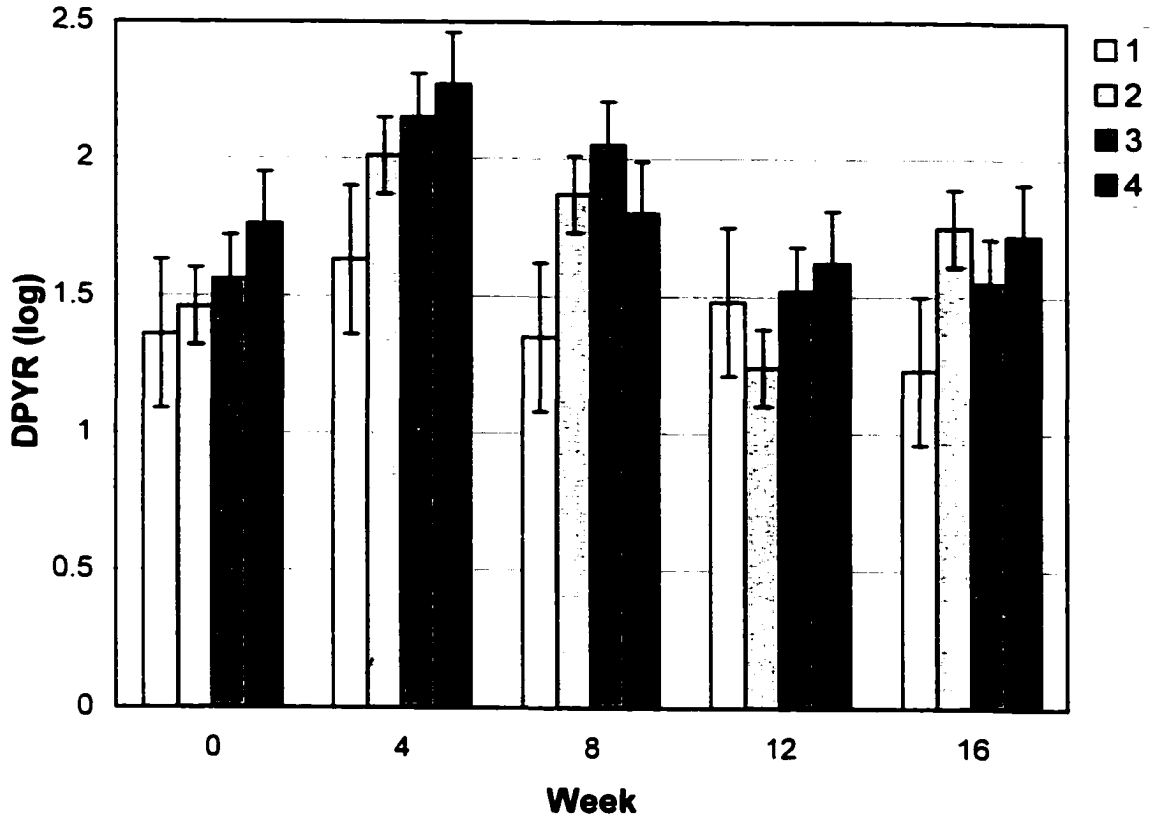

Figure 3 F. A plot showing the association between log values of deoxypyridinoline crosslinks (DPYR) concentration and radiographic callus grades at 16 weeks (1=slight, 2=mild, 3=moderate, and 4=marked). The sample at time 0 was collected preoperatively and the other samples 4, 8, 12, and 16 weeks after surgery. Data are expressed as least squared means +/- standard error of the mean.

Discussion

Overall, the results of this study suggest that serum bone markers may be useful for evaluating fracture healing and the development of postoperative osteomyelitis. The application of our model to clinical cases with respect to changes in serum bone marker concentration is unknown. The model used in our study was a severe non-union model; a 10-mm mid diaphyseal defect was created and a sclerosing agent was used on the fragment ends to prevent fracture healing (Chapter 2). An osteoinductive treatment (Ad-BMP-2) was used in the study and there have been no studies evaluating the association between treatment with Ad-BMP-2 and serum bone marker concentration. Rabbits healed by bridging-callus formation rather than defect ossification in the 16-week study period (Chapter 3), and the effect of type of healing on bone marker concentration is unknown. Therefore the association between bone marker concentration and the phases of fracture healing (inflammation, repair, and remodeling) may be difficult to determine from this study.

The rabbit was chosen as the animal model for this study (Chapter 2), and although there have been no studies specifically evaluating the difference in serum bone marker concentration between species a difference would be expected based on differences in body weight, activity, and metabolism. In our study rabbits had a higher OC, lower BS-ALP, and higher DPYR compared to human reference values. These differences may reflect assay variability between laboratories; however, more likely indicate alterations in bone metabolism based on the body weight, activity, and age of the rabbits. The higher OC and lower BS-ALP values are difficult to explain particularly in light of the results of this study where there was an association between the changes in

concentration of the two markers. Other studies, however, have found a lack of association between OC and BS-ALP.[25,41] Further, different types of fractures result in different trends in the changes in bone marker concentration.[22] For example, vertebral compression fractures did not alter OC concentration,[22] and hip fracture repair resulted in an increase in OC whereas hip prosthesis did not, possibly because the fracture site was removed.[41] The change in DPYR and PYR concentration was also found to be dependent on fracture type.[22] The results of our study, however, support the pursuit of future studies using clinical cases in the target species to evaluate the use of serum bone marker for assessing fracture healing.

There was a significant change in all serum bone markers over time. Serum markers of bone formation (BS-ALP and OC) decreased at week 4, peaked at week 8, then decreased to values lower than those at time 0; whereas the marker of bone resorption (DPYR) peaked at week 4, then decreased. These results suggest that in general there was an initial phase of bone resorption with minimal bone mineralization, particularly in infected rabbits, followed by bone formation, reflecting the phases of fracture healing.[22] This finding is supported by the results of nuclear scintigraphy where a correlation between external callus formation and Tc-PO4 uptake, an indication of hydroxyapatite formation, was found only after 4 weeks (Chapter 4). Because samples were assayed by time period, the difference between time periods may be attributed to interassay variability; however, there were similar trends with all bone markers, therefore this is unlikely.

Samples were collected at 0, 4, 8, 12, and 16 weeks. Repeated blood collection from rabbits would not have been possible, because of both local damage to blood vessels

and systemic signs associated with blood loss. Further, the cost of analysis of serum bone markers precluded sample analysis at additional time periods in this study, and there were also time constraints associated with the overall study design. Therefore, future studies evaluating serum bone marker concentration should be performed at more frequent intervals earlier in the course of fracture healing to assess the clinical value of these markers.

The results of this study overall are supported by previous studies. One study evaluating human subjects with normally healing tibial shaft fractures reported a similar trend with BS-ALP initially decreasing at 1 week and then increasing throughout the study.[25,36] In the same study, OC increased postfracture, then decreased reaching a minimum at week 5, and then increased thereafter.[25] In another study, OC and ALP concentrations were higher at 6 weeks compared with immediately postfracture, and at 12 weeks was not different from concentrations before surgery.[20] Osteocalcin was also reported to increase 72-hours after fracture, however the difference in this study was not statistically significant.[40] Urinary PYR and DPYR were found to increased 1 week post fracture, peak between 4 and 8 weeks, and returned to normal by week 24.[22] Therefore, our study as well as others, support a change in bone marker concentration after fracture with an initial period of bone resorption and minimal bone formation, followed by a period of bone formation, which is associated with the phases of fracture healing.

In our study we found a weak correlation between OC and BS-ALP; however, there was a better correlation between the change in OC and BS-ALP. In another study there was no association between OC and total ALP and the dissociation between OC and total ALP was not explained by liver disease. The authors concluded that it reflected the

different aspects of osteoblastic function.[41] Bowles and coworkers, also reported that total ALP increased while BS-ALP decrease initially postfracture, and there was no association between BS-ALP and OC during the first few weeks postfracture.[25] The weak correlation between BS-ALP and OC may reflect the release of OC in association with bone resorption and bone formation.[25] variation in osteoblastic function, or variability associated with the individual rabbit and the assay.

The initial high BS-ALP and OC at time 0 is difficult to interpret; however, it probably reflects the young age of the rabbits. The rabbits used in the study were skeletally mature (9 months) and the femoral growth plates were closed; however, these rabbits may still have been actively mineralizing bone. Another study,[25] however, showed no effect of age on BS-ALP and OC concentrations in human subjects with fractures varying in age from 16 to 64 years. Alternatively, transportation and changes in housing may also have led to the higher concentration of BS-ALP and OC at the beginning of the study.

The physiological processes associated with the release of serum bone markers are complex and there are numerous factors that affect serum bone marker concentration. Changes in bone markers postfracture reflect bone resorption and formation associated with the actual fracture and repair, osteonecrosis associated with the initial injury and surgical treatment, soft tissue trauma, lameness, reduced activity, immobilization or physical unloading of the limb, bone remodeling, infection, hemorrhage, and systemic disease.[22] The complexity is illustrated by the effect of bodyweight and change in body weight on the results of the analyses in our study. Although these variables altered the analysis there was no correlation between OC and BS-ALP and pre-operative body

weight. Other studies did not find a correlation between weight/height and OC concentration in humans; however there was a positive correlation between BS-ALP and height/weight.[25] Interestingly, there was no effect of lameness; however, the effect of reduced weight bearing on the affected limb may have been counteracted by altered gait and increase in weight bearing on the contralateral limb. The lack of association between bone marker concentration and external callus and lysis grade may also be a result of interactions between bone formation and resorption with both healing and osteomyelitis. Additionally circadian, seasonal, age-related, and hormonal-factors, as well as different methods of sample collection and analysis are thought to affect bone marker concentration. A large variability between individuals in serum bone marker concentration following fracture and during fracture repair has been reported,[39,40] and was also found in our study. The large variability between individuals as well as the interassay variability may have resulted in the low level of statistical significance between groups in our study.

In the current study, OC was measured as the intact molecule, which has a high variability and low stability. The N-terminal mid fragment can also be measured and there is less variation in measurements and it is more stable for storage,[22] but it may be falsely elevated because there may be multiple fragments associated with a single molecule. In our study, blood samples were collected at approximately the same time each day and were stored similarly, however there was approximately 2 months difference in time between sample collection in the first and last rabbit and there was a 4-month variation between the initial and final sample collection, which may account for some variability over time. Mature female rabbits were used and some variability

associated with hormonal changes may have existed. Despite the numerous factors affecting serum bone marker concentration the results of this study suggest that they may be useful for evaluating fracture healing.

Serum bone markers may be useful for evaluating the presence of infection. Rabbits with infection had lower serum BS-ALP and OC and a higher DPYR concentration at 4 weeks. When a combination of markers were used to predict whether the rabbit was infected or not, the overall accuracy was 96% at 4 weeks (Table 1), which is higher than that achieved with imaging modalities.[8-10] The use of serum bone markers for evaluating infection early is supported by the lack of radiographic bone lysis in infected rabbits at 4 weeks (Chapters 2 and 3). However, in clinical cases the time from injury and surgery to the development of osteomyelitis is variable and unknown; therefore serial measurements of serum bone marker concentration would be needed.

The low BS-ALP may have been a reflection of reduced bone formation in the infected rabbits. However, it may also be an indication of the effect of systemic disease on bone formation, because the infected rabbits showed signs of inappetence, lameness, and weight loss, as well as sepsis requiring euthanasia in some cases. The effect of systemic disease is supported by the correlation between BS-ALP and body weight at euthanasia, and the reduced significance of infection when these variables were included in the analysis. Hemorrhagic shock has been shown to increase osteonecrosis, reduce osteoblastic function, and subsequently cause a decrease in OC at 72 hours after experimental fracture and hemorrhagic shock in mice.[40] During the 16-week course of the study, rabbits had approximately 12.5% of blood volume collected, which should not have altered serum bone marker concentration; however, the combination of blood loss

and infection may have caused a decrease in BS-ALP. We found no association between body weight at euthanasia or change in body weight and OC. Similarly, studies evaluated OC in humans and found that systemic disease did not affect OC, but BS-ALP was not evaluated.[41] The OC followed a similar trend to BS-ALP at 4 weeks, but OC was increased in infected rabbits at 16 weeks whereas BS-ALP was not. The increase in OC in infected rabbits at 16 weeks may be a combination of both OC release from bone resorption as well as bone formation associated with sclerosis and proliferation in infected rabbits. Osteocalcin was found not to be beneficial for evaluating chronic osteomyelitis in human patients because of the wide ranges in concentration and different factors affecting OC concentration.[30] In a dog model of an infected femoral fracture stabilized with an intramedullary pin, OC and BS-ALP were increased 1 and 2 weeks after fracture and infection, reaching a peak at 2 weeks.[31] The duration of the latter study was only 4 weeks and there were no non-infected animals, making it difficult to evaluate the effect of the fracture versus the infection on serum bone marker concentration.

The DPYR was higher in infected rabbits at all time periods, which is a reflection of bone degradation. This was supported by rabbits with a higher radiographic lysis grade having a significantly higher concentration of DPYR, and is similar to another study showing an increase in ICTP concentration in infected fractures.[31] The ICTP was not evaluated in this study because there are no commercially available kits to measure ICTP in rabbits.

Other measurements used to evaluate infection such as erythrocyte sedimentation rate and C-reactive protein, were not measured in our study, but may be useful to

measure inflammation and infection concurrently with serum bone markers in future studies.

Serum markers may also be useful for evaluating fracture healing. Overall, rabbits with a higher external callus grade had higher BS-ALP. Bone-specific alkaline phosphatase is used *in vitro* to determine expression of BMP-2. Rabbits treated with Ad-BMP-2 had a higher external callus grade and bridging-callus formation compared to control rabbits (Chapter 3), but there was no significant difference between treatment groups in BS-ALP; however, the increase in BS-ALP in rabbits with higher external callus grade may be an indication of the over expression of BMP-2. Although it appeared that there was a higher OC concentration at 8 and 12 weeks and a higher DPYR concentration at 4 and 8 weeks in rabbits that had a higher external callus grade, this was not statistically significant in this study because of the high variability. Further, external callus grade is a subjective evaluation, which may have also added variability. A grade-4 was assigned if the external callus was large and bridging, and it appear that rabbits with a grade-4 callus had the highest values of serum bone markers, and then after reaching a peak there was a decline in these values. Nuclear scintigraphy findings followed a similar trend (Chapter 4). Additionally, there was a trend for rabbits with bridging-callus to have a greater decrease in OC from time 0 at 16 weeks. These results support those of other studies that reported an increase in marker concentration after fracture, and then a more rapid decline in marker concentration in patients with normal union.[20] The trend for an increase in DPYR with increase in external callus formation may actually be a reflection of the interaction between the presence of infection causing lysis and the greater bone proliferation and callus formation associated with infection. Alternatively, rabbits with a

larger callus may have had more bone for resorption resulting in a higher DPYR. Another study found an increase in ICTP after fracture, and there was a trend for patients with delayed healing to have higher concentrations at 2 weeks after fracture.[39]

In conclusion, serum bone markers may be useful for distinguishing normal union from delayed- or non-union and infected from non-infected fractures. It is unlikely that one serum bone marker will be adequate; however, using multiple markers, concentrations for healing versus non-healing and infected versus non-infected fractures may be established. Future studies in the target species, using additional serum bone markers, and at earlier, more frequent time periods are required.

References

1. Yelin E, Callahan LF. The economic cost and social and psychological impact of musculoskeletal conditions. Arthritis Rheum 1995; 38:1351-1362.
2. Praemer A, Furner S, Rice DP. Musculoskeletal conditions in the United States, Park Ridge IL. Am Acad Orthop Surg 1992, p85-124.
3. Johnson EE, Urist MR, Finerman AM. Resistant nonunion and partial or complete segmental defects of long bones. Clin Orthop Rel Res 1992; 277:229-237.
4. Auer JA, Watkins JP. Treatment of radial fractures in adult horses: An analysis of 15 clinical cases. Equine Vet J 1987; 19: 103-110.
5. Sanders-Shamis M, Bramlage LR, Gable AA. Radius fractures in the horse: A retrospective study of 47 cases. Equine Vet J 1986; 18:432-437.
6. Crawford WH, Fretz PB. Long bone fractures in large animals. A retrospective study. Vet Surg 1985; 14:295-302.
7. Hance SR, Bramlage LR, Schneider RK, et al. Retrospective study of 38 cases of femur fractures in horses less than one year of age. Equine Vet J 1992; 24:357-363.
8. Letts RM, Afifi A, Sutherland JB. Technetium bone scanning as an aid in the diagnosis of atypical acute osteomyelitis in children. Surg Gynechol Obstet 1975; 140:899-902.
9. Munoz P, Bouza E. Acute and chronic osteomyelitis and prosthesis-related infections. Bailliere's Clinical Rheum 1999; 13:129-147.
10. Abiri MM, DeAngelis GA, Kirpekar M, et al. Ultrasound detection of osteomyelitis. Investigative Radiology 1992; 27:111-113.

11. Russell RGG. The assessment of bone metabolism in vivo using biochemical approaches. Horm Metab Res 1997; 29: 138-144.

12. Bettica P. Moro L. Robins SP. et al. Bone-resorption markers galactosyl hydroxlysine. pyridinium crosslinks. and hydroxyproline compared. Clin Chem 1992; 38:2313-2318.

13. Garnero P. Shih WJ. Gineyts E. et al. Comparison of new biochemical markers of bone turnover in late postmenopausal osteoporotic women in response to alendronate treatment. J Clin Endocrin Metab 1994; 79:1693-1700.

14. Bollen AM. Kiyak HA. Eyre DR. Longitudinal evaluation of a bone resorption marker in elderly subjects. Osteoporosis Int 1997; 7:544-549.

15. Turner AS. Alvis M. Myers W. et al. Changes in bone mineral density and bone-specific alkaline phosphatase in ovariectomized ewes. Bone 1995; 17:395S-402S.

16. Kurdy NMG. Serology of abnormal fracture healing: The role of PIIINP. PICP. and BsALP. J Orthopaedic Trauma 2000; 14: 48-53.

17. Hauschka PV. Lian JB. Gallop PM. Direct identification of the calcium-binding amino acid. gamma-carboxyglutamate in mineralized tissue. Proc Natl Acad Sci USA 1975; 72:3925-3929.

18. Lian JB. Gundberg CM. Osteocalcin: Biochemical considerations and clinical applications. Clin Orthop Rel Res 1988; 226:267-271.

19. Price PA. Poser JW. Raman N. Primary structure of the gamma carboxy glutamic acid containing protein from bovine bone. Proc Natl Acad Sci USA 1976; 73:3374-3375.

20. Nyman MT, Paavolainen P, Forsius S, Lamberg-Allardt C. Clinical Evaluation of fracture healing by serum osteocalcin and alkaline phosphatase. Annales Chirurgiae et Gynaecologiae 1991; 80:289-293.

21. Price PA, Williamson MK, Lothringer JW. Origin of the vitamin K-dependent bone protein found in plasma and its clearance by kidney and bone. J Biol Chem 1981; 256:12760.

22. Ohishi T, Takahashi M, Kushida K, Hoshino H, Tsuchikawa T, Naitoh K, Inoue T. Changes in biochemical markers during fracture healing. Arch Orthop Trauma Surg 1998; 118;126-130.

23. Obrant KJ, Merle B, Bejui J, Delmas PD. Serum bone-gla protein after fracture. Clin Orthop Rel Res 1990; 258:300-303.

24. Akesson K, Vergnaud Ph, Delmas PD, Obrant KJ. Serum osteocalcin increases during fracture healing in elderly women with hip fracture. Bone 1995; 16:427-430.

25. Bowels SA, Kurdy N, Davis AM, et al. Serum osteocalcin, total and bone-specific alkaline phosphatase following isolated tibial shaft fracture. Ann Clin Biochem 1996; 33:196-200.

26. Mallmin H, Ljunghall S, Larsson K. Biochemical markers of bone metabolism in patients with fracture of the distal forearm. Clin Orthop Rel Res 1993; 295:259-263.

27. Ingle BM, Hay SM, Bottjer HM, Eastell R. Changes in bone mass and bone turnover following distal forearm fracture. Osteoporosis Int 1999; 10:399-407.

28. Oni OOA, Mahabir JP, Iqbal SJ, Gregg PJ. Serum osteocalcin and total alkaline phosphatase levels as prognostic indicators in tibial shaft fractures. Injury 1989; 20: 37-38.

29. Emami A, Larsson A, Petrén-Mallmin M, Larsson S. Serum bone markers after intramedullary fixed tibial fractures. Clin Orthop Rel Res 1999; 368:220-229.

30. Peters KM, Rosendahl T, Heller KD, Weigmann R, Zilkens KW. Osteocalcin levels in chronic osteomyelitis. Arch Orthop Trauma Surg 1994; 114:53-55.

31. Philipov JP, Pascalev MD, Aminkov BY, Grosev CD. Changes in serum carboxyterminal telopeptide of type I collagen in an experimental model of canine osteomyelitis. Calcif Tissue Int 1995; 57:152-154.

32. Raekallio J, Mäkinen PL. Alkaline and acid phosphatase activity in the initial phase of fracture healing. Acta Path Microbiol Scandinav 1969; 75:415-422.

33. Volpin G, Rees JA, Ali SY, Bently G. Distribution of alkaline phosphatase activity in experimentally produced callus in rats. J Bone Joint Surg 1986; 68B: 629-634.

34. Urist MR, Mazet R, McLean FC. Pathogenesis and treatment of delayed union and non-union. J Bone Joint Surg 1954; 36A: 931.

35. Lal SK, Jacob KC, Nagi ON, Annamalai AL, Nair CR. Variations of some plasma components after closed fractures. J Trauma 1976; 16: 206.

36. Bowles SA, Kurdy N, Davis AM, France MW. Changes in serum bone-specific alkaline phosphatase following tibial fracture. Ann Clin Biochem 1997; 34:690-691.

37. Leung KS, Fung KP, Sher AHL, Li CK, Lee KM. Plasma bone-specific alkaline phosphatase as an indicator of osteoblastic activity. J Bone Joint Surg 1993; 75B:288-292.

38. Brozmanová E, Škrovina B. Serum enzyme activity in bone tumors and osteomyelitis (LDH, GOT, GPT, CPK, CHE, ALP, AP, PP, ALD). Neoplasia 1977; 24:109-117.

39. Joerring S, Krogsgaard M, Wilbek H, Jensen LT. Collagen turnover after tibial fractures. Arch Orthop Trauma Surg 1994; 113:334-336.

40. Wichmann MW, Arnoczky SP, DeMaso CM, Ayala A, Chaudry IH. Depressed osteoblast activity and increased osteocyte necrosis after closed bone fracture and hemorrhagic shock. J Trauma: Injury, Infection, and Critical Care 1996; 41:628-633.

41. Slovik DM, Gundberg CM, Neer RM, Lian JB. Clinical evaluation of bone turnover by serum osteocalcin measurements in a hospital setting. J Clin Endocrin Metab 1984; 59:228-230.

42. Kjaersgaard-Anderson P, Pedersen P, Kristensen SS, Schmidt SA, Pedersen NW. Serum alkaline phosphatase as an indicator of heterotopic bone formation following total hip arthroplasty. Clin Orthop Rel Res 1988; 234:102-109.

43. Kurdy NMG, Bowles S, March DR, Davies A, France M. Serology of collagen types I and III in normal healing of tibial shaft fractures. J Orthop Trauma 1988; 12:122-126.

44. Antoniou J, Huk O, Zukor D, Eyre D, Alini M. Collagen cross-linked N-telopeptide as a marker for evaluating particulate osteolysis. Proc 43rd Ann Mtg Orthop Res Soc 1997.

45. Rico H, Villa LF. Serum tartrate-resistant acid phosphatase (TRAP) as a biochemical marker of bone remodeling. Calcif Tissue Int 1993; 52:149-150.

46. Lawton DM, Andrew JG, Marsh DR, Hoyland JA, Freemont AJ. Mature osteoblasts in human non-union fractures express collagen type III. J Clin Pathol Mol Pathol 1997; 50:194-197.

SUMMARY AND CONCLUSIONS TO THESIS

The results of this study underscore the challenge of developing new methods for treatment and early diagnosis of infected non-union. We were able to develop an infected non-union model, which was useful for evaluating gene transfer of BMP-2 for enhancing fracture healing. However, as with clinical cases of non-union and osteomyelitis, there was considerable morbidity and mortality associated with the infected non-union model. Modifications to this model, including the use of supportive therapy, the dose of *S. aureus*, and the use of sodium morrhuate, should be evaluated prior to future studies using this model.

Treatment with Ad-BMP-2 enhanced the amount and rate of external callus formation in both non-infected and infected non-union models. Therefore, it was concluded that Ad-BMP-2 is effective for stimulating a healing response in the presence of infection. However, there was minimal new bone formation in the fracture defect. While the specific reasons for this could not be determined from this study because of inadequate control groups, the use of the sclerosing agent on the bone ends is the most logical explanation. Based on the *in vitro* study evaluating the effect of the sclerosing agent on the transduction efficiency of the adenoviral vector, it would appear that at low concentrations of the sclerosing agent transduction is not affected. Although the concentration of the sclerosing agent at the time of treatment with Ad-BMP-2 was unknown, it was presumed to be low because of the 48-hour delay between surgery and treatment.

The sclerosing agent, however, damaged the bone ends adjacent to the defect, as well as some of the soft tissue and vessels in the defect area. Hence, it is likely that there was a lack of cells for the adenovirus to transduce. While this model is particularly harsh, it could reveal an important limitation with *in vivo* gene therapy; that is, if there is extensive soft tissue, vascular, and bone damage associated with a traumatic fracture, there may be insufficient cells for viral transduction, resulting in inadequate transgene expression. The use of *ex vivo* gene transfer may overcome the problem; however, *ex vivo* gene transfer is technically more demanding, time consuming, and the fate of the transduced cells in an infected non-union is unknown. Further studies are required to evaluate the use of *ex vivo* gene transfer of BMP-2 in infected non-unions. Because there is usually a poor blood supply associated with severe traumatic fractures, the use of an angiogenic growth factor, such as vascular endothelial growth factor (VEGF), in combination with BMP-2 could produce more favorable results, and this should also be evaluated in future studies.

Several limitations with the use of nuclear scintigraphy for early diagnosis of osteomyelitis associated with long-bone fractures were identified. While both Tc-PO and -CIPRO were useful for distinguishing infected from non-infected fractures late in the study, neither method was reliable at the earliest time point (4 weeks). The lack of specificity for diagnosing osteomyelitis using Tc-PO is most likely associated with both an increase in blood flow to the area and an increase in bone metabolism associated with fracture healing. While the lower than expected specificity with Tc-CIPRO was difficult to explain, it was most likely related to an increase in blood flow to the bone associated with surgery and healing in both infected and non-infected rabbits resulting in false

positive results in non-infected rabbits. A decrease in blood flow as a result of the use of the sclerosing agent as well as abscessation may have caused false negative results in infected rabbits. Although there were some trends observed, Tc-PO was not useful for differentiating fractures that developed a bridging-callus from those that did not; however, this may be a reflection of the model and type of healing. The use of nuclear scintigraphy in conjunction with other methods, and performing sequential scans may be more useful for assessing fracture healing and diagnosing osteomyelitis.

Serum bone markers, on the other hand, may be useful for early diagnosis of osteomyelitis in patients with long-bone fractures. The changes in serum bone marker concentration appeared to reflect the phases of fracture healing, and there was a high accuracy for differentiating infected from non-infected fractures at 4 weeks when multiple markers were used. Further studies in the target species are required to more accurately assess the value of serum bone markers for this purpose.

In conclusion, while the results of our study suggest that Ad-BMP-2 stimulated healing in our model, future studies evaluating different methods of gene therapy and combinations of growth factors for enhancing healing in infected non-unions are required. The use of nuclear scintigraphy and serum bone markers for assessing fracture healing and for early diagnosis of osteomyelitis should be evaluated further at earlier and more frequent time points.